CHARACTERIZATION, MODELLING, PREDICTION AND INHIBITION OF NAPHTHENATE DEPOSITS IN OILFIELD PRODUCTION

by

MOHAMMED MURTALA AHMED

Submitted for the Degree of Doctor of Philosophy in

PETROLEUM ENGINEERING

Institute of Petroleum Engineering
Heriot-Watt University
Edinburgh, UK

September 2010

ABSTRACT

The production of acidic or sometimes heavier crudes often leads to the formation of either calcium naphthenate or sodium carboxylate soap emulsions during oil production operations. This problem has been recognised as a major flow assurance problem in the oil industry. In this work, both harder calcium naphthenates and more emulsion–like sodium carboxylates have been studied and these are viewed as "end members" in the spectrum of field naphthenate deposits which may occur. In this thesis, four related aspects of naphthenate deposits are studied, as follows: (i) **Characterization** of various field naphthenates samples from different parts of the world, involving naphthenic acid extraction method development and subsequent extract analysis using electrospray mass spectrometry (ESMS) and atmospheric pressure chemical ionisation mass spectrometry (APCI MS) techniques. It was observed that different naphthenic acid extraction and analysis methods affected the naphthenic acid identification and apparent composition; (ii) **Geochemical** studies have been carried out on various crude oils which form calcium naphthenate deposits, sodium carboxylate soaps and emulsions. Biomarker correlation analysis was employed on the aliphatic and aromatic fractions of the crude oil samples using gas chromatography (GC) and gas chromatography mass spectroscopy (GCMS); (iii) **Thermodynamic modelling** of naphthenate formation was carried out, and both a simple thermodynamic pH change naphthenate model and a full naphthenate precipitation model have been developed. This thermodynamic model describes the chemistry of a simple partitioning "pseudo" naphthenic acid which may form calcium naphthenate "precipitate", according to a solubility product type description. This model has been used in a wide sensitivity study which makes some predictions about the way a precipitating Ca-Naphthenate (CaN) system behaves and these predictions have been confirmed experimentally; (iv) **Naphthenate chemical inhibition** studies have been performed in order to develop a methodology for the mitigation of these deposits. Static "inhibition efficiency" tests have been conducted using 8 different naphthenate inhibitors in order to determine the most appropriate methodology for testing and also the effectiveness of these chemicals in preventing the formation of calcium naphthenates and sodium carboxylate soap emulsions.

ACKNOWLEDGEMENTS

I would like to express my sincere gratitude to my supervisor, Professor Ken Sorbie, for his invaluable guidance, motivation, encouragement, and support throughout the course of my PhD. It would have been very difficult for me to have reached this point in my academic journey, without the leadership, technical criticism, and support from him which is highly appreciated.

My endless gratitude goes to my parents for their prayers and moral support through the course of my study. I am sure they will be more than happy to see me achieve what I have dreamt off long ago. All assistance and concern from my brothers, sisters, friends, and well wishers is highly appreciated.

I am also grateful to Petroleum Technology Development Fund (PTDF) for their sponsorship and all assistance from Kano State Government is also acknowledged.

My sincere gratitude goes to FAST III sponsors (Baker Hughes, BP, BWA Water Additives, Champion Technologies, Chevron, Clariant Oil Services, ConocoPhillips, Halliburton, MI Swaco, Nalco, Petrobras, Petronas, REP, Rhodia, Saudi Aramco, Shell, Statoil and Total) and all the members of the Flow Assurance and Scale Team for making my stay at Heriot-Watt a memorable one. I would particular like to thank Dr. Eric Mackay, for all his support on both academic and non-academic issues throughout my stay at Heriot-Watt University which will certainly be some of the great highlights that I will always remember. I thank all my colleagues in the scale office for the wonderful times we shared and the long office hours spent together during my PhD which I am sure I will always remember.

I am also grateful to Dr. Darrell L. Gallup of Chevron and Dr. Robin E. Westacott of Chemical Engineering, Heriot-Watt University for agreeing to examine this thesis. Their time invested in reading and evaluation of this thesis was invaluable.

I would like to acknowledge Christine Graham, of Chemistry Department, Heriot-Watt University for her assistance and Rebecca Dodds of M-Scan for the ESMS and APCI-MS analysis.

Finally, I am sincerely grateful to my beloved wife Zainab, and my son Mahmud. Her patience, encouragement, support, and prayers throughout the roller-coaster of this PhD is highly appreciated. She made unique contributions at every step during my research period and that really made things a lot much easier.

TABLE OF CONTENTS

LIST OF FIGURES

LIST OF TABLES

NOMENCLATURE

Acid-IER	Acid ion exchange resin
APCI-MS	Atmospheric pressure chemical ionization mass spectrometry
API	American petroleum institute
At %	Atomic percent
Arn	Tetra protic acid
BF3	baron trifloride
BSE	Back-scattered electrons
Ca^{++}	Calcium ions
$CaCl_2.6H_2O$	Calcium chloride hexahydrate
CaN	Calcium naphthenate
CPI	Carbon preference index
CO_2	Carbon dioxide
Conc.	Concentration
Cur	Curtain gas
EDAX	Energy dispersive X-ray
eV	electron volt
ESEM/EDAX	Enviromental scanning electron microscope/energy dispersive x-ray
ESMS	Electrospray mass spectrometry
FT-ICR-MS	Fourier transform ion cyclotron mass spectrometry
FT-IR	Fourier transform infrared
g	Grams
GAA	Glacial acetic acid
GC	Gas chromatography
GCMS	Gas chromatography mass spectroscopy
GCMSMS	Gas chromatography mass spectroscopy mass spectroscopy
$[HA]_{oi}$	Initial molar concentration of acid in the oil phase
$[HA]_{wf}$	Final molar concentration of acid in the water phase
$[OH]_f$	Final molar concentration of hydroxyl ion
$[H^+]_f$	Final molar concentration of the hydrogen ion
HCO_3^-	Bicarbonate ion
HTGC	High temperature gas chromatography
IPA	Isopropyl alcohol
ITMS	Ion-trap mass spectroscopy
ISO	Ion spray voltage
K^+	Potassium
$KCaA_2$	Solubility product
K_{ow}	Partition coefficient
K_w	Ionic product of water
KOH	Potassium hydroxide
kV	Kilo volts
LCMS	Liquid chromatogram mass spectrometry
l	Litre
M	Molar concentration
MeOH	Methanol

Mg	Milligram
MIC	Minimum inhibitor concentration
ml	Milli litre
M_{sol}	Mass of solid
M.wt	Molecular weight
MS	Mass spectrometry
m/z	Mass to charge ratio
n	Number of carbon atoms
Na^+	Sodium ion
NaCl	Sodium chloride
Na_2CO_3	Sodium carbonate
$NaHCO_3$	Sodium hydrogen carbonate
NaN	Sodium naphthenate
NaOH	Sodium hydroxide
NEB	Nebulizer gas
NMR	Nuclear magnetic resonance spectroscopy
OEP	odd-even carbon number preference
Ph	Phytane
pH_f	Final brine pH
pKa	Acid dissociation constant
ppm	Parts per million
Pr	Pristane
R-COOH	Carboxylic acid general formula
rpm	revolution per minutes
SIM	Single ion monitoring
t	Time
TAN	Total acid number (mg KOH/g Oil)
TBR	Tube blocking rig
TIC	Total ion chromatogram
TLC	Thin layer chromatography
TOC	Total organic carbon
UV	Ultraviolet
V_o	Volume of oil
V_w	Volume of water
V_T	Total volume
VPO	Vopor pressure osmmometry
W%	Weight percentage
%WCut	Percentage watercut
^oC	Degree centigrade
Z	Homologous series
~	Approximately
%	Percentage
μm	Micron

LIST OF PUBLICATIONS

Murtala A. Mohammed and K. S. Sorbie, 20-22 April 2009: *Spectroscopic Determination of Naphthenic Acid Composition from Various Calcium Naphthenate Field Deposits*. SPE 121633 at the International Symposium on Oilfield Chemistry, The Woodlands, Texas, USA (2009).

Murtala A. Mohammed, K. S. Sorbie and Andrew, G. Shepherd, August 2009. *Thermodynamic Modelling of Naphthenate Formation and Related pH Change Experiments*. SPE Production & Operation Journal, Page 466-472.

Murtala A. Mohammed and K. S. Sorbie, October 2009. *Naphthenic Acid Extraction and Characterization from Naphthenate Field Deposits and Crude Oils Using ESMS and APCI-MS*. Colloids and Surface A: Physiochemical and Engineering Aspect, Volume 349, Issues 1-3, page 1-18).

Murtala A. Mohammed and K. S. Sorbie: *Thermodynamic Modelling of Calcium Naphthenate Formation Using Naphthenic Acid Extract from Field Deposits*. Accepted for publication in Colloids and surface journal (in press).

Murtala A. Mohammed and K. S. Sorbie: Geochemical studies of calcium and sodium naphthenates forming crude oils from various parts of the world in relation to flow assurance. *In progress.*

Murtala A. Mohammed, K. S. Sorbie and J. P. Vijn: Chemical mitigation of naphthenate deposits and sodium carboxylate emulsions by interface crowding inhibitors. *In progress*

CHAPTER 1: INTRODUCTION

The worldwide high demand for crude oil as a source of energy in recent years has led oil companies to go into the development, exploration and production of heavier crudes. These crudes may have high total acid number (TAN), or sometimes they may be slightly biodegraded. These heavy or slightly biodegraded crudes are mostly acidic in nature and the acidity is predominantly caused by the indigenous acids present within the crude oil (Rousseau *et al.,* 2001), which are referred to as naphthenic or carboxylic acids in the oil industry. However, in some cases when these crudes are produced along with water this can lead to the formation of metal naphthenates. These may be either soft emulsion type substances referred to as "sodium naphthenate/carboxylate soap" or hard type deposits known as "calcium naphthenate". They are formed during oil production due to changes in chemical and physical properties of both crude oil and formation water (Rousseau *et al.,* 2001; Gallup *et al.,* 2002; Goldszal *et al.,* 2002; Dyer *et al.,* 2003; Havre *et al.,* 2003; Vindstad *et al.,* 2003; Ese and Kilpatrick, 2004; Laredo *et al.,* 2004; Shepherd *et al.,* 2005). The precise mechanism by which these metal naphthenates form is discussed in detail later in this thesis.

Calcium naphthenate deposits or carboxylate soap formation are among a number of flow assurance problems in the petroleum industry. In most cases, naphthenate formation poses a very serious concern within the oil industry and therefore, its identification, prevention or mitigation is necessary. The production problems associated with the formation of metal naphthenates are reported to occur mostly in the surface facilities i.e. in the separators, hydrocyclones, heat exchangers and other production equipment (Rousseau *et al.,* 2001; Vindstad *et al.,* 2003), although it was recently suggested that it can also cause some formation damage in the reservoir (Sarac and Civan, 2007). However, no field cases have yet been reported of naphthenate formation damage.

It has been reported in the literature that certain crude oils produced from both onshore and offshore fields in a range of places, including Angola, Congo, Cameroon and Nigeria, the North Sea (United Kingdom), the Norwegian continental shelf (Norway), South East Asia

(China, Indonesia, Malaysia), South America (Venezuela and Mexico) have naphthenate/ carboxylate soap flow assurance problems (Rousseau *et al.,* 2001; Gallup and Star, 2004; Hurtevent and Ubbels, 2006). Naphthenate formation in these fields hinders oil production and can result in unplanned plant shutdown, loss of production and off-specification export oil quality control problems. Therefore, it is important to understand the chemistry of these crude oils and their formation waters, as well as the changes in the physical parameters that occur during oil production to enable us to address this type of flow assurance problem. Prevention of production losses by understanding this phenomenon can save oil companies millions of dollars by providing them with the data they require well before any problems arise. Ultimately, this will also give the oil companies an opportunity to design new improved production facilities to mitigate the naphthenate/carboxylate soap problems.

This thesis is focused on understanding the chemical composition of calcium naphthenate/carboxylate soaps and the thermodynamic prediction modelling and chemical mitigation of these deposits/emulsions. The thesis consists of 8 chapters. This chapter has given a brief review of what naphthenates are.

Chapter 2 is a detailed literature review of the occurrence and structures of naphthenates, naphthenic acid characterization and also their presence in crude oils, as well as studies on naphthenates formation prediction modelling and naphthenate inhibition.

Chapter 3 describes all the experimental methods used for the extraction of naphthenic acid from calcium naphthenate deposits and sodium carboxylate/emulsion soaps, crude oil geochemical analysis, naphthenate precipitation/sensitivity experiments and also the method development for the chemical “inhibition” of naphthenate deposits and carboxylate soaps.

Chapter 4 present results from the extraction and characterization of various field calcium naphthenate deposits, sodium carboxylate/emulsion soap and crude oil extracts, using electrospray mass spectrometry (ESMS) and atmospheric pressure chemical ionisation

mass spectrometry (APCI-MS) techniques. Results from calcium naphthenate re-precipitation and subsequent naphthenic acid extraction from the laboratory formed precipitate are also discussed in this chapter.

Chapter 5 describes the geochemical analysis of naphthenate forming crudes i.e. calcium naphthenate and carboxylate soaps from the flow assurance perspective. Results from the crude oil fractions biomarker analysis using gas chromatography (GC) and gas chromatography mass spectrometry (GCMS) are extensively covered in this chapter.

Chapter 6 presents a thermodynamic naphthenate prediction model which describes the theoretical, experimental and modelling results of; (i) simple pH change experiments, (ii) naphthenate precipitation experiments and (ii) other sensitivity studies.

Chapter 7 presents results from the chemical mitigation (inhibition) methods development for calcium naphthenate, carboxylate soap and emulsion forming crudes. Results from static inhibition efficiency experiments using 8 different naphthenate inhibitors on calcium naphthenate extract, sodium carboxylate/emulsion extracts and emulsion forming crude oil are discussed in this chapter. An attempt to carry out naphthenate dynamic inhibition efficiency experiments is also discussed.

Chapter 8 gives an overview of the conclusions of this study and recommendations for future research work in this area.

In the Appendix, the theoretical derivation method for the naphthenate model is described (Appendix A).

CHAPTER 2: LITERATURE REVIEW

2.1 NAPHTHENATES

In an oilfield production system, naphthenate deposition is one of a number of flow assurance problems affecting crude oil productivity. The formation of these substances has been of great concern to many producing companies, because of their negative effect on oil production and the fact that preventing their formation can often be very difficult. There are two main types of naphthenates that have been reported in the field i.e. the hard type of sticky deposit known as "calcium naphthenate" and the soft fluid/emulsion type known as "sodium carboxylates/emulsions". Formation of both of these types of naphthenate deposit (calcium naphthenate or sodium carboxylate/emulsion) has been observed in various oil producing areas of the world. Naphthenate deposits/emulsions are known to be associated with problems such as blockage of surface equipment, shutdown of offshore installations, increase in the cationic content of crudes and the formation of oil sludges (Gallup *et al.,* 2002; Vindstad *et al.,* 2003; Gallup and Star, 2004; Smith, 2004;). Calcium naphthenate deposits are usually observed at the oil-water interface during oil production and tend to harden on exposure to air and this may increases the difficulty of their removal and disposal. The calcium naphthenate deposits may accumulate over time and have been reported to cause unplanned shutdowns and at times off-spec products (Vindstad *et al.,* 2003).

2.2 GENERAL MECHANISM FOR NAPHTHENATE FORMATION

The key factors believed to be responsible for the formation of naphthenates can be categorised as (a) chemical parameters - such as crude oil composition, brine composition, and brine pH, and (b) physical parameters such as pressure, temperature, shear and % watercut (Turner and Smith, 2005). The literature regarding these two categories of naphthenate formation (calcium naphthenate or sodium carboxylate/emulsion) will be discussed in a later section. However, the fundamentals of how naphthenates form will be described in this section. Several researchers in the literature have attempted to describe the basic mechanism of naphthenate formation. The crude oil composition is considered to play a significant role in the naphthenate formation mechanism. The key factor regarding crude

oil composition for the naphthenate mechanism is the types of naphthenic acid present in the crude oil, as well the concentration level. The brine composition is also important, particularly the cationic content of the brine, which determines the precise mechanism of naphthenate formation. Most of the hard field deposits, i.e. calcium naphthenates, have been shown to contain calcium ions (Ca^{++}), although in certain instances, the samples contain mainly monovalent ions such as sodium (Na^{+}) or potassium (K^{+}), as reported by Gallup *et al.,* (2002) and Turner and Smith (2005). The cationic composition of the field samples is also tied to the naphthenate type, with the calcium rich deposit referred to as calcium naphthenate and the sodium rich sample referred to as sodium carboxylate or sodium naphthenate emulsion, as suggested by Turner and Smith (2005). The brine composition is known to play a significant role in the basic naphthenate formation mechanism. The brine pH entirely depends on the pressure and the carbonate system chemistry ($CO_2/H^{+}/Ca^{2+}/HCO_3^{-}$). At downhole conditions, where pressure is high and brine pH is often relatively low, the naphthenic acids remain protonated and in the crude oil and consequently there is no naphthenate formation. Rousseau *et al.,* (2001) described the naphthenate appearance mechanism as being dependent on the pH increase that occurs during crude oil production, due to carbon dioxide (CO_2) being evolved from the brine leading to an increase in brine pH (Rousseau *et al.,* 2001; Goldszal *et al.,* 2002; Dyer *et al.,* 2003; Shepherd *et al.,* 2005). The overall pressure and temperature drop as the crude oil flows from the reservoir to the separator. This decrease is necessary in order to be able to separate the crude oil and produced fluids into various components. The "naphthenic acid" from the crude oil, represented by the general formula R-COOH (Goldszal *et al.,* 2002), collects at the oil-water interface, due to the chemistry of the functional group. The change of the brine pH (from lower to higher) causes the formation of surface active naphthenates, RCOO- anion (Rousseau *et al.,* 2001) at the oil-brine interface until pH equilibrium is attained. The mechanism of reaction for the naphthenate formation has been described by Goldszal *et al.,* (2002) as follows:

$$RCOOH + OH^{-} \leftrightarrow RCOO^{-} + H_2O \qquad (2.1)$$

Depending on the cationic composition of the brine, the naphthenate anions will bond with the metal ions to form insoluble substances i.e. metal naphthenates. The most common known types are the calcium and sodium naphthenates. The two possible reaction mechanisms are as follows:

$$2RCOO^- + Ca^{2+} \leftrightarrow (RCOO)_2Ca \quad (2.2)$$

$$RCOO^- + Na^+ \leftrightarrow RCOONa \quad (2.3)$$

Calcium naphthenate formation has been observed at brine pH greater than about 6 (Goldszal *et al.,* 2002; Rousseau *et al.,* 2001; Turner and Smith, 2005) whilst sodium carboxylate/ emulsion has been seen at slightly higher brine pH i.e. ~8.5 (Gallup *et al.,* 2005; Turner and Smith, 2005). The reaction and formation of these naphthenates usually occurs at the oil-water interface and they tend therefore to move along through the production system with the oil and the produced fluids (Ese and Kilpatrick, 2004). The effect of various physical parameters i.e. temperature and shear have been described by Turner and Smith, (2005). The temperature effect has been considered to be a key physical parameter influencing naphthenate formation as it speeds up the kinetics of naphthenate formation. Gallup *et al.,* (2004) have reported that temperature variation between offshore pipelines and land terminals enhanced the formation and precipitation of sodium carboxylate. However, the detailed mechanism of how temperature affects naphthenate formation is still not well understood. The crucial importance of shear in naphthenate formation has been highlighted by Turner and Smith, (2005). Shear usually plays a significant role by generating smaller water droplets that provide larger interfacial areas, which tend to lead to a more stable emulsion, and also favours more naphthenate formation. In addition, a detailed review on the effects of shear on emulsion behaviour can be found in Petex (1990) and Ajienka *et al.,* (1993). Variation of % watercut has also been observed to influence the formation of naphthenate, although the precise mechanism for this phenomenon has not been fully explained (Turner and Smith, 2005). Later in this thesis (Chapter 6), a thermodynamic model which explains the effect of watercut on the quantity of naphthenate produced will be presented. Based on the proposed naphthenate formation

mechanism of Rousseau *et al.,* (2001), several successful static experiment attempts have been made to form naphthenates under laboratory conditions (Havre, 2002; Dyer *et al.,* 2003; Mediaas *et al.,* 2005; Dyer *et al.,* 2006;). Formation of naphthenate under laboratory conditions has been recently used in prediction modelling, inhibition efficiency experiments and other sensitivity studies and work in all of these areas will be reported later in this thesis.

2.3 CRUDE OIL COMPOSITION

Crude oil is a very complex mixture of hydrocarbons of various molecular weights and other organic compounds, which occur in geologic formations under certain conditions. The crude oil also contains small amounts of sulphur, oxygen and nitrogen, as well as various metallic constituents, particularly vanadium, nickel, iron and copper (Speight, 1999). The crude oil also contains a wide range of naphthenic acids, depending on the oil and the level of biodegradation which has occurred. In this work, the concern is more with the presence of the naphthenic acids in the crude oil because of their central role in naphthenate formation. The naphthenic acid composition of the crudes varies from one to another and it has been the traditional practice to measure naphthenic acid concentration using the Total Acid Number measurement (TAN) which gives the total acid composition of the crude oil. TAN is measured in units of mg KOH/g of crude oil, as discussed in more detail later in this Chapter. However, Meredith *et al.,* (2000) noted that TAN measurement does not give an accurate naphthenic acid composition of any crude oil, since substances like dissolved hydrogen sulphide (H_2S), dissolved carbon dioxide (CO_2), phenols and some inorganic acids, may affect the final measured TAN value. They also noticed that there was no distinct correlation between total acid number and naphthenic acid concentration in most crude oils which were analysed. Nevertheless, they found some small degree of correlation between TAN and naphthenic acid concentration. This may be due to the fact that the crude oils analysed are from the same geological formation and they are therefore expected to be of similar properties. Sorbie *et al.,* (2005) have presented data from a variety of sources about the range of naphthenate forming crudes and there is no definite correlation between TAN and naphthenic acid concentration from the crudes. Some naphthenate forming crudes

were observed to have very high TAN and low naphthenic acid content (8.2 mgKOH/g and 20 ppm) whilst others show the opposite; i.e., low TAN and high acid content (0.5 mgKOH/g and 5000 ppm) (Smith, 2004).

Origin and structure of naphthenic acid in crude oil

It has been documented in the literature for over a century that quite complicated mixtures of naphthenic acids are present in different types of hydrocarbon sources. Naphthenic acids can be represented by the general molecular formula, $C_n H_{2n+z} O_2$, where, n is the carbon number and Z represents a homologous series. Z value can be from zero down to a negative integer and represents the hydrogen deficiency which usually occurs when a ring is included in the naphthenic acid structure. The Z value is zero in the case of fatty acids, or negative, depending on the number of aromatic rings. Although the term naphthenic acid was originally used in the petroleum industry to define acids with cycloaliphatic derivatives, all organic acids, including acyclic and aromatics present in the crude oil are frequently referred as "naphthenic acid" (Brient, 1995; Meredith *et al.,* 2000; Qian *et al.,* 2001). Almost all crude oils contain some amount of naphthenic acids. Heavy crudes from geologically young formations or biodegraded crudes (from either formation or reservoir) have high acid content whilst paraffinic crudes are associated with low acid content (Seifert *et al.,* 1969). Complex naphthenic acid structures with more than one carboxylic acid functional groups have been found (Tomczyk *et al.,* 2001; Baugh *et al.,* 2004) as well as those containing heterotoms, which were seen in certain crude oils (Robbins *et al.,* 1998; Tomczyk *et al.,* 1998 and 2001; Qian *et al.,* 2001; Rudzinski *et al.,* 2002). Some examples of naphthenic acid structures for different values of Z are presented below, in Figure 2.1.

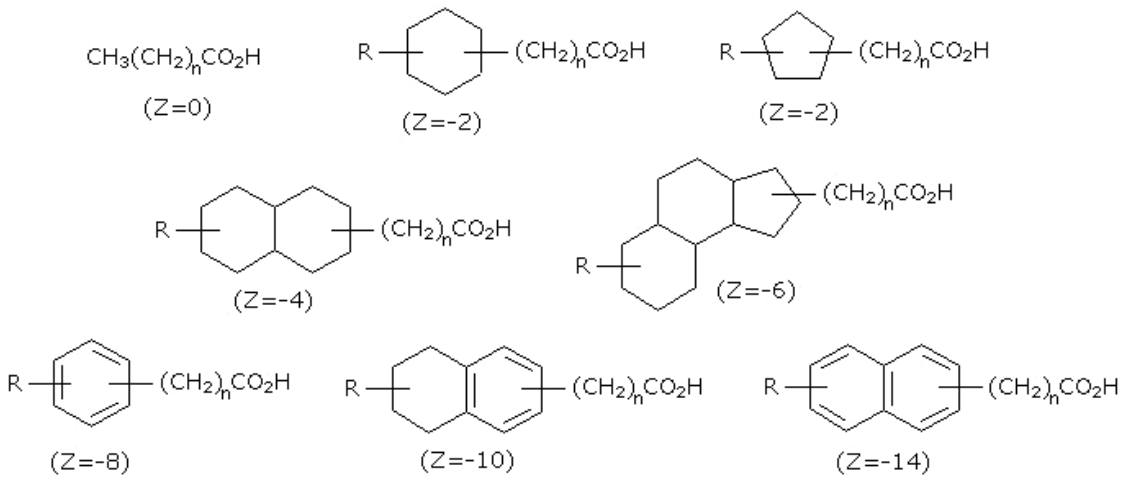

Figure 2.1: Naphthenic acid structures where Z describes the hydrogen deficiency, R is an alkyl (Brandal, 2005).

The acid content of crude oil varies from non detectable levels to as high as 4%, depending on the type of oil (Dzidic *et al.,* 1988; Jones *et al.,* 2001). These carboxylic or naphthenic acids, as they are more commonly known in the petroleum industry, are considered very important because of the corrosion problems they usually caused at the refinery during crude oil refining (Aceredo *et al.,* 1999). They also exhibit surfactant properties (Babaian-Kibala *et al.,* 1998) and are used for commercial purposes such as preservatives and in the paint industry.

Crude oils with higher naphthenic acid content have been reported in the North Sea (UK and Norway Sectors), Venezuela, Mexico, California, West Africa and the South East Asia (Robbins *et al.,* 1998; Skippins *et al.,* 2000; Rousseau et al., 2001; Sartori *et al.,* 2001; Laredo et al., 2004; Mediaas et al., 2005; Turner and Smith, 2005). Naphthenic acid concentration and distribution are thought to be dependent on the level of biodegradation of the crude oil (Meredith *et al.,* 2000; Jones *et al.,* 2001). Further work by Meredith *et al.,* (2000) using 30 crudes showed that undegraded oils were mainly dominated by saturated acids whilst the degraded oils contained higher molecular weight acids. Total acid number measurement of crude oils is usually carried out using either colourimetric or potentiometric titrations (D974 and ASTM D664) which give an indication of the total acid present in the crude oil. Crude oil TAN has been found to vary in different crudes

depending on many parameters responsible for the crude oil acidity. Sartori *et al.,* (2001) reported that crude oils will typically have TAN values in the range 0.2 to 10 mg KOH/g. Furthermore, crudes with TAN value greater than 0.5 mgKOH/g of oil are considered as having a high total acid number (Robbins *et al.,* 1998). TAN measurement does not specify the various types of acid structure present in the crude oil, as shown in the wok of Qian *et al.,* (2001); they showed for a South American crude that there are more than 30 groups of naphthenic acids with various ranges of carbon number between 15 to 55 and Z distribution between -2 to -22. .

2.4 NAPHTHENIC ACID CHARACTERISATION

The term naphthenates in this thesis refers to both calcium naphthenate and sodium carboxylate/emulsion substances. Although, each different class of substance is known to have its own peculiar characteristics, e.g. regarding the formation mechanism and composition, this thesis is focussed mainly on calcium naphthenate with a smaller amount of work being presented on sodium carboxylate/ emulsions. Awareness of sodium carboxylate /emulsion problems has been around since the late 1960s, whilst the calcium naphthenate problem only came to light in the mid 1990s. This does not mean that calcium naphthenate problems did not exist before this time, but rather if they did occur they were not recognised as such or were described chemically in other ways. Formation of calcium naphthenates in the field may typically be quite small, e.g. around 10 mg solid/litre of crude oil, as reported. This quantity may appear insignificant, but it should be viewed as a cumulative effect arising from the very large throughput volume of oil and brines during production (Vindstad *et al.,* 2003; Pearson, 2004).

As exploration and exploitation of heavier crudes continues, then the tendency for naphthenate formation will increase. This will increase the need within the oil industry for naphthenate characterisation in order to understand the composition of the main components in the formed naphthenates. Techniques for naphthenic acid extraction have been known for some time for other purposes prior to the understanding that these species can cause flow assurance problems due to the formation of metal naphthenates. Qualitative naphthenic acid characterisation has been carried out using several analytical techniques

which includes various methods such as mass spectrometry (MS) (Koike *et al.,* 1992; St. John *et al.,* 1998; Tomczyk *et al.,* 2001; Holowenko *et al.,* 2002) and gas chromatography mass spectrometry (GC-MS) (Gallup *et al.,* 2002; Rudzinski *et al.,* 2002; Gallup, 2004). These methods have been used in combination with Fourier transform ion cyclotron resonance mass spectrometry (FT-IR) and /or nuclear magnetic resonance (NMR) spectrometry (Marshall *et al.,* 1998). Naphthenic acid characterisation from various samples showed very different acid compositions can occur depending on the sample (naphthenate) type and the specific field involved. Several of these researchers have documented their work on the naphthenic acid compositions using various extraction methods and analytical techniques, as well as looking at sensitivity parameters which may also have some influence on the detection of naphthenic acid composition from the sample.

Naphthenic acid characterisation in calcium naphthenate deposits, sodium carboxylate/emulsion and crude oil.

Methods for naphthenic acid characterisation from calcium naphthenate deposits have been available for some time, and many workers have used different extraction and characterisation techniques in order to determine the naphthenic acid distributions in various samples across the world. Direct characterisation of the naphthenic acid extract from the field deposit is usually carried out using soft ionisation mass spectrometry, which involves little or no fragmentation of the naphthenic acid species. Furthermore, high temperature gas chromatography (HTGC) and liquid chromatography mass spectrometry (LCMS) techniques are also sometimes used for naphthenic acid characterisation. The latter techniques are based on the derivatised methyl esters formed from the naphthenic acids, using derivatisation agents. The most common derivatisation agent reported so far is BF3/methanol mixture (Jones *et al.,* 2001; Tomczyk *et al.,* 2001; Baugh *et al.,* 2004; Hao *et al.,* 2005;; Saab *et al.,* 2005). Nevertheless, in some instance poor derivatisation recoveries have been reported in acid extracts containing aromatic rings (Jones *et al.,* 2001). Some of the techniques for derivatisation yield better results than others.

Hsu *et al.,* (2000) used mass spectrometry to characterise naphthenic acids in crude oil samples, using various techniques including chemical ionisation, fast ion bombardment, atmospheric pressure chemical ionisation (APCI) and electrospray ionisation in both positive and negative ion modes. Their work showed that negative-ion mode APCI using acetonitrile as a mobile phase yields a good spectrum compared to the other techniques studied in his work. Hsu *et al., (2000)* reported a naphthenic acid distribution in the range of m/z 300 to ~ m/z 750. Other researchers (Goldszal *et al.,* 2002; Headley *et al.,* 2002; Rogers *et al.,* 2002) use electrospray mass spectrometry (ESMS) for naphthenic acid characterisation, which is often used and results will be reported in this thesis using this technique. The ESMS technique revealed good responses in terms of the naphthenic acid determination, since the naphthenic acid extracts generated for the mass spectrometry are not fragmented. The technique could detect naphthenic acid at very low concentrations and was shown to detect naphthenic acid concentration in hydrocarbons at as low as 0.1mg/l (Headley *et al.,* 2002). Barrow, (2003) used Fourier-transform ion cyclotron mass spectrometry (FT-ICR MS) to quantify naphthenic acid distribution in naphthenate forming crudes. The results revealed a distribution of lower molecular weight naphthenic acids in the range of m/z 300 to m/z 600. Further analysis of calcium naphthenate samples and the corresponding source crude oil was carried out by Baugh *et al.,* (2004) using various techniques such as elemental analysis and nuclear magnetic resonance (NMR). The total acid number (TAN) measurement from these studies showed that the molecular weight values for both crude and naphthenate are between 430 g/mol to 330 g/mol. These results are in agreement with those of Vindstad *et al.,* (2003) who reported that the naphthenic acid molecular weight of naphthenate sample from North Sea was 330 g/mol. However, analysis of the naphthenate sample for the determination of naphthenic acid content using vapor pressure osmometry (VPO), high temperature gas chromatography (HTGC) and liquid chromatography mass spectrometry (LCMS) gave different results. The results using these techniques showed two different classifications of naphthenic acids: a lower molecular weight naphthenic acid with values around m/z 350 and a higher molecular weight naphthenic acid in the range of m/z 1230 (Baugh *et al.,* 2004). However, the limitation is that the MS settings do not allow for direct comparison of the different naphthenic acid concentration intensities or the interaction between the two classes of acids

identified (lower and higher molecular weight naphthenic acids) during the mechanism for the formation of naphthenates. It was claimed by Baugh *et al.,* (2004) that four carboxylic acid functional groups would be present in the acid structure and this was further confirmed by vapour pressure osmometry (VPO) and subsequent mass spectrometry (MS) results. Both of these analytical techniques indicated the presence of naphthenic acids with the molecular weight at around m/z 1230 from the naphthenate deposit. Moreover, it was also claimed that the group of naphthenic acids with the molecular weight at around m/z 1230 were the ***dominant*** naphthenic acid group in the naphthenate deposit. However, later work by other researchers (including work in this thesis) showed that is not always the case, as some naphthenate samples may have predominantly lower molecular naphthenic acids in addition to the higher molecular weight naphthenic acids (Shepherd *et al.,* 2005). An empirical formula for the higher molecular weight naphthenic acid (m/z 1230) was proposed by Baugh *et al.,* (2004) to be approximately $C_{80\text{-}81}H_{142\text{-}180}O_8$ and the naphthenic acid involved was named "ARN". Further analysis of the naphthenate sample using FT-ICR MS, 2D-nuclear magnetic resonance (NMR) and pyrolysis mass spectrometry by Baugh *et al.,* (2005a) concluded that most of the acid species in the naphthenate sample are ARN acids. The characterisation of the naphthenic acids was carried out on the derivatized acid extract from the naphthenate deposit. An illustration of a possible ARN structure, based on the 2D NMR of the naphthenic acid derivatives obtained from a field naphthenate sample from Baugh *et al.,* (2005b) is shown in Figure 2.2 below.

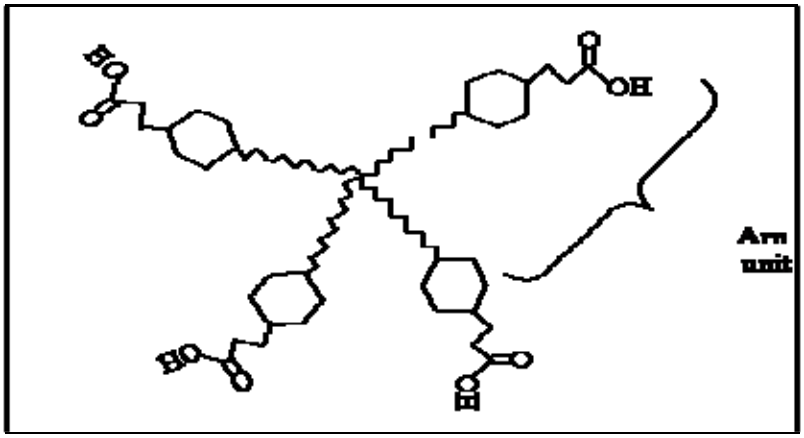

Figure 2.2: Proposed most likely structure of ARN acid, based on results by Baugh et al., 2005b. The ARN unit represents the hydrocarbon skeleton and the single carboxylic acid attached to a side chain, in turn attached to a cycloaliphatic ring.

Further extensive characterisation of the ARN naphthenic acid present in the naphthenate sample from a North Sea field was carried by Lutnaes *et al.,* (2006) and they were able to establish a more precise structure of the ARN acid species. These authors suggested that the predominant component within the ARN acid family would be composed of six rings and also speculated that the acid is likely to be of biological archaeal bacteria origin. However, few kinetic routes for ARN formation were suggested by the authors in their paper. The proposed ARN acid structure suggested by Lutnaes *et al.,* (2006) is presented in Figure 2.3 below:

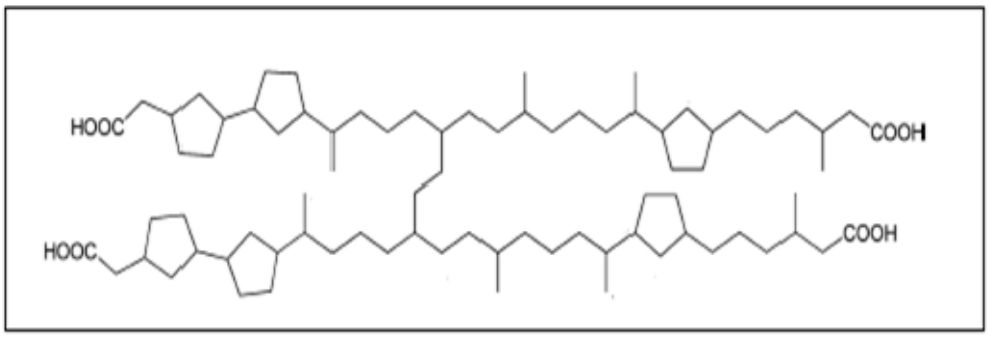

Figure 2.3: Proposed predominant structure of ARN acid (Lutnaes et al., 2006).

Sensitivity studies regarding the favourable ionisation of particular acid species during the mass spectrometry (MS) part of the analysis, as well as the use of different ionisation solvent and ion spray voltage settings were reported by Shepherd, (2008). The results from this study revealed that using different ionisation solvents favoured certain naphthenic acid determinations; that is, a different apparent distribution of naphthenic acids was observed depending of the various solvents used. The results showed that atmospheric pressure chemical ionisation mass spectrometry (APCI-MS) could detect the presence of a very low amount of higher molecular weight naphthenic acid in a sample. Most of the work presented by these authors is based on samples from particular fields and each also uses different techniques of either extraction or analysis and some cases in both. No extensive study of various naphthenate samples across the world, using the same extraction and analytical characterisation has been reported in the literature. These issues will be addressed in this thesis in order to enable us to understand the naphthenic composition of

samples from different part of the world and ultimately to give an insight into the possible mechanisms that are involved.

Sodium carboxylate/emulsion characterisation has also been in place for some time and various analytical methods (such as energy dispersive X-ray, EDAX, and X-ray diffraction, XRD) have indicated that sodium carboxylate sludge consists of approximately 30% water, 50% oil, and 20% of C_{28} to C_{30} carboxylate salts, which are mostly in sodium form (Gallup and Star, 2004). A detailed analysis of sodium carboxylate emulsions from an South East Asian field, using analytical techniques such as gas chromatography mass spectroscopy (GCMS) and nuclear magnetic resonance (NMR), was presented in Gallup *et al.,* (2002 and 2005). The results showed the presence of predominantly linear acid (acyclic) species in these field samples. The acids identified are mostly fatty acids containing carbon numbers between 28 to 30, and molecular weights in the range of 396 and 452 g/mol (Gallup *et al.,* 2002). This type of carboxylate emulsion is associated with crude oil that has low total acid number (TAN), as reported by Turner and Smith (2005). The presence of lower molecular weight naphthenic acids, mostly acyclic, has been reported from the analysis of sodium carboxylate emulsion and corresponding crudes, using electrospray mass spectroscopy (ESMS). In addition, small quantities of naphthenic acids with m/z 620 and m/z 1240 were also reported (Gallup *et al.,* 2005). The stability of these sodium carboxylate viscous emulsions was considered to be due to the incorporation of materials such as paraffin, barite and clay materials. It was also suggested that as low as 5% wt of minerals in the production fluids is sufficient to generate a viscous sludge from the carboxylate emulsion (Gallup *et al.,* 2002). Sodium carboxylate sludge resulting from an emulsion pad was analysed by Gallup *et al.,* (2005) and the authors suggested an empirical formula for the sodium carboxylate soap to be $C_{38}H_{78}O_4Na$ which is presented structurally in Figure 2.4 below.

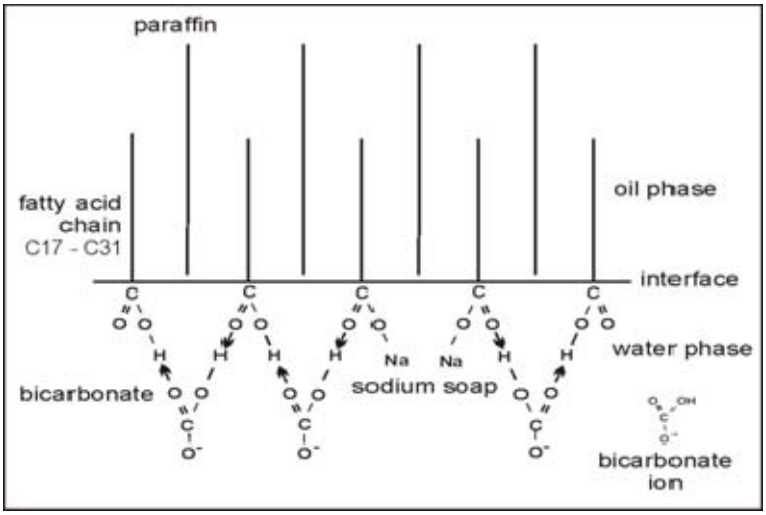

Figure 2.4: Sodium carboxylate soap emulsion structure proposed by Gallup *et al.,* 2004 and Gallup *et al.,* 2005.

In further studies of sodium emulsion formed from production fluids in the South East Asian field by Gallup *et al.* (2007), the sample was characterised using various analytical techniques including ultraviolet (UV), Fourier transform infrared (FT-IR), electrospray mass spectroscopy (ESMS) and ion-trap mass spectroscopy (ITMS) and Fourier transform ion cyclotron resonance-mass spectroscopy (FTICR MS). The results reported by authors from the ESMS revealed the presence of predominantly *n*-alkanoic acids, i.e. C_8 to C_{40} acyclic naphthenic acids in most cases; minor traces of bicyclic and alkylbenzoic acids were also detected. Detailed characterisation of acyclic naphthenic acid has shown preferential dominance of even carbon number over odd carbon number acid species. Surprisingly, the authors reported some traces of a cluster at around m/z 1242, which correspond to the ARN acid species. Recently, an analysis of another sodium soap emulsion from an Asian production field, using atmospheric pressure chemical ionisation mass spectrometry (APCI-MS) and high temperature gas chromatography (HTGC), showed a different type of acid classification from the sodium emulsion samples analysed. The APCI-MS results revealed the presence of predominantly alkylbenzoic naphthenic acids with minor traces of C_{58} acyclic naphthenic acid, as opposed to the usual *n*-alkanoic acid, which have been identified as the common acids found in sodium carboxylate emulsions. The samples analysed also did not show the preferred distribution of even carbon numbers acids over odd (Gallup *et al.,* 2010). The literature review presented here regarding

naphthenic acid characterisation led to the first objective of the project i.e. "characterisation of the various calcium naphthenate, sodium carboxylate/emulsions and crude oil samples from various part of the world". This is aimed at understanding more about the different acid compositions present in the various samples.

2.5 CRUDE OIL GEOCHMEISTRY

The study of the geochemistry of crude oils has been the central role of petroleum geochemistry, which is mainly used in oil prospect evaluation. The study of petroleum geochemistry entails issues regarding the origin of the source rocks which ultimately lead to petroleum formation/generation and maturation, migration from the source rock to the reservoir and reservoir dynamics, and biodegradation. Crude oil geochemistry is traditionally focused on the study of particular hydrocarbon fractions in the crude oil. Traditionally, this subject has placed very little emphasis on the naphthenic acid composition of the crude oil. Even where naphthenic acid compositions of crude oils were studied, it was viewed from the biodegradation point of view rather than attempting to relate this to flow assurance matters. The occurrence of carboxylic acids in crude oils has been documented since the early part of the 20th century and this has been reviewed recently (Seifert *et al.,* 1969; Gallup *et al.,* 2007). Numerous acid extraction techniques from crude oils have steadily improved over the years, and more efficient new methods will undoubtedly lead to the identification of additional compounds for classification (Saab *et al.,* 2005). Naphthenic acids occur naturally as part of the components of crude oils (Seifert *et al.,* 1969; Fan, 1991; Tomczyk *et al.,* 2001). They form an integral part of the acids that are usually present in the oil at different concentrations, depending on the nature of the location from which the oil is sourced. Generally, carboxylic acids occur in crude oil as a result of insufficient maturation of the source rock that generates the crude oil, or the oil has undergone some sort of biodegradation by bacteria (Tissot and Walte, 1978). Furthermore, carboxylic acids have been reported in deposits of naturally biodegraded oil (Nascimento *et al.,* 1999; Meredith *et al.,* 2000) as well as in crude oil that has been biodegraded in the laboratory (Roques *et al.,* 1994; Watson *et al.,* 2002). However, although correlation of naphthenic acids in crude oils with the basic geochemistry

parameters has been attempted in the past, it has not been approached from the flow assurance perspective (Fan, 1991; Nascimento *et al.,* 1999; Kim *et al.,* 2005). It is only recently that this correlation has been attempted for the purpose of sodium carboxylate emulsion prediction (Gallup *et al.,* 2007). Apart from some of the most fundamental measurements for geochemical analysis, which include TOC, vitrinite reflectance and carbon isotope studies, there is also more advanced biomarker identification (Peters and Moldowan, 1993). Geochemically, direct analysis of the crude oil sample can be carried out for some biomarkers. However, due to the presence of trace concentrations of some species like the heteroatom species, separation of a particular fraction prior to any analytical study is generally desirable. The crude oil samples are usually separated into **aliphatic**, **aromatic** and **polar fractions**, using either liquid column elution chromatography (LC) or thin layer chromatography separation (TLC). In some cases, asphaltenes are first precipitated using *n*-heptane and column chromatography is then applied on the maltenes (Weiss *et al.,* 2000; Fan and Buckley, 2002). Geochemical characterisation using gas chromatography (GC), gas chromatography mass spectroscopy (GCMS) and gas chromatography mass spectroscopy mass spectroscopy (GCMSMS) are well established techniques in geochemistry study of the various hydrocarbon fractions (aliphatic and aromatics). These techniques find a wide applicability because of their response to some sensitive parameters, such as thermal maturation, concentration level and biodegradation (Peters and Moldowan, 1993).

The application of biomarkers (biological marker indicators) in the petroleum has been well established in this area to correlate between an oil sample and the original petroleum source rock in terms of obtaining relevant information with regard to organic matter in the source rocks, environmental conditions during its deposition and burial, thermal maturity experienced by the rock or oil, degree of biodegradation, certain aspects of lithology, and age (Baugh, 1993; Peters and Moldowan, 1993). These biomarkers are defined as compounds derived from organisms that are preserved in sediments, the geological record and ultimately in oils. Linking the biomarker with the specific family of organism gives an opportunity to identify the family's fossil record. Indeed, even when the original fossils of an organism are *not* found, its chemical markers are useful to trace the organisms history

and the role during certain period of time. This has been a powerful tool in petroleum geochemistry. Biomarker correlation is carried out by studying the various crude oil fractions (aliphatic and aromatic) using GC, GCMS and GCMSMS techniques, in addition to other non-biomarker geochemical parameters, to provide the most reliable information required. The distribution of the normal *n*-alkanes is best seen from the GC spectrum, whilst the most wide used biomarker parameters i.e. steranes and terpanes (hopanes) are obtained from the GCMS spectrum. An example of the identification of these compounds (*n*-alkanes, hopanes and steranes) in a GC chromatogram of a whole crude oil is shown in Figure 2.5 whilst a typical chromatogram of hopane and steranes is presented in Figures 2.6 and 2.7 respectively.

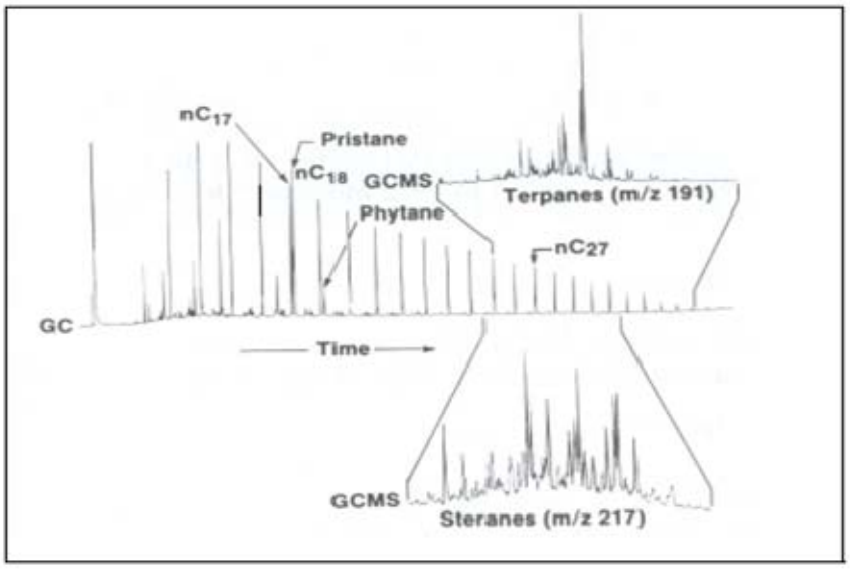

Figure 2.5: Identification of hydrocarbon biomarkers during GC analysis (Peters and Moldowan, 1993).

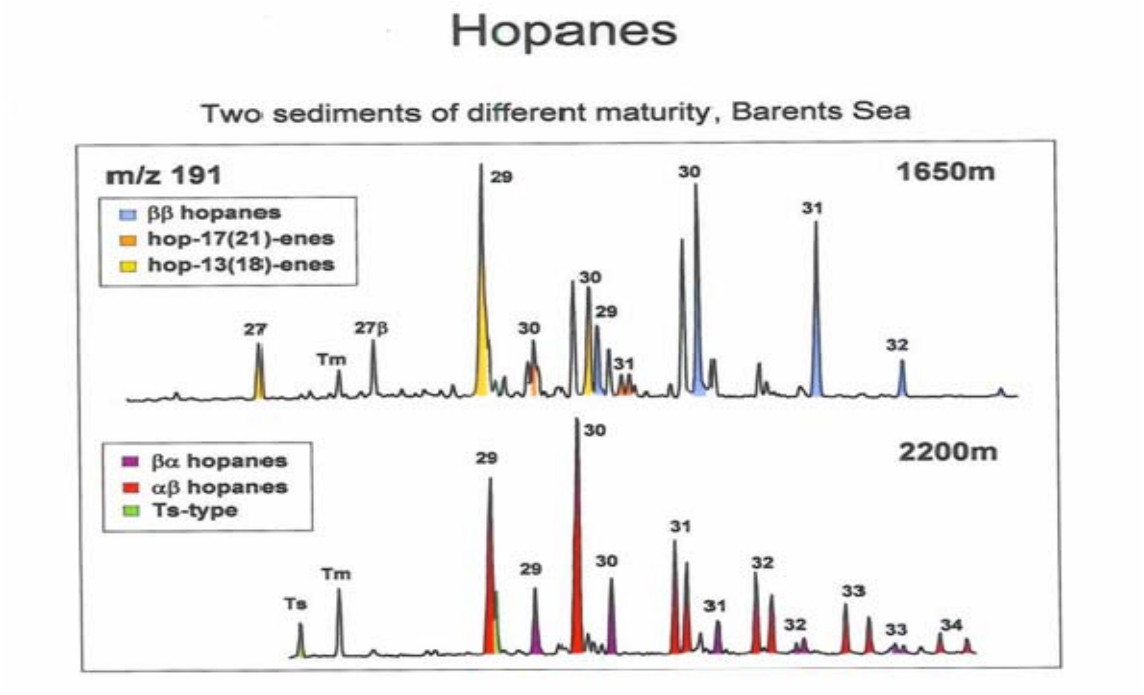

Figure 2.6: Chromatogram of two sediments of different maturity, Barents Sea from Paul Farrimond biomarker identification guide.

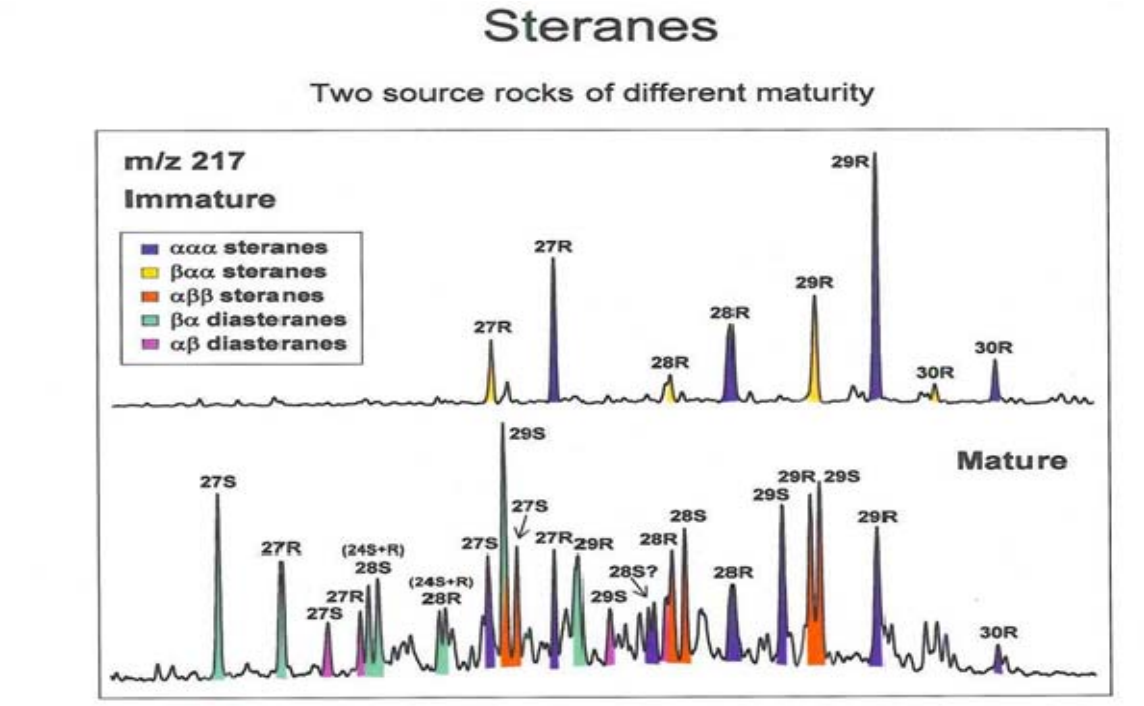

Figure 2.7: Chromatogram of two source rocks of different maturity from Paul Farrimond biomarker identification guide.

Several biomarker parameters were calculated using some of the biomarker ratios from the *n*-alkanes, hopanes and steranes for biodegradation studies (Barnard and Bastow, 1991; Kim *et al.,* 2005; Meredith *et al.,* 2000; Nascimento *et al.,* 1999; Peters and Moldowan, 1993;), correlation between biodegradation and naphthenic acid species (Kim *et al.,* 2005; Klein *et al.,* 2006), and maturity studies and comparison between oil maturities (Meredith *et al.,* 2000; Peters and Moldowan, 1993). Before the work in this thesis, virtually no correlation has been looked at in the literature regarding flow assurance concerns (such as naphthenate deposition) by studying the crude oil geochemistry. This missing activity in the literature led to the second objective of this thesis: to study the biomarkers of various calcium naphthenate and sodium carboxylate/emulsion forming crudes and to try to relate them to the likelihood of formation of these substances. If there is actually some correlation, then this could be used as an alternative predictive tool in flow assurance studies; that is, if certain biomarker species are shown to correlate well with different types of naphthenate problem (calcium naphthenate or sodium carboxylate emulsion formation), then this would provide with either a predictive tool – or at least a "warning" method –for anticipating such naphthenate problems in future.

2.6 NAPHTHENATE PRECIPTATION PREDICTION MODELING

Very little has been published on naphthenate precipitation prediction modelling and, at present, to my knowledge, there is no commercially available naphthenate predictive model. However, attempts have been made to model the interaction of carboxylic acids with metal cations which were reported in the early part of the 20th century. Further modelling work was carried out by Stenius and Zilliacus (1971), using fatty acids in aqueous brine to investigate the aggregation of soaps, whilst Somasundaran *et al.,* (1984) modelled changes in interfacial tension to obtain a thermodynamic understanding of the formation of pre-micellar soap aggregate. In later years, Havre (2002) carried out some interesting modelling of naphthenic acids in solvent-brine systems. However, basic thermodynamics could not explain the differences in predicted and calculated values of bulk properties from his results. The only explanation the author suggested was that this was possibly due to micelle formation. Recently, a comprehensive detailed naphthenate

thermodynamic model has been put forward by Sorbie *at al.,* (2005). This model attempts to fully describe the basic mechanism for naphthenate formation, considering all the chemical and physical changes that tend to influence the formation of naphthenates during the production process. The authors pointed out the key parameters that are required for modelling possible naphthenate formation i.e. the naphthenic acid dissociation constants (K_a), the water-oil partitioning coefficient (K_{ow}) and solubility product (K_{Ca_A2}). The effect of pH was also fully considered in the naphthenate thermodynamic modelling. Brandal (2005), reported in his work about the equilibria involved when naphthenic acids are introduced into an oil-water system. He further summarises the fundamental processes taking place in the bulk solution as oil-water partitioning, self-association in oil, self-association in water and interaction with other fractions. In this work Sorbie's thermodynamic naphthenate predictive model has been studied in much more detail in that: (a) a wide range of sensitivity calculations were carried out using this model; (b) the predictions from this model have been used to design 3 types of experiments where definite predictions of the outcome of the various experiments was made, and (c) experiments which directly test the predictions from the thermodynamic naphthenate prediction model were carried out.

2.7 NAPHTHENATE INHIBITION

Naphthenate inhibition is very crucial in oil production where the crude oil and the water properties are prone to either calcium naphthenate or sodium carboxylate/emulsion formation. In order to reduce or completely inhibit the extent of naphthenate formation, chemical mixtures of various compositions are traditionally injected into the well production stream. Naphthenate formation is known to occur when the aqueous pH exceeds the pKa of the naphthenic acids in the oil phase. This could be achieved by injecting short-chain organic acids which will keep the aqueous pH low and will ultimately hinder the formation of naphthenates (Goldszal *et al.,* 2002). An acid injection approach has been the common method used to control the formation of calcium naphthenate (Hurtevent and Ubbels, 2006; Smith and Turner, 2003, 2005; Vinstad *et al.,* 2003). Acetic acid is the most commonly used chemical for the inhibition of naphthenate formation worldwide (Ese and

Kilpatrick, 2004; Brocart *et al.,* 2005; Lutnaes *et al.,* 2005). The application of this acid to lower the water pH to ≤ 6 has been reported to produce the minimum level of naphthenate deposits (Rousseau *et al.,* 2001; Ese and Kilpatrick, 2004; Shepherd *et al.,* 2005). It has been reported that maintaining the pH below 6 achieves no further improvement on the naphthenate inhibition, but rather can result in a stabilised emulsion, which may eventually worsen the problem (Melvin *et al.,* 2008). The typical method of application varies from continual injection in severe cases to batch injection in milder situations. Acid demulsifiers, consisting of acetic acid in an aromatic solvent mixture and non-acid demulsifiers consisting of ethoxylates have also shown to significantly reduce deposition (Gallup, 2004). It was also reported that the use of phosphoric acids and phosphoric based products, rather than acetic acid, are very effective on sodium carboxylate emulsions (Gallup *et al.,* 2005), although the authors draw some attention to certain limitations regarding phosphoric acid usage. Other types of acids and their products, such as sulphonic and hydrochloric acids, have been used in the past to inhibit naphthenate formation (Vinstad *et al.,* 2003; Smith and Turner, 2005). The use of inhibitors rather than acid is becoming common in the petroleum industry due to the vast logistics involved in deploying large volumes of acid solutions. Recently, Gallup *et al.,* (2010) reported the use of some naphthenate inhibitors that were able to inhibit the formation of sodium soap emulsion in a South East Asian field. These inhibitors were tested on sodium soap emulsion that could not be inhibited using the available acidic demulsifier. The mechanism by which these new inhibitors work was suggested to be via complexation.

2.8 SUMMARY AND CONCLUSIONS

In this chapter, a wide literature review has been presented which describes our current understanding of the basic mechanisms of naphthenate formation. The variables believed to influence naphthenate formation have been discussed in detail. In particular, the role of the crude oil composition has a central role in naphthenate formation and the subsequent production problems which can occur. A review of the origin and structure of naphthenic acid in crude oil was also presented. The literature review was also directed at the key objectives of this thesis which are framed in the following 4 topics: (i) the characterisation

of naphthenic acid in calcium naphthenate deposits and sodium carboxylate emulsion; (ii) the role of the crude oil geochemistry; (iii) naphthenate precipitation modelling, and (iv) the chemical inhibition of naphthenate deposits. The objectives of each of these 4 topics are listed below.

The information presented in this Chapter is seen as the basis from which the objectives of the thesis were derived. The main objectives within each of the 4 topics described above are as follows:

1) Characterisation of naphthenate field samples i.e. calcium naphthenate, sodium carboxylate/emulsion and crude oils for naphthenic acid classification. The main objectives are:

- Method development for the naphthenic acid extraction from calcium naphthenate, sodium carboxylate/emulsion and crude oil field samples.
- To characterize the extracted naphthenic acid using ESMS and APCI-MS techniques.
- To carry out re-precipitation experiment using the extracted naphthenic acid and compare the results with the results from the field samples.
- Carry out elemental composition studies on the formed naphthenate as well as the field naphthenates for comparisons.

2) Geochemical studies of naphthenate forming crudes i.e. calcium naphthenate and sodium carboxylate/emulsion. The main objectives are:

- To carry out crude oil separation into various components of aliphatic, aromatic and polar fractions and also measure the TAN value of the crude oils.
- To analyse the aliphatic and aromatic fractions using GC and GCMS for biomarker parameters studies.
- To use the biomarker and non-biomarkers parameters for possible correlations with respect to either calcium naphthenate or sodium carboxylate/emulsion formation.

3) Thermodynamic precipitation model prediction; and the objectives are:

- To carry out thermodynamic pH change experiments and compare the results with the simple model prediction.
- To carry out naphthenate precipitation experiments and compare the results with the model prediction.
- Conduct sensitivity studies and their effect on the naphthenate formation such as presence of bicarbonate, variable calcium concentration, brine pH, temperature effect, shear effect and watercut ratio.

4) Naphthenate inhibition studies for calcium naphthenate and sodium carboxylate; and the objectives are:

- To develop a laboratory method for testing various calcium naphthenate inhibitors on both calcium naphthenate deposits and sodium carboxylate emulsions.
- To carry out sensitivity studies such as the effect of temperature of the efficiency of these inhibitors.

CHAPTER 3: EXPERIMENTAL METHODS

3.1 INTRODUCTION

This chapter gives the detailed description of all the experimental procedures used in the course of this PhD research, including all the methods developed for; (i) the naphthenic acid extraction procedures (for calcium naphthenate, sodium carboxylate soaps and crude oil) samples which will be described and discussed in Chapter 4, (ii) the methodology used in the crude oil chromatographic separation and TAN analysis for the geochemistry studies described in Chapter 5, (iii) the techniques used in the naphthenate re-precipitation experiments for the thermodynamic pH change and naphthenate precipitation modelling work in Chapter 6, and (iv) the static naphthenate inhibition efficiency experiments described in Chapter 7. The brine pH measurement procedure is also described. The equipment/apparatus specifications and settings used for the analysis of naphthenic acid extracts, crude oil fractions, precipitates and oil samples are fully explained in this chapter.

3.2 DEVELOPMENT OF NAPHTHENIC ACID EXTRACTION PROCEDURES AND ANALYSIS OF EXTRACTS

One of the key objectives of this research, as outlined in Chapter 1, is to understand the naphthenic acid composition of the various naphthenate field samples (calcium naphthenate, sodium carboxylate soaps and their corresponding crude oil samples). For example, some researchers have reported that certain calcium naphthenate field deposits are composed principally of higher molecular weight naphthenic acids. In contrast, work carried out in this research showed these calcium naphthenate deposits were made up of a combination of both lower and higher molecular weight naphthenic acids. Because of this controversy, the present research aimed to develop a rigorous naphthenic acid extraction technique which digested all of the deposit. This was then used in an extensive study of various field samples from different parts of the world. This research has developed a clearer understanding of the effect of using different spectroscopic methods of analysis to study the distribution of the naphthenic acid composition in the extracts viz. the

electrospray mass spectrometry (ESMS) and atmospheric pressure chemical ionisation mass spectrometry (APCI MS) techniques.

A number of field calcium naphthenate deposits were used from different geographical regions for naphthenic acid extraction, as follows: North Sea, Norway, South East Asia, and West Africa. Sodium naphthenate/carboxylate samples from the North Sea, Asia and the Middle East were also studied. Corresponding crude oil samples from some of the fields were also analysed. Different extraction techniques were studied and the most efficient one of these was employed as a reference method which was used throughout the course of this research. The naphthenic acid extracts were analysed using electrospray mass spectrometry (ESMS) and atmospheric pressure chemical ionisation mass spectrometry (APCI-MS) to determine their naphthenic acid composition and distribution.

3.2.1 Methods of extraction of Naphthenic acids from calcium naphthenate deposits

All the field naphthenate samples used in the naphthenic acid extraction procedures in this work were surface facility samples from various fields around the world. These field naphthenate samples were treated as received. Two conventional techniques for the naphthenic acid extraction from the field deposits were used (Methods 1 and 2) along with a modified technique (Method 3) which is described in detail below. The modified extraction technique (Method 3) used in this study was developed based on the fact that the higher molecular weight naphthenic acid components in the deposit (referred to as ARN (Baugh *et al.,* 2004)) have low solubility in toluene solvent i.e. ARN solubility in toluene is low — thought to be approximately 0.5 to 0.6 wt% at room temperature. This implies that the ratio of cleaned naphthenate deposit to toluene solvent should be 0.5: 100 on a weight scale; this would be 0.5g ARN in 116ml for effective ARN extraction to be achieved. The extraction stirring time in the modified method is significantly increased to approximately 25 hours to ensure complete dissolution of the naphthenate in the toluene solvent, compared with around 2 to 3 hours in Methods 1 and 2. This Method 3 technique always led to the complete digestion of all of the naphthenate deposits tested (apart from some sand, when it is present).

Treatment of the field naphthenate deposit and acid extraction (Method 1)

The calcium naphthenate deposit was initially ground with mortar and pestle. About **300g** was washed with 500ml of acetone (Analar VWR) solution at room temperature under mechanical agitation for one hour. The sample was filtered using Schleicher and Schuell 597 HY hydrophobic silicone coated filter paper, reground, and then treated with a second portion of 500ml acetone for one hour, under mechanical agitation. The process was repeated using methylene chloride (dichloromethane), toluene, isooctane (2, 2, 4-trimethyl pentane) and methylene chloride (dichloromethane) respectively, with each solvent mixture agitated for one hour under mechanical agitation, and then at each stage the solvent was removed by vacuuming.

Extraction of naphthenic acid from the treated (cleaned) sample was then carried out by adding 400ml of 3M HCl and 300ml of toluene to 100g of the cleaned naphthenate sample. The mixture was stirred magnetically and mechanically for 2 to 3 hours. The solution (fluid organic phases) was filtered using Schleicher and Schuell 597 HY hydrophobic silicone coated filter paper, under vacuum. The toluene solvent in the filtrates was removed using a rotary evaporator at a temperature between 40^{o}C and 50^{o}C. The naphthenic acid extract and sludge were analysed using ESMS (electrospray mass spectrometry) and APCI-MS (atmospheric pressure chemical ionisation mass spectrometry) techniques to determine the naphthenic acid compositions.

Treatment of the field naphthenate deposit and acid extraction (Method 2)

In Method 2, the calcium naphthenate field deposit was ground with mortar and pestle. About 50g of the ground naphthenate samples was treated with 100ml of toluene (Analar VWR) solution at room temperature under mechanical agitation for one hour. This was then filtered using Schleicher and Schuell 597 HY hydrophobic silicone coated filter paper under vacuum. Extraction of naphthenic acid from the cleaned sample was carried out using a mixture of 100ml solution of 3M HCl/ glacial acetic acid (50:50 ratio) and 200ml of toluene under magnetic and mechanical stirring for 2 to 3 hours. An additional 250ml of toluene (Analar VWR) was added to effect proper extraction and this solution was kept

under agitation for 30 minutes. Fluid organic phases were filtered using Schleicher and Schuell 597 HY hydrophobic silicone coated filter paper by vacuuming and the solvent in the filtrate was removed using a rotary evaporator at a temperature between 40^{o}C and 50^{o}C. The extract and sludge were analysed using ESMS (electrospray mass spectrometry) and APCI-MS (atmospheric pressure chemical ionisation mass spectrometry) techniques for different naphthenic acid compositions.

Treatment of the field naphthenate deposit and acid extraction (Method 3--modified)

As in Methods 1 and 2, again in Method 3, the calcium naphthenate field deposit samples were ground with mortar and pestle. 50g of the ground deposit was washed with 85ml of acetone (Analar VWR) solution at room temperature under agitation for one hour. The sample was filtered using Schleicher and Schuell 597 HY hydrophobic silicone coated filter paper, reground and then treated with a second portion of 85ml acetone for one hour under mechanical agitation. The process was repeated using 85ml of methylene chloride (dichloromethane), toluene, isooctane (2, 2, 4-trimethyl pentane) and methylene chloride (dichloromethane) respectively, with each solvent mixture agitated for one hour under mechanical agitation, and then at each stage the solvent was removed by vacuuming. The sample obtained is hereafter referred to as “cleaned naphthenate deposit”.

Extraction of naphthenic acid from the cleaned deposit was carried out by adding 100ml of 3M aqueous HCl and 350ml toluene solvent to the cleaned naphthenate sample and the mixture was stirred magnetically for 25 hours until the entire cleaned naphthenate sample was completely dissolved. The solution (fluid organic phase) was filtered using Schleicher and Schuell 597 HY hydrophobic silicone coated filter paper under vacuum and the toluene solvent in the filtrate was removed using a rotary evaporator at a temperature between 40^{o}C and 50^{o}C. The resulting solution (presumed naphthenic acid extracts) was analysed using ESMS (electrospray mass spectrometry) and APCI-MS (atmospheric pressure chemical ionisation mass spectrometry) techniques for different naphthenic acid composition.

3.2.2 Method of extraction of naphthenic acid from sodium carboxylate/emulsion

The extraction of naphthenic acid from sodium carboxylate soaps/emulsion field samples in this study was slightly different from the procedures described above for calcium naphthenate. The rigorous solvent cleaning of the sodium carboxylate soaps/emulsion samples i.e. with methylene chloride (dichloromethane), toluene, isooctane (2, 2, 4-trimethyl pentane) led to the sample dissolution before the naphthenic acid extraction stage; hence, a simplified method of naphthenic extraction was used in all the sodium carboxylate soaps/emulsion samples studied. A mild cleaning of the field sample with acetone was employed two to three times to make sure that traces of oil entrained within the field sodium carboxylate soaps/emulsion sample were removed prior to naphthenic acid extraction.

Treatment of the field sodium carboxylate/emulsion and acid extraction

50g of the sodium carboxylate/emulsion field sample was weighed and washed with 100ml of acetone (Analar VWR) solution at room temperature under slight mechanical agitation for 20 minutes. The washing process was repeated for a second time (and in a few cases for up to 3 times) until a clear acetone solution was observed. The clear acetone solution was then decanted slowly and subsequently filtered under vacuum, using Schleicher and Schuell 597 HY hydrophobic silicone coated filter paper, to make sure that the acetone solution was completely removed prior to acid extraction.

Extraction of naphthenic acid from the washed sodium carboxylate/emulsion was carried out by adding 100ml of 3M aqueous hydrochloric acid (HCl) and 350ml toluene solvent to the cleaned sample. The mixture was then stirred magnetically for 30 minutes to achieve complete dissolution and extraction of the naphthenic acid into the toluene phase. The solution (fluid organic phase) was filtered using Schleicher and Schuell 597 HY hydrophobic silicone coated filter paper under vacuum and the toluene solvent in the filtrate was removed using a rotary evaporator at a temperature between 40^{o}C and 50^{o}C. The resulting solution (presumed naphthenic acid extracts) was analysed using ESMS

(electrospray mass spectrometry) and APCI-MS (atmospheric pressure chemical ionisation mass spectrometry) techniques to determine the naphthenic acid compositions.

3.2.3 Methods of extraction of naphthenic acid from crude oil

Naphthenic acid extraction from the crude oil samples in this study was carried out using two different techniques as follows: (i) using an ion exchange resin (Acid-IER method) as described by Mediaas *et al.,* (2003); and (ii) using alcoholic potassium hydroxide (KOH). In both cases, the extracted naphthenic acid is subsequently characterized by using electrospray mass spectrometry (ESMS) and atmospheric pressure chemical ionisation mass spectrometry (APCI-MS). The naphthenic acid extraction using the ion exchange resin used QAE Sephadex A-25, a sugar based resin (poly-1, 6-glucose) with diethyl-(-2-hydroxy-propyl) aminoethyl ion exchange groups. The general reaction mechanism of the QAE Sephadex is described as follows: QAE Sephadex A-25 resin (Acid-IER) is in the form: Acid-IER-Cl

Activation of the resin:

$$\text{Acid-IER-Cl} + HCO_3^- \rightarrow \text{Acid-IER-}HCO_3 + Cl^-$$

Extraction of the acids onto the resin:

$$\text{Acid-IER-}HCO_3 + HA \rightarrow \text{Acid-IER-A} + H_2CO_3$$

Recovery of the extracted acids from the resin:

$$\text{Acid-IER-A} + HCOOH \rightarrow \text{Acid-IER-OOCH} + HA \text{ (extracted acid)}$$

The other method, using alcoholic potassium hydroxide (KOH) crude oil extraction technique, is based on the principle that the crude oil sample is reconditioned by treating with glacial acetic acid at 60^{o}C for 24 hours. This treatment should convert any calcium naphthenate that may have been formed into naphthenic acids and then the dry crude oil is extracted with potassium hydroxide in methanol, which makes the naphthenate soluble in methanol. The methanol layer is decanted after acidification with 5% hydrochloric acid. The naphthenates are converted to naphthenic acid and dissolved in toluene.

Acid-IER Extraction technique on crude oil samples (based on the methodology of Mediaas et al., 2003)

1) Activating the Acid-IER resin (QAE Sephadex A-25)

1.1. The total acid number (TAN) of the crude oil from which the naphthenic acids are to be isolated was measured, and the required amount of Acid-IER was calculated. The Acid-IER capacity is approximately 2.5 mmol acid equivalents per gram of resin.

1.2. The quantity of Acid-IER from 1.1 was transferred to a filter funnel (40-90μ pore size) and 1M Na_2CO_3/$NaHCO_3$ solution was run through slowly i.e. 75ml of the solution per gram Acid-IER.

1.3. The activated Acid-IER was washed by draining de-ionized water through it until the filtrate pH is approximately 7 and the remaining water was removed by vacuuming. Usually 75ml water per gram Acid-IER is used.

1.4. The Acid-IER was then saturated with methanol by draining it through. Methanol saturation maximized isolation yield. 25ml methanol per gram Acid-IER was usually used.

2) Extraction of acids onto the resin

The activated Acid-IER (described above) and the crude oil sample were transferred to a suitably sized beaker. This was gently stirred with a floating stirrer for about 16 hours, allowing sufficient time to extract all the acids onto the resin (Acid-IER). Extraction was carried out at room temperature and atmospheric pressure.

3) Removal of non-acidic components from the resin

3.1. The oil was drained off the Acid-IER through Whatman grade 41 filter paper (20-25μ) using vacuum filtration.

3.2. The Acid-IER was washed with batches of 5ml toluene per gram Acid-IER for 5 minutes to extract the heavy oil components and then drained using a vacuum. The washing was repeated 3 more times, until the drained toluene solution was clear.

3.3. The washing procedure was repeated using 2:1 toluene/methanol mixture to achieve complete removal of non-acidic components.

3.4. The filtrates from steps 3.1 to 3.3 were re-filtered twice using 589 blue ribbon Schleicher & Schuell filter paper (2 μm) to ensure that no Acid-IER was left.

4) Recovery of the extracted acids

4.1. The Acid-IERs from both filters (as described in 3 above) were transferred to a beaker with 1:1 toluene/methanol (50ml/g Acid-IER) and 1M formic acid (3.5ml/g Acid-IER) and stirred for 3 to 4 hours.

4.2. The liquid was drained off the Acid-IER using Whatman grade 41 filter paper (20-25 μm) under a vacuum. The Acid-IER was repeatedly washed with batches of 2:1 toluene/methanol mixture (10ml/g Acid-IER), until the drained liquid was clear. The filtrate was re-filtered with 589 blue ribbon Schleicher & Schuell filter (2 μm) and then transferred to a pre-balanced round bottom flask.

4.3. The process (4.1) was repeated using 0.5ml/g Acid-IER 1M formic acid.

4.4. Step 4.2 was repeated.

4.5. Extracts from steps 4.2 and 4.4 were mixed and the solvents evaporated, including any residual formic acid, using a rotary evaporator at (60^{o}C, 120 rpm).

Alcoholic potassium hydroxide (KOH) Extraction technique on crude oil samples

120ml of the crude oil sample and 1000ppm of glacial acetic acid (GAA) were weighed into a bottle and then shaken for 10 minutes. The resulting crude oil-glacial acetic acid mixture was then kept for 24 hours at 60^{o}C. The bottle containing the crude oil sample was then allowed to cool and the dry crude oil sample was removed for naphthenic acid extraction. 100ml of the dry crude oil sample was weighed into a separate bottle and 100ml of 1M potassium hydroxide in methanol (KOH/MeOH) was added to the dry crude oil sample and the bottle was shaken for 10 minutes at 200 rpm using an automatic shaker. An emulsion layer was formed at the bottom of the bottle, whilst a solution layer of KOH/MeOH was observed at the top of the bottle, after it was allowed to settle for about 2 minutes. The KOH/MeOH upper layer was removed using a syringe and allowed to stand for 24 hours. 75ml of this KOH/MeOH solution was then placed into a new bottle and protonated by adding 30g of toluene solution (~35ml). The whole solution was neutralized to pH 2 using 5% hydrochloric acid (HCl); this was checked with litmus paper and was thoroughly mixed for 10 minutes and allowed to separate (Methanol mixes with the salt water and drops to the bottom, while the toluene solvent remains on the top). About 20 ml of the toluene phase (top layer) was removed using a syringe and the toluene solvent was then removed using a rotary evaporator at 60^{o}C. The extract was now analysed using

electospray mass spectrometry (ESMS) and atmospheric pressure chemical ionisation mass spectrometry (APCI-MS) to determine the naphthenic acid composition analysis.

3.2.4 Naphthenic acid extraction from laboratory re-precipitated calcium naphthenate precipitate

The main objective for developing the extraction procedure from the laboratory precipitated calcium naphthenate is to test whether there is any similarity between the naphthenic acid composition of the field deposit analysed and the later naphthenic acid extracted from the re-precipitation experiment. Naphthenic acid extract from the modified method (Method 3) described in section 3.2.1 was used in the calcium naphthenate re-precipitation experiment and the laboratory work was carried out at room temperature. The synthetic brine (water phase) was composed of 25000 ppm Na^{+} (as NaCl) and 20000 ppm Ca^{++} (as $CaCl_2.6H_2O$) ,whilst the oil phase consist of 10000 ppm naphthenic acid extract dissolved in toluene. The brine is degassed and pH adjusted to 9 and 9.5 prior to the re-precipitation experiment as follows:

A standard bottle test was used in this study, with 50ml of extracted naphthenic acid in toluene added to 50ml of synthetic brine, which has been pH adjusted (pH: 9.0 and 9.5).

(1) Extracted naphthenic acid from Method 3 extract was dissolved in toluene— 1.00g/100ml of extract in toluene (equivalent to 10000 ppm). The solution was allowed to stand for 24 hrs, for complete dissolution.

(2) Synthetic brine (composition: 25000 ppm Na^{+} and 20000 ppm Ca^{++}) was prepared by dissolving 63.55g NaCl and 109.32g of $CaCl_2.6H_2O$ in a litre of distilled water and allowed to stand for 24hrs for complete dissolution.

(3) The brine solution was filtered using a vacuum pump (Filter paper size: 0.45μ), and then degassed overnight prior to pH adjustment.

(4) The degassed brine was pH adjusted to pH 9 and pH 9.5 using 10% sodium hydroxide (NaOH) solution.

(5) 50 ml of pH adjusted brine phase was added to 50 ml of extracted naphthenic acid in toluene phase in a bottle.

(6) The bottle was shaken for 1 minute in a fume cupboard.

(7) The mixture was allowed to stand in contact for 10 minutes. .

(8) The precipitate was filtered, and was left to dry overnight in a fume cupboard.

(9) 5g of the dried precipitate was re-dissolved in 10 ml 3M hydrochloric acid (HCl) and 25 ml toluene. The mixture was stirred using magnetic stirrer in a fume cupboard for 30 minutes for complete dissolution of the precipitate.

(10) The fluid organic phase was filtered using Schleicher and Schuell 597 HY hydrophobic silicone coated filter paper under vacuum.

(11) The solvent was evaporated in the filtrate using a rotary evaporator at a temperature between 40^{o}C and 50^{o}C and the presumed naphthenic acid extract was analysed using electrospray mass spectrometry (ESMS) and atmospheric pressure chemical ionisation mass spectrometry (APCI-MS) techniques to characterize the acid composition in the extract.

3.2.5 Analysis of naphthenic acid extracts by ESMS and APCI-MS

The naphthenic acid extract analyses in this study were carried out using either electospray mass spectrometry (ESMS) or atmospheric pressure chemical ionisation mass spectrometry (APCI-MS). For many samples, both ESMS and APCI MS were performed and the results compared. The basic principle upon which both ESMS and APCI-MS work is the "soft" ionisation technique, where the ions analysed in the mass spectrometry are generated without thermally fragmenting them in the ionisation process. The ESMS and APCI-MS techniques differ with respect to how ionisation is induced. In ESMS, ionisation is achieved as a result of the potential difference between the spray needle and the cone, along with rapid but gentle solvent evaporation, whilst in APCI-MS, the analyte solution goes into the pneumatic nebuliser and the solvent is evaporated in a heated quartz tube prior to interacting with the corona discharge, creating ions for mass spectrometry analysis (http://www.chm.bris.ac.uk/ms/theory/apci-ionisation.html). Preferential ionisation of higher molecular weight acids with APCI-MS over ESMS was also reported when tested on some commercial naphthenic acids samples (Chang *et al.,* 2000), with at least one order of magnitude more sensitivity. Formation of unwanted clusters (multimers) from the APCI-

MS technique during the analysis of the higher molecular weight naphthenic acids was also reported (Rudzinski *et al.,* 2002).

The ESMS analysis was performed using a PE-Sciex API 150EX single quadrupole mass spectrometer in a negative ion mode, with nitrogen both as nebulizer gas and curtain gas at a flow rate of 6 litre/min and pressure of 60 psi. Source temperature used was 350^{o} C and the needle voltage for ion spray was -4.5 kV. Samples were introduced using a Harvard pump with flow rate between 1 and 10 µl/min and mass spectra were recorded from m/z 115 to m/z 2000 for the purpose of naphthenic acid identification. The APCI measurements were carried out using a PE-Sciex API 150EX mass spectrometer with a heated nebulizer source. Nitrogen was used as both nebulizer and curtain gas, with gas pressures of 10 and 12 psi respectively. Nebulizer current voltage and temperature were -6 kV and 400^{o}C

3.3 CRUDE OIL CHROMATOGRAPHIC SEPARATION, ANALYSIS AND TAN MEASUREMENT

Crude oil chromatographic separation was carried out on all the crudes used in this work, in order to carry out certain biomarker studies, as described below. Chromatographic separation was carried out using liquid column elution techniques for all the crude oil samples analysed and the fractions separated were analysed using gas chromatography (GC) and gas chromatography mass spectrometry (GCMS). In this study, calcium naphthenate, sodium carboxylate soaps and emulsion forming crudes from different parts of the world were used. Total acid number (TAN) measurement was also carried out for some of the crude oil samples and the detailed experimental procedures for this are also explained below.

3.3.1 Crude oil liquid column separation technique

A standard vertical glass column was used for the separation of crude oil into various fractions i.e. aliphatic, aromatic and polar (NSO). There are three different stages in the separation process: (i) column preparation— the glass column was thoroughly cleaned with petroleum ether and a small piece of cotton wool was used to tightly block the drain end of the column. The column was filled with a slurry of silica in petroleum ether using a “tap-

fill" procedure to form a stationary phase filling up to two thirds of the column length. A layer of alumina (about 1 cm) was added above this, followed by the layer of the crude oil sample to be separated (the crude oil sample was mixed with alumina to form a fine grained powder) and this was then covered by another layer of alumina (about 1 cm) on top of the sample, (ii) sample preparation— 60g of the crude oil sample was mixed with 2g of alumina to achieve a fine grained powered substance prior to loading onto the column, and (iii) elution development— elution of the various fractions was based on the polarity of the different components in the crude oil samples, with the aliphatic fraction being eluted first using 70ml of petroleum ether, followed by the aromatic fractions, using 70ml (30% dichloromethane (DCM) and 70% petroleum ether) and finally the polar fraction, using 70ml of methanol. Each of the eluted fractions was collected in a separate conical flask and the solvent was evaporated using a rotary evaporator and subsequent complete evaporation to dryness, using nitrogen, prior to analysis.

3.3.2 Chromatographic analyses of the fractions

The fractions analysed in this study were the aliphatic and aromatic fractions from the various crude oil samples, using gas chromatography (GC) and gas chromatography mass spectrometry (GCMS) for biomarker studies.

Gas chromatography (GC) analysis

Gas chromatography (GC) analysis of aliphatic and aromatic hydrocarbon fractions of the crude oil samples separated was carried out using a HP 5890 gas chromatograph fitted with an HP-5 (30m X 0.25mm X 0.25μm film thickness) silica capillary column. The oven temperature was programmed from 50^{o}C to 300^{o}C at 4^{o}C per minute and held at the final temperature for a period of 20 minutes. Helium carrier gas was used with a flow rate of 2ml/minute. The following peaks, i.e. pristane (pr), phytane (ph), *n*-C_{17} and *n*-C_{18}, were measured from the GC traces. Both the retention time and the corresponding area of the peaks were measured using the automatic integration method on the computer.

Gas chromatography mass spectrometry (GCMS) analysis

Samples from the crude oil separation were analysed by gas chromatography mass spectrometry (GCMS) in selected ion monitoring mode, using the HP5970II mass selective detector. The GC was fitted with a HP-1 flexible silica capillary column (60mm X 0.32m i.d.; 0.25μm film thickness), using splitless injection. The GC oven temperature was programmed from 40^{o}C to 300^{o}C at 4^{o}C per minute and held at the final temperature for 20 minutes with helium as the carrier gas (flow rate of 1ml/minute). Different ions were monitored in single ion monitoring (SIM) mode for this analysis. The peaks of interest in this study from the m/z chromatograms were integrated automatically, using the RTE integrator, and the corresponding areas were used. For those peaks that suffered co-elution or were too small to be automatically integrated, a manual method was used and the corresponding areas of the peaks measured.

3.3.3 Total acid number (TAN) measurements of crude oil samples

The total acid number (TAN) measurement has been a well established technique in the oil industry and is traditionally determined by non-aqueous titration as described in the *ASTM D 664, Standard Test Method for Acid Number of Petroleum Products by Potentiometric Titration*. Total acid number (TAN) can generally be defined as the amount of acid and acid-like material in the oil sample. In other words, it is considered as the amount in milligrams of strong base required to neutralise the acidity in one gram of oil sample. The end point obtained is referred as the total acid number (TAN usually in units of mg of KOH) value and is mathematically expressed as:

$$\mathrm{TAN} = \frac{\mathrm{base}_{\mathrm{volume}} * \mathrm{base}_{\mathrm{concentration}} * \mathrm{base}_{\mathrm{M.W}}}{\mathrm{crude\ oil\ sample\ weight}}$$

where the $\mathrm{base}_{\mathrm{concentration}}$ is the molar concentration of the base and $\mathrm{base}_{\mathrm{M.W}}$ is the molecular weight of the base used. In this study, a DMP Titrino 785 Metrohem automatic titrator was used for the determination of the total acid number (TAN) for various crude oil samples, as a preliminary indication of degree of acidity.

Depending on the expected value of the acid number from the crude oil sample, 0.1g to 10g of the well-mixed crude oil sample was weighed out into the titration vessel for total acid number (TAN) determination. The general guide used in the total acid number (TAN) determination is shown in the table 3.1 below.

Expected acid number mg KOH/g sample	Sample weight (g)	Weighing accuracy (mg)
0.05 to 0.9	10 ± 2 g	100 mg
1 to 4.9	5 ± 0.5 g	20 mg
5 to 19	1 ± 0.1 g	5 mg
20 to 99	0.25 ± 0.02 g	1 mg
100 to 250	0.1 ± 0.01 g	0.5 mg

Table 3.1: General guide for sample weights in the determination of TAN

An appropriate weight of crude oil sample was weighed into the titration vessel and 50 to 125ml of the solvent (toluene/IPA/H_2O— in the ratio of 500ml/495ml/5ml) was added and the whole mixture was titrated with 0.1mol/L of c(KOH—potassium hydroxide) solution. The titer determination of the c(KOH) was carried out using potassium hydrogen phthalate (KH phthalate) prior to the total acid number determination and the titer value factor incorporated in the calculation formula. Approximately 200 mg of potassium hydrogen phthalate (KH phthalate) was weighed out into a beaker and dissolved in 40 ml of distilled water, followed by the addition of 20 ml isopropyl alcohol (IPA). The solution was then titrated with potassium hydroxide until the first end point and the titer value calculated as follows:

$$\text{Titer} = \frac{\left[\frac{C00}{C01}\right]}{EP1}$$

Where;

C00 = weight of KH phthalate in mg

C01 = 20.423 (1 ml c(KOH) = 0.1 mol/L, corresponds to 20.423 mg KH phthalate)

EP1 = titrant consumption up to the endpoint, in ml.

The mathematical expression for the total acid number (TAN) calculation after the titration was carried out is expressed as:

$$\text{TAN} = \frac{(\text{Titrant consumption-Solvent blank}) * \text{Molarity of titrant} * \text{Factor on titrant} * \text{Molar mass of KOH (56.106)}}{\text{Sample weight}}$$

3.4 STATIC NAPHTHENATE PRECIPITATION TESTS

The procedure for all the naphthenate precipitation experiments performed during this research in static bottle test experiments is described in this section. The basic experiment is where a pH adjusted brine (to pH ~ 9 – 9.5) containing calcium ions is shaken with an oil (toluene) phase containing a certain concentration of extracted naphthenic acids. A solid calcium naphthenate then may form at the interface. This section describes the details of the composition of the various types of brine used, the pseudo oil phase compositions, as well as the nature of the different types of experiments i.e. the pH change experiment, the naphthenate precipitation experiment and the determination of the calcium concentration in the oil phase.

3.4.1 Brine Compositions

All the brines used during the course of this study are synthetic brines of various compositions prepared in an aqueous medium. The brines were prepared in the laboratory using distilled water and mineral salts purchased from VWR. Brines were prepared in 500ml, 1litre or 2 litre batches, depending on the demands of each type of experiment. For example, when required in a 1 litre batch, this was prepared by weighing the correct amount of the required salts and dissolving in approximately 750 ml of distilled water to achieve complete dissolution before being transferred to a graduated 1 litre flask which was then topped up to the mark using distilled water. Brine solutions used in this research were prepared using sodium chloride (NaCl) and calcium chloride hexahydrate ($CaCl_2.6H_2O$). The various compositions of brines used in these studies were as follows:

(i) 25000 ppm Na^+ and 20000 ppm Ca^{++}

(ii) 25000 ppm Na^+ and 15000 ppm Ca^{++}

(iii) 25000 ppm Na^+ and 10000 ppm Ca^{++}

(iv) 25000 ppm Na^+ and 5000 ppm Ca^{++}

(v) 25 000 ppm Na^{+} and 1000 ppm Ca^{++}

(vi) 25000 ppm Na^{+} and 500 ppm Ca^{++}

3.4.2 Oil phase

The description of an oil phase in the field implies the actual composition of the crude oil. However, for the purposes of this research, the "oil phase" is generally a naphthenic acid extract from the field deposits or a crude oil dissolved in toluene solvent i.e. either calcium naphthenate, sodium carboxylate soaps/emulsion. The extracts from naphthenate field samples are presumed to comprise 100% naphthenic acid content, while the toluene solvent is considered to be the synthetic oil. To prepare a known concentration of naphthenic acid in the oil phase (say 10000 ppm[**]), 1g of the naphthenic acid extract was dissolved in 100ml of toluene solvent and then subsequent concentrations i.e. of the oil phases were prepared from the stock solution**.**

[**]***Note:*** *Throughout this thesis, whenever 1 ppm of naphthenic acid in the oil phase is referred, this is actually* (ρ_o/ρ_w) *mg/L of the substance. In the aqueous phase, 1 ppm of any quantity is the normal 1 mg/L.*

3.4.3 pH change experiment

This particular type of experiment is the simpler version of the naphthenate precipitation experiment in which there was no actual formation of precipitate but rather just a pH change in the brine when the (pH adjusted) brine and oil phase were shaken together. Extracted naphthenic acid from naphthenate field deposit, as described in section 3.2.1, was dissolved in toluene solvent in a volumetric flask at a concentration of 1g/100ml (1%w/v ≡ 10000ppm), which was then taken as the stock solution. Various naphthenic acid solutions in toluene were then prepared from the stock solution at concentrations ranging from 0.1 wt% (1000 ppm), 0.25 wt% (2500 ppm), 0.5 wt% (5000 ppm), 0.75 wt% (7500 ppm) and 1.0 wt% (10000 ppm). Synthetic brine solution (water phase) was prepared (composition: 25000 ppm Na^{+} and 20000 ppm Ca^{++}) by dissolving 63.55g NaCl and 109.32g of $CaCl_2.6H_2O$ in a litre of distilled water. The solution was allowed to stand for 24 hours for complete dissolution, and was filtered using a 0.45μm filter before use. Brine samples were

pH adjusted to initial pH values 6, 5, 4 and 3. At these low brine pH values precipitation did not occur, as metal naphthenates do not precipitate when the solution pH value is below 6, with a buffered system (Laredo *et al.,* 2004).

The oil phase (naphthenic acid extract in toluene) and brine (at initial pH) phases were then brought into contact: 5 ml of the adjusted pH brine phase (water phase) were mixed with 5 ml of the naphthenic acid samples in the toluene (oil phase) for each corresponding concentration i.e. 1000, 2500, 5000, 7500 and 10000 ppm. The bottles were shaken for 30 seconds in a fume cupboard and the samples were left to partition before the oil phase was decanted, and the final brine pH measured

3.4.4 Method of naphthenate precipitation experiment

The aim of this was to carry out an experiment to determine the effect of naphthenic acid and calcium ions concentration on the formation of naphthenate. The precipitation experiment was carried out for several naphthenate extracts studied during this research work, using either calcium naphthenate deposit or sodium carboxylate/emulsion sample extract. The concentration of the naphthenic acid in the toluene (oil phase) varies from experiment to experiment depending on the particular work in question, but the most common ranges used in this study were 0.1 wt% (1000 ppm), 0.25 wt% (2500 ppm), 0.3 wt% (3000 ppm), 0.5 wt% (5000 ppm), 0.75 wt% (7500 ppm) and 1.0 wt% (10000 ppm). Also, the typical brine composition (water phase) used in this part of the work was 25000 ppm Na^+ and 20000 ppm Ca^{++} was obtained by dissolving 63.55g NaCl and 109.32g of $CaCl_2.6H_2O$ in a litre of distilled water, though, in some sections of this work, a fixed concentration of Na^+ (25000 ppm) was used, while varying the Ca^{++} concentrations (500, 1 000, 5000, 10000 and 20000 ppm). In every case, the synthetic brine was prepared using distilled water and was allowed to stand for 24 hours to achieve thorough dissolution prior to pH adjustment. The synthetic brine solution was then filtered using a 0.45μm filter and thereafter pH adjusted to either pH 9 or pH 9.5, using 10% sodium hydroxide solution (NaOH),

The naphthenate precipitation experiment was performed by bringing 10 ml of the oil phase (naphthenic acid in toluene) into contact with the water phase (pH adjusted synthetic brine) in a bottle. The oil/brine mixture was shaken for 30 seconds in a fume cupboard and then allowed to settle for 10 minutes. The precipitate formed was filtered, using 589 blue ribbon Schleicher & Schuell filter paper (2 μm) and allowed to dry in a fume cupboard for 24 hours. The mass of the formed precipitate was measured and final brine pH measured.

3.4.5 Environmental scanning electron microscopy/energy dispersive x-ray (ESEM/EDAX) analysis

The objective of using this type of analysis on some of the naphthenate field deposits and laboratory generated naphthenate precipitates was to gain some insights into and information about the morphology of the metal naphthenate deposits (ESEM), along with the elemental composition of these naphthenates (EDAX). Scanning electron microscopy (SEM) and environmental scanning electron microscopy (ESEM) have been in used for a long time in structural characterization. It is documented that when a sample is examined with an electron beam, three different signals can be created: (i) secondary electrons, (ii) backscattered electrons and (iii) X-rays. The secondary electrons are usually ejected after an interaction with the primary electrons of the beam and are known to have low energy (less than 50 eV). Back-scattered electrons (BSE) are the primary beam electrons which have left the sample due to static collisions and have energies ranging from 50 eV up to the accelerating voltage of the beam. The principle on which scanning electron microscopy (SEM) works is by bombarding the surface of a material with a beam of electrons and detecting either secondary electrons or back-scattered electrons, since X-rays give poor resolution compared to the other two. A virtual image is then generated from the signals emitted by the samples and the resolution of scanning electron microscopy (SEM) is a measure of the smallest feature observable by the instrument, which is usually in the Å or nm range.

Due to the need for a higher vacuum and extensive sample preparation with scanning electron microscopy (SEM), the environmental scanning electron microscopy (ESEM)

mode of operation is often used in "wet" solid characterization studies. The operational procedure in ESEM does not require any sample preparation, as analysis can be carried out directly on the original solid materials. The sample chamber and the beam column are separated by multiple pressure limiting apparatus. The column remains at high pressure, while the chamber sustains pressure of at least 4.6 Torr (Philips, 1996). Inert gas is used to control the pressure of the chamber. Ionisation in the sample chamber eliminates the charging effects and is used to amplify the secondary electron signal, which is measured in the ESEM detector (Philips, 1996). In most cases, ESEM machines have in-built EDAX capabilities, to be able to use the energy produced as a result of the incidence of the primary electron beam. The EDAX detectors measure the quantity of the emitted X-rays as a function of energy.

The ESEM presents images of the material compositions whilst EDAX measures the elemental compositions. ESEM/EDAX was performed in this study using an XLM Philips model. The instrument is operated with nitrogen and the beam energy used was 20 KeV. Two different measurements were carried out on each of the samples.

3.4.6 Sensitivities study experiment

The main objective of this part of the study was to look at a range of sensitivity parameters i.e. shear effect, bicarbonate concentration, temperature (60^{o}C), and % watercut and their effects on the formation of naphthenate precipitates in the laboratory. In all these experiments, the oil phase (naphthenic acid extract in toluene) at various naphthenic acid concentrations was obtained from different calcium naphthenate field deposits and the water phase (pH adjusted synthetic brine) had a composition of 25000 ppm Na^{+} and 20000 ppm Ca^{++}.

Shear effects

The rate of shear has a significant role in the process of naphthenate formation. This is established in this work, where experiments have been carried out to study how shear can affect the rate of naphthenate formation. Naphthenic acid extract from field calcium naphthenate deposits at various acid concentrations (1000, 3000 and 7500 ppm) was used,

with brine composition of 25000 ppm Na^+ and 20000 ppm Ca^{++}. The synthetic brine was filtered with 0.45µ filter using a vacuum pump, degassed for about 2 hours and pH adjusted to pH 9 using 10% sodium hydroxide. 10 ml of the oil phase and 10 ml of the brine phase were mixed and bottle shaken for 30 seconds prior to observation of the interface for any naphthenate precipitation. The bottles containing the mixed phases (oil and brine) were allowed to stand for 2 weeks and the precipitate was observed at the interface on daily basis for 2 weeks. At the end of two weeks the precipitate was filtered using 589 blue ribbon Schleicher & Schuell filter paper (2µ) and left overnight for the solvent to dry. The final mass of the precipitate was weighed and the final filtered brine pH was also measured.

Bicarbonate ($NaHCO_3$) effect

In this experiment, the effect of the addition of sodium hydrogen carbonate ($NaHCO_3$) to the brine at various concentrations (i.e. 300 ppm, 600 ppm and 900 ppm) was studied. The synthetic brine compositions remain same as above (25000 ppm Na^+ and 20000 ppm Ca^{++}) in addition to the $NaHCO_3$ added. The naphthenic acid concentrations in the oil phase were 1000, 3000 and 7500 ppm. The synthetic brine was filtered, degassed and pH adjusted prior to mixing. 10 ml of each phase (oil and brine) were mixed in a bottle and the bottle was shaken for 30 seconds and allowed to settle for 10 minutes before the precipitate was filtered using 589 blue ribbon Schleicher & Schuell filtered paper (2µ) and left overnight for the solvent to dry. The final mass of the precipitate formed was weighed and the final brine pH was also measured.

Temperature effect

The effect of temperature (at 60^oC) on the rate of naphthenate precipitation was investigated in this experiment. The brine composition used was (25000 ppm Na^+ and 20000 ppm Ca^{++}) and the naphthenic acid concentrations in the oil phase were 1000, 3000 and 7500 ppm. The brine was filtered using 0.45µ filter, degassed and pH adjusted to pH 9. The oil and brine phases were heated separately in a water bath for about 1 hour to attain the desired temperature. The heated phases (oil and brine) were then mixed together and the bottle was shaken for 30 seconds. The precipitate was allowed to settle for 10 minutes

before the being filtered using 589 blue ribbon Schleicher & Schuell filter paper (2μ) and left overnight for the solvent to dry. The mass of the precipitate formed was weighed and the final brine pH was also measured.

Percentage watercut (%)

The essence of this experiment was to see the effect of the oil-water mixing ratio on the precipitation of naphthenates and two types of experiments were carried out as follows: (i) constant V_o but variable V_o/V_w ratio experiment (with V_o/V_w = 1 : 0.25 to 1 : 10), and (ii) constant $V_{total} = V_o + V_w$ experiment but variable V_o/V_w = 10% Wcut to 91% Wcut. In both types of experiments the naphthenic acid concentration in the oil phase was 3,000 ppm and the synthetic brine composition was 25000 ppm Na^+ and 20000ppm Ca^{++}. The prepared brine was filtered using 0.45μ filter, degassed and pH adjusted to pH 9 using 10% sodium hydroxide, prior to phase mixing.

The constant V_o but variable V_o/V_w ratio experiment: the oil-water mixing ratios used in the experiment are shown in 3.2 below:

V_o (ratio) and ml	V_w (ratio) and ml	% Watercut = 100* (R/1+R) where R = V_w/V_o
1 = 20 ml	0.25 = 5 ml	20
1 = 20 ml	0.50 = 10 ml	33
1 = 20 ml	0.75 = 15 ml	43
1 = 20 ml	1.00 = 20 ml	50
1 = 20 ml	2.00 = 40 ml	67
1 = 20 ml	5.00 = 100 ml	83
1 = 20 ml	10.00= 200 ml	91

Table 3.2: Summary of the V_o and V_w used in the experiment for Constant V_o but variable V_o/V_w

The oil and brine phases were mixed and the bottle was shaken for 30 seconds before it was allowed to settle for 10 minutes. The precipitate which was formed was filtered using 589 blue ribbon Schleicher & Schuell filter paper (2μ) and left overnight in a fume cupboard to

enable the solvent to evaporate. The mass of the precipitate was weighed in each case and the final brine pH was also measured.

The constant $V_{total} = V_o + V_w$ experiment but variable V_o/V_w = 10% Wcut to 91% Wcut: the oil and water volumes used in these experiment are presented in table 3.3 below:

% Watercut = 100* (R/1+R) where R = V_w/V_o	V_o (ml) = volume of oil phase to make up total volume of 40ml (ml)	V_w (ml) = represent the corresponding %Wcut. (ml)
10	36.00	4.00
20	32.00	8.00
33	26.67	13.33
43	22.86	17.14
50	20.00	20.00
67	13.33	26.67
83	6.67	33.33
91	3.64	36.36

Table 3.3: Summary of the V_o and V_w used and the corresponding % watercut for $V_{total} = V_o + V_w$ experiment.

The oil and brine phases were mixed and the bottle was shaken for 30 seconds before being allowed to settle for 10 minutes. The precipitate formed was filtered using 589 blue ribbon Schleicher & Schuell filter paper (2μ) and left overnight in a fume cupboard to enable the solvent to evaporate. The precipitate was weighed the final brine pH measured in each case.

3.5 INHIBITION EFFICIENCY TESTS

The main objective of the naphthenate "inhibition efficiency" experiments described here was to develop a methodology to evaluate the various commercially available naphthenate inhibitors. Eight different naphthenate inhibitors were tested on calcium naphthenate deposit extracts, sodium carboxylate soap extracts and emulsion forming crude oil samples to determine the "minimum inhibition concentration" (MIC). This "MIC" is not determined in the way that is usual for conventional scale inhibitors, which act on mineral scales such

as barium sulphate and calcium carbonate. These inhibitors were tested using a static two phase oil/brine bottle test experiment at room temperature and the best performing inhibitor was then tested a higher temperature (60^{o}C). An attempt was made to carry out a modified tube blocking experiment to enable the inhibitors to be tested at higher temperature and pressure conditions. However, many set backs were encountered while trying to achieve this.

3.5.1 Static inhibition experiment

Eight different naphthenate inhibitors supplied by 3 chemical service companies for the naphthenate studies were used on extracts from field samples. The inhibitors supplied have active concentration ranging from 20% to 50% and are all oil phase soluble i.e. they are all deployed in the oil phase. The inhibitors are denoted as follows: CNI 1, CNI 2, CNI 3, CNI 4, CNI 5, CNI 6, CNI 7, and CNI 8. The synthetic brine composition used in the experiment was (25000 ppm Na^{+} and 20000 ppm Ca^{++}), pH adjusted to pH 9.

Inhibitor stock solutions with active concentration of 10000 ppm were prepared (assuming 100% activity) by weighing 10g and dissolving in 1 litre of toluene solution. Thereafter, the actual 10000 ppm of the inhibitor concentration was prepared based on the inhibitor % active concentration. For example, CNI 1 has 40% active concentration; so the quantity used to prepare 10000 ppm stock solution was:

X g/L = 10g * (10000/active concentration)

i.e. X g = 10g * (10000/4000) = 25g/L or 2.5g/100ml, which was dissolved in toluene to give 10000 ppm active concentration at 40% active concentration and was referred to as inhibitor stock solution. Various concentrations of 500 ppm (0.05%), 400 ppm (0.04%), 300 ppm (0.03%), 200 ppm (0.02%), 100 ppm (0.01%) and 40 ppm (0.004%) active concentration of the inhibitor in toluene were subsequently prepared from the naphthenate inhibitor stock solution as follows:

500 ppm = {(500/10000) * 50} = 2.5 ml of the stock solution in 50 ml with toluene.

400 ppm = {(400/10000) * 50} = 2.0 ml of the stock solution in 50 ml with toluene.

300 ppm = {(300/10000) * 50} = 1.5 ml of the stock solution in 50 ml with toluene.

200 ppm = {(200/10000) * 50} = 1.0 ml of the stock solution in 50 ml with toluene.
100 ppm = {(100/10000) * 50} = 0.5 ml of the stock solution in 50 ml with toluene.
40 ppm = {(40/10000) * 50} = 0.2 ml of the stock solution in 50 ml with toluene.

These concentrations of naphthenate inhibitors in toluene are prior to mixing with the oil phase. The naphthenic acid concentrations in the oil phase used in these studies were 1000 ppm, 3000 ppm or 7500 ppm, depending on the experiment. Naphthenic acid in toluene was then mixed with the naphthenate inhibitor in toluene at 1:1 ratio to give the corresponding oil phase. This oil phase was then brought into contact with pH adjusted synthetic brine and the bottle was shaken for 30 seconds and subsequently the mixture was allowed to settled for 10 minutes before observations were made to determine the minimum inhibition concentration (MIC) value. The oil phase was separated from the water phase and the final brine pH measured. In all cases, a control experiment was carried out as a reference. An explanation of how the mixing calculation was carried out is presented in Table 3.4.

Name	% Activity	Concentration required (v/v) before mix	Concentration (v/v) after mix	Volume of each used (ml)
HA in crude oil	??	15000 ppm	7500 ppm	10ml
Inhibitor in toluene (CNI 1)	40	500 ppm	250 ppm	10 ml
	40	400 ppm	200 ppm	10 ml
	40	300 ppm	150 ppm	10 ml
	40	200 ppm	100 ppm	10 ml
	40	100 ppm	50 ppm	10 ml
	40	40 ppm	20 ppm	10 ml

Table 3.4: Summary of the values for mixing calculation for the inhibition efficiency experiment.

This experiment was carried out for all the 8 naphthenate inhibitors, using calcium naphthenate extract and sodium carboxylate soaps. For the emulsion forming crude oil sample, a naphthenic acid extract from a calcium naphthenate deposit was used to "spike" the crude oil at various concentrations, prior to addition of the naphthenate inhibitor. However, in two experiments, direct inhibition was carried out on the emulsion forming crude oil sample. The experiment at higher temperature ($60^{o}C$) was performed by heating

the oil phase (naphthenic acid in toluene together with naphthenate inhibitor in toluene) and synthetic brine separately, prior to mixing. All the experiments were carried in duplicate.

3.5.2 Dynamic inhibition experiment

A dynamic naphthenate inhibition experiment was carried in order to try to replicate field production conditions as closely as possible in terms of temperature and pressure. A standard tube blocking rig (TBR) was modified with various filters being used instead of a capillary coil to detect the formed naphthenates as the pressure drop across this filter increased. However, the dynamic naphthenate experiment could not form adequate precipitates to block the filter even after 4 to 5 hours. A number of modifications were attempted to improve this apparatus but no success was achieved and no dynamic naphthenate results are presented in this thesis.

CHAPTER 4: CHARACTERIZATION OF FIELD NAPHTHENATES (CAN AND NAN) AND CRUDE OIL SAMPLES

4.1 INTRODUCTION

In this Chapter, detailed results are presented from the study and analyses of field naphthenate samples; i.e. calcium naphthenates (CaN), sodium carboxylates/emulsions (NaN) and crude oils. The experimental extraction techniques for these samples and the spectroscopic analyses applied to the extracts (ESMS and APCI-MS) have been fully described in Chapter 3. The calcium naphthenate deposits analysed are from; (i) North Sea-Norway (**HD** and **HDN**), (ii) North Sea-UK (**WB** and **BLK** samples), (iii) Asia (**BBAY**), and (iv) West Africa (**WAE**). The sodium carboxylate/emulsion samples characterized are from; (i) South East Asia-Malaysia (**MLY 53L, MLY 35L**, **TK-52S**, **TK-38S)**, (ii) South East Asia- Indonesia (**DLG 53-1**, **DLG 53-2, SEJD, SGS, WS-B04, WS-B06, WS-B07, W07W** and **B07B**), (iii) South East Asia-Brunei (**BRN)**, (iv) North Sea-UK (**NSA**), whilst crude oil samples are from; (i) North Sea-UK (**BLK C**) , (ii) North Sea-Norway (**HD C and HDN C**). The calcium naphthenate (CaN), sodium carboxylate/emulsion (NaN), and crude oil samples used in this thesis were supplied by various oil and chemical companies who sponsor the FAST JIP at Heriot-Watt University.

4.2 CALCIUM NAPHTHENATE SAMPLE ANALYSIS

Brief descriptions of the calcium naphthenate deposits used in this work are presented in Table 4.1 below:

Sample (s)	Location of Naphthenate Deposits	Physical Description
HD and HDN	North Sea (Norway sector)	Hard, shining, dark brown, sticky deposit
WB and BLK	North Sea (UK sector)	Hard, dark brown, quite sticky deposit
BBAY	Asia	Hard, dark brown, non-sticky deposit
WAE	West Africa	Hard, light brown, non-sticky deposit

Table 4.1: Brief description of the calcium naphthenate samples used in this work.

Three different naphthenic acid extraction techniques described in Section 3.2.1 were used in this study. However, the extraction procedures for Methods 1 and 2 (as described in Chapter 3, section 3.2.1) were only carried out on sample HD, which led to the generation of sludges due to incomplete digestion of the cleaned deposit, as compared to Method 3 (where complete digestion was achieved). Naphthenic acid extraction from the remaining samples HDN, WB, BLK, BBAY and WAE was carried out using Method 3 extraction procedures. Extracts (presumed to be naphthenic acids extracted from these calcium naphthenate deposits) were analysed using electrospray mass spectrometry (ESMS) and atmospheric pressure chemical ionisation mass spectrometry (APCI-MS). When applying these techniques, two distinct distribution patterns of the composition of the naphthenic acids were noticed. A summary of the identification of the naphthenic acids extracted from calcium naphthenate deposit samples is presented in Table 4.2 below.

Sample (s)	Description
HD 1	Naphthenic acid extract from Method 1 technique
HD 2	Naphthenic acid extract from Method 2 technique
HD S1	Sludge from Method 1 technique
HD S2	Sludge from Method 2 technique
HD 3	Naphthenic acid extract from Method 3 technique
HDN 3	Naphthenic acid extract from Method 3 technique
WB 3	Naphthenic acid extract from Method 3 technique
BLK 3	Naphthenic acid extract from Method 3 technique
BBAY 3	Naphthenic acid extract from Method 3 technique
WAE 3	Naphthenic acid extract from Method 3 technique

Table 4.2: Identification of the extracted naphthenic acid extracts from deposits.

The spectra from extracts HD, HDN and WB showed a broad distribution of lower molecular weight naphthenic acids and a small but significant ion peak at around m/z 1230, indicating the presence of ARN acid species. In contrast, the spectra from extracts BLK,

BBAY and WAE revealed minor traces of lower molecular weight naphthenic acids (acyclic, monocyclic, bicyclic and alkylbenzoics) in the region of m/z 200 to m/z 650 and a very pronounced ion peak at around m/z 1230, corresponding to the presence of ARN acid species.

ESMS analyses of calcium naphthenate extracts

Analysis of the extracts was carried out by taking representative amounts of each of the following samples – HD 1, HD 2, HD S1, HD S2, HD 3, HDN 3, WB 3, BLK 3 and BBAY 3. These were treated with a small volume of glacial acetic acid/toluene (1:1 v/v) solution, to wash and dissolve any possible solid material present, and the resulting solutions were washed with a small volume of water. The organic layer from each of these samples was removed and diluted with toluene/2-propanol (IPA) (35:65 v/v) and 0.1% (v/v) ammonia was added. Analyses were carried out on the prepared (diluted) samples in a negative ion mode ESMS with mass spectra recoded from m/z 115 to m/z 2000. The background spectrum of the solvent used in the analysis is shown in Figure 4.1. The spectrum contains significant ions of ~m/z 155 (C_9 monocyclic naphthenic), m/z 205.1 (C_{13} alkylbenzoic naphthenic) and m/z 521.1 (C_{35} acyclic naphthenic). There are no corresponding acid components for the ions with m/z 249.0 and m/z 385.0 peaks in the spectrum.

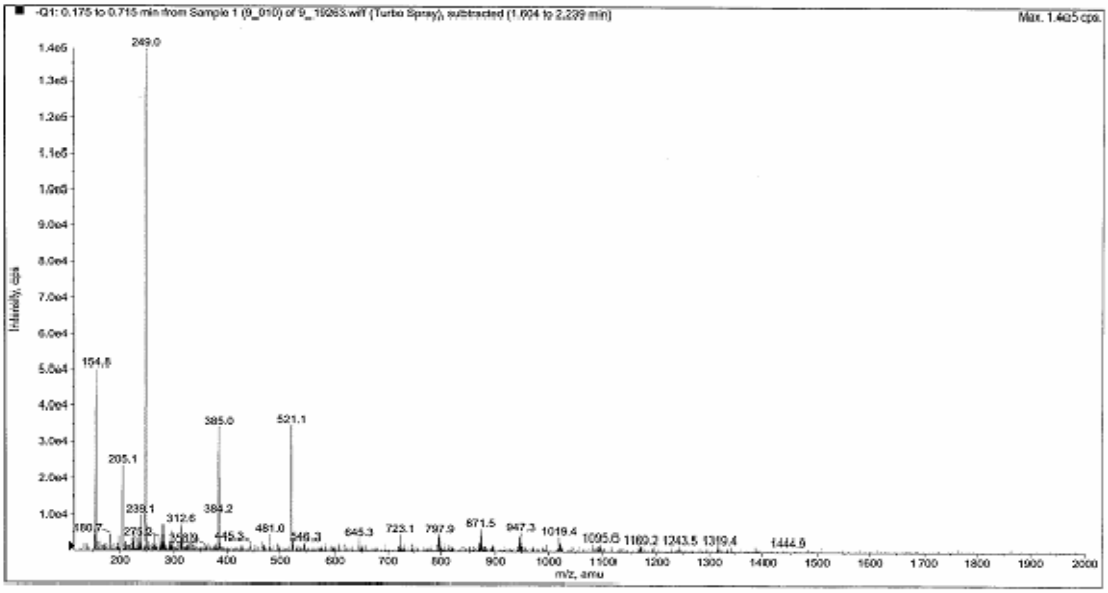

Figure 4.1: ESMS background spectrum.

Naphthenic acid extracts analysed using ESMS from samples HD 1, HD 2, HD S1, HD S2, HD 3 and HDN 3 are shown in Figures 4.2 to 4.7. These spectra show the presence of two distinct major classes of naphthenic acid families, as follows: (i) a range of lower molecular weight naphthenic acids with broad distribution from around m/z 200 to m/z 650, and (ii) a narrow band of higher molecular weight naphthenic acids between m/z 1230 to m/z 1240. The presence of intermediate molecular weight naphthenic acids was also seen in the spectra. The cluster of pronounced peaks at around m/z 1230 from the spectra was observed which is attributed to the presence of 4-protic naphthenic acid referred to as ARN (Baugh *et al.,* 2004).

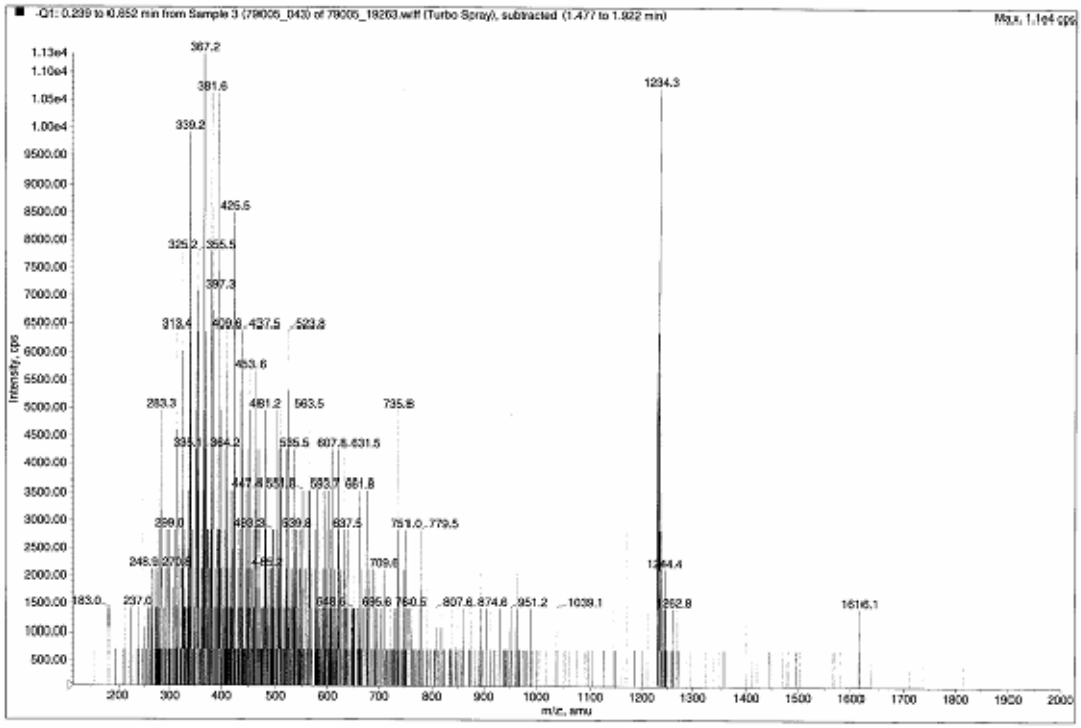

Figure 4.2: ESMS spectrum for the naphthenic acid extract from sample HD 1.

Spectra of sludges from the Methods 1 and 2 extraction techniques show the presence of both lower and higher molecular weight naphthenic acids species, as shown in Figures 4.4 and 4.5, which may be associated with the efficiency of the extraction method used. For example, the Figure 4.3 spectrum shows evidence for the ions of lower molecular weight naphthenic acids (acyclic, monocyclic, bicyclic and alkylbenzoics) and a pronounced cluster of ions corresponding to higher molecular weight naphthenic acids. The presence of

acyclic (C_{20} to C_{29} and C_{31}), C_{22} monocyclic, bicyclic (C_{17} and C_{21}) and weaker evidence of alkylbenzoic naphthenic acids are also seen in the spectrum, although alkylbenzoic naphthenic acids were seen in some spectra (e.g. Figure 4.5). The ESMS spectrum of the extract from HDN 3 sample, presented in Figure 4.7, revealed a significantly abundant distribution of lower molecular weight naphthenic acids from m/z ~200 to m/z 650 and a much smaller ion peak at m/z ~1230, indicating the presence of higher molecular weight naphthenic acid species (ARN). The wide range of the lower molecular weight naphthenic acids present is composed of acyclic (C_{10} to C_{25}, C_{27} to C_{29} and C_{36}), monocyclic (C_{11}, C_{13} to C_{28} and C_{30} to C_{32}), bicyclic (C_{11} to C_{13}, C_{15} to C_{22}, C_{24}, C_{25} and C_{27}) and alkylbenzoics (C_8 to C_{21}, C_{23}, C_{25} to C_{27} and C_{31}). The WAE 3 sample extract was only analysed using APCI-MS technique for the determination of naphthenic acid composition.

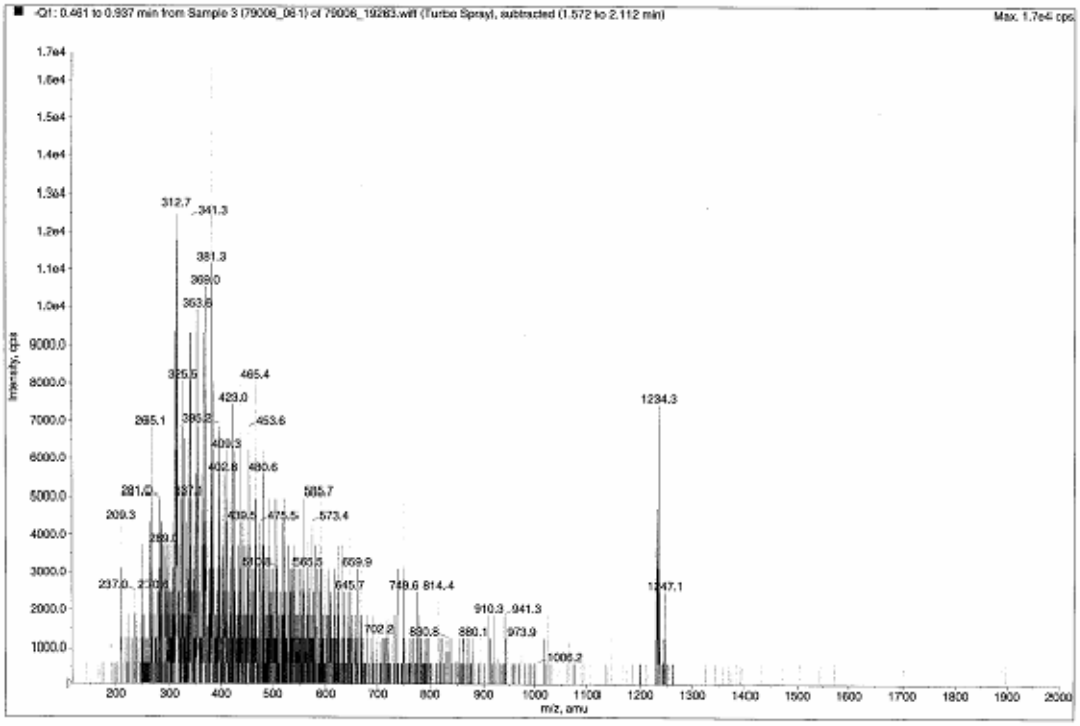

Figure 4.3: ESMS spectrum for the naphthenic acid extract from sample HD 2.

Figure 4.8 shows the spectrum of extract from sample WB 3, in which minor distributions of lower molecular weight naphthenic acids are present in the region of m/z 200 to m/z 500. A small ion peak at m/z 1229.5 was also noticed from the spectrum, which indicates the

presence of higher molecular weight naphthenic acid (ARN). However, a significant ion peak at m/z 312.9 was clearly seen which may be related to the "ARN" acid species fragment (with z = 4). Spectra of the naphthenic acid extracts from samples BLK 3 and BBAY 3 showed the presence of a distribution of lower molecular weight naphthenic acid species in the range of m/z 200 to m/z 600 with no indication of higher molecular weight acid species around m/z 1230, as can be seen in Figures 4.9 and 4.10 respectively.

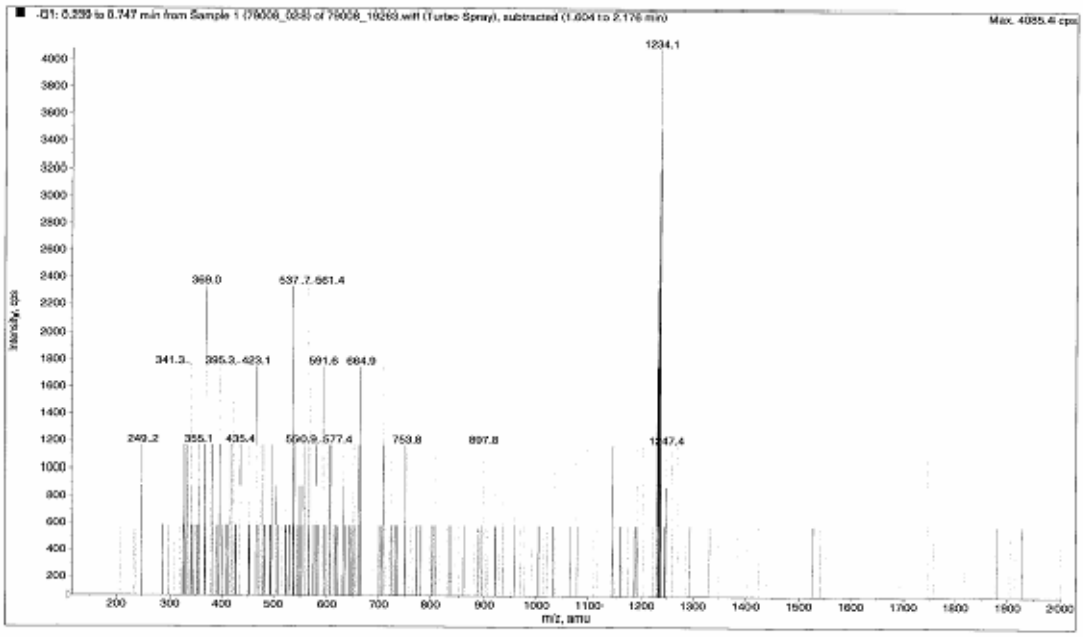

Figure 4.4: ESMS spectrum for the naphthenic acid extract from sample HD 1 sludge.

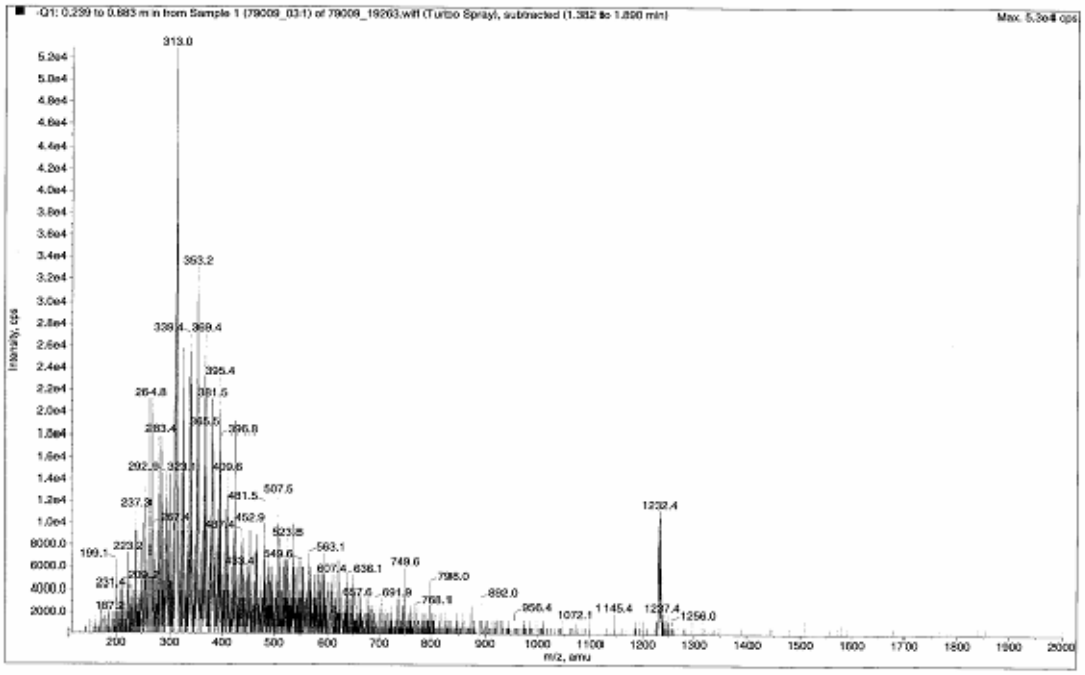

Figure 4.5: ESMS spectrum for the naphthenic acid extract from sample HD 2 sludge.

The spectrum of sample BLK 3 (Figure 4.9) showed evidence of acyclic (C_{20} to C_{24}), monocyclic (C_{20} to C_{24}) and C_{21} alkylbenzoic naphthenic acids, together with weaker evidence of other lower molecular weight naphthenic acids. The spectrum in Figure 4.10 for sample BBAY 3 showed the presence of acyclic (C_{19} to C_{22}) naphthenic acids with weaker evidence of different acid species, viz. monocyclic, bicyclic and alkylbenzoic naphthenic acids. In the ESMS spectra in both Figures 4.9 and 4.10, pronounced ion peaks at m/z 313 and m/z 312.9 were observed respectively. These are strongly suspected to be the z = 4 charged molecular ion fragment of the higher molecular weight naphthenic acid referred as 'ARN'. Normally ARN acid species (4-protic naphthenic acids) are detected at around m/z 1230 (if z = -1) but it is possible that 4 charged ions may be formed. Hence, is believed that the dominant ion peak at around m/z 313 from the spectra is an indication of such a molecular ion.

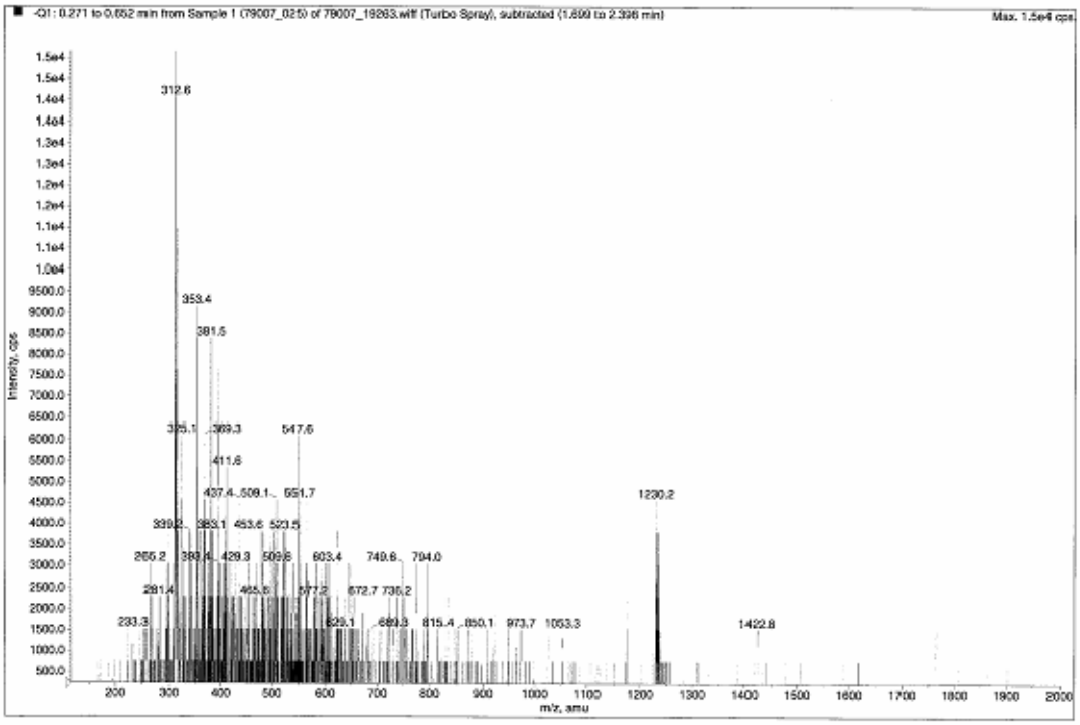

Figure 4.6: ESMS spectrum for the naphthenic acid extract from sample HD 3.

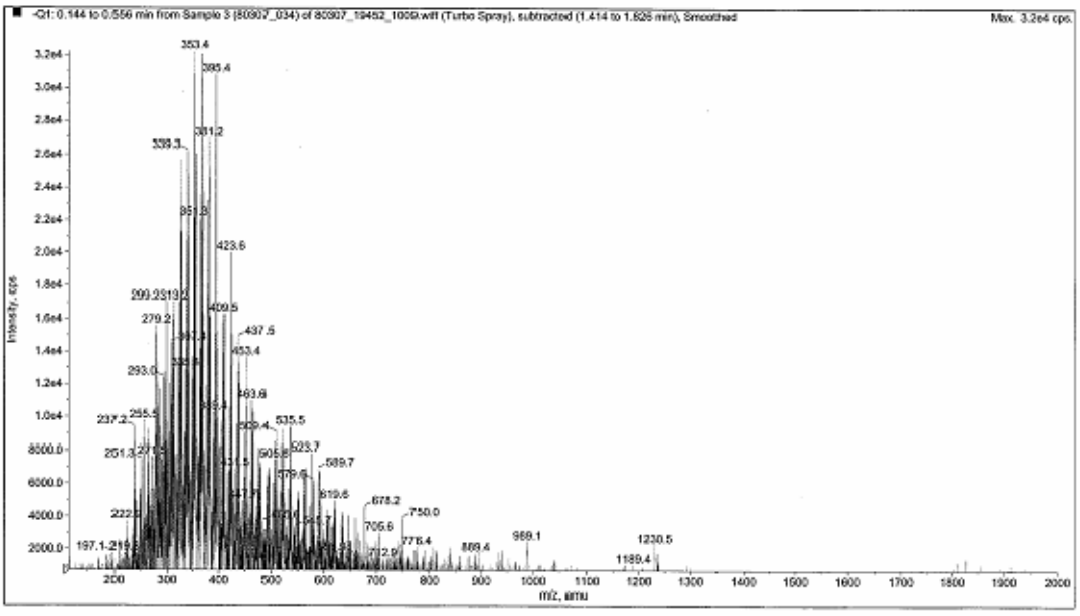

Figure 4.7: ESMS spectrum for the naphthenic acid extract from sample HDN 3.

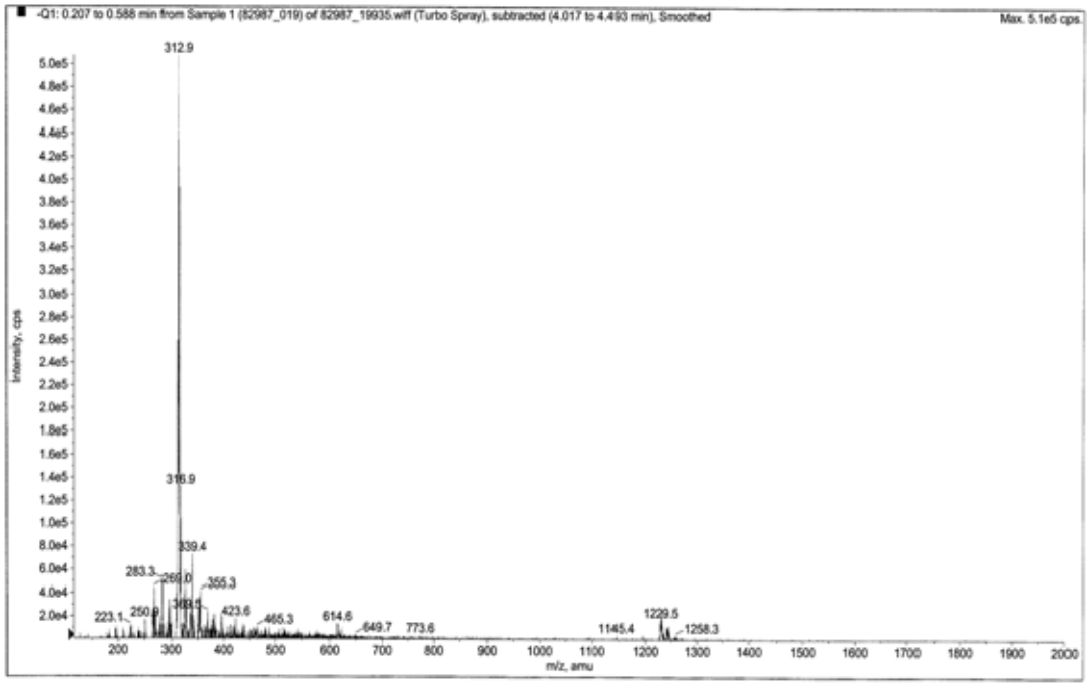

Figure 4.8: ESMS spectrum for the naphthenic acid extract from sample WB 3.

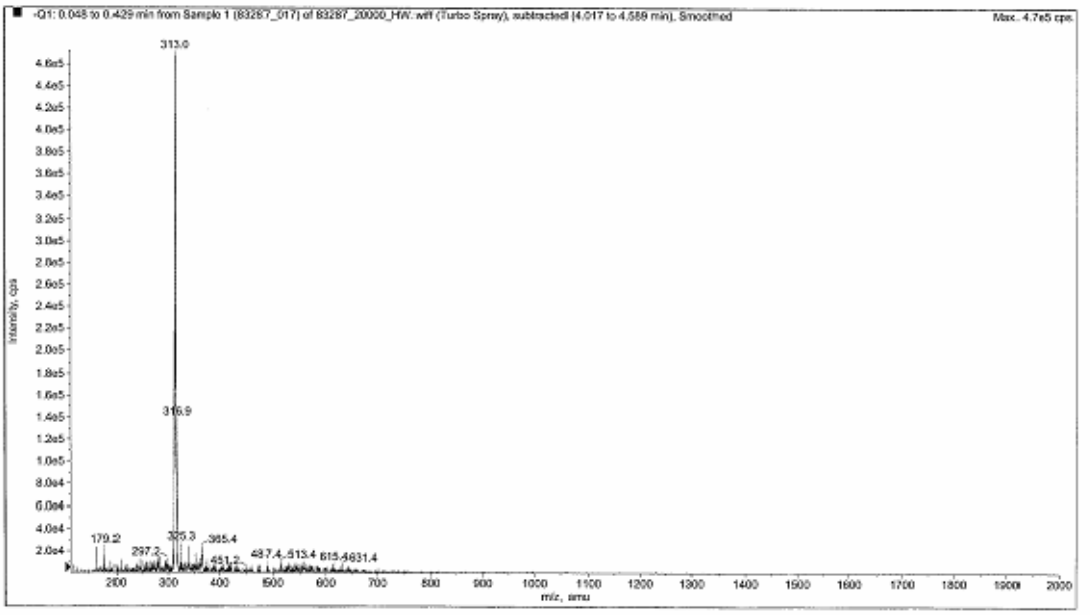

Figure 4.9: ESMS spectrum for the naphthenic acid extract from sample BLK 3.

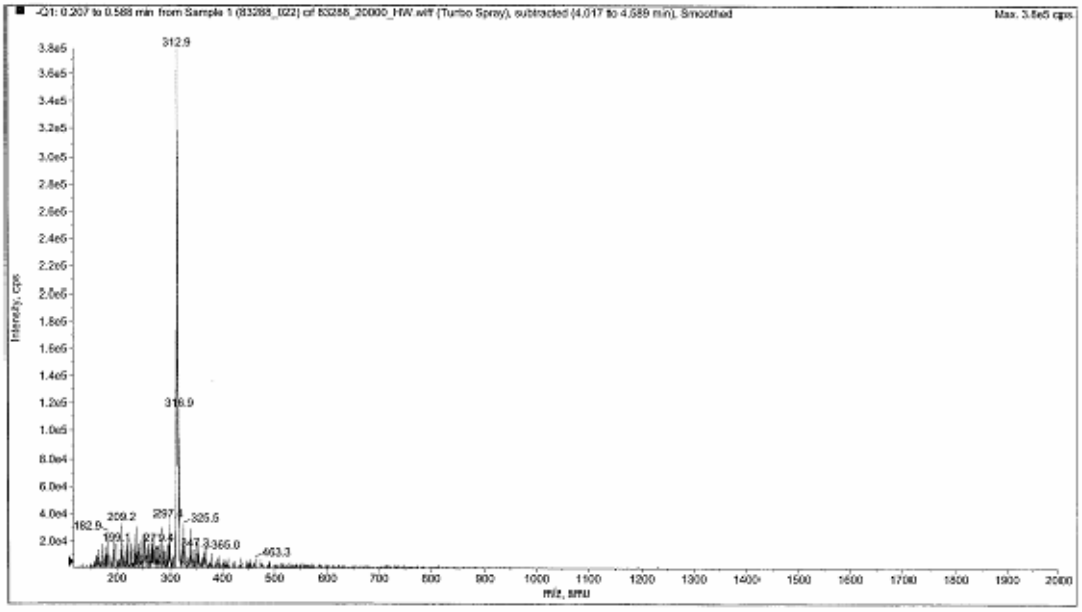

Figure 4.10: ESMS spectrum for the naphthenic acid extract from sample BBAY 3.

APCI-MS of calcium naphthenate extracts analyses

Six different extracts - viz. samples (HD 1, HD 2, HD 3, HDN 3, WB 3, BLK 3, BBAY 3 and WAE 3) - were analysed using the atmospheric pressure chemical ionisation mass spectrometry (APCI-MS) technique. A representative amount of each of the presumed naphthenic acid extracts was dissolved in a small volume of glacial acetic acid/toluene (50:50 v/v) solution to dissolve any solid materials and the resulting solution was washed with the equivalent volume of water. The organic layer from the above samples was diluted with hexane/2-propanol (IPA) (35:65 v/v) with approximately 0.1% (v/v) ammonia added. Analysis was carried out on the prepared (diluted) samples in negative ion mode APCI-MS with the spectra recorded from m/z 115 to m/z 2000. Background spectra for the different batch of samples analysed were obtained with the presence of significant m/z 136.1, 145.1, 161.0, 220.3, 227.5, 254.8 and 288.0 ions present. The following acid species were also detected: m/z 227.5 (C_{14} acyclic naphthenic) and 254.8 (C_{16} acyclic naphthenic). Figures 4.11 and 4.12 present the APCI-MS spectra of naphthenate deposit extracts (HD 1 and HD 2) using Methods 1 and 2 extraction techniques.

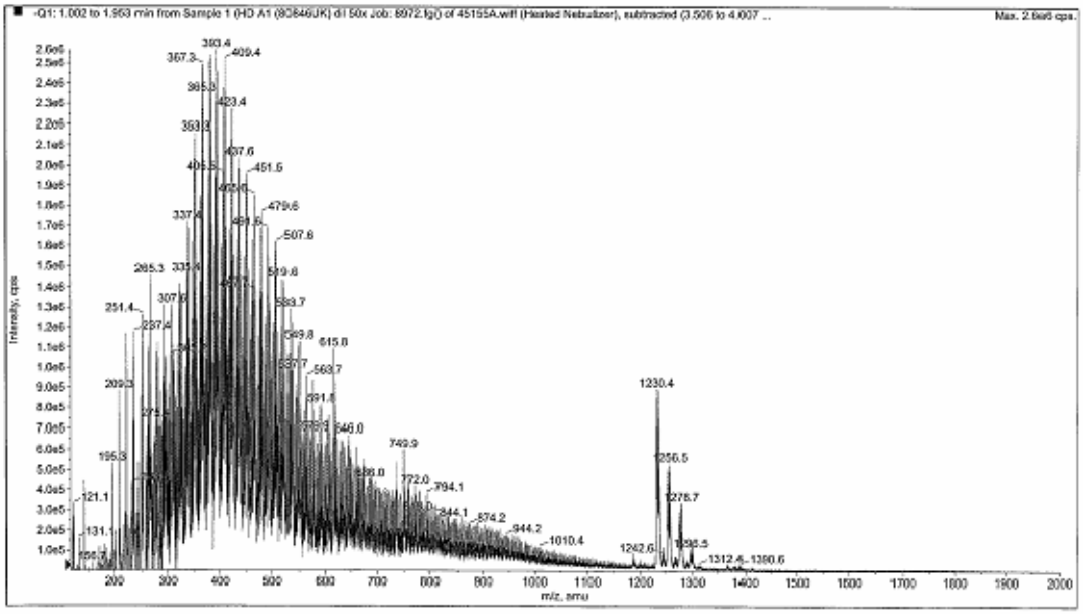

Figure 4.11: APCI-MS spectrum for the naphthenic acid extract from sample HD 1.

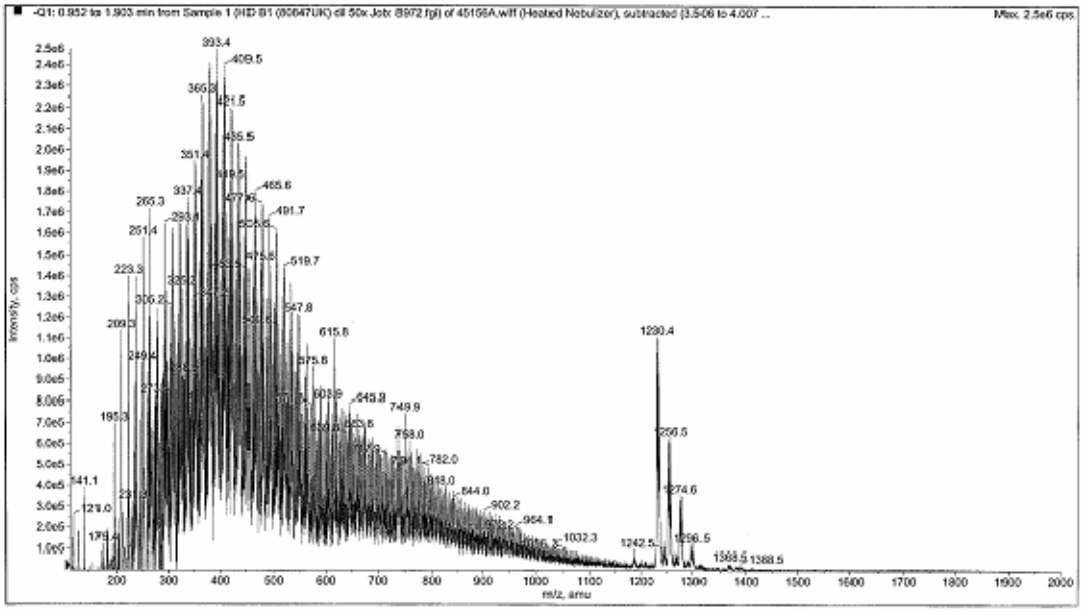

Figure 4.12: APCI-MS spectrum for the naphthenic acid extract from sample HD 2.

These figures showed that a range of acyclic and monocyclic (C_{17} to C_{55}), bicyclic (C_{12} to C_{55}) and alkylbenzoic (C_{17} to C_{55}) naphthenic acids were predominantly present in the spectra. The identification of these molecular weight naphthenic acids (acyclic,

monocyclic, bicyclic and alkylbenzoic) was carried out routinely, using software which uses the accurate atomic masses (of C, O, H) from the spectra to identify the various types of naphthenic acid, in addition to the pronounced higher molecular weight naphthenic acid ion peak (ARN) at around m/z 1230 similar to the spectra of samples HD 3, HDN 3 and WB 3**,** as shown in Figures 4.13 to 4.15 respectively.

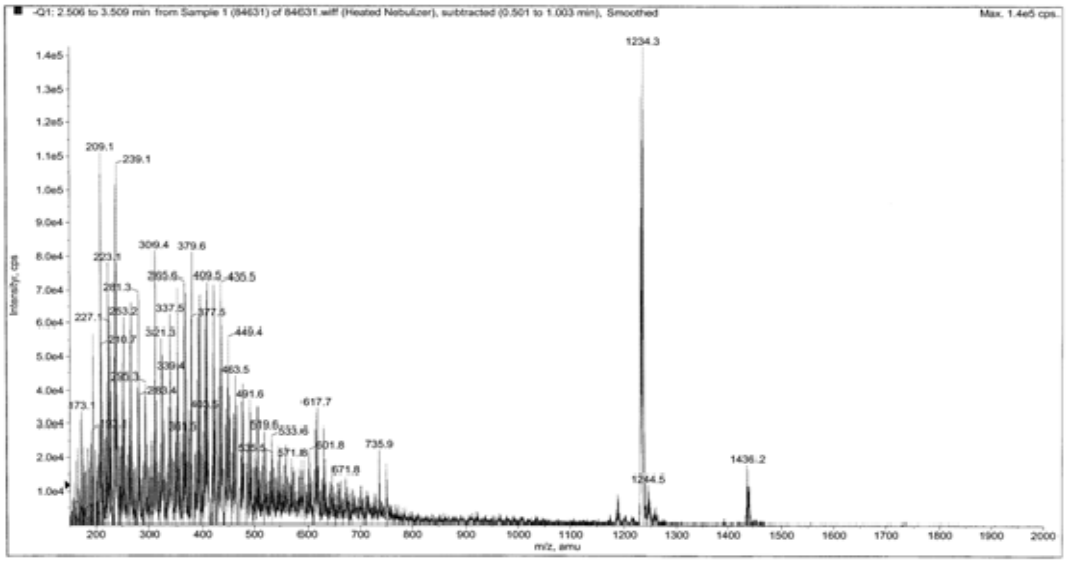

Figure 4.13: APCI-MS spectrum for the naphthenic acid extract from sample HD 3.

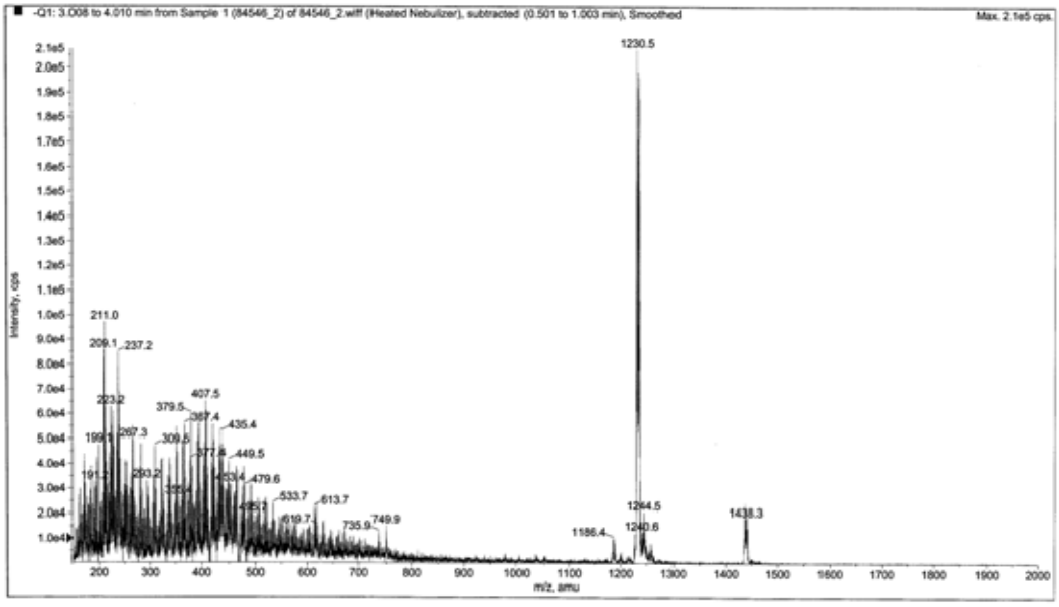

Figure 4.14: APCI-MS spectrum for the naphthenic acid extract from sample HDN 3.

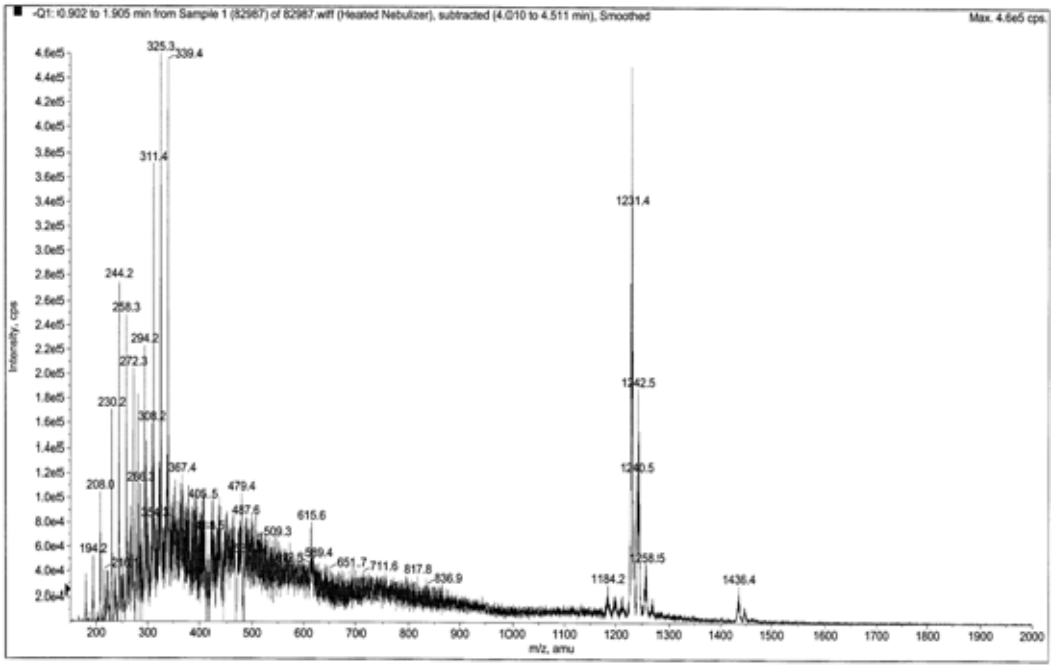

Figure 4.15: APCI-MS spectrum for the naphthenic acid extract from sample WB 3.

The APCI-MS spectra of samples BLK 3, BBAY 3 and WAE 3 are presented in Figures 4.16 to 4.18. The spectra showed weak evidence of acyclic, monocyclic, bicyclic and alkylbenzoic lower molecular weight naphthenic acids. A cluster of ions from m/z 1225 to m/z 1290 was detected in Figure 4.16, providing strong evidence for the presence of higher molecular weight naphthenic acids (ARN) whilst the Figure 4.17 spectrum revealed weak evidence of further naphthenic acids of mass greater than m/z 690. However, the responses were very weak relative to the background noise of the sample. Also a cluster of ions was detected between m/z 950 and m/z 1125 which may possibly be associated with multimerization of some lower molecular weight naphthenic acids, although some of the ions within these clusters correspond to ions indicating the presence of naphthenic acids. The presence of strong clusters of ions corresponding to ARN acids was also observed in the spectrum at around m/z 1225 to m/z 1265.

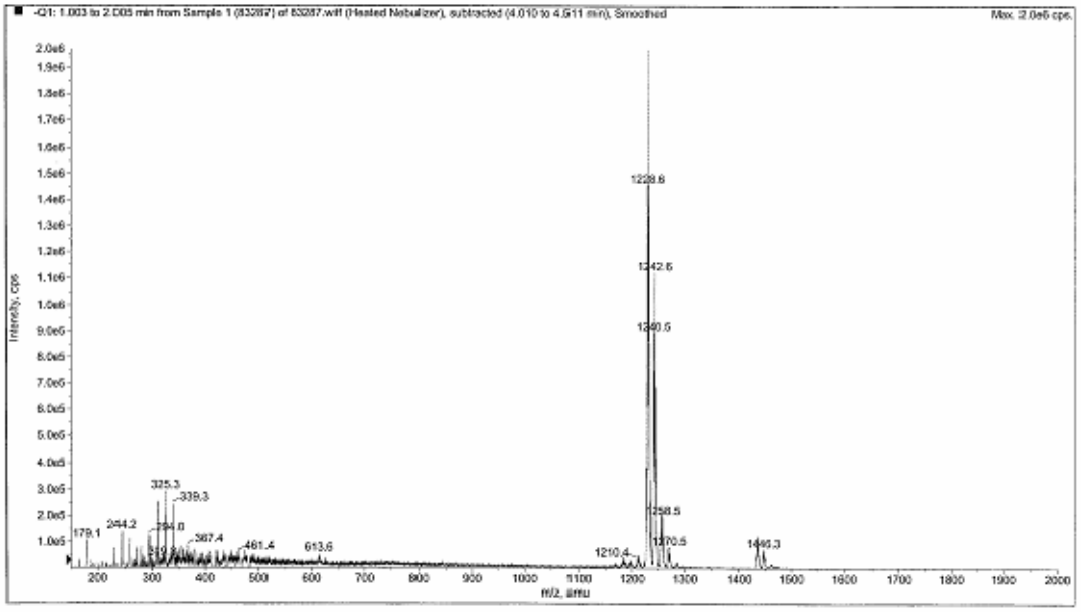

Figure 4.16: APCI-MS spectrum for the naphthenic acid extract from sample BLK 3.

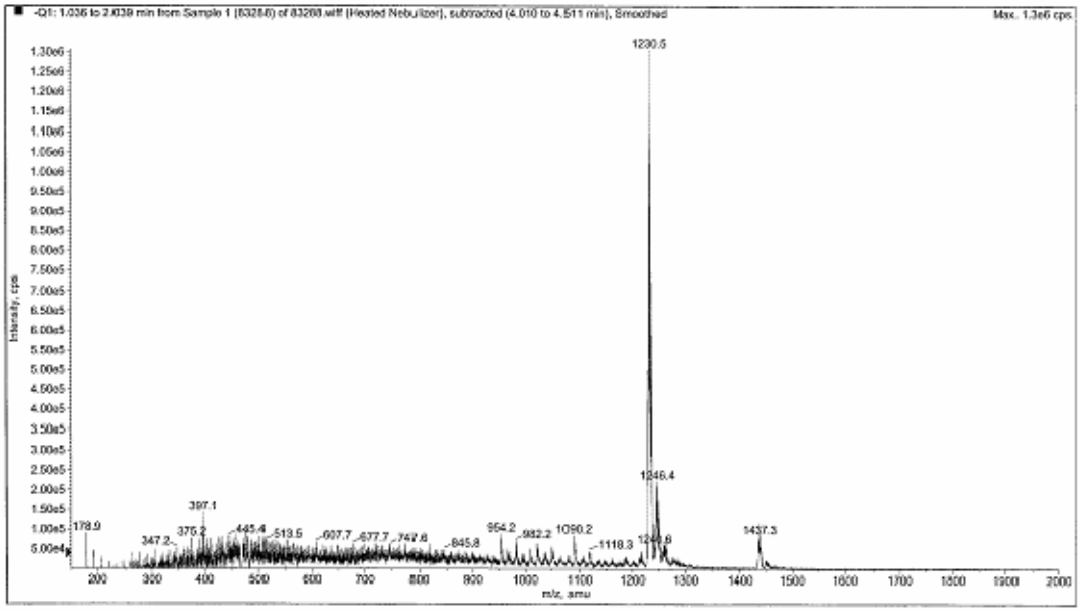

Figure 4.17: APCI-MS spectrum for the naphthenic acid extract from sample BBAY 3.

The spectrum of the extract from sample WAE 3 is presented in Figure 4.18, in which no significant lower molecular weight naphthenic acid species were observed. A significant pronounced ion peak at m/z 1234.5 was present which is associated with the presence of higher molecular weight naphthenic acid (ARN). In addition, in some spectra (BLK 3,

BBAY 3 and WAE 3) a cluster of ions of unknown origin were detected at m/z 1430 to m/z 1460. However, it should be noted that a cluster of this mass range was also seen in the ARN reference standard run under the same conditions, and therefore the appearance of these ion peaks in the sample extract spectra may be related.

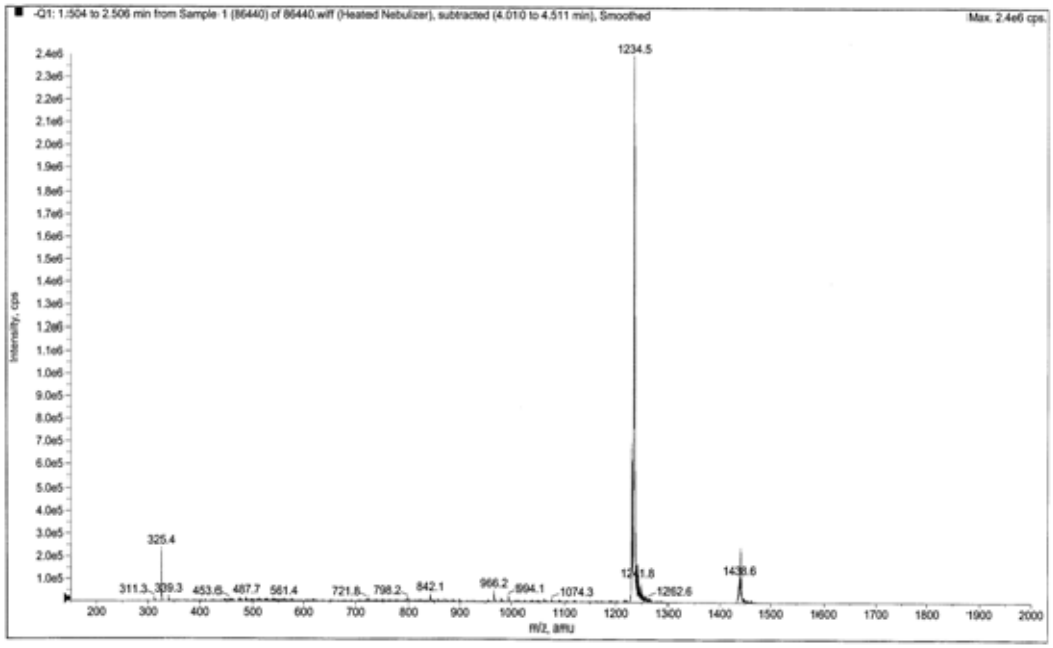

Figure 4.18: APCI-MS spectrum for the naphthenic acid extract from sample WAE 3.

4.3 ANALYSES OF SODIUM CARBOXYLATE/EMULSION NAPHTHENATE SAMPLES

Sodium carboxylate/emulsion samples used in this thesis research work were sourced from South East Asia i.e. from three different oil producing countries (Malaysia, Indonesia and Brunei) and the North Sea (United Kingdom) regions. Naphthenic acid extraction from these samples was carried out using the procedure explained in Chapter 3, Section 3.2.2. Extracts from these sodium carboxyalate emulsion samples were analysed using electrospray mass spectrometry (ESMS) and atmospheric pressure chemical ionisation mass spectrometry (APCI-MS) for naphthenic acid compositional study. Two different naphthenic distribution patterns were observed, (i) a wide range of lower molecular weight naphthenic acid (acyclic, monocyclic and alkylbenzoic) in the range of m/z 200 to m/z 600

and (ii) a sequence of acyclic naphthenic acids with an interesting pattern of preferential presence of even-over-odd carbon numbered acids. A general description of the sodium carboxylate/emulsion samples studied in this thesis is presented in Table 4.3 below:

Sample (s)	Location of Sodium Carboxylate/emulsion	Physical Description
MLY 53L, MLY 35L, TK-52S and TK-38S	South East Asia (Malaysia)	Cream to light brown, either light or thick emulsion
DLG 53-1, DLG 53-2, SEJD, SGS, WS-B04, WS-B06, WS-B07, B07W and B07B	South East Asia (Indonesia)	Brown, black, thick, or cream to ash coloured sludge or emulsion
BRN	South East Asia (Brunei)	Light brown, very thick emulsion
NSA	North Sea	Soft, dry, dark brown to light black coloured sludge

Table 4.3: Brief descriptions of the sodium carboxylate/emulsion samples used in this research studies.

Each category of the sodium carboxylate/emulsion samples was observed to have a similar distribution of naphthenic acid compositions, from the extracts analysed. Therefore, a representative selection of each category is discussed in this thesis. It is also worth noting that in some instances, the samples are from the same production field but different wells.

ESMS of sodium carboxylate/emulsion extracts analyses

The preparatory procedure for the extracts from sodium carboxylate/emulsion samples was carried out same as in the calcium naphthenate extract above. Prior electrospray mass spectrometry analyses (ESMS) were carried out on the prepared (diluted) samples in negative ion mode and the spectra were recorded from m/z 115 to m/z 2000. The background spectrum of the solvent used in the analyses of the sodium carboxylate/emulsion extracts is shown in Figure 4.19. This spectrum contains only one

significant identifiable acid ion species at m/z 197.1 (C_{12} monocyclic naphthenic acid), which may increases the response of the corresponding acid species in the extract.

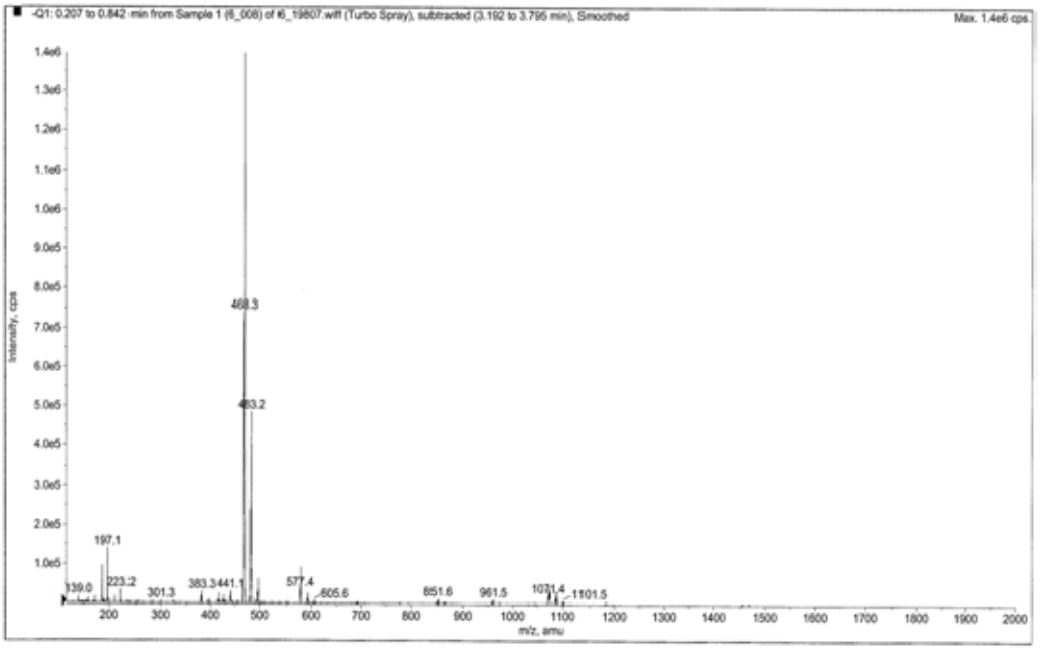

Figure 4.19: ESMS background spectrum.

The ESMS spectrum of the extract from sample TK-38S is presented in Figure 4.20, in which mainly lower molecular weight naphthenic acids are observed. The presence of acyclic (C_{20} and C_{24}), monocyclic (C_{12}, C_{22}, C_{24} and C_{25}), bicyclic (C_{24} and C_{28}) and alkylbenzoic (C_{28} and C_{29}) naphthenic acids was revealed. No traces of higher molecular weight naphthenic acid (ARN) from the spectrum were observed. Extracts from MLY 53L, MLY 35-L and TK-52S samples show naphthenic acid compositions of lower molecular weight naphthenic acids in the range of m/z 200 to m/z 650 from the spectra.

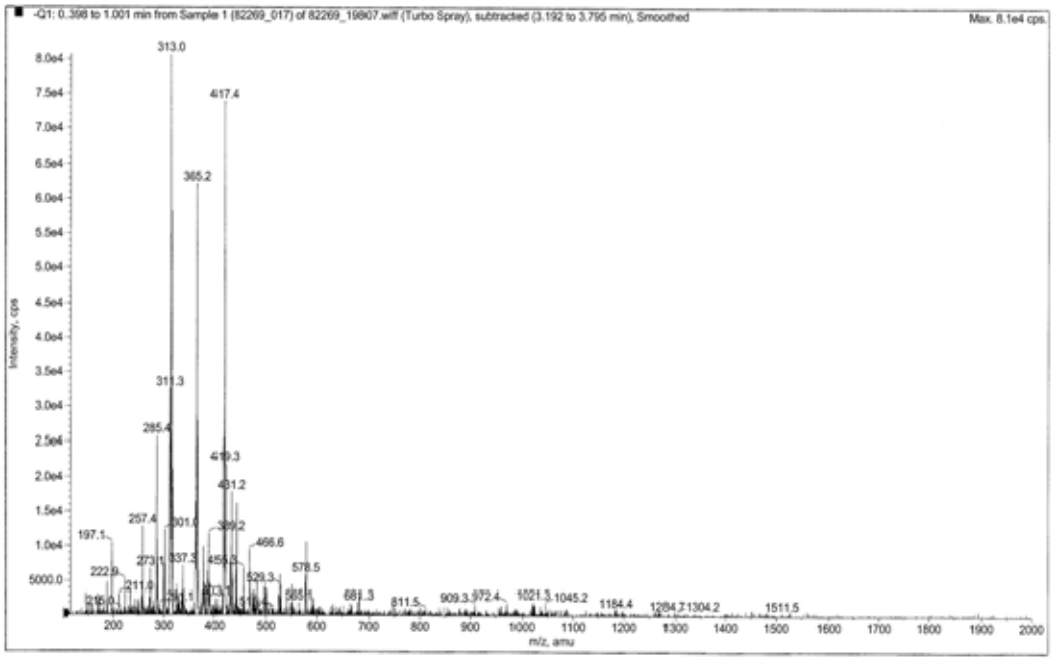

Figure 4.20: ESMS spectrum for the naphthenic acid extract from sample TK-38S.

Naphthenic acid extracts analysed from the sodium carboxylate sludge sample (DLG 53-2) and the crude oil emulsion (DLG 53-1) using ESMS show a wide range of different acid families, viz. acyclic, monocyclic, bicyclic and alkylbenzoic naphthenic acids. For example, ESMS analysis of sample DLG 53-1, presented in Figure 4.21, shows evidence of naphthenic acids corresponding to acyclic (C_{20} to C_{25}), monocyclic (C_{24} and C_{25}), bicyclic (C_{14}, C_{24} to C_{29}) and alkylbenzoic (C_{21} to C_{36}). Figure 4.22 presents the ESMS spectrum of sample DLG 53-2 where a wide range of acyclic, monocyclic and bicyclic naphthenic acids have been identified along with a few alkylbenzoic (C_{26} and C_{28}) naphthenic acids. The dominant acids identified in this sample were acyclic naphthenic acids (C_{16} to C_{29}), monocyclic naphthenic acids (C_8 to C_{28}) and bicyclic naphthenic acids (C_{14} to C_{28}). In both spectra of the samples analysed, there was no evidence of any presence of ions with m/z greater than 1000, i.e. no evidence for the presence of ARN acids in these samples. The remaining sodium carboxylate samples (from Indonesia) analysed showed a distribution of the lower molecular weight naphthenic acid i.e. acyclic, monocyclic, bicyclic and alkylbenzoic. There was no trace of ARN acid species in the spectra.

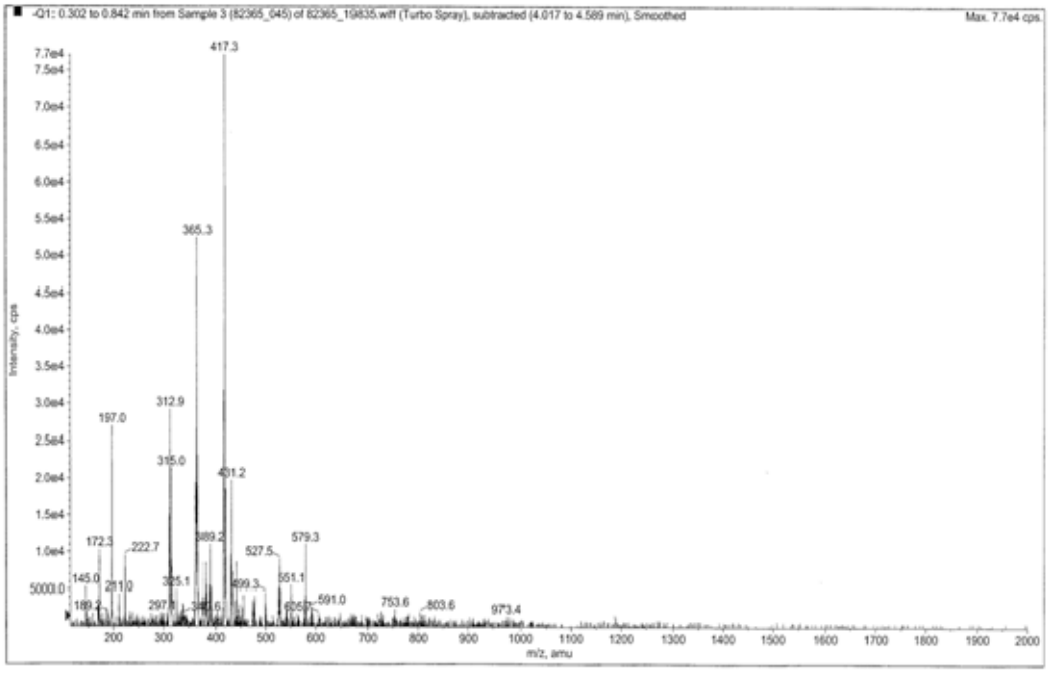

Figure 4.21: ESMS spectrum for the naphthenic acid extract from sample DLG 53-1.

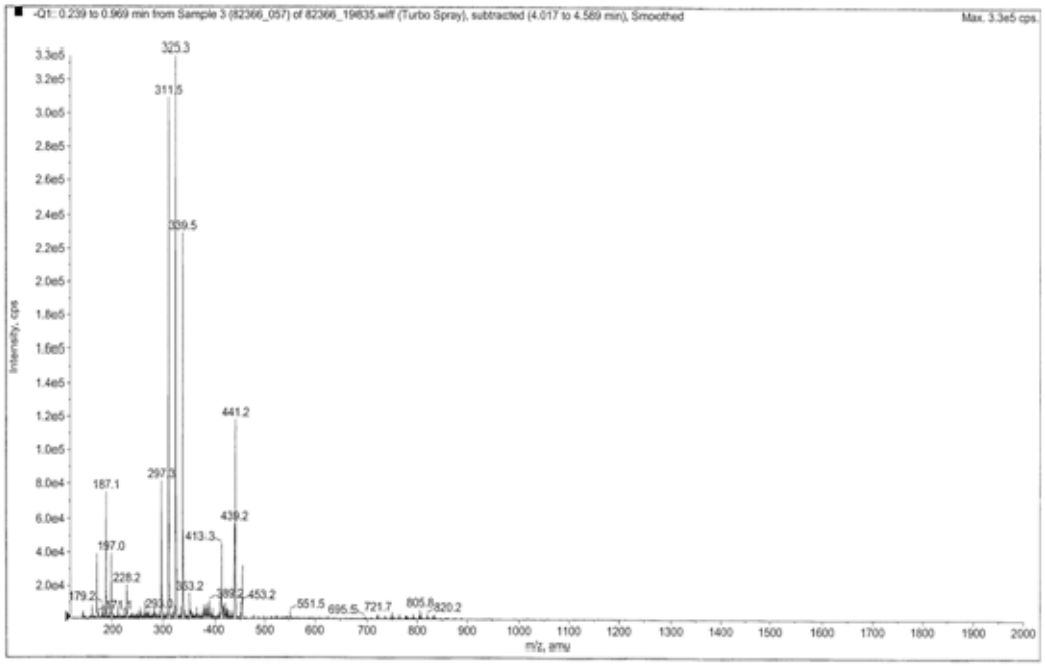

Figure 4.22: ESMS spectrum for the naphthenic acid extract from sample DLG 53-2.

The ESMS analysis of the extract from the sodium naphthenate sample (BRN) revealed a wide range of different lower molecular weight naphthenic acid families; viz acyclic, monocyclic, bicyclic and alkylbenzoic naphthenic acids. The spectrum of the ESMS analysis is presented in Figure 4.23, with the dominant cluster of ions appearing at around m/z 310 to m/z 318, with several of the ions within the cluster corresponding to some naphthenic acid species. However, the origin of this cluster within the sample is unknown and the clusters may be influencing the relative intensities of other ions present in the sample.

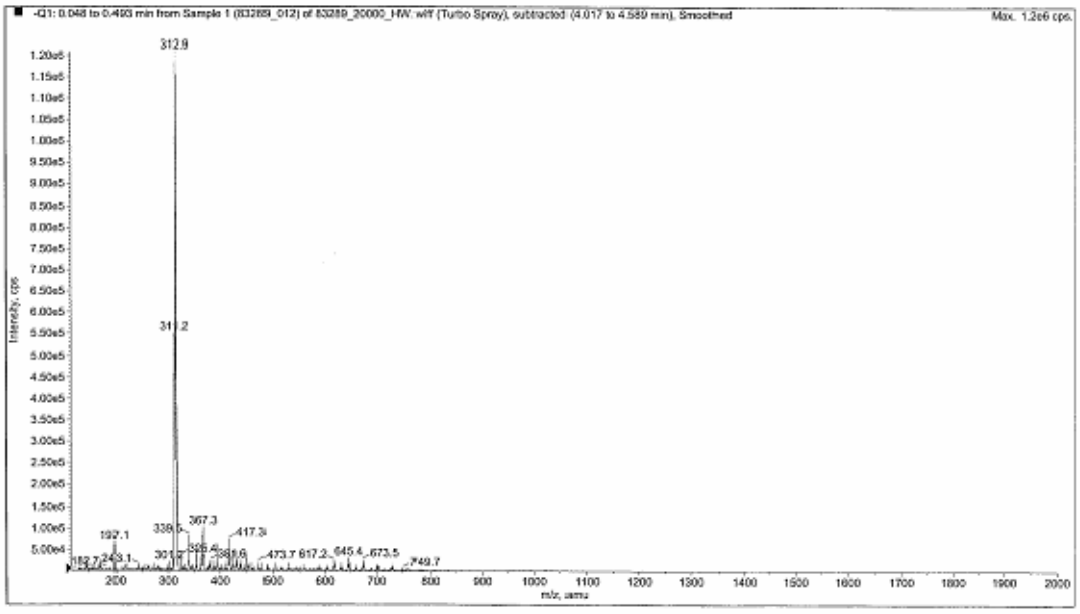

Figure 4.23: ESMS spectrum for the naphthenic acid extract from sample BRN.

The presence of low intensity ranges of acyclic (C_{10}, C_{16}, and C_{20} to C_{30}), monocyclic (C_9, C_{12}, C_{20}, C_{24} and C_{25}), bicyclic (C_{24}, C_{28} and C_{29}) and alkylbenzoic (C_{14}, C_{22} and C_{28}) naphthenic acid species were observed. Looking at the spectrum, there was some detection of clusters of ions between m/z 590 and m/z 735 (possibly part of an ion series). Although some of the ions within the cluster correspond to ions indicating the presence of naphthenic acids, the origins cannot be ascertained and it is not considered consistent with the typical ARN acid mass distribution. There was no evidence of higher molecular weight naphthenic acid species in these spectra.

The extract from sample NSA was only characterized using the atmospheric pressure chemical ionisation mass spectrometry (APCI-MS) technique to determine the naphthenic acid composition in the extract.

APCI-MS analyses of sodium carboxylate/emulsion extracts

Sample preparation prior to APCI-MS analysis was the same as for the ESMS case above. The prepared samples were analysed in the negative ion mode APCI-MS with mass spectra recorded from m/z 115 to m/z 2000. The background spectrum of the solvent used in these analyses is shown in Figure 4.24. The spectrum contains the following significant ion species at m/z 197.0 (C_{12} monocyclic naphthenic acid) and m/z 211.0 (C_{13} monocyclic naphthenic acid) which may increase the response of the corresponding acid species in the extract.

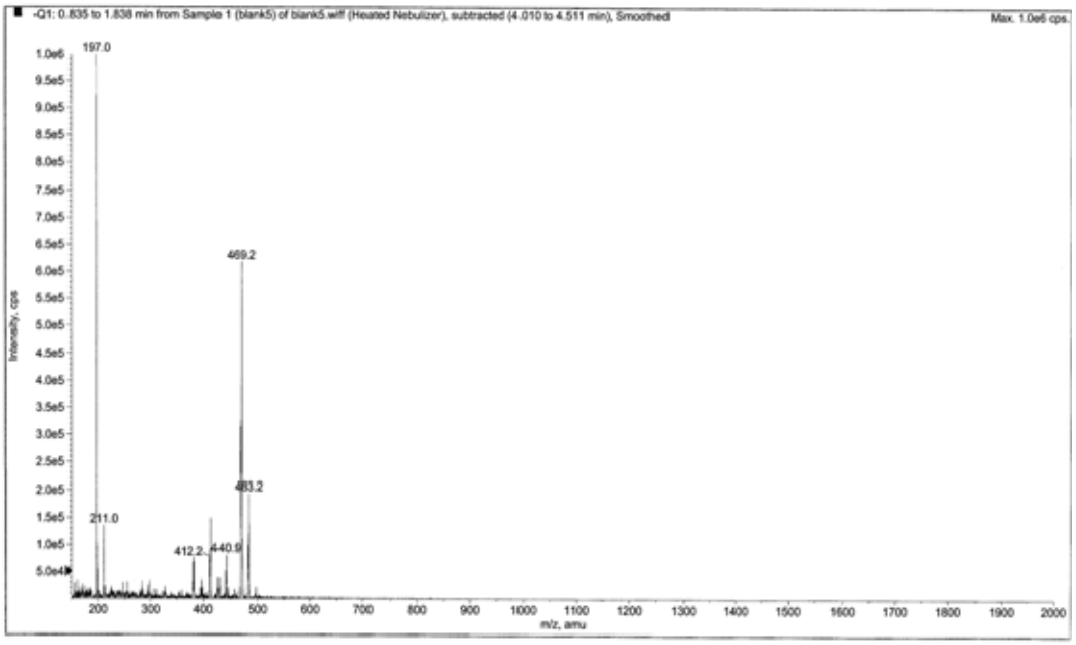

Figure 4.24: APCI-MS background spectrum

The APCI-MS spectrum of the naphthenic acid extract from sample TK-38S is presented in Figure 4.25. Lower molecular weight naphthenic acids i.e. acyclic, monocyclic, alkylbenzoic and traces of bicyclic were observed from the spectrum. The range of these

naphthenic acids present is as follows: acyclic (C_{28} and C_{29}), monocyclic (C_{10}, C_{24} and C_{29}), alkylbenzoic (C_{25}, C_{27}, and C_{29} to C_{31}), and some weak evidence of bicyclic (C_{16} to C_{46}) naphthenic acids. Also, some evidence of naphthenic acid of mass greater than m/z 680 has been detected; however, the responses are very weak relative to the background noise for the sample

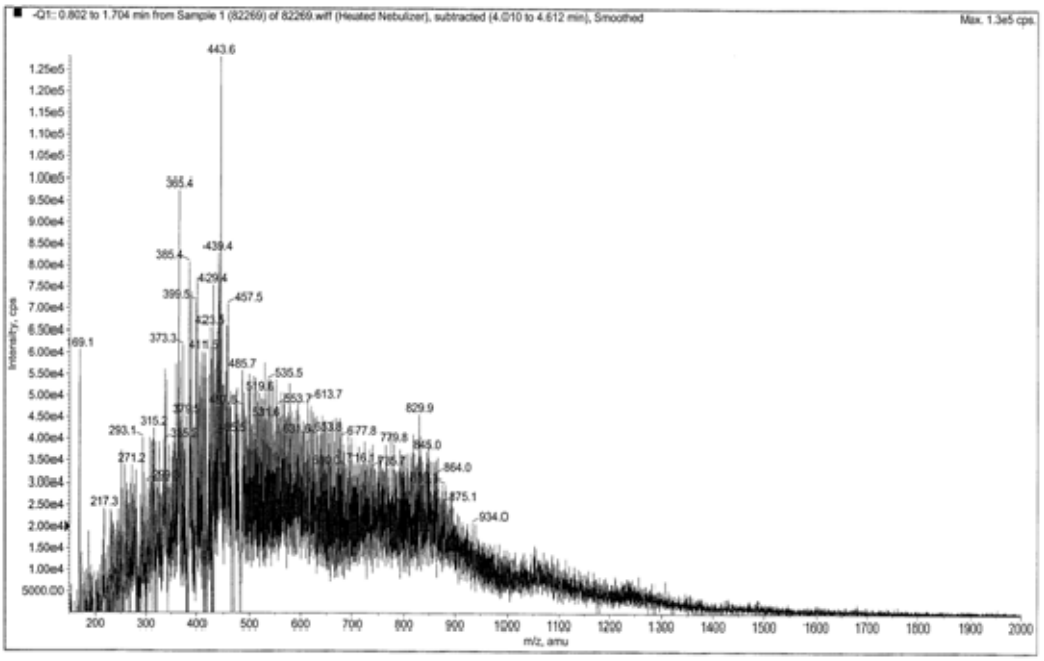

Figure 4.25: APCI-MS spectrum for the naphthenic acid extract from sample TK-38S.

Figures 4.26, 4.27 and 4.27a presents the APCI-MS spectra of extracts from samples DLG 53-1, DLG 53-2 and the expanded DLG 53-2 spectrum, respectively. The crude oil emulsion extract spectrum (DLG 53-1) shows a range of lower molecular weight acids in the range of m/z 150 to m/z 500, with a predominance of acyclic naphthenic acids (C_{20}, C_{24}, C_{26}, C_{28}-C_{30}, C_{32} and C_{34}) while traces of C_{24} monocyclic naphthenic acid, C_{30} bicyclic naphthenic acid and alkylbenzoic naphthenic acids (C_{30}-C_{32}) have been detected in the spectrum in Figure 4.26. The spectrum of the crude oil emulsion extract also shows the presence of further naphthenic acids of mass greater than m/z 680; however, the response of those ions was relatively weak compared to the peaks for the naphthenic acids ions at the lower mass range of m/z 150 to m/z 500. The ions observed are at m/z 829.9 and m/z 857.9, which could correspond to the C_{57} and C_{59} acyclic naphthenic acids, although there

is no clear evidence for other acidic species in this mass range, but they may be associated with multimerisation of some lower molecular weight naphthenic acids.

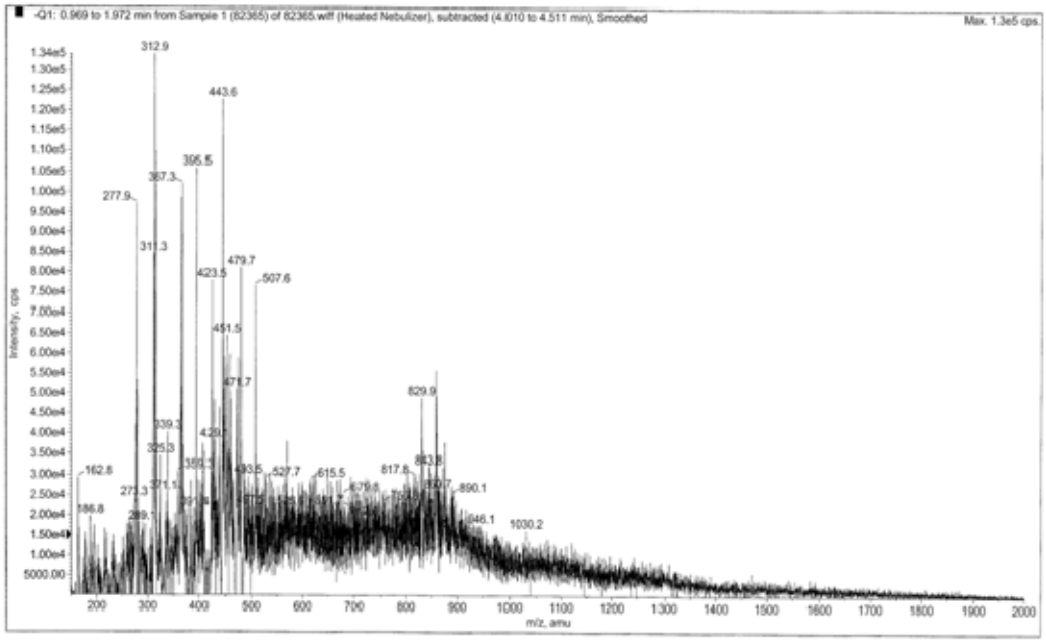

Figure 4.26: APCI-MS spectrum for the naphthenic acid extract from sample DLG 53-1.

The APCI-MS spectrum of the extract from the sodium carboxylate sludge (DLG 53-2) sample reveals an interesting result, where a sequence of acyclic naphthenic acids (C_{19} to C_{36}) was clearly identified with very minor trace evidence of monocyclic naphthenic acids (C_{10} and C_{26}-C_{30}), as can be seen from Figure 4.27. The acyclic naphthenic acid distributions from the spectrum in Figure 4.27a showed a predominance of even-over-odd carbon number distribution and a similar trend has already been reported with the crude oils from the same petroleum basin from where these samples were obtained (Curiale *et al.,* 2005).

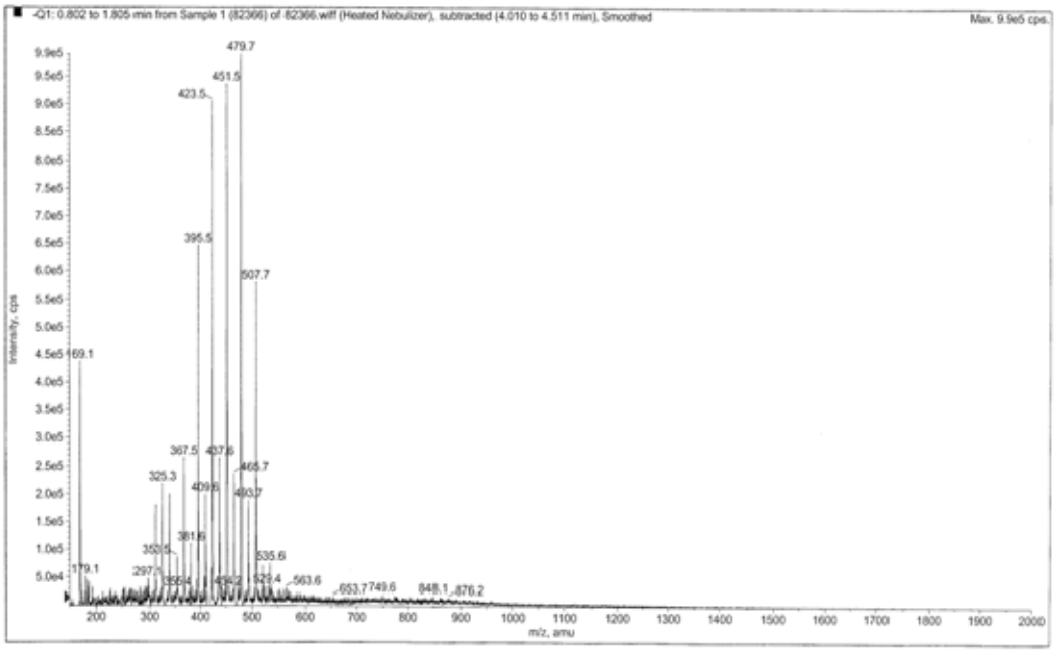

Figure 4.27: APCI-MS spectrum for the naphthenic acid extract from sample DLG 53-2.

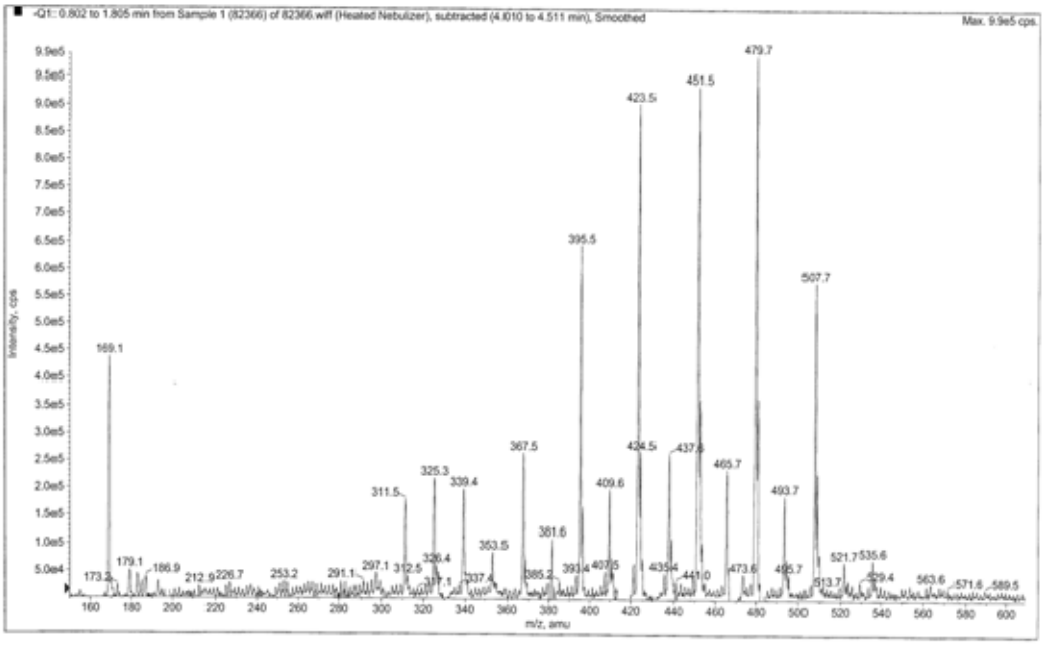

Figure 4.27a: APCI-MS spectrum for the naphthenic acid extract from sample DLG 53-2—Expanded version.

The APCI-MS spectrum of the sodium naphthenate extract (BRN) is presented in Figure 4.28. This spectrum revealed an interesting result where a sequence of acyclic naphthenic acids (C_{20} to C_{36}) was clearly identified. C_{24} monocyclic naphthenic acid was also detected in the spectrum, with minor trace evidence of monocyclic (C_{16}, C_{18}, C_{20}, C_{22}, C_{23}, C_{25} to C_{38} and C_{42} to C_{45}), bicyclic (C_{16}, C_{18}, C_{20}, C_{24}, C_{26}, C_{27}, C_{29} to C_{33}, C_{35} and C_{37}) and alkylbenzoic (C_{18}, C_{21}, C_{24}, C_{25}, C_{27}, C_{29} to C_{31}, C_{33} to C_{35}, C_{37} and C_{38}) naphthenic acid species. The acyclic naphthenic acid distributions from the spectrum showed a predominance of even-over-odd carbon number distribution in Figure 4.28a. A similar trend has already been reported with the crude oil samples from the petroleum basin where sample DLG 53-2 was sourced. The spectrum also showed some distribution of further naphthenic acids of mass greater than m/z 665. However, the responses are relatively weak compared to the background noise of the sample. Clusters of ions between m/z 670 to m/z 935 were detected (possibly part of an ion series). Although some of the ions within these clusters correspond to ions indicating the presence of naphthenic acids, the origin of these clusters is unknown.

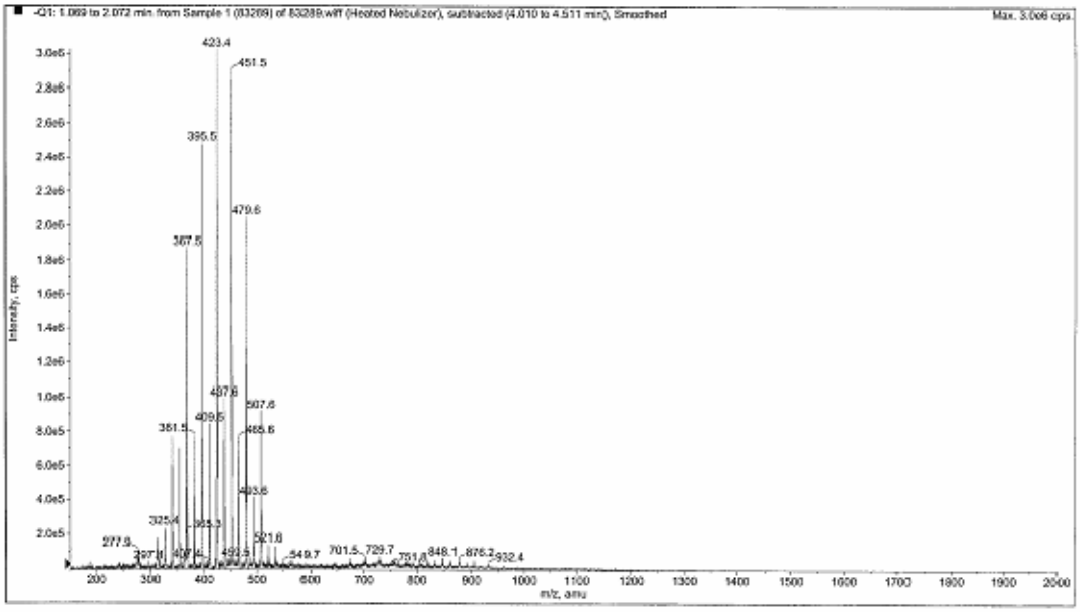

Figure 4.28: APCI-MS spectrum for the naphthenic acid extract from sample BRN.

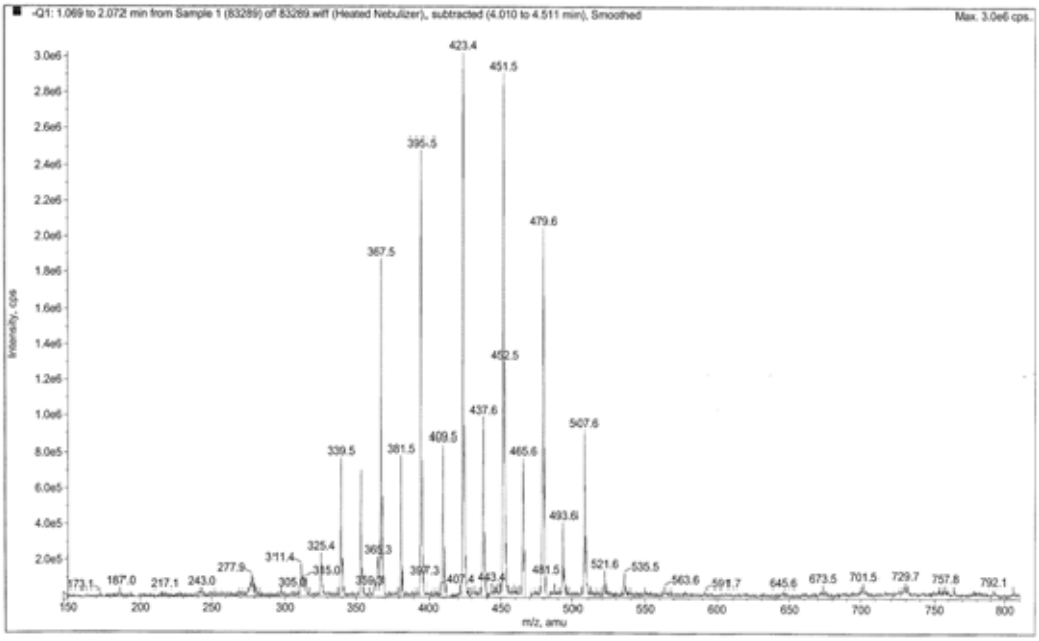

Figure 4.28a: APCI-MS spectrum for the naphthenic acid extract from sample BRN—Expanded version.

The APCI-MS extract analysis of sample NSA is shown in Figure 4.29. The presence of bicyclic naphthenic acid with very few acyclic, monocyclic and alkylbenzoic naphthenic acid species was observed in this spectrum. The presence of C_{24} acyclic, C_{24} monocyclic, C_{28} alkylbenzoic and bicyclic (C_{18}, C_{24} and C_{28}) naphthenic acids was observed. In addition, weak evidence was also seen for the presence of acyclic (C_{18} to C_{23} and C_{25} to C_{40}), monocyclic (C_{14}, C_{18} to C_{23} and C_{25} to C_{40}), bicyclic (C_{21} to C_{23}, C_{25} to C_{27} and C_{29} to C_{40}) and alkylbenzoic (C_{21} to C_{27} and C_{29} to C_{40}) naphthenic acids. The presence of further naphthenic acids of mass greater than m/z 595 was seen. However, the responses are weak relative to the background noise of the sample, and are hence difficult to identify. In all the extracts analysed from the sodium carboxylate/emulsion samples, there was no trace of higher molecular weight naphthenic acid (ARN).

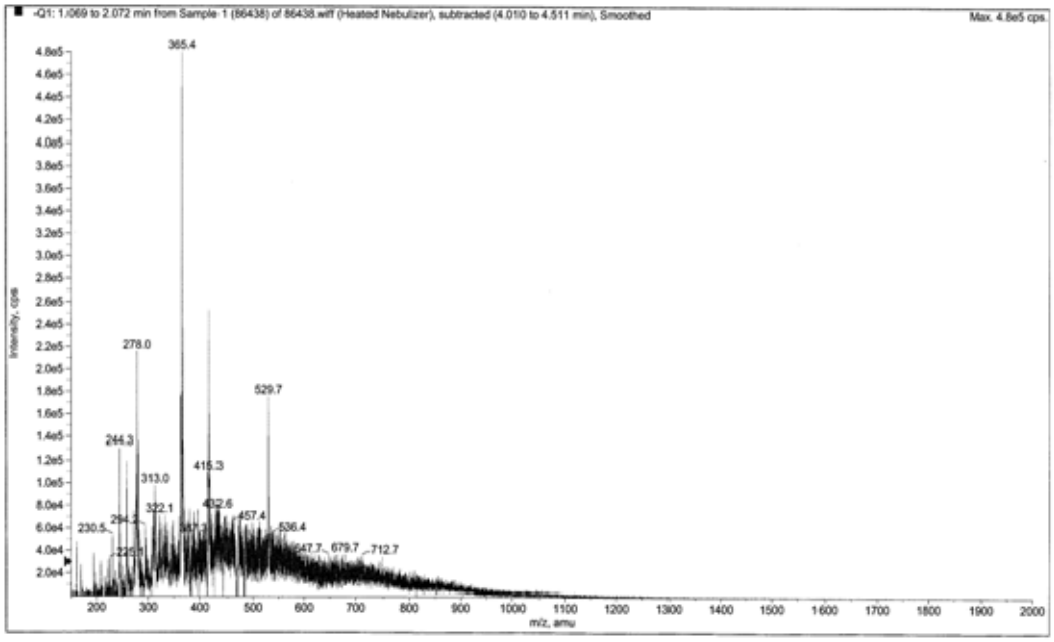

Figure 4.29: APCI-MS spectrum for the naphthenic acid extract from sample NSA.

4.4 ANALYSES OF CRUDE OIL SAMPLES

Two crude oil samples from the North Sea (from UK and Norway) were used for the naphthenic acid extraction and characterization. The extraction procedure used was an Acid-IER resin and alcoholic potassium hydroxide (KOH) procedure which is fully described in Chapter 3, Section 3.2.3. The characterization of the naphthenic acid extracts was carried out using ESMS and APCI-MS techniques as already described in detail above. Direct spectroscopic analysis, i.e. ESMS and APCI-MS of the crude oil samples, was also conducted and the results reported in this section. Results from the two different methods of naphthenic acid extraction are quite similar. A general description of the crude samples used in this study and an overview of extract identification for ESMS and APCI-MS analyses are presented in Table 4.4 below:

Sample	Location of Crude Oil	Physical Description
HD C	North Sea (Norway Sector)	Brown thick crude
HDN C	North Sea (Norway Sector)	Brown thick crude
BLK C	North Sea (UK Sector)	Dark brown, very thick crude
HD CR	North Sea (Norway Sector)	Naphthenic acid extract from the resin extraction
HDN CA	North Sea (Norway Sector	Naphthenic acid extract from alcoholic KOH extraction
BLK CR	North Sea (UK Sector)	Naphthenic acid extract from resin extraction

Table 4.4: Brief description of the crude oil samples and the corresponding extracts used in this research studies.

ESMS analyses of crude oils and crude oil extracts using (Acid-IER and alcoholic KOH)

Aliquots of the extracts (HD CR, HDN CA and BLK CR) were treated and prepared for ESMS analysis as in the above samples, as described in Section 4.2.1. Figures 4.30 and 4.31 show the spectra of the samples (HD CR and BLK CR) extracted using Acid-IER resin technique (Mediaas *et al.,* 2003). The spectra showed a wide range of lower molecular weight naphthenic acids in the range (m/z 200 to m/z 600) which correspond to the ion species of acyclic, monocyclic, bicyclic and alkylbenzoic naphthenic acids. The presence of identifiable acyclic (C_{15} to C_{40}), monocyclic (C_{14} to C_{29}), bicyclic (C_{14} to C_{27}) and alkylbenzoic (C_{15} to C_{22}) naphthenic acids are observed in Figure 4.30.

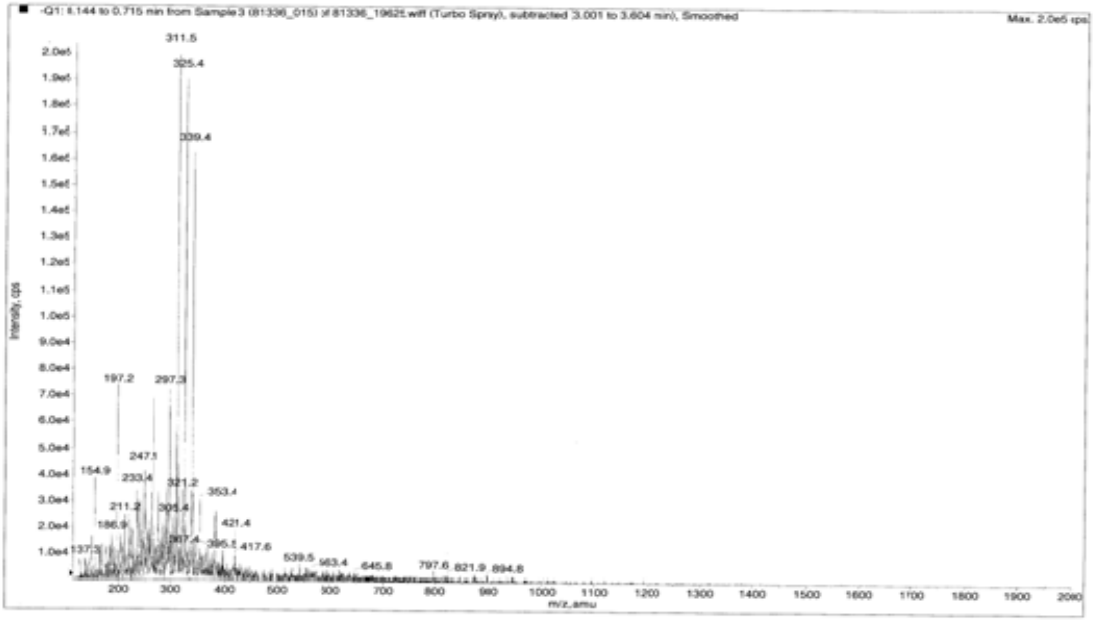

Figure 4.30: ESMS spectrum for crude oil extract (Acid-IER) sample HD CR.

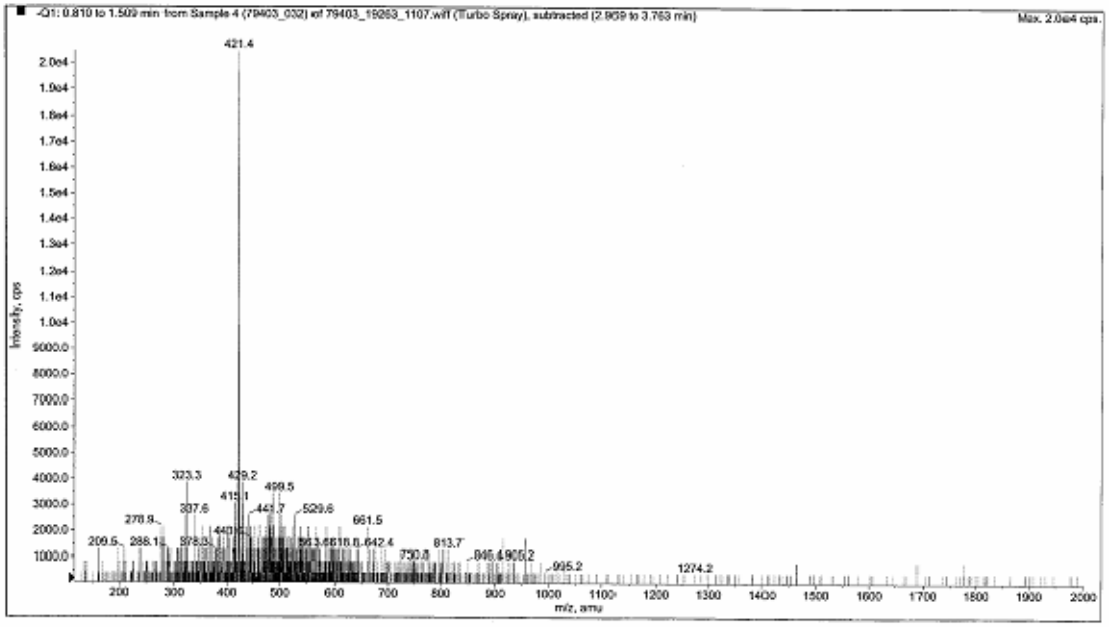

Figure 4.31: ESMS spectrum for crude oil extract (Acid-IER) sample BLK CR.

The sample BLK CR spectrum revealed the presence of acyclic (C_{11} and C_{13} to C_{26}), monocyclic (C_9 to C_{22}, C_{24} and C_{28}), bicyclic (C_{15} to C_{21}) and alkylbenzoic (C_9 to C_{24}) naphthenic acids species. However, there was no clear evidence of the presence of higher

molecular weight naphthenic acids (ARN), although a very weak signal was observed at around m/z 1230 in Figure 4.31. This may be too low to be reported as the presence of a definite ARN acid. The ESMS spectrum of the crude oil sample HD C is presented in Figure 4.32, and this is dominated by five significant ions out of which two ion peaks (m/z 249.0 and m/z 385.1) are not readily assigned to any of the targeted acids groups (i.e. lower to higher molecular weight naphthenic acids), whilst the remaining three provide evidence for the ions indicating the presence of the following acids: C_{13} alkylbenzoic (m/z 205.0; weak evidence), C_9 monocyclic (m/z 155.2) and C_{35} acyclic (m/z 521.0). However, the spectrum is not typical of a naphthenic acid distribution. There was no evidence for the presence of high molecular weight acids (ARN) in the crude oils spectra.

The naphthenic acid extract analysis of the sample HDN CA from the potassium hydroxide (KOH) extraction technique was carried out using APCI-MS.

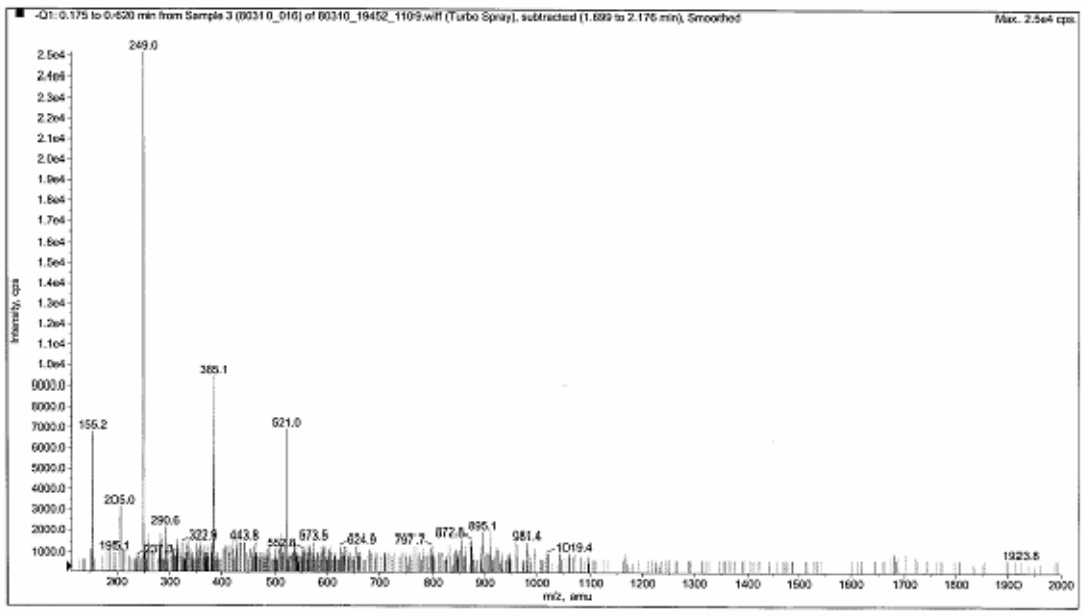

Figure 4.32: ESMS spectrum for crude oil sample HD C.

APCI-MS analyses of crude oils and crude oil extracts (Acid-IER and alcoholic KOH)

The crude oil Acid-IER extract samples (HD CR and BLK CR) were prepared for APCI-MS analysis in a similar way to those analysed previously and the spectra are presented in Figures 4.33 and 4.34 respectively. The spectrum of extract sample HD CR (Figure 4.33) revealed the presence of a wide range of lower molecular weight naphthenic acids (acyclic, monocyclic, bicyclic and alkylbenzoic), including acyclic (C_{16} to C_{48}), monocyclic (C_{10} to C_{48}), bicyclic (C_{15} to C_{48}) species and some traces of alkylbenzoic naphthenic acids. There was no indication of any ARN acid species in the spectra, which may be related to the level of higher molecular naphthenic acid concentration in the crude oil sample. The spectrum of the extract BLK CR presented in Figure 4.34 showed the presence of a wide range of lower molecular weight naphthenic acids (acyclic, monocyclic, bicyclic and alkylbenzoic) and some weak evidence of higher molecular weight naphthenic acid (ARN) ion peaks. The presence of acyclic (C_{10} to C_{32}, C_{34} and C_{42}), monocyclic (C_{10}, C_{11}, C_{13} to C_{30}, C_{38} and C_{42}), bicyclic (C_{11} to C_{27}, C_{29} and C_{42}) and alkylbenzoic (C_{10} to C_{28} and C_{30}) naphthenic acids were also noted in the spectrum. Also a cluster of ions from m/z 1229 to m/z 1238 was detected, providing weak evidence for the presence of ARN acids in the extract. In addition, the presence of a high mass ion cluster at m/z 1180 to m/z 1220 was also observed, with two of the ions within this cluster indicating the presence of naphthenic acids. However, the origin of these clusters could not be properly ascertained and is not considered consistent with typical ARN acid mass distribution.

The spectrum of the naphthenic acid extract (HDN CA) from the alcoholic potassium hydroxide (KOH) extraction procedure is shown in Figure 4.35. A broad distribution of lower molecular naphthenic acids was observed. The naphthenic acid distribution from the spectrum is in the range of m/z 200 to m/z 650. Presence of acyclic (C_{19} to C_{24} and C_{26} to C_{36}), monocyclic (C_{15} to C_{36} and C_{38}), bicyclic (C_{14} to C_{35} and C_{37}) and alkylbenzoic (C_{17} to C_{35}) naphthenic acid species are observed. In addition, an indication for the weak evidence of acyclic (C_{15} to C_{18}, C_{25} and C_{37} to C_{42}), monocyclic (C_{14}, C_{37} and C_{39} to C_{42}), bicyclic (C_{12}, C_{13}, C_{36}, C_{38} to C_{42}) and alkylbenzoic (C_{15}, C_{16} and C_{36} to C_{42}) naphthenic acids were seen from the spectrum. There was some weak evidence of further naphthenic acids of mass greater than m/z 620. However, the responses are weak relative to the background

noise of the sample from the spectrum, hence; those peaks could not properly be identified. No trace of higher molecular weight naphthenic acid (ARN) is seen in this spectrum. The naphthenic acid distribution from sample HDN CA is quite similar to that of sample HD CR.

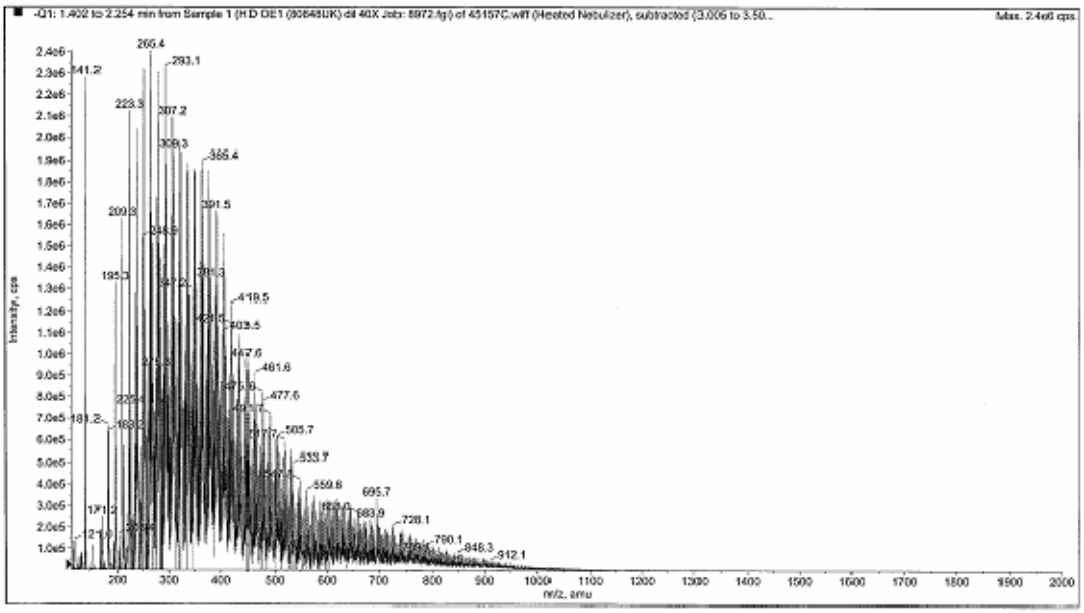

Figure 4.33: APCI-MS spectrum for crude oil extract (Acid-IER) sample HD CR.

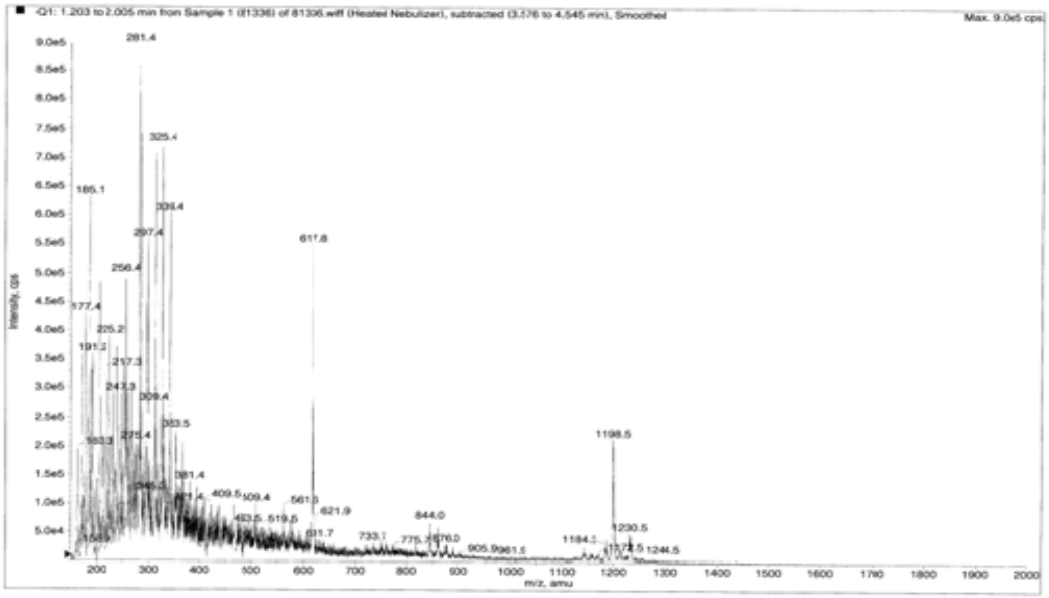

Figure 4.34: APCI-MS spectrum for crude oil extract (Acid-IER) sample BLK CR.

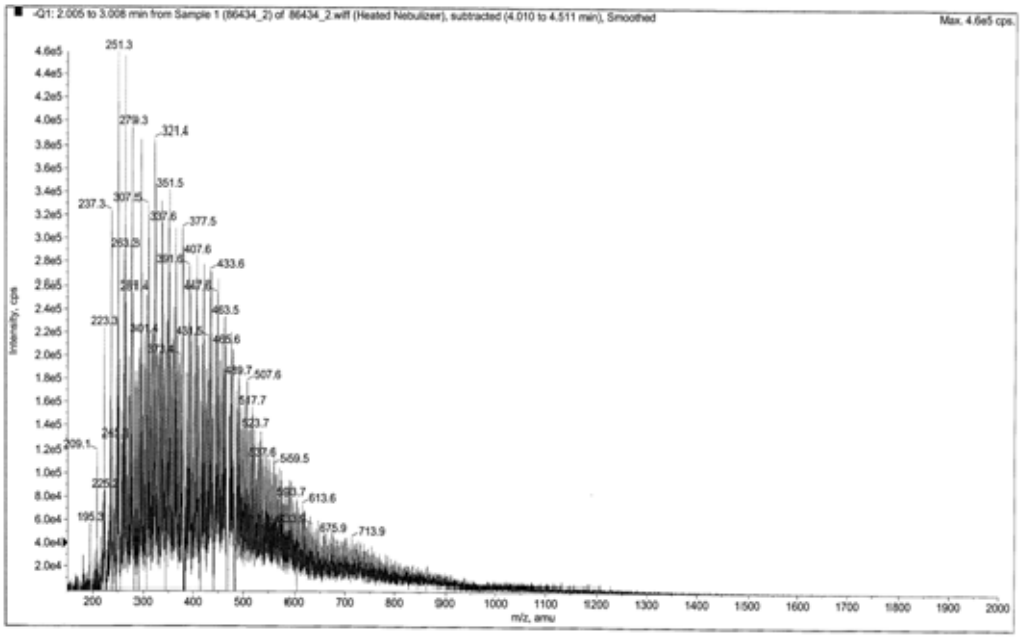

Figure 4.35: APCI-MS spectrum for crude oil extract (alcoholic KOH) sample HD CA.

4.5 RE-PRECIPITATION EXPERIMENT—EXTRACTION AND ANALYSES

The experiment was carried out using naphthenic acid extract from sample HDN 3 and pH adjusted brine (pH 9 and pH 9.5). The main reason for carrying out this particular type of experiment is to address the following specific question:

If a given naphthenic acid deposit is fully digested (using the procedure described in Chapter 3, Section 3.2.4) and then it is re-precipitated, do we obtain (i) a deposit of the same composition as the original? or (ii) a deposit based on selective deposition/precipitation of only certain (probably higher molecular weight) naphthenic acid components?

This has some very important consequences for a range of issues concerned with naphthenate field management, the experimental determination of deposit composition and naphthenate inhibitor testing. The fully digested deposit, for which the APCI-MS spectrum is shown in Figure 4.14, was re-precipitated as shown in Figure 4.36. It was clearly observed that abundant naphthenate deposit forms at both pH values. This deposit is the re-precipitated original field deposit and it is of great interest to establish if the composition of

this deposit closely resembles the original one and, more specifically to establish if it still includes a significant fraction of the lower molecular weight species present in the original deposit.

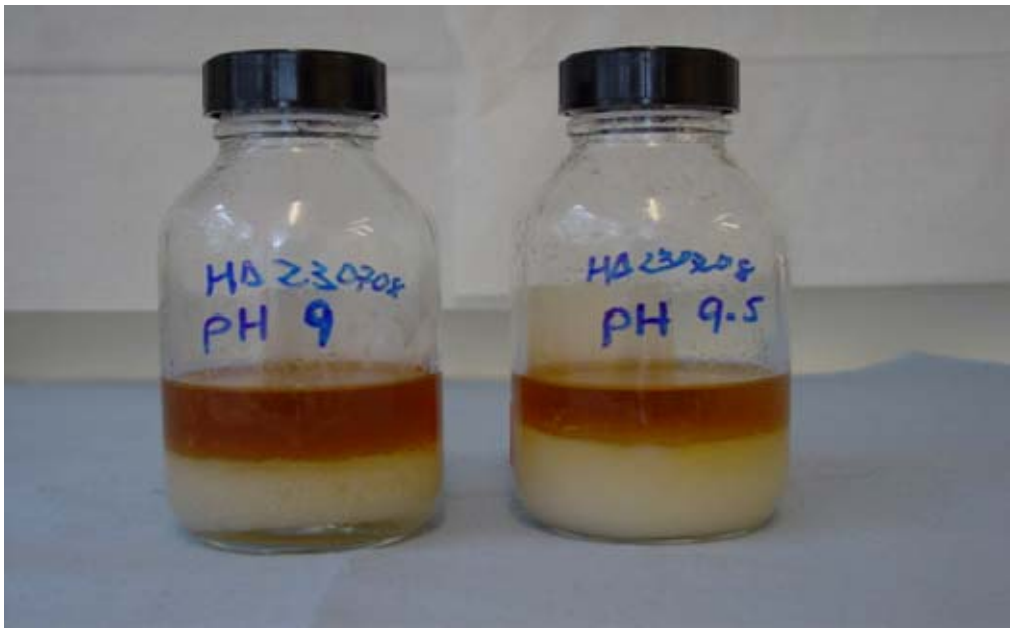

Figure 4.36: Re-precipitation bottle experiment at pH 9 and pH 9.5 using oil phase an water phase.

ESMS and APCI-MS analyses of the dissolved precipitate obtained from the re-precipitation experiment (presumably pure calcium naphthenate) are presented in the spectra shown in Figures 4.37 and 4.38, respectively.

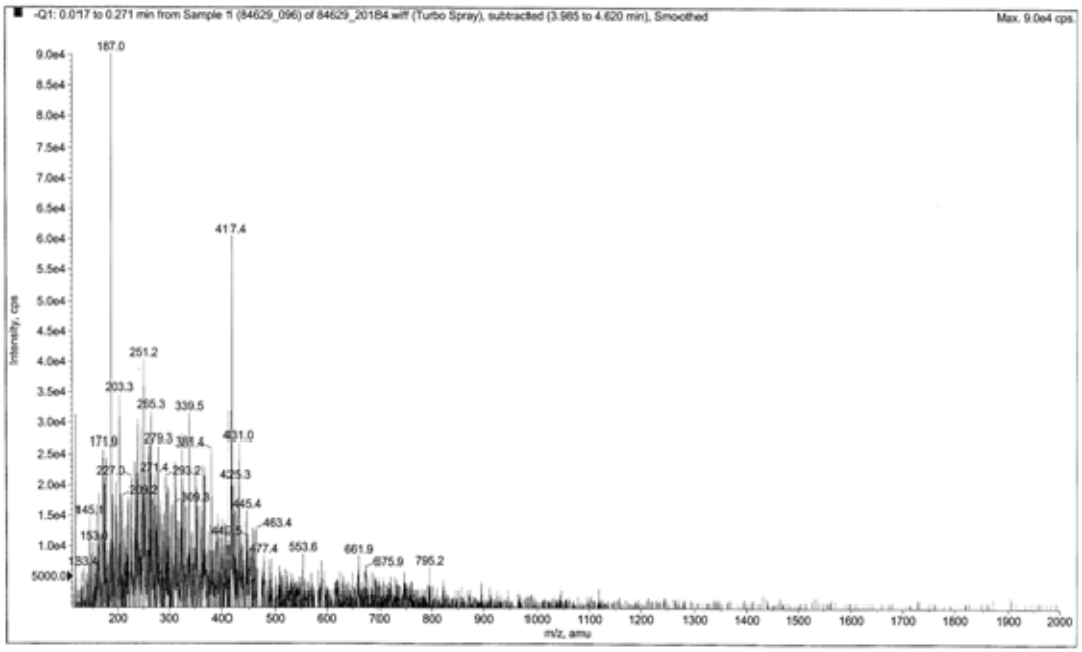

Figure 4.37: ESMS spectrum for the naphthenic acid extract from re-precipitation experiment.

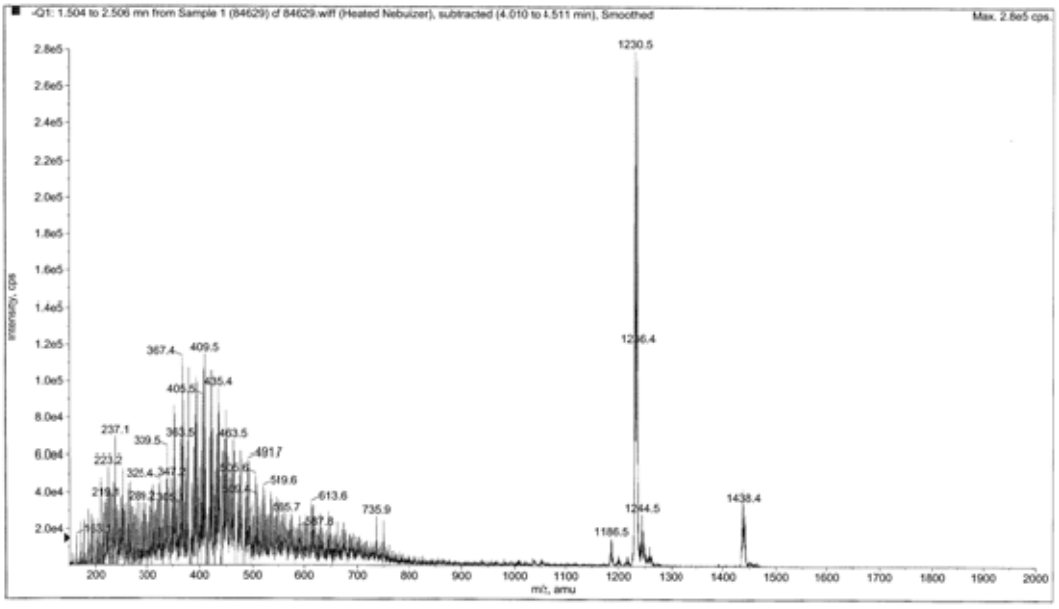

Figure 4.38: APCI-MS spectrum for the naphthenic acid extract from re-precipitation experiment.

The spectra clearly show that both lower and higher molecular weight naphthenic acids are present in both the original and re-precipitated samples. The lower molecular naphthenic

acids appeared in the range of m/z 200 to around m/z 700 consisting of acyclic, monocyclic, bicyclic and alkylbenzoic naphthenic acids and a very clear ion peak at m/z 1230.5 corresponding to "ARN" acid species was observed from the APCI-MS spectrum in Figure 4.38. Comparison of APCI-MS spectra (Figure 4.38) of the naphthenic acid extract from the laboratory formed calcium naphthenate (pure sample) with the naphthenic acid extract from field calcium naphthenate deposit (Figure 4.14) shows an almost exact replica of the original spectrum, with the presence of both lower molecular naphthenic acids in the region of m/z 200 to around m/z 700 and higher molecular weight naphthenic acid at around m/z 1230. The spectrum from the re-precipitated samples shows a distribution of lower molecular weight naphthenic acids comprising acyclic (C_{21} to C_{24} and C_{26} to C_{33}), monocyclic (C_{24} to C_{34}), bicyclic (C_{13} to C_{17} and C_{24} to C_{32}) and alkylbenzoic (C_{15}, C_{25}, C_{27} and C_{29} to C_{31}) acid species. In addition, a cluster of ion peaks at M/z 1225 to m/z 1270 was detected with a strong ion peak at m/z 1230.5 corresponding to the presence of ARN acids. Furthermore, an observation of a cluster of ions at m/z 1430 to m/z 1465 of unknown origin was made. However, it should be noted that similar ion clusters of this mass range were seen in the ARN reference standard under the same conditions. A direct comparison of the two APCI-MS spectra of the original HDN 3 sample deposit and the re-precipitated HDN 3 deposit is presented in Figure 4.39 where it is clearly observed that the spectra are virtually identical and have similar distributions of naphthenic acids.

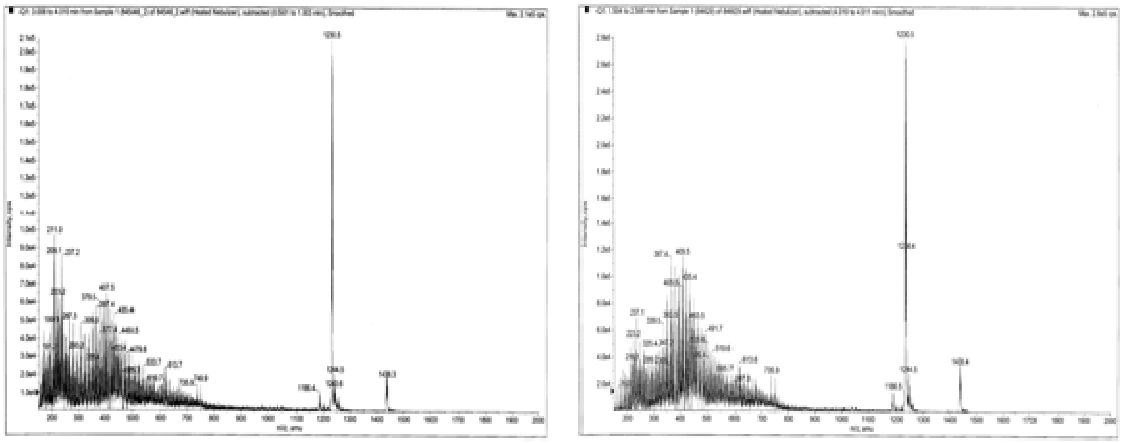

Figure 4.39: APCI-MS spectrum for the naphthenic acid extracts from calcium deposit and re-precipitation experiment.

4.6 COMPARISON BETWEEN ESMS AND APCI-MS TECHNIQUES

In an earlier part of this chapter, it was obvious that extracts analysed using ESMS show a somewhat different pattern of naphthenic acid distribution to those extracts analysed using APCI-MS techniques. The principle on which the two spectroscopic techniques (ESMS and APCI-MS) work is by utilising a "soft" ionisation mechanism. The method involves the generation of ions without thermally fragmenting them for mass spectrometry analysis. The two techniques (ESMS and APCI-MS) differ in the details of precisely how ionisation is induced. In ESMS, ionisation is achieved as a result of a potential difference between the spray needle and the cone along with rapid but gentle solvent evaporation. In APCI-MS, the analyte solution goes into the pneumatic nebuliser and the solvent is evaporated in a heated quartz tube prior to interacting with the corona discharge, creating ions for mass spectrometry analysis. In APCI-MS, ionisation due to charge transfer is facilitated with polar molecules during the corona discharge. It can be expected that charge transfer will be favoured by the presence of ARN acid species. This may explain the low level of lower molecular weight naphthenic acid species in the APCI spectrum compared to the ESMS. Preferential ionisation of higher molecular weight acids with APCI-MS over ESMS was also reported when tested on some commercial naphthenic acids samples (Chang *et al.,* 2000) with the higher molecular weight species showing at least one order of magnitude more sensitivity. Formation of unwanted clusters (multimers) from the APCI-MS technique during the analysis of the higher molecular weight naphthenic acids was also reported (Rudzinski *et al.,* 2002). Comparisons between the ESMS and APCI-MS spectra revealed a clear distinction regarding the intensities of higher molecular weight to lower molecular weight naphthenic acids. In their studies, Hsu *et al.,* (2000) showed that the ESMS signal was an order of magnitude lower than APCI-MS, but only for low polarity solvents. This might be attributed to enhanced charge transfer in the APCI source with more polar solvents. In ESMS, the samples are injected in an ionized form, by addition of an alkali, for instance. Rudzinski *et al.,* (2002) compared both APCI-MS and ESMS sources with standard acid mixtures as well as individual naphthenic acid solutions. For example, the ESMS spectra of samples HD 1, HD 2, HD 3, WB 3 and WB CR showed a similar trend of naphthenic acid distribution with a broad range of lower molecular weight naphthenic acids in the region around m/z 200 to m/z 700 and some clusters of ion peaks at

around m/z 1230 to m/z 1300, which is considered to be associated with the higher molecular weight naphthenic acids (ARN) (Thomas *et al.,* 2005). These higher molecular weight naphthenic acids, referred to as "ARN" acids, are identified again from the spectra, using software which can accurately detect the species based on accurate molecular weights. These particular clusters of "ARN" peaks have now been observed very frequently by many workers in the field. The corresponding APCI-MS spectra of the above mentioned samples revealed distinctively the enhancement of the ARN acid which are clearly speciated and this can be seen (for example) in Figures 4.2 and 4.11. However, the ESMS spectra of sample BLK 3 and BBAY 3 show very weak evidence of the lower molecular weight naphthenic acids, with no indication of ARN acids, whilst the APCI-MS spectra clearly show the presence of pronounced ARN acid ion peaks as can be seen (for example) in Figures 4.9 and 4.16. The sensitivity parameters were reported to influence the detection level of naphthenic acids in the samples analysed. Shepherd *et al.,* (2008), showed that factors such as ion spray voltage (ISV), nebulizer gas (NEB) and curtain gas flow rates (CUR) as well as the type of solvent used (depending on the polarity) all play a significant role in the detection of higher molecular weight naphthenic acid (ARN) species.

4.7 ELEMENTAL COMPOSITION OF CALCIUM NAPHTHENATE SAMPLES

The morphological appearance of the various samples studied in this thesis has been described in Table 4.1 above, with different types of textures from sticky to non-sticky, light brown to dark brown and hard to slightly soft. The techniques used to study the morphology and elemental composition of these deposits are Environmental Scanning Electron Microscopy and energy dispersive X-ray (ESEM - EDAX). ESEM/EDAX analysis of field calcium naphthenate field deposit was carried out and the results are presented in this chapter. Figure 4.40 presents the ESEM images obtained for the field calcium naphthenate deposit samples (HD, HDN, WB and BBAY). The images from the ESEM analysis revealed heterogeneous surfaces which represent non-crystalline hydrocarbon matrices with a range of trace compounds.

The mass and atomic weight percentages for the samples analysed and shown in Figure 4.40 are presented in Table 4.6 below, as given by EDAX. Each result presented in Table 4.6 in percentage (%) is the average of two measurements. The results revealed that the field calcium naphthenate deposits are mainly composed of carbon and oxygen whilst the predominant cation present in the deposit is calcium as well as some amount of sodium in smaller proportions. However, the ESEM/EDAX measurements show other inorganic scales entrained within the calcium naphthenate deposit samples analysed.

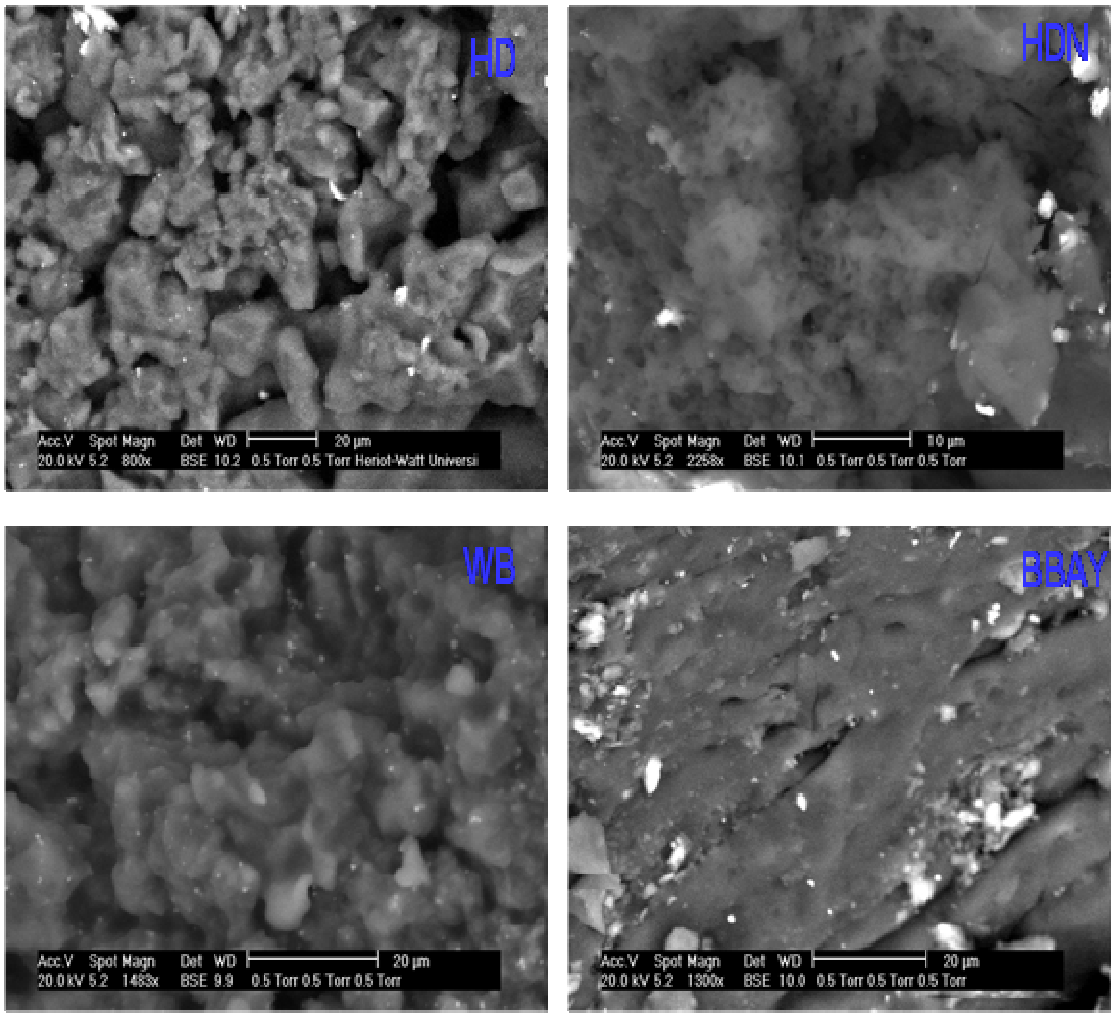

Figure 4.40: ESEM images for calcium naphthenate samples HD, HDN, WB and BBAY.

Table 4.6 shows a good correlation for the main cation present in the field samples. The deposit samples analysed are calcium naphthenate field samples and it was observed that

the % atomic weight composition of the calcium ion is much higher than the % atomic weight composition of the sodium ion. This is expected of calcium naphthenate as a product of interphase reaction between the naphthenic acids in the crude oil with the calcium cation in the formation water. The carbon/calcium ratio calculated for the samples analysed showed a lower value as compared to the carbon/sodium ratio.

Field	**HD**		**HDN**		**WB**		**BBAY**	
Element	Wt %	At %	Wt %	At %	Wt %	At %	Wt %	At %
C	91.91	95.30	88.74	92.98	92.88	95.41	85.69	90.55
O	4.40	3.42	7.26	5.71	4.80	3.7	9.78	7.76
Na	0.39	0.21	0.12	0.06	0.36	0.2	0.22	0.12
Mg	X	X	X	X	0.13	0.07	0.45	0.23
Al	X	X	X	X	X	X	0.38	0.18
Si	X	X	0.2	0.09	0.13	0.06	0.83	0.38
S	0.35	0.13	0.32	0.12	0.34	0.13	0.24	0.09
Cl	0.30	0.11	0.18	0.06	0.55	0.19	X	X
Ca	2.66	0.83	2.84	0.89	0.80	0.25	1.52	0.48
Fe	X	X	0.35	0.08	X	X	0.9	0.2
C/Ca		114.82		104.47		381.64		188.65
C/Na		453.81		1549.67		477.05		754.58

Table 4.5: EDAX data for some field calcium naphthenate deposit samples analysed

4.8 ESMS AND APCI-MS DATA ANALYSIS

Electrospray mass spectrometry (ESMS) and atmospheric pressure chemical ionisation mass spectrometry (APCP-MS) data for the extracts analysed from calcium naphthenate deposit samples (HD 2 and BBAY) and sodium carboxylate/emulsion samples (DLG 53-2 and BRN) were plotted and presented in Figures 4.41 and 4.42 respectively. It was observed from Figure 4.41 that the plot for sample HD 2 shows a broad distribution in the m/z range of ~200 to 650 which corresponds to the distribution of lower molecular weight naphthenic acid species. A small but pronounced peak of ions was detected at around m/z

1230 to m/z 1239 in the plot which can be positively associated with the presence of high molecular weight acid (Baugh *et al.,* 2004). . However, the APCI-MS data plot for the extract from sample HD 2 indicates much more speciation of the higher molecular weight naphthenic acid (ARN) with a similar distribution of the lower molecular weight naphthenic acids as in ESMS data plot. The ESMS data plotted for the extract from sample BBAY indicates some naphthenic acid distribution within the m/z 200 to 650, showing an ion intensity response, although a strong ion peak was seen at around m/z 313. This strong ion peak at around m/z 313 was associated with the ARN (m/z 1230) ion fragment which was suspected to be thermally fragmented during the ESMS analysis. The APCI-MS plot of sample BBAY shows a pronounced ion peak plotted at around m/z 1230 which corresponds to the ARN acid species.

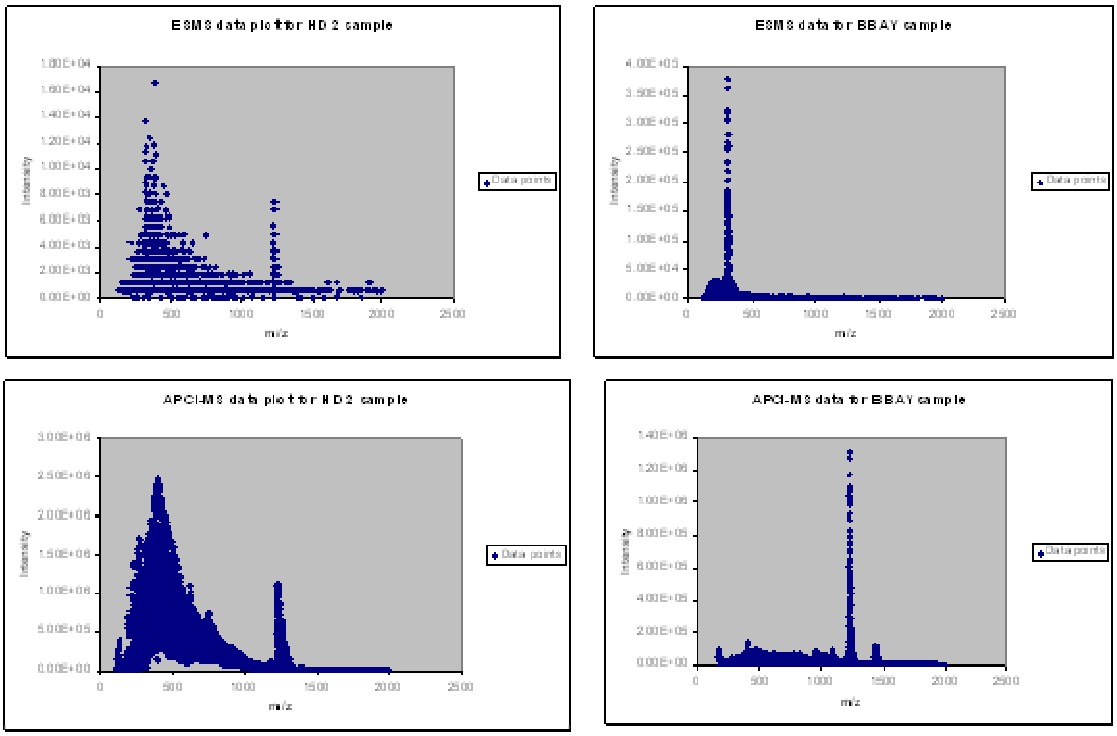

Figure 4.41: ESMS and APCI-MS data plot for calcium naphthenate deposit samples HD 2 and BBAY.

This plot for the two samples, HD 2 and BBAY, clearly shows two types of naphthenic acid distributions as follows; (i) abundant lower molecular weight naphthenic acids with small but pronounced higher molecular weight naphthenic acid and (ii) very few traces of lower molecular weight naphthenic acid with significant presence of a higher molecular

weight naphthenic acid species. The data plot from the sodium carboxylate/emulsion samples DLG 53-2 and BRN presented in Figure 4.42 shows that both the ESMS and APCI-MS data plots have similar distribution of naphthenic at around m/z 200 to m/z 550, which corresponds to distribution of lower molecular weight naphthenic acids. In all the sodium carboxylate/emulsion samples analysed in this thesis, there was no sample which shows any indication of the presence of higher molecular weight naphthenic acids (ARN).

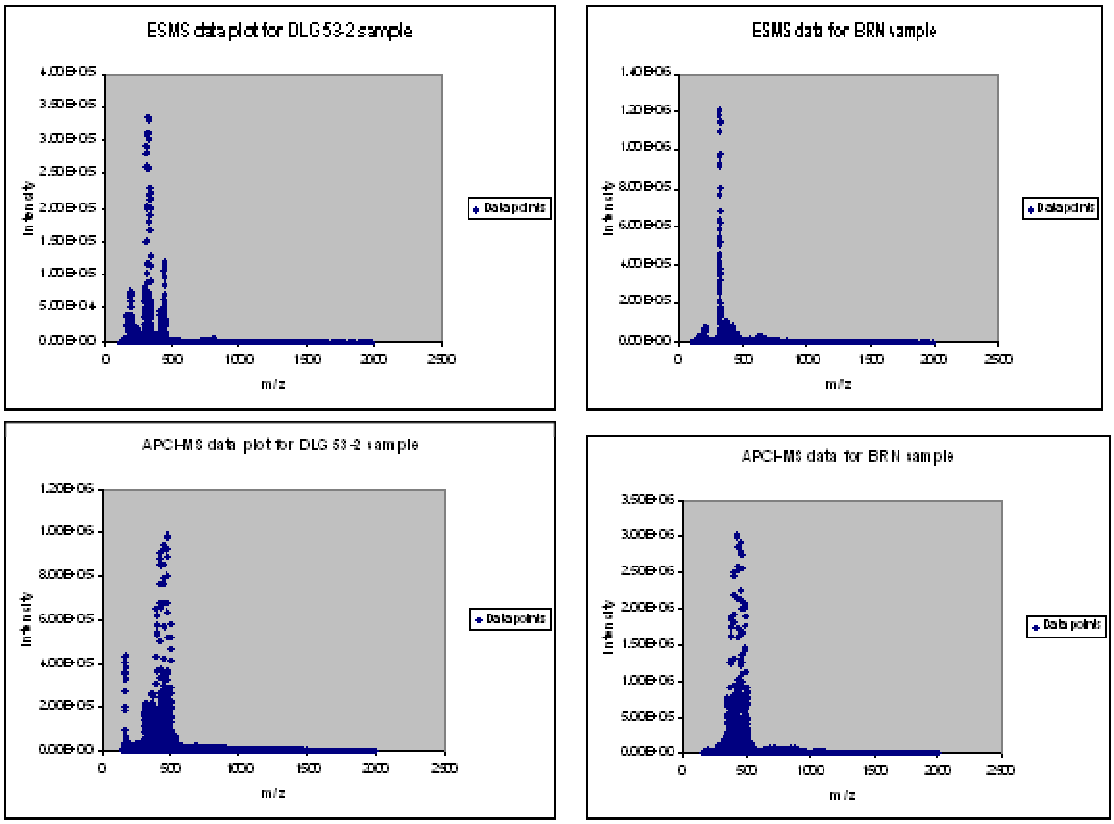

Figure 4.42: ESMS and APCI-MS data plot for sodium carboxylate/emulsion samples DLG 53-2 and BRN.

4.9 SUMMARY AND CONCLUSIONS

The analyses and characterization of field naphthenate deposit samples (i.e. calcium naphthenate, sodium carboxylate/emulsion and crude oils) has led to the development of a series of techniques resulting in a procedure for reliably extracting and characterizing the naphthenic acid present in these samples. The extraction methods developed here led to the

full digestion of all of the organic components in the calcium and sodium naphthenate field deposits. A range of different extraction techniques, the re-precipitation experiment and subsequent naphthenic acid extraction, soft ionisation sources (i.e. ESMS and APCI-MS) were studied to achieve the best method for naphthenic acid characterization. The two different mass spectrometry techniques (ESMS and APCI-MS) used in this work showed that APCI-MS gives a favoured ionisation of naphthenic acids, particularly for samples with traces of higher molecular weight naphthenic acid (ARN) species. However, in some instances, fragmentation of the higher molecular weight naphthenic acids was suspected during ESMS analysis. The suspected fragment ion is usually seen in the spectrum as a pronounced peak at around m/z ~313 (probably the z = 4 species). This type of behaviour has also been observed by other researchers, although the information is yet to appear in the published literature.

Calcium naphthenate deposit samples

The ESMS analyses of the naphthenic acid extract from samples (HD 1 and HD 2) using the Methods 1 and 2 extraction techniques reveal the presence of both lower and higher molecular weight naphthenic acids with a broad abundant distribution of lower molecular weight naphthenic acids. In addition, analyses of the remaining sludges (samples HD S1 and HD S2) gave a similar pattern of acid distribution in lower proportion compared to the main extracts. The main reason for developing the modified extraction technique (Method 3) was to address the issue of the ARN acid's solubility in toluene, which is the principal extraction solvent in this study. ESMS spectra of the extract from sample HD 3 revealed the presence of a wide range of lower molecular weight naphthenic acids between m/z 200 and m/z 600 and clusters of ARN acids ion peaks at around m/z 1230 to m/z 1235 similar to those from the Method 1 and 2 extraction techniques. However, analyses of extracts from samples WB 3, BLK 3 and BBAY 3 gave a slightly different distribution of acids, with weak evidence of lower molecular weight naphthenic acid and a strong ion peak at around m/z 313, which is suspected of being the ARN acid fragment, generated due to the electrospray ionisation technique (with z = 4). Although this has not yet been proven, others working in a similar area have also observed this pattern. The APCI-MS spectra of all the extracts from samples (HD 1, HD 2, HD 3, HDN 3, WB 3, BLK 3, BBAY 3 and

WAE 3) present favoured ionisation of the ARN acids with very distinct peaks between m/z 1230 to m/z 1310, in addition to showing evidence of lower molecular weight naphthenic acids at around m/z 200 to m/z 700. From the results, these differences in the lower molecular weight acid distributions are believed to be field specific. Although the APCI-MS technique yields a favoured ionisation of higher molecular weight naphthenic acids, it is believed that it leads to the formation of multimers at masses greater than m/z 800, which are observed in some samples; this type of pseudo naphthenic acid formation has been previously reported in the literature (Rudzinski *et al.,* 2002). Therefore, it can be concluded that naphthenic acid composition in calcium naphthenate deposits is field specific, with some composite of two types of naphthenic acid (i.e. lower and higher molecular weight) in various proportions whilst others almost completely consist of higher molecular weight naphthenic acid (ARN).

Sodium carboxylate/emulsion deposit samples

Extract sample analyses of TK-38S, DLG 53-1 and DLG 53-2 using ESMS and APCI-MS revealed the presence of acyclic, monocyclic and alkylbenzoic naphthenic acids in all samples with weak evidence for the presence of bicyclic naphthenic acid. The APCI-MS spectra of TK-38S and DLG 53-1 showed the presence of further naphthenic acids of mass greater than m/z 680. However, the response was weak relative to the background noise of the sample. Interestingly, the APCI-MS spectrum of DLG 53-2 shows a sequence of acyclic (C_{19} to C_{36}) naphthenic acid distribution with the preference of even-over-odd carbon number acyclic naphthenic (fatty) acids. This phenomenon can be attributed to the geochemical history of the petroleum system (Curiale *et al.,* 2005). Naphthenic acid distribution of sample BRN using ESMS and APCI-MS technique was very similar to DLG 53-2, with a predominance of acyclic naphthenic (fatty) acid and preference of even-over-odd carbon number acid distributions. Characterization of the sample NSA using APCI-MS has shown the presence of bicyclic naphthenic acid with trace evidence for the presence of acyclic, monocyclic and alkylbenzoic naphthenic acids. In all the sodium carboxylate/emulsion samples analysed, there was no evidence of ARN acid species.

Crude oil samples

The ESMS spectra of the naphthenic acids extracted from the crude oil using Acid-IER techniques for samples HD CR and BLK CR show relative distributions of the different classes of lower molecular weight naphthenic acids (acyclic, monocyclic, bicyclic and alkylbenzoic) . There was little indication of ARN acids, whilst the APCI-MS spectrum of the extract from sample BLK CR reveals the presence of lower molecular weight naphthenic acids and also traces of ARN acids ion peaks at a very low level. The presence of a low level of ARN acids in the crude oil, or even the inability to detect them in some crude oil samples using the Acid-IER extraction procedure, can be attributed to the concentration of the naphthenic acids present in crude oil. Furthermore, analysis of sample HDN CA (from an alcohol/KOH extraction procedure) revealed a broad distribution of lower molecular weight naphthenic acids i.e. acyclic, monocyclic, bicyclic and alkylbenzoic. The distribution of the lower molecular weight naphthenic acids in sample HDN CA (from the alcohol/KOH method) is similar to sample HD CR (from the Acid-IER method)

Extract from re-precipitation experiments

The APCI-MS spectra of both naphthenic acid extracts from the re-precipitation experiment and field calcium naphthenate deposit gives almost identical distributions of naphthenic acid compositions. In each case, two distinct classes were observed (lower and higher molecular weight naphthenic acid species). Also, the distributions of these acid classes from the spectra are observed to be in very similar ranges of m/z. Hence, we have conclusively established that, for that particular calcium naphthenate sample (Sample HDN 3), the composition of the deposit contains mainly lower molecular weight naphthenic acids along with a small but significant % of the higher molecular weight naphthenic acid species.

Elemental composition (ESEM/EDAX) of calcium naphthenate

The ESEM/EDAX analyses of the calcium naphthenate deposits (HD, HDN, WB and BBAY) have shown that they contain carbon, oxygen and calcium in various ratios as the main components. Sodium and other ions were also present in the EDAX composition. The % level of sodium is observed to be much lower than the % of calcium.

CHAPTER 5: GEOCHEMISTRY OF NAPHTHENATES FORMING CRUDES

5.1 INTRODUCTION

Petroleum geochemistry involves the application of chemical principles to study the origin, migration, accumulation and alteration (biodegradation) of crude oils. Petroleum is generally considered to primarily consist of carbon and hydrogen, in addition other elements present in various proportions. Geochemically, petroleum is thought to be generated from the decomposition and / or thermal maturation of organic matter and this organic matter originates from plants and algae. The accumulated petroleum in the reservoir is found to contain some biological indicators (biomarkers) which are incorporated in the oil. Biomarkers are defined as compounds derived from organisms that are preserved in sediments, the geological record and ultimately in oils. Linking the biomarker with a specific family of organism gives an opportunity of identifying the family's fossil record. However, even when the original fossils of an organism are not found, its chemical markers are useful to trace the organism's history and the role in oil composition during certain periods of time (geological eras). Organic geochemists have been using biomarkers to correlate data between an oil sample and the original petroleum source rock in terms of obtaining relevant information with regards to organic matter in the source rock, environmental conditions during its deposition and burial, thermal maturity experienced by the rock or oil, the degree of biodegradation and some aspects of lithology, and age (Baugh, P. T., 1993 and Peters and Moldowan, 1993). The detection of various biomarkers can be carried out using gas chromatography (GC), gas chromatography mass spectrometry (GC-MS) and gas chromatography mass spectrometry mass spectrometry (GC-MS-MS) spectroscopic techniques.

In this study, an attempt is being made to use the knowledge of the geochemistry (both biomarker and non-biomarker parameters) as a tool to address naphthenate formation. 11 different types of crude oil samples (calcium naphthenate, sodium carboxylate and emulsion forming crudes) were used in this work.

The crude oil samples were separated into various component fractions (aliphatic, aromatic and polar) and the aliphatic and aromatic fractions were subsequently analysed using GC and GC-MS techniques in both selected ion monitoring (SIM) and full scan modes for biomarker analysis. An overview of the crude oil samples studied is summarised in Table 5.1.

Sample code	Crude oil classification
HD--- North Sea (Norway sector)	Calcium naphthenate forming crude
BLK--- North Sea (UK sector)	Calcium naphthenate forming crude
KUT--- South East Asia	Sodium carboxylate/naphthenate forming crude
BRN--- South East Asia	Sodium carboxylate/naphthenate forming crude
ML 53L--- South East Asia	Sodium carboxylate/naphthenate forming crude
ML 35L--- South East Asia	Sodium carboxylate/naphthenate forming crude
HDN--- North Sea (Norway sector)	Calcium naphthenate forming crude
SAC 1--- Middle East	Emulsion forming crude
SAC 2--- Middle East	Emulsion forming crude
BP B--- Africa	Calcium naphthenate forming crude
BP C--- Africa	Calcium naphthenate forming crude

Table 5.1: Brief description of the different types crude oil samples used in this work.

5.2 TOTAL ACID NUMBER (TAN) ANALYSES

The total acid number (TAN) measurement has been used as an indication of the acid composition of a crude oil. It can be defined as the amount of strong base (in mg) that is required to neutralise the acidity in one gram (g) of crude oil sample. The detailed procedure for TAN measurement has been fully described in Chapter 3, Section 3.3.3. Different crude oil samples, i.e. calcium naphthenate, sodium carboxylate and emulsion

forming crudes, were studied. The results of the total acid number measurements are presented in Table 5.2.

Sample code	Crude oil classification	TAN (mg KOH/g)--Measured	API—from literature
HD	CaN forming crude	2.50	25.0^{o}
BLK	CaN forming crude	0.20	35.0^{o}
KUT	NaN forming crude	0.48	35.0^{o}
BRN	NaN forming crude	0.50	37.0^{o}
ML 53L	NaN forming crude	N/A	N/A
ML 35L	NaN forming crude	N/A	N/A
HDN	CaN forming crude	2.51	25.0^{o}
SAC 1	Emulsion forming crude	0.40	34.0^{o}
SAC 2	Emulsion forming crude	0.41	34.0^{o}
BP B	CaN forming crude	2.10	19.0^{o}
BP C	CaN forming crude	2.20	19.0^{o}

Table 5.2: Showing the total acid number values (TAN) measured and API gravity values from the literature.

Measurement of crude oil TAN does not give detailed information on the acidic content of the crude oil but rather it gives an indication of the total acid composition in the crude oil. Furthermore, Meredith *et al.,* (2000) found that dissolved hydrogen sulphide (H_2S), dissolved carbon dioxide (CO_2), inorganic acids and some contaminants, such as inhibitors or detergents, will also affect the final measured TAN value. The precise effects of components on the TAN value are most likely to be time and concentration dependent. The relation between TAN value and naphthenic acid concentration [HA] has been studied for some selected crude oil samples (Meredith *et al.,* 2000) and it was observed that there was no specific trend in this plot.

Figure 5.1 presents a plot of the crude oil API values versus TAN for calcium naphthenate, sodium carboxylate/emulsion, and emulsion forming crude oils from different parts of the world.

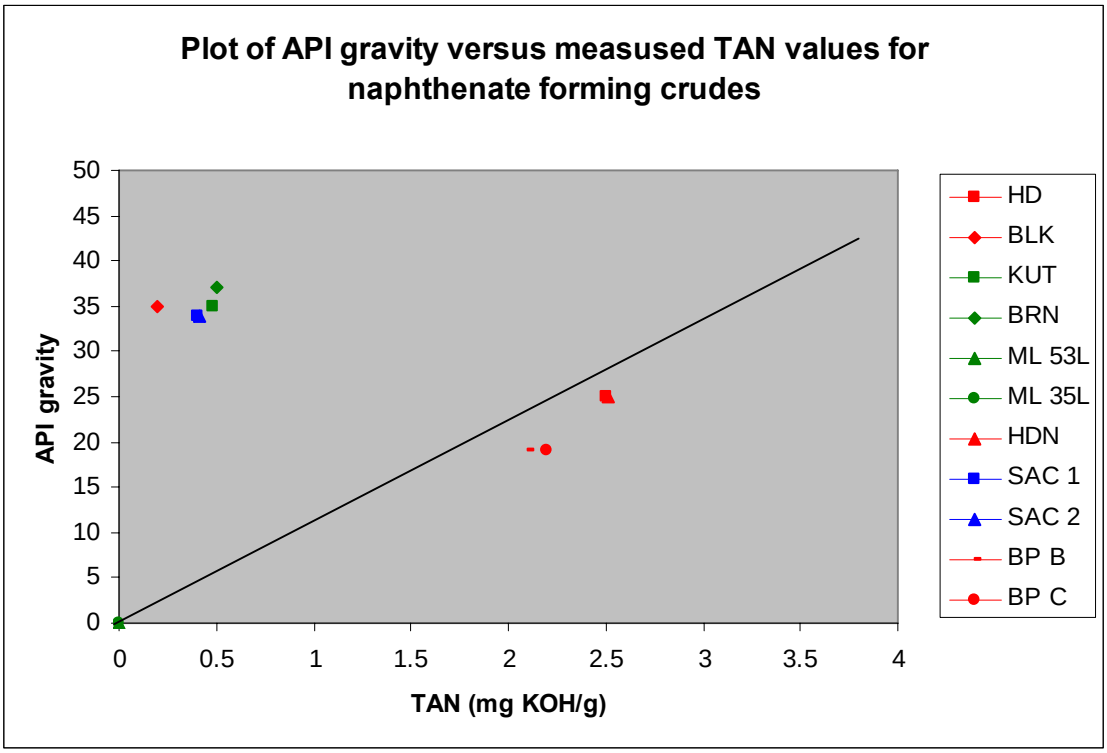

Figure 5.1: Plot of API as function of TAN for calcium naphthenate, sodium carboxylate and emulsion forming crude oil samples from different parts of the world.

The red coloured samples are calcium naphthenate forming crudes, the green are the sodium carboxylate/emulsion forming crudes whilst the blue represent the emulsion forming crudes. There is no clear trend correlating TAN and API for the series of naphthenate forming crude oils studied in this thesis, as can be seen from Figure 5.1 above. It was observed from the graph that calcium naphthenate forming crude oils tend to have lower API than sodium carboxylate and emulsion forming crude oils. However, one of the calcium naphthenate forming crude oil samples was found to have high API and low TAN. Generally, all the carboxylate and emulsion forming crude oil samples were noticed to have intermediate to high API and low TAN values. The information about TAN and API measurements does not give a definite clue about what sort of flow assurance problem

would be encountered during crude oil production, but rather it gives some idea of the total acid components present in the crude oil sample.

5.3 GEOCHEMICAL ANALYSES

Two different analytical techniques are used in the analyses of the crude oil fractions (aliphatic and aromatics) i.e. gas chromatography (GC) and gas chromatography mass spectrometry (GC-MS). The GC is a direct method whilst the GC-MS technique combines two separate procedures: gas chromatography and mass spectrometry. Both techniques are quite well-established and have been applied in different areas. In petroleum geochemistry, GC-MS is predominantly used in the analysis of more complex compounds apart from *n*-alkanes, i.e. steranes and triterpanes; these compounds are normally present in petroleum in very low concentrations and therefore their detection and quantification only becomes practical using GC-MS. In this chapter, an attempt is being made to use depositional (source), maturity and biodegradation parameters in relation to the deposition of all types of naphthenates.

Gas chromatography (GC) analyses

Parameters calculated from the GC analysis are Pristane/Phytane (Pr/Ph) ratio, Pristane/nC$_{17}$ (Pr/nC$_{17}$), Phytane/nC$_{18}$ (Ph/nC$_{18}$), CPI (carbon preference index), and OEP (odd-even preference) index. These parameters are explained in some detail below but the results of these calculations are summarized in Table 5.3 below. In the samples analysed in Table 5.3, samples (i) HD, BLK, HDN, BP B and BP C are calcium naphthenate forming crude oils; (ii) KUT, BRN, ML 53L and ML 35L are sodium carboxylate/emulsion forming crude oils; and (ii) SAC 1 and SAC 2 are emulsion forming crude oils.

Sample Code	Pr/Ph	Pr/nC_{17}	Ph/nC_{18}	CPI	OEP
HD (CaN)	1.08	0.61	0.67	1.10	0.95
BLK (CaN)	0.88	1.23	1.53	1.09	0.93
KUT (NaN)	4.07	1.50	0.50	1.44	1.00
BRN (NaN)	1.70	0.42	0.28	1.32	0.99
ML53L(NaN)	4.06	0.98	0.31	1.35	1.01
ML35L(NaN)	4.03	1.06	0.33	1.34	1.01
HDN (CaN)	0.97	0.65	0.80	1.05	0.94
SAC 1 (E)	0.35	0.12	0.41	1.19	0.95
SAC 2 (E)	0.39	0.12	0.37	1.19	0.97
BP B (CaN)	0.91	N/A	N/A	N/A	N/A
BP C (CaN)	1.34	0.29	0.23	1.24	1.04

Table 5.3: The various parameters calculated from the GC traces of the aliphatic fractions of the 11 different oil samples.

Key:

CaN = Calcium naphthenate forming crude oil

NaN = Sodium carboxylate emulsion crude oil

E = Emulsion forming crude oil

Pristane/Phytane ratio (Pr/Ph)

This ratio is commonly used because pristane (Pr) and phytane (Ph) are measured quite easily using gas chromatography (GC). The Pr/Ph ratio has been used to indicate the redox potential of source sediments, and a ratio of less than one (<1) usually indicates anoxic source-rock deposition whilst oxic conditions are indicated by Pr/Ph > 1 (Didyk *et al.,* 1978). Caution has to be exercised as it has been suggested that the Pr/Ph ratio from low maturity samples should not be used, and that this should be done only for samples within the oil-generative window (Volkman and Maxwell, 1986). The pristane/phytane ratio (>3) often indicates terrestrial organic matter input under oxic conditions, as can be seen from samples KUT, ML 53L and ML 35L in Table 5.3. Valid conclusions from the Pr/Ph ratio alone on the redox potential of source sediments are very difficult, due to the influence of maturity and source effects; hence, other geochemical data should be used in conjunction

with this ratio. The pristane/phytane ratio can also be used to distinguish oils from carbonate source rocks which can be seen from Table 5.3 where SAC 1 and SAC 2 samples show a very low pristane/phytane ratio of 0.35 and 0.39 respectively.

Isoprenoid/n-alkane ratio [(Pr/nC_{17}) and (Ph/nC_{18})]

Pristane and phytane are isoprenoids with the common likely source from the phytyl side chain of chlorophyll **a** in phototrophic organisms and bacteriochlorophyll **a** and **b** in purple sulphur bacteria. Archaea were also considered to be other likely sources for pristane and phytane (Rowland *et al.,* 1990). The ratio of pristine/nC_{17} or phytane/nC_{18} is sensitive to maturity, although also affected by other factors such as source and biodegradation, therefore it is much more convenient to use this parameter in studying oils which are related and non-biodegraded. The ratio is calculated by using the peak areas from gas chromatography (GC). The isoprenoid/n-alkane ratio i.e. pr/nC_{17} or ph/nC_{18} decreases with the oil thermal maturity due to the fact that the increase in thermal maturity of the oil leads to n-alkane generation from kerogen, by cracking.

Carbon preference index (CPI) and odd-to-even predominance (OEP)

The carbon preference index (CPI) is also specifically related to maturity, although other factors like source and biodegradation do affect the response of the parameter. The CPI is the ratio of the odd carbon number ranging from C_{25} to C_{33} over the even carbon number ranging from C_{26} to C_{34} of the alkanes and this is calculated from the GC ion peaks. The CPI ratio and the improved OEP (odd even preference) ratio have been in use for some times in petroleum geochemistry analysis, and ratios significantly above or below 1.0 indicate low thermal maturity. This parameter is influenced by the source, as can be seen from samples KUT, BRN, ML 53L and ML 35L, although the samples are relatively mature, but their CPI is still significantly higher than 1.0.

Gas chromatography mass spectrometry (GCMS) analyses

Parameters calculated from the gas chromatography mass spectrometry (GCMS) analyses for the 11 aliphatic and aromatic fractions included maturity and depositional/source related effects. It was hoped that looking at these biomarker parameters, it might be possible to

relate them to the different categories of calcium naphthenate, sodium naphthenate or emulsion forming crude oils. If such a relationship existed, it might then be possible to predict whether naphthenate deposits of any type would occur by studying the crude oil sample prior to the start of production operations.

Biomarker maturity parameters are quite useful for determining the thermal history of petroleum deposits and their related source rocks. Several studies have shown that many maturity parameters are also dependent on certain properties of the source rock itself (Mackenzie *et al.,* 1980; Moldowan *et al.,* 1994). The maturity parameters considered in this study were sub-divided into hopane and sterane related parameters and are measured using selected ion monitoring (SIM) from the GCMS.

SAMPLE	%22S	%20S	% ββ	% Ts	% C_{29}Ts	C_{35} homo	% Dias./sterane	% Oleanane
HD	57	56	53	72	42	1.02	42	0
BLK	59	45	52	74	40	1.15	36	0
KUT	56	26	25	37	59	0.32	22	46
BRN	61	37	49	36	16	0.45	25	15
ML 53L	56	45	36	44	22	0.36	27	50
ML 35L	56	41	33	45	22	0.41	26	51
HDN	56	61	56	65	37	1.00	41	0
SAC 1	58	49	52	31	9.0	1.26	13	0
SAC 2	58	47	53	30	9.0	1.29	9.0	0
BP B	57	55	59	57	37	0.85	48	0
BP C	56	44	50	44	36	0.80	44	0

Table 5.4: Hopane and sterane parameters of the oil samples, calculated from the GC-MS analysis.

Key:

%22S = % {22S/ (22S + 22R)}C_{32} αβ hopane; **%20S** = % C_{29} {20S / (20S + 20R)}sterane ; **%ββ** = C_{29} αββ/ (αββ + ααα) sterane ; **%TS** = % {Ts/ (Ts + Tm)}; **%29Ts** = %{(C_{29}Ts / (C_{29}Ts + C_{29}αβ)) hopane}; **C_{35} homo** = (C_{31} 22R / C_{30} hopane); **% Dias. Ratio** = %{ Diasteranes / (diasteranes + steranes)}; **% Oleanane** = % {Oleanane/ (oleanane + C30 αβ hopane)}.

Note: The description of the biomarker parameters calculated as indicated in the *Key* are as follow:

$$\%22S = 100 * \left(\frac{C_{32}17\alpha,21\beta\ 22S\ hopane}{\left(C_{32}17\alpha,21\beta\ 22S\ hopane + C_{32}17\alpha,21\beta\ 22R\ hopane\right)} \right)$$

$$\%20S = \ 100 * \left(\frac{C_{29}5\alpha,14\alpha,17\alpha\ sterane\ 20S}{C_{29}5\alpha,14\alpha,17\alpha\ sterane\ 20S + C_{29}5\alpha,14\alpha,17\alpha\ sterane\ 20R} \right)$$

$$\%\beta\beta = \ 100 * \left(\frac{C_{29}5\alpha,14\beta,17\beta\ sterane\ 20S + 20\mathrm{R}}{C_{29}5\alpha,14\beta,17\beta\ sterane\ 20S + 20\mathrm{R} + C_{29}5\alpha,14\alpha,17\alpha\ sterane\ 20S + 20\mathrm{R}} \right)$$

$$\%Ts = \ 100 * \left(\frac{18\alpha - 22,29,30 - trisnorneohopane}{18\alpha - 22,29,30 - trisnorneohopane + 17\alpha - 22,29,30 - trisnorhopane} \right)$$

$$\%29Ts = \ 100 * \left(\frac{C_{29}Ts\ hopane}{C_{29}Ts\ hopane + C_{29}\alpha\beta\ \ hopane} \right)$$

$$C_{35}\ Homo = \left(\frac{C_{31}R\ hopane}{C_{30}\alpha\beta\ hopane} \right)$$

$$\%Dias.Ratio = \ 100 * \left(\frac{C_{27}13\beta,17\alpha\ diasteranes\ 20S + 20\mathrm{R}}{\left(C_{27}13\beta,17\alpha\ diasteranes\ 20S + 20\mathrm{R}\ \right) + \left(\ \left(C_{27}5\alpha,14\alpha,17\alpha\ sterane\ 20S + 20R\right) + \left(C_{27}5\alpha,14\beta,17\beta\ sterane\ \ 20S + 20R\right)\ \right)} \right)$$

$$\%Oleanane = \left(\frac{18\alpha(H) - oleanane}{\left(18\alpha(H) - oleanane + C_{30}\alpha\beta\ hopane\right)} \right)$$

Sterane Isomerization

The parameter **{20S/ (20S + 20R)}** (%) is one of the most commonly used molecular maturity parameters in petroleum geochemistry. It is used to calculate the measured ratio of either C_{27} or C_{29} ααα sterane from m/z 217 and is based on the relative abundance of the 20S isomer compared with the biologically-inherited 20R stereochemistry. This parameter attains equilibrium at around 50 to 55% (Mackenzie *et al.,* 1980). In the 11 oil samples studied here, values increase progressively from around 26% in sample KUT to 61% in the HDN sample as shown in Table 5.4. In addition, like some other geochemical parameters, organofacies and biodegradation can also affect the ratio. For example it was reported that partial biodegradation of sterane in an oil can result in an increase in C_{27}, C_{28} and C_{29} sterane ααα %{ 20S / (20S + 20R)} to above 55%, presumably by selective removal of the ααα 20R epimer by bacteria (Seifert and Moldown, 1978). The {αββ/(αββ+ααα)}(%) isomerization ratio increases from non-zero values to about 70% and usually attains an equilibrium end point between 67% to 71% (Seifert and Moldowan, 1986). This maturity parameter shows the greater thermal stability of the αββ sterane isomers compared with the biologically-derived ααα forms. It is widely applicable due to its application beyond the start of the oil window. A graphical plot of maturity parameters {20S/ (20S + 20R)} (%) *vs.* {αββ/ (αββ+ααα)} (%) is presented in Figure 5.2 which shows an increase of oil maturity from the sodium naphthenate forming crude oil samples (KUT and BRN) to calcium naphthenate forming crude oil samples (HD, BLK, HDN, BP B and BP C). All the naphthenate and emulsion forming crude oil studied here are relatively mature (based on the maturity parameter calculations), although some crude oil samples were found to be more mature than others. Crude oil sample KUT can be classified as low maturity while ML 53L, ML 35L and BRN are medium maturity oil samples and samples SAC 1, SAC 2, BLK, BP B, BP C, HD and HDN as high maturity oil samples, as shown in Figure 5.2.

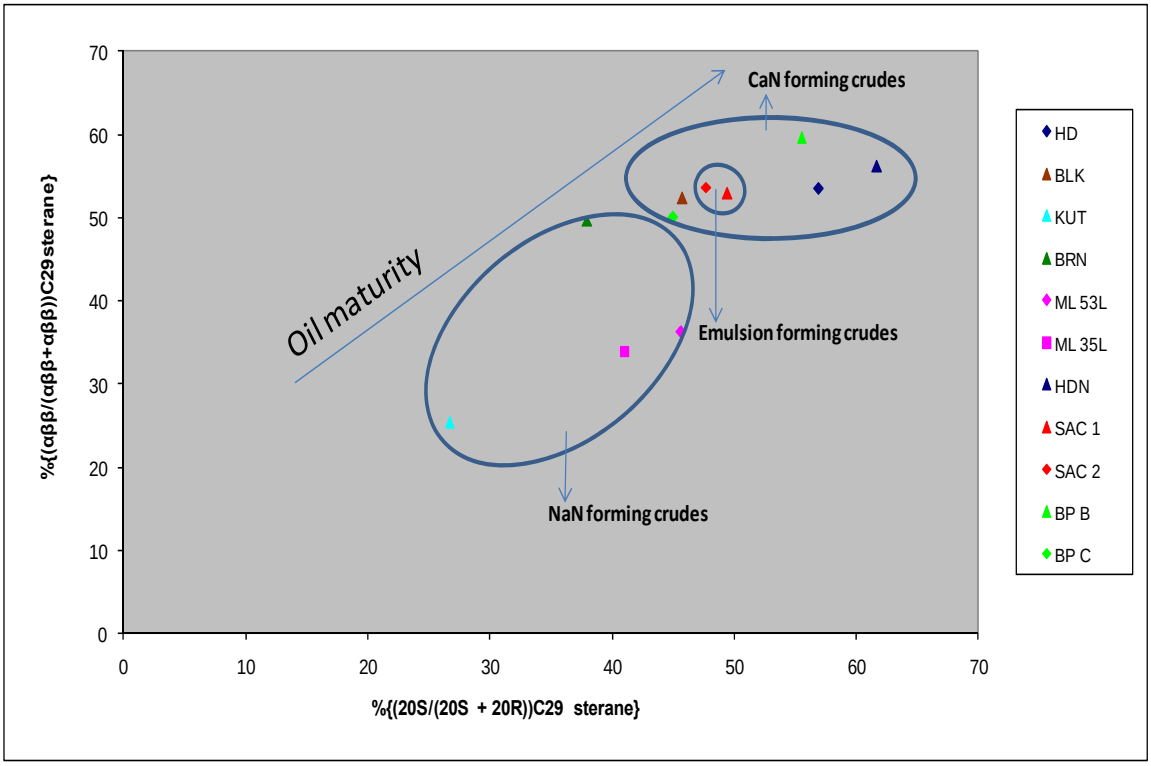

Figure 5.2: Biomarker maturity parameter cross-plots showing the progressive increase of these parameters with increasing maturity.

Ts/ (Ts + Tm)

This quantity ***Ts/(Ts+Tm)*** is often used in petroleum geochemistry as a maturity parameter, despite its dependence on both organic facies and the depositional environment. It increases with increasing maturity in samples of common source or consistent organic facies (Peters and Moldowan, 1993). Oil samples generated from different organic facies may not give a consistent % Ts increase with increasing oil maturity. In this study, the {Ts/ (Ts + Tm)} (%) parameter increases from <35% in sodium naphthenate forming crudes (SAC 1, SAC 2, BRN, ML 53L and Ml 35L) and rises progressively to >65% in the calcium naphthenate forming crudes (HD, BLK and HDN), as presented in Table 5.4.

C_{29}Ts/ (C_{29}Ts + C_{29} 17α (H)-hopane

This parameter is similar to %Ts and is also used as a maturity indicator in oil samples. The %$C_{29}T_S$ shows a similar geochemical characteristic as %Ts, and is quite abundant in oils, except that there is high tendency of coelution with C_{29} 17α (H)-hopane, which usually hinders its reliable usage. In this study it was also observed that the ratio increases with oil

maturity, which can be viewed as an increase from the sodium naphthenate forming crudes to calcium naphthenate forming crudes. Therefore a cross plot between {Ts/ (Ts + Tm)} (%) versus {C_{29}Ts/ (C_{29}Ts + C_{29} 17α (H)-hopane} shows a correlation of both parameters, increasing with the maturity of the oil samples, with the exception of KUT sample, as can be seen in Figure 5.3.

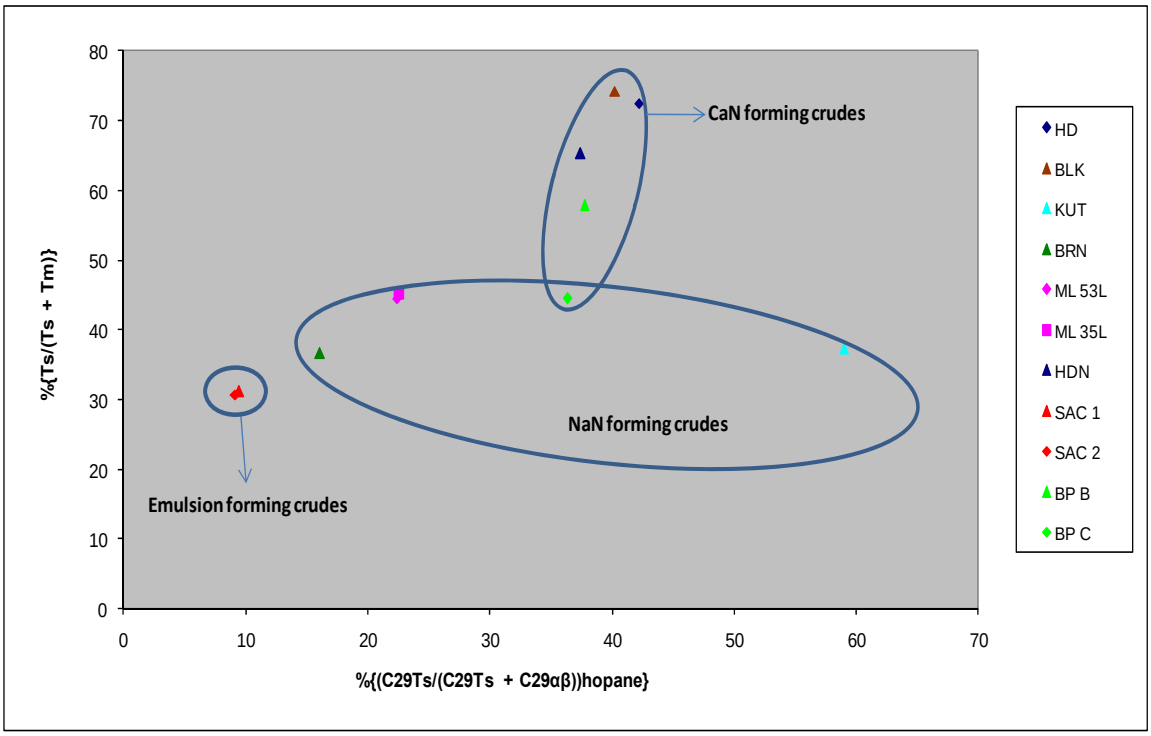

Figure 5.3: Plot of two maturity and source dependent parameters: % {(Ts/ (Ts + Tm)} and % {(C_{29}Ts/ (C29Ts + C_{29}αβ)) hopane.

22S/(22S + 22R) homohopane isomerisation

This parameter is calculated from the ratio of C_{31} to C_{35} 17α-homohopane from the m/z 191 GCMS spectra of all the oil samples analysed. The biologically produced hopane precursors carry a 22R configuration which is gradually converted to a mixture of 22R (biological epimer) and 22S (geological epimer) diastereomers. The ratio {22S/ (22S + 22R)} (%) reaches equilibrium at around 57% to 62% during oil maturation (Seifert and Moldowan, 1986). Generally, oil with a homohopane ratio of 50% to 54% is considered to have barely entered oil generation whilst a ratio in the range of 57% to 62% indicates the main stage of oil generation which can be seen from Table 5.4 above. It was observed that

all the sodium carboxylate and calcium naphthenate forming crude oil samples analysed (HD, BLK, KUT, BRN, BRN, ML 53L, ML 35L, HDN, SAC 1, SAC 2, BP B and BP C) showed a homohopane ratio ranging from approximately 57% to 62%. This means that all the crude oils analysed are from source rocks that are within the oil generative stage.

Oleanane index:

Oleanane is a biological marker diagnostic of certain higher plants, and has been suggested as a marker for angiosperms i.e. flowering plants (Ekweozor *et al.,* 1979). The parameter {Oleanane/ (Oleanane + C_{30} hopane)} (%) provides information on the age of the source rock that produced a particular oil sample. Oleanane was discovered to evolve in the cretaceous geological age, along with angiosperms (Moldowan *et al.,* 1994), Epimer ratios can also be used to indicate thermal maturity. The contribution of these angiosperms to the source rock during the deposition process usually leads to oils generated with medium to high wax content present in them. From the eleven (11) oil samples analysed in this study, samples KUT, BRN, ML 53L and ML 35L contain oleanane, as shown in Table 5.4. These samples that contain oleanane are sodium carboxylate forming crudes. The % oleanane index varies from 15% in sample BRN to around 51% in sample ML 35L shown in Figure 5.4 below. It was observed that the calcium naphthenate and the emulsion forming crude oils do not contain any traces of oleanane.

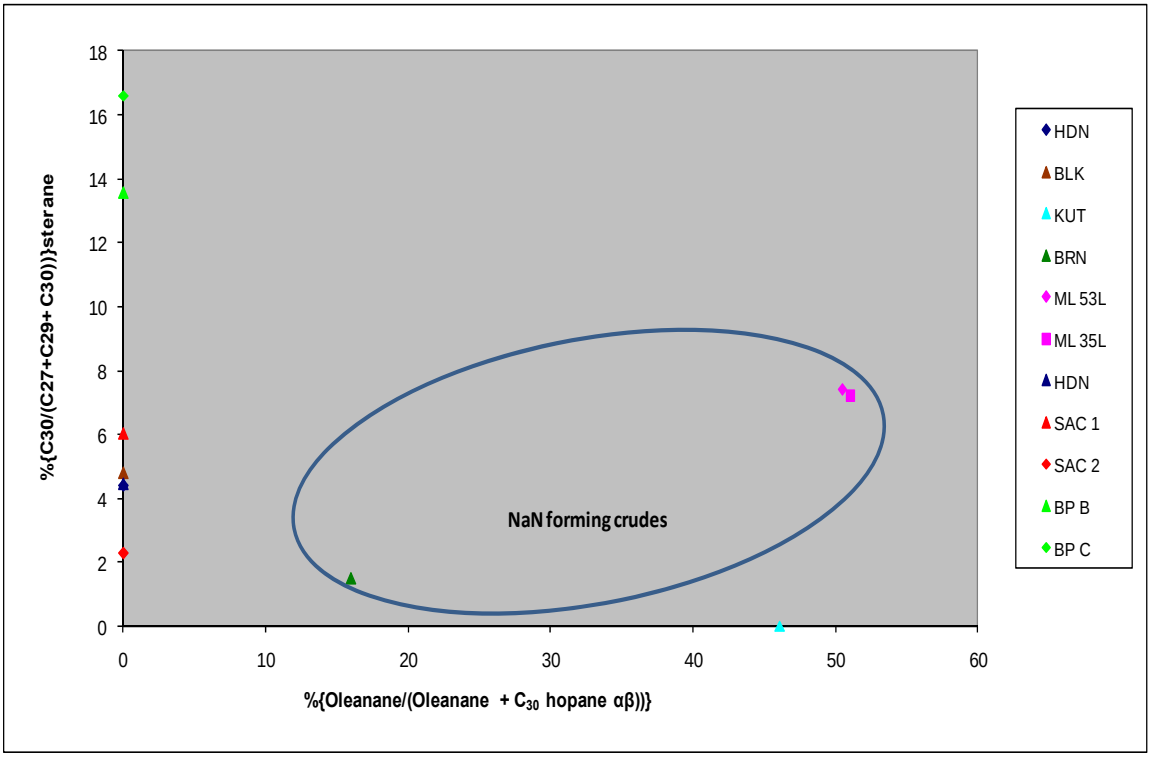

Figure 5.4: Plot of %{(C_{30}/ (C_{27} + C_{29} + C_{30}))} sterane versus oleanane index to identify oil samples that contain land plant inputs.

Diasteranes/steranes parameter

Diasteranes are rearranged steranes with 13β, 17α (H) 20S and 20R (major isomer) and 13α, 17β (H) 20S and 20R (minor isomer) stereochemistries. Diasteranes/steranes ratio is often used to distinguish carbonate from clay-rich source rocks (Barakat *et al.,* 1997). However, the ratio can also be useful for maturity determination, but only when the oils being compared are from the same source-rock organic facies. In this study, the diasterane ratios are calculated from peak parameters in the m/z 217 and m/z 218 chromatograms. Analysis was carried out using three different categories of oil samples: emulsion forming crude oils, sodium carboxylate forming crude oils and calcium naphthenate forming crude oils. A plot of the %diasterane ratio versus %Ts is presented in Figure 5.5, clearly showing two distinct groupings. The sodium carboxylate and emulsion forming crude oil samples i.e. KUT, BRN. ML 53L, ML 35L, SAC1 and SAC 2 studied here have clustered in one area while the calcium naphthenate forming crude oil (HD, BLK, HDN, BP B and BP C) samples are also grouped in another area. This type of categorisation can possibly be used

to differentiate between the sodium carboxylate/emulsion forming crude oils and the calcium naphthenate forming crude oils. It can be seen from Figure 5.5 that the sodium carboxylate/emulsion forming crudes have lower values % diasterane whereas the calcium naphthenate forming crude oil samples have higher %diasterane ratios. In petroleum geochemistry, % diasterane ratio parameter is used in differentiating oil samples sourced from carbonate source rock from those sourced from clay-rich source rocks. A lower value of % diasterane is associated with oil samples from carbonate source rocks whilst higher value is usually from clay-rich source rocks. However, higher diasterane ratio could also result from higher thermal maturity (Seifert and Moldowan, 1978).

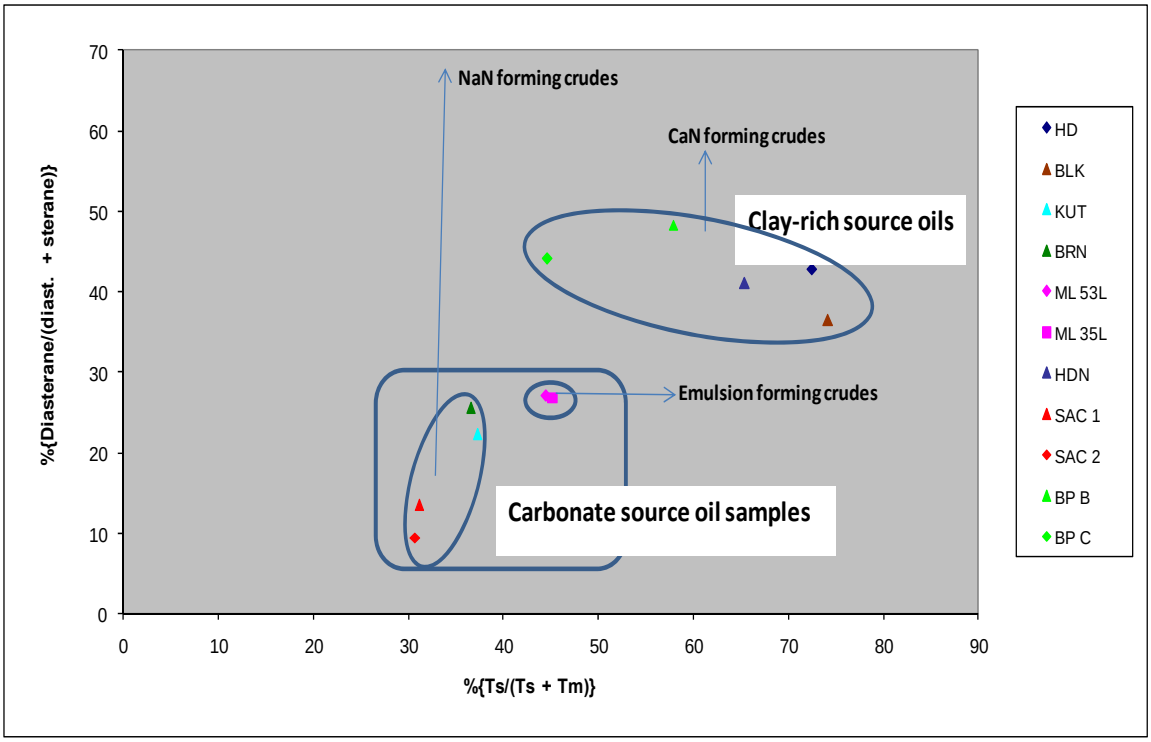

Figure 5.5: A plot of %{ Diasterane/ (diasterane + sterane)} versus %(Ts/ Ts + Tm) used to show different categorisation of sodium carboxylate/emulsion forming crudes and calcium naphthenate forming crudes.

Biodegradation

Biodegradation in petroleum studies is the activity of living organisms altering the composition of the crude oil. The living organism (eubacteria, fungi, and possibly archaea) consume saturated and aromatic hydrocarbon components; therefore, the process is

considered to be an oxidation mechanism producing carbon dioxide (CO_2) and partially oxidised species, such as organic acids (Peters and Moldowan, 1993). The *n*-alkanes of the saturated fraction are considered the most readily degraded components in petroleum (Ronald, 1981) and the process of biodegradation triggers a great deal of oil property variation; e.g. decreases in API gravity and subsequent increases in viscosity, NSO and trace metal composition, etc. The *n*-alkane biodegradation eventually leads to the formation of monocarboxylic acids. In this study, for example, depletion of lower molecular weight *n*-alkanes from samples HD and BLK total ion chromatograms were observed, which can be seen in Figures 5.6 and 5.7, respectively. However, the *n*-alkane ion chromatogram (m/z 85) of the HD sample presented in Figure 5.8 reveals the presence of a lower molecular carbon number *n*-alkane which suggests cycles of biodegradation and topping up with fresher oil to restore the *n*-alkanes. This type of oil mixing at the reservoir, between the non-biodegraded and biodegraded, has been reported by the producer in that particular oil field, due to the nature of the geological structural formation. Sample KUT showed some slight biodegradation which is shown in the total ion chromatogram (TIC) i.e. Figure 5.9, whilst the TIC of sample BRN presented in Figure 5.10 shows a normal distribution of *n*-alkanes. The degree of the oil biodegradation can be further assessed when there is evidence of pristane and phytane from the total ion chromatogram. Peters and Moldowan, (1993) proposed an oil biodegradation scale based on the degree of biodegradation that was categorised from level 1 up to level 10. The level 1 Peters and Moldowan (P & M) scale represents crude oil samples which are undegraded (unaltered *n*-alkanes), whilst level 10 refer to crude oil samples which are severely degraded to the level where hopanes and disateranes are absent.

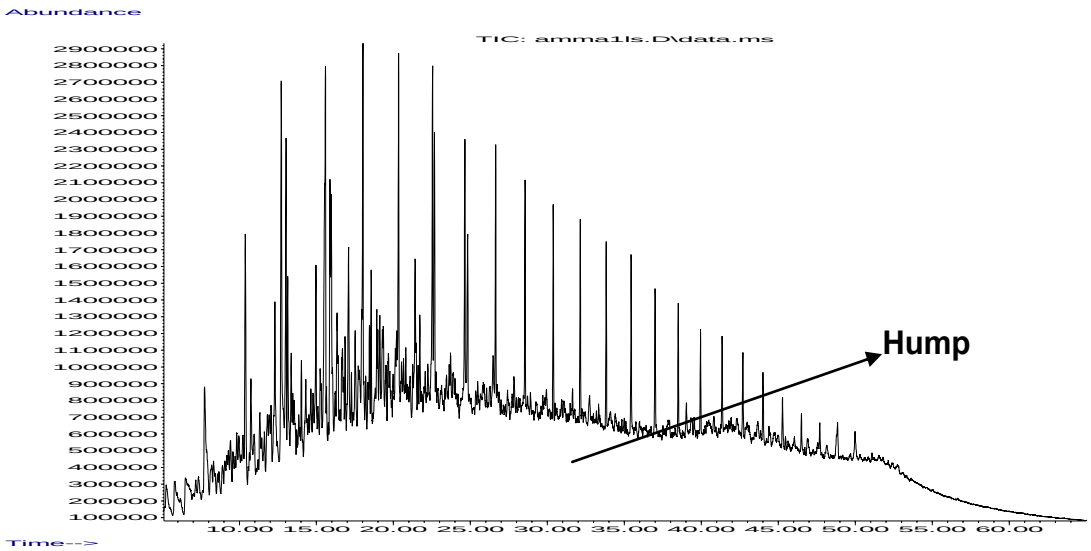

Figure 5.6: Total ion chromatogram (TIC) of aliphatic for sample HD,

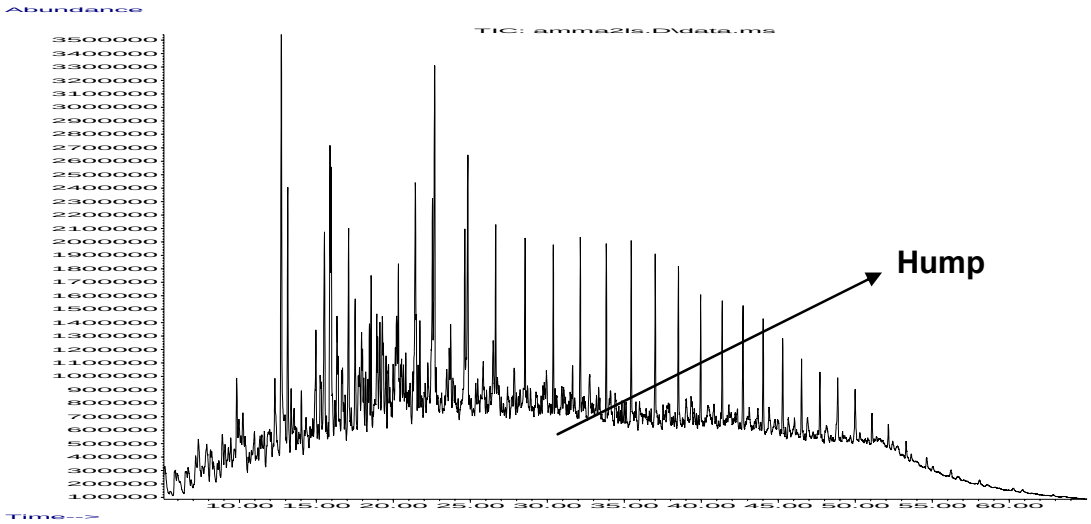

Figure 5.7: Total ion chromatogram (TIC) of aliphatic for sample BLK.

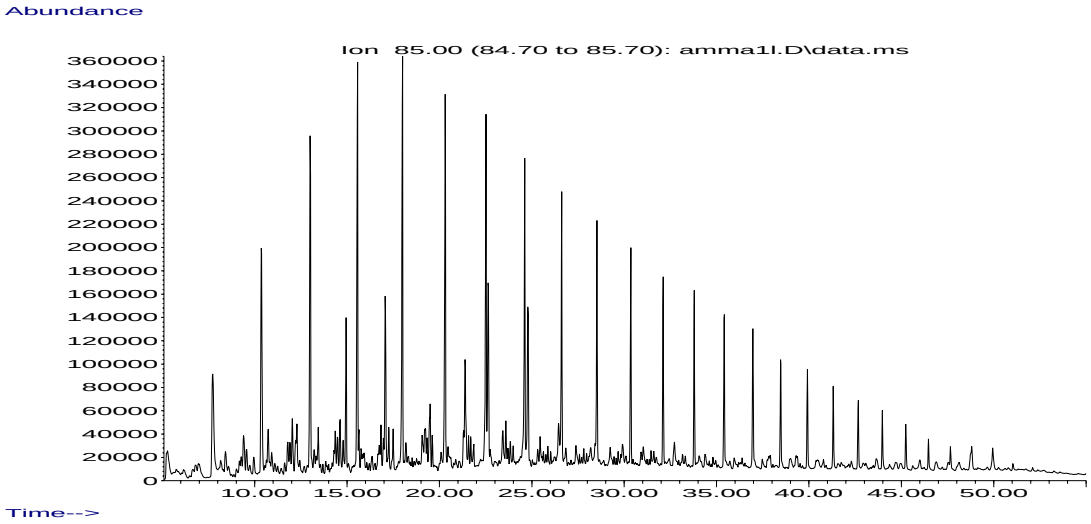

Figure 5.8: Aliphatic fraction ion chromatogram (m/z 85) for sample HD.

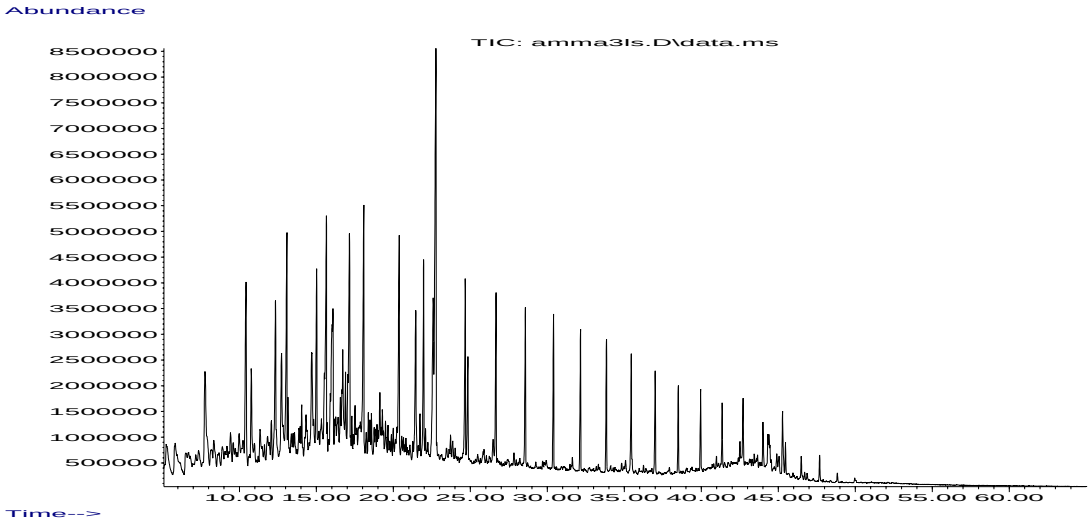

Figure 5.9: Total ion chromatogram (TIC) of aliphatic for sample KUT.

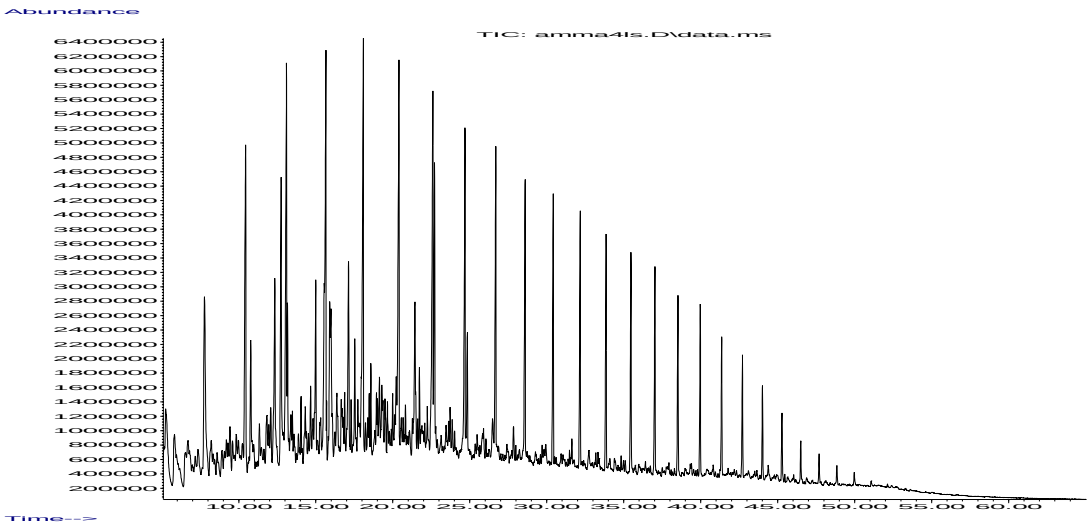

Figure 5.10: Total ion chromatogram (TIC) of aliphatic for sample BRN.

5.4 SUMMARY AND CONCLUSIONS

This chapter deals with the organic geochemistry of the crude oils as it relates to calcium naphthenate, sodium carboxylate and emulsion formation. These techniques have been applied to all 11 crude oils used in this study. Determination of the total acid number (TAN) of the naphthenate forming crude oils revealed that most of the calcium forming crudes has a higher TAN, whereas the sodium carboxylate/emulsion forming crude oil samples showed low to moderate TAN. However, some calcium naphthenate forming crude oil may have a low TAN which was seen from sample BLK in Figure 5.1 above. No good correlation between the TAN values and the naphthenate forming character of the crudes was observed. Nor was there a good correlation between TAN and the API gravity for most of the samples in this work. A reasonable guide was established i.e. the higher the TAN value then the higher the API gravity and subsequently the tendency of that crude oil sample to form calcium naphthenate deposits during oil production. Although that is not always the case, as there are some crude oil samples with low TAN and API yet still form calcium naphthenate. Therefore, formation of calcium naphthenate or sodium carboxylate/emulsion is much more associated with the particular acid composition in the crude oil.

The gas chromatography (GC) and gas chromatography mass spectrometry (GCMS) of the aliphatic fractions for oil samples HD, BLK, KUT, BRN, ML 53L, ML 35L, HDN, SAC 1, SAC 2 and BP B and BP C revealed that:

(i) Samples HD, BLK, HDN, SAC 1, SAC 2, BP B and BP C are more mature than samples KUT, BRN, ML 53L and ML 35L, based on the plots of the maturity parameters.

(ii) Samples HD, BLK, HDN, BP B and BP C have higher diasterane ratios whilst samples KUT, BRN, ML 53L, ML 35L, SAC 1 and SAC 2 have low diasterane ratios. Oil samples with a higher diasterane ratio are usually sourced from clay-rich source rocks and those with low diasterane ratio are associated with carbonate source rocks.

(iii) Samples KUT, BRN, ML 53L, ML 35L indicated some presence of oleanane biomarkers, due to likely contribution of flowering plant leaves during the source rock deposition, hence these oils are expected to have medium to high wax content.

(iv) The total ion chromatograms (TIC) of samples HD and BLK shows an indication of slight biodegradation (presented in Figures 5.6 and 5.7) as compared to KUT and BRN (Figures 5.9 and 5.10) and, as expected from the point of geochemistry, that biodegradation leads to an increases in the crude oil acidity, which invariably results in naphthenate problems (sodium or calcium naphthenate). The geochemistry study here of the naphthenate forming crudes has revealed that the calcium naphthenate forming crude oils are generally more biodegraded than the sodium carboxylate and emulsion forming crudes. However, this is not invariably the case, as there are some exceptions.

Formation of these naphthenates is of great concern to the global oil industry as it causes a number of flow assurance and phase separation problems. Presently, naphthenate formation is only apparent when the problem has started occurring in the field; i.e. it cannot be predicted in advance. However, this study proposes a method to predict which crudes are likely to form calcium naphthenate or sodium carboxylate emulsion, based on the geochemical data from the crude oil. This method is at a preliminary stage but it offers

some promise of being able to predict naphthenate formation as soon as a crude oil sample is available. Tentatively, it can conclude that the sodium carboxylate and emulsions forming crudes are less mature and less biodegraded than the calcium naphthenate forming crudes, but this is just a preliminary result and further detailed work must be carried out on different oil samples before making firm conclusions on this matter.

CHAPTER 6: THERMODYNAMIC MODELLING OF NAPHTHENATE FORMATION

6.1 INTRODUCTION

The prediction and prevention of soft emulsion type sodium naphthenate and hard calcium naphthenate deposits is an important issue in oil exploration and production. A detailed description of how these substances form has been available for some time in the literature. Modelling of other organic scales which may also hinder production output (for example asphaltene) has been well advanced and can be carried out using predictions derived from polymer solution thermodynamic, colloidal stability and fractal aggregation theories (Mullins *et al.,* 2007). The information is used to predict the initial onset of asphaltene precipitation when a particular fluid approaches its bubble point (Idem and Ibrahim, 2002).

A general overview of the interactions between carboxylic/naphthenic acids and metal cations has been available in literature for some time. In the early years of this type of study, work by Langmuir and Schaefer (1937) presented a model description of the adsorption of a stearic acid monolayer as a function of pH. Since then, further modelling work has appeared on such topics as fatty acids in aqueous brine systems, changes in interfacial tension to understand the formation of pre-micellar soap aggregates and phase equilibria for the extraction of carboxylic acids from solvent systems using carbon dioxide (Stenius and Zilliacus, 1971; Somasundaran *et al.,* 1984; Kuzmanovic *et al.,* 2005). At present, models which can predict the formation of either calcium or sodium naphthenates are not currently available commercially, to the best of our knowledge. Therefore, this current chapter will present results on a naphthenate model developed at Heriot-Watt University. Both modelling predictions and experimental verification will be described, as well as outlining a number of sensitivity studies which have been carried out. It is hoped that this preliminary naphthenate modelling will eventually lead to more general models incorporating pressure and temperature (PVT) behaviour closer to that found in the field operations. Some naphthenate precipitation sensitivity studies were also carried out and the results are presented in this thesis.

6.2 MODEL DESCRIPTION

The modelling work in this chapter describes two types of naphthenate experiment : i) simple "pH change" experiments in which no calcium naphthenate precipitation occurs, and ii) full calcium naphthenate "precipitation" experiments where a solid deposit (denoted CaN) forms. The current model description for naphthenate formation was first formulated by Sorbie in 2001 and further details are available in Sorbie *et al.,* (2005). In this study, the full derivation of the model description was revised and the revised model was used in making experimental predictions as well as carrying out a number of sensitivity studies, which will be fully described later in this chapter.

The main reason for the original development of the naphthenate thermodynamic equilibrium model was to analyse the mass transfer of naphthenic acid [HA] between the oil phase and the brine phase and its possible precipitation mechanism. However, in order to predict naphthenate precipitation, the theory shows that we must know the following quantities:

a) the **partition coefficient** of the naphthenic acid, HA, between the oil and the water phases, K_{ow};

b) the naphthenic acid **dissociation constant** in water, pK_a;

c) the **solubility product**, K_{caA2} (or other similar solubility parameter), of the naphthenate deposit.

A general view of the naphthenate deposition mechanisms across the spectrum of naphthenate "scales," from sodium-rich emulsions to calcium naphthenate deposits, was put forward by Sorbie *et al.,* (2005). This work took the view that, to prevent naphthenate problems, a view of both the basic mechanism(s) through which they formed and a thermodynamic model to quantitatively describe their formation needed to be developed. An outline mechanism for the formation of naphthenate deposits had been presented previously by Rousseau *et al.,* (2001). Subsequent studies have used this conceptual mechanism to study deposition in both model and field naphthenate systems (Sorbie *et al.,* 2005).

6.3 THERMODYNAMIC PH CHANGE EXPERIMENT

This type of experiment demonstrates the effect of naphthenic acid [HA] mass transfer from the oil phase to the water phase (brine) when coming into contact and equilibrating. No naphthenate precipitate or emulsion was observed, because these experiments were performed at lower values of initial pH (pHi $\leq$ 6), even with the presence of buffers. However, a change in pH of the brine phase may be observed as a result of mass transfer of the naphthenic acids between the phases. There is a tendency for the naphthenic acid to partition between the oil and water phases during oil production. Once in the water phase, the weak acids dissociate in accordance with normal equilibrium. However, with the exception of low-molecular weight acids, naphthenic acids are relatively insoluble in water (Havre, 2002). The partition coefficient from the oil phase into the water phase (K_{ow}) therefore tends to increase as the molecular weight of the naphthenic acid decreases. For a single naphthenic acid, this mass transfer process is governed by the two main quantities: the oil-water partition coefficient, K_{ow}, and the acid dissociation constant, K_a. The study is aimed at using the model to use measured final brine pH (pH_f) in "pH change experiments" from which the quantities, K_{ow} and K_a can then be calculated. The final brine pH was measured after coming into contact with different concentrations of extracted naphthenic acid dissolved in toluene at initial brine pH values of 6, 5, 4, and 3.

Theory of Naphthenate Thermodynamic Modelling

The naphthenate precipitation model is illustrated in Figure A1 in Appendix A where a full derivation of the equations is given, and the notation is explained. The model is defined by the initial (known) conditions, $[HA]_{oi}$, $[Ca^{2+}]_{wi}$, pH_i (i.e., $[H^+]_i$), and $[OH^-]_I$; and the final seven unknowns are $[HA]_{of}$, $[HA]_{wf}$, $[Ca^{2+}]_{wf}$, pH_f (i.e., $[H^+]_f$), $[A^-]_{wf}$, $[OH^-]_f$, and m_{sol} (the mass of solid "precipitate" CaA_2). The four parameters in the model are K_{ow}, K_a, K_w, and K_{CaA2} and only the first three apply if there is no precipitation (pH change only). The seven final unknown quantities in the model can be found by numerically solving the seven equations 1, 2, 3, 4, 6, 7 = 8 and 9 = 10 in Appendix A and are summarized in Table A2**.**

When there is no naphthenate precipitation (just pH change), the seven equations can be successively reduced by substitution down to one or two chosen solution variables. This

can be done in various ways, but the two unknown variables, $[HA]_{wf}$ and $[H^+]_f$ have been chosen to be solved. This leads to the following two equations:

$$[HA]_{oi} = [HA]_{wf}\left[\frac{1}{K_{ow}} + \frac{V_w}{V_o} + \frac{K_a . V_w}{[H^+]_f . V_o}\right] \quad \text{..... (1)}$$

and

$$\left([H^+]_i - [OH^-]_i\right) = [H^+]_f - \frac{1}{[H^+]_f}\left(K_w + K_a[HA]_{wf}\right) \quad \text{..... (2)}$$

which gives 2 equations with 2 unknowns that have been solved numerically by the Newton-Raphson method applied in a spreadsheet. Once $[HA]_{wf}$ and $[H^+]_f$ have been found, the remaining five unknowns can be found readily using the appropriate equations given in Appendix A.

Experimental and Modelling Results

pH Change Experimental Results

In all these pH change experiments, a decrease in pH from an initial value of pH_i (6, 5, 4, and 3) to a final value pH_f below this initial value was observed. This decrease is as expected from the model equations previously presented, and is caused by the transfer of the naphthenic acids from the oil phase to the interface and/or to the bulk of the brine (water phase). The magnitude of the change in the brine pH, after coming into contact with the oil phase to the final value pH_f, depends on the values of the parameters K_{ow} and K_a, as well as the known initial input values (at $t = 0$) of the brine pH and the initial naphthenic acid concentration in the oil phase. The higher the naphthenic acid concentration in the oil phase, the more acid transfers to the brine phase, thereby decreasing the brine pH to a lower value. It was also observed that, at a very low initial brine pH value (i.e., $pH_i = 3$) and high concentration of naphthenic acid in toluene (i.e., 10000 ppm)**, the final brine pH value (pH_f) change was less drastic than the change for a high initial pH value (i.e., $pH_i = 6$). At an initial brine pH of 3, the solution is already very acidic; therefore, there is little

opportunity for any substantial mass transfer effect of naphthenic acid. The experimentally measured final brine pH (pH_f) for the various initial brine pH values is presented in Table 6.1 below.

> ***Note:** Throughout this thesis, whenever 1 ppm of naphthenic acid in the oil phase is referred, this is actually (ρ_o/ρ_w) mg/L of the substance. In the aqueous phase, 1 ppm of any quantity is the normal 1 mg/L.*

	Final brine (measured) pH_f Initial $[HA]_{oi}$ in toluene				
Initial pH of Brine (pH_i)	0.1 wt% (0.0033M)	0.25 wt % (0.0083M)	0.5 wt% (0.0166M)	0.75 wt% (0.025M)	1.0 wt% (0.0333M)
6	5.5	5.1	4.8	4.2	3.5
	5.4	5.0	4.7	4.0	3.4
5	5.0	4.5	4.2	4.0	3.3
	4.9	4.4	4.1	3.9	3.2
4	3.9	3.5	3.0	2.8	2.5
	3.8	3.3	2.9	2.7	2.4
3	3.0	207	2.5	2.2	2.0
	2.9	2.6	2.4	2.1	1.9

Table 6.1: Experimentally measured final brine pH (pH_f) for the various initial brine pH values.

Graphical plots of experimental final brine pH (pH_f) vs. initial % naphthenic acid concentration in toluene ($[HA]_{oi}$) are presented in Figures 6.1 to 6.4, for initial brine pH values 6, 5, 4, and 3, respectively. Note that each pH change experiment was performed in duplicate, and the result of each repeat experiment is shown in Figures 6.1 to 6.4. The reproducibility of these experiments is clearly very good. It can be observed from Figures 6.1 and 6.2 (pH_i = 6 and 5) that there is a sharp decrease in the pH_f value as the concentration of naphthenic acid in toluene increases, there is a sharp decrease in the pH value to minimum values of pH_f = 3.45 and 3.25, respectively, at 1 wt% $[HA]_{oi}$. At the

lowest initial pH value (pH_i = 3) in Figure 6.4, a steady decrease was noticed to pH_f = 1.95 at 1 wt% $[HA]_{oi}$. At lower brine pH, the [HA] is present more in the protonated form and therefore remains in the oil phase, whereas at a higher pH, more mass transfer of naphthenic acid into the brine phase occurs. These pH change experimental results are summarized for all experiments, in Figure 6.5**,** and these results were modelled using the thermodynamic model described above.

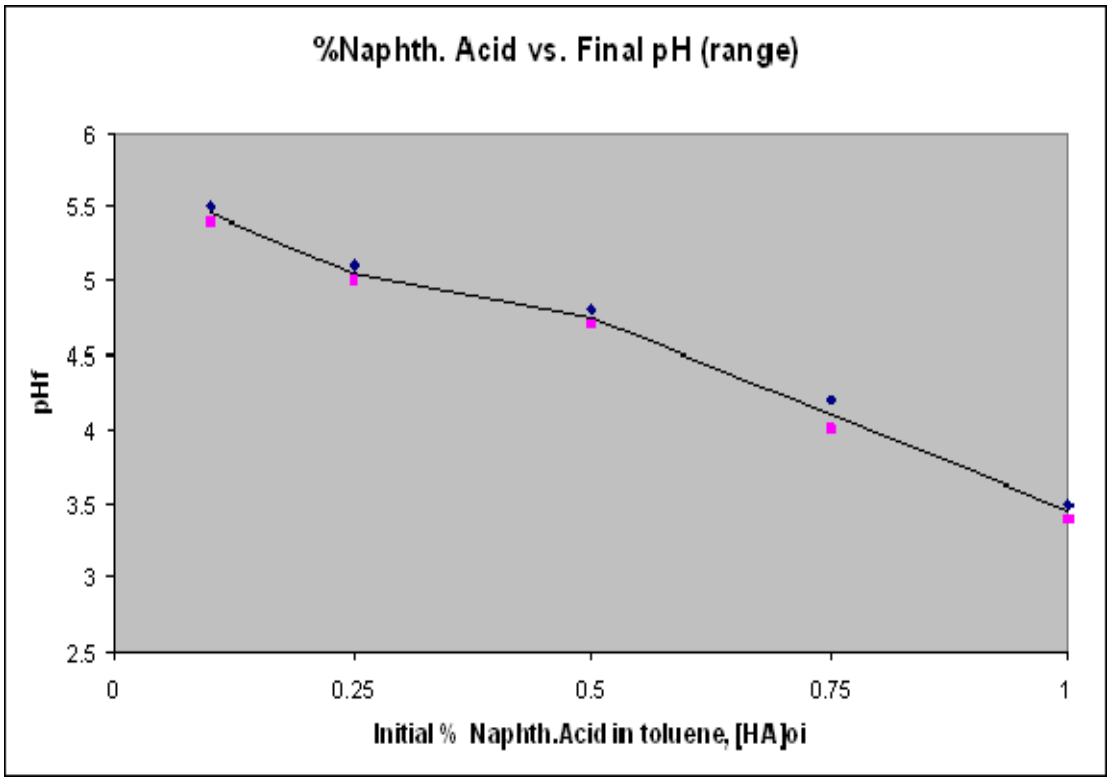

Figure 6.1: Plot of experimental pH_f values for a system vs. % naphthenic acid in toluene with pH_i = 6.

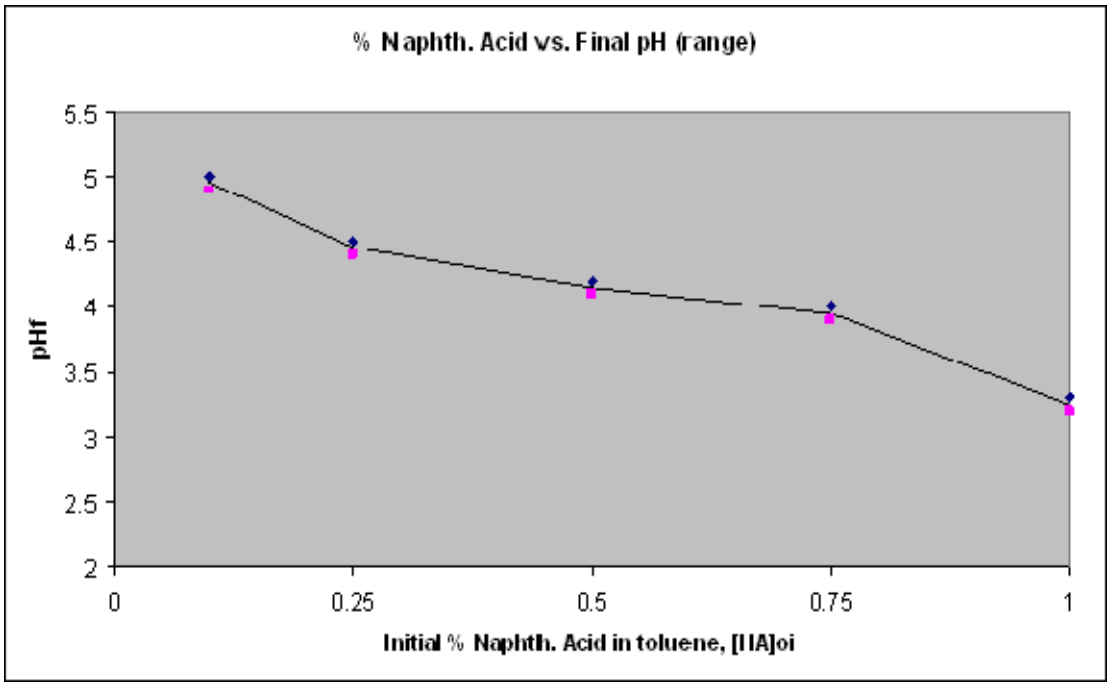

Figure 6.2: Plot of experimental pH_f values for a system vs. % naphthenic acid in toluene with $pH_i = 5$.

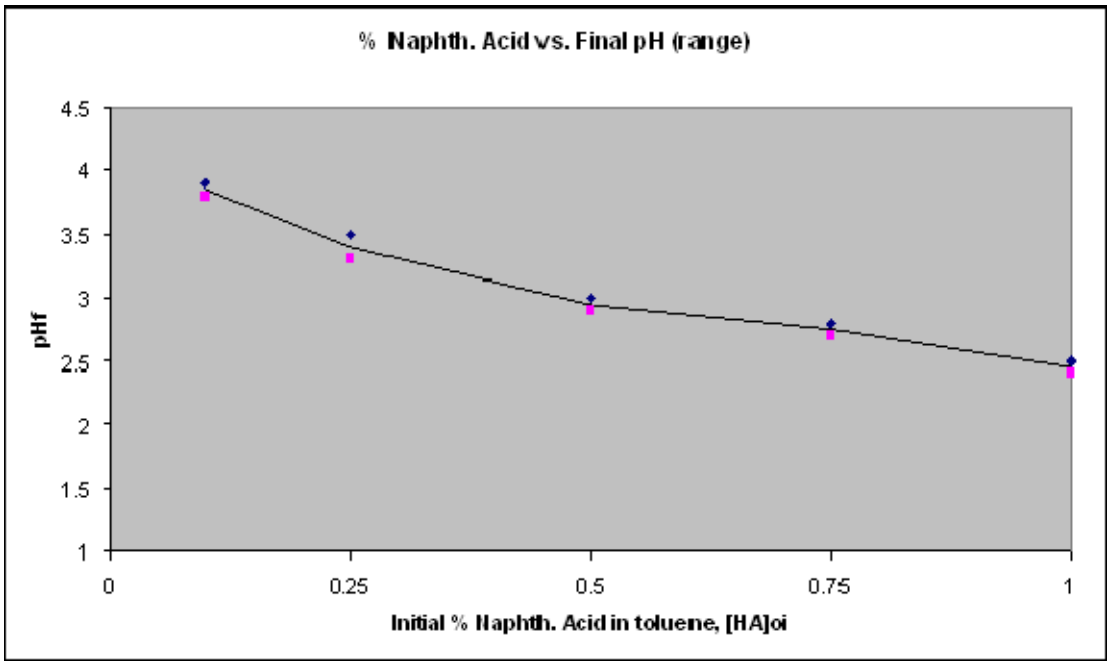

Figure 6.3: Plot of experimental pH_f values for a system vs. % naphthenic acid in toluene with $pH_i = 4$.

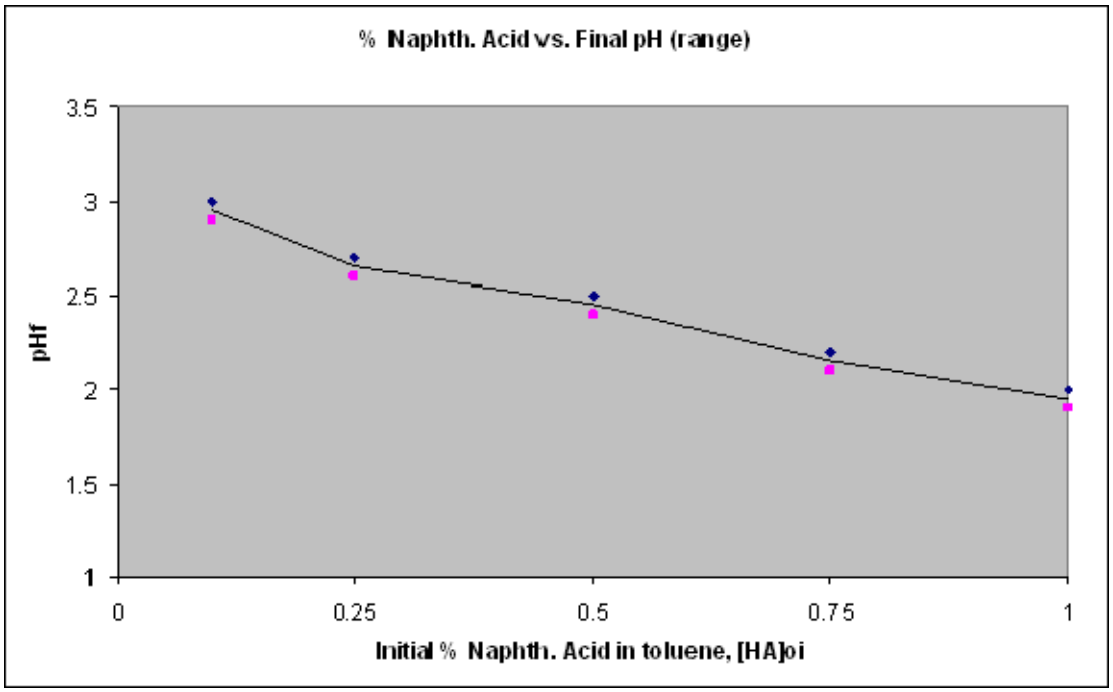

Figure 6.4: Plot of experimental pH_f values for a system vs. % naphthenic acid in toluene with $pH_i = 3$.

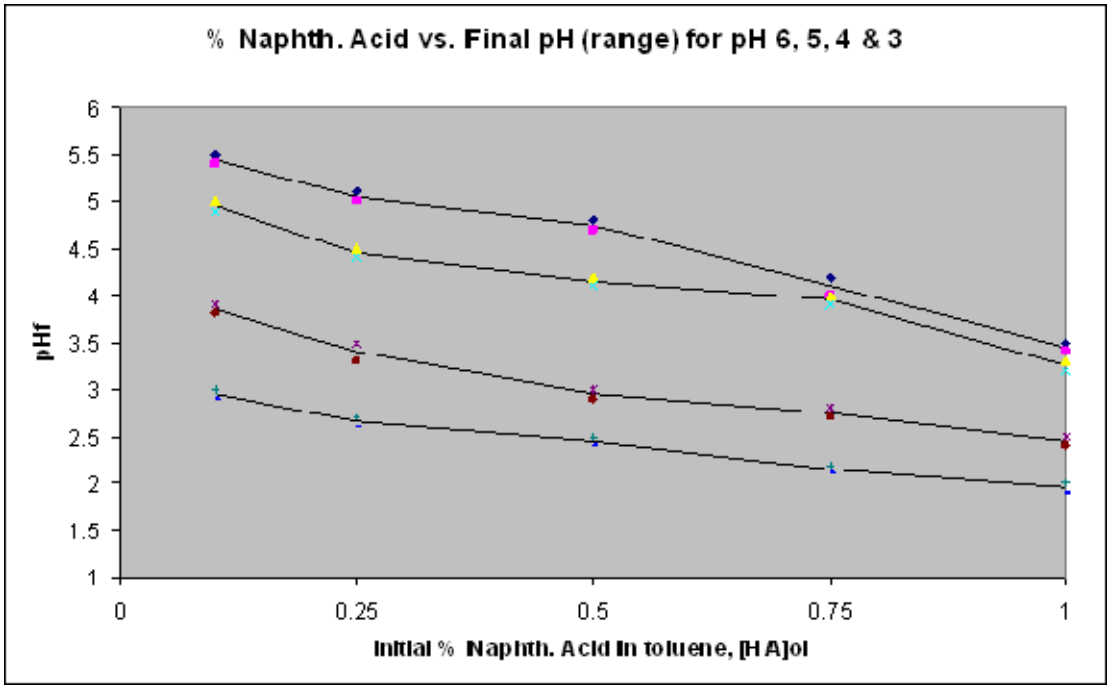

Figure 6.5: Summary of the plot of experimental pH_f values for a system vs. % naphthenic acid in toluene with $pH_i = 6$, 5, 4 and 3.

Modelling Results—Approach 1

The model equations for the pH change experiments were solved by estimating the values of the acid dissociation constant (K_a) and partition coefficient (K_{ow}), and then calculating the final brine pH (pH_f) for the various initial brine pH_i of 6, 5, 4, and 3, and initial naphthenic acid $[HA]_{oi}$ concentrations of 0.0033 M (0.1 wt%), 0.0083 (0.25 wt%), 0.0166 (0.5 wt%), 0.025 (0.75 wt%), and 0.0333 (1.0 wt%). Virtually all dissociation constants of naphthenic acids (K_a) in the literature are found to be in the range of, $K_a = 1\times10^{-4}$ to 1×10^{-6} (pKa = 4 to 6). In addition, it is well known that naphthenic acids are quite sparingly soluble in water and therefore the partition constant, K_{ow} (defined in Eq. 1), is expected to be low, in the order of $\sim10^{-5} - 10^{-3}$ (Havre, 2002).

By a process of trial and error, using the model, the values $K_a = 7.0\times10^{-5}$ and $K_{ow} = 3.0\times10^{-2}$ were found to give the best overall fit to the experimental data. Table 6.2 gives the final pH (pH_f) values calculated for the initial pH values 6, 5, 4, and 3 using the values $K_a = 7.0\times10^{-5}$ and $K_{ow} = 3.0\times10^{-2}$. A plot of these calculated pH_f vs. initial naphthenic acid concentration $[HA]_{oi}$ is presented in Figure 6.6. Comparing the graph summarizing the experimental data (Figure 6.5) with that of the modelling data (Figure 6.6), the two plots show qualitatively similar trends, with a progressive decrease of the final pH value from a higher value to a lower pH. For the higher initial pH values of (pH_i = 6 and 5), a moderate qualitative agreement was seen between the modelling results and experiment for these fixed values of K_a and K_{ow}, although the "quantitative" agreement was poor. However, it is evident that using fixed values of K_a and K_{ow} cannot give a good qualitative representation for the observed behaviour at lower initial pH values. For pH_i = 3, the experimental final pH_f was ~2, whereas, the model prediction is that the pH hardly changes at all. To determine why the model is not reproducing experimental observations correctly, an alternative modelling approach was examined, as explained in the following section.

	pH_i = 6	**pH_i = 5**	**pH_i = 4**	**pH_i = 3**
↓ $[HA]_{oi}$	pH_f	pH_f	pH_f	pH_f
0.1 wt% (0.0033M)	4.08	4.06	3.84	2.99
0.25 wt% (0.0083M)	3.88	3.87	3.72	2.99
0.50wt% (0.0166M)	3.73	3.72	3.62	2.98
0.75 wt% (0.025M)	3.65	3.64	3.55	2.98
1.0 wt% (0.0333M)	3.58	3.58	3.50	2.99

Table 6.2: Calculated values of the final brine pH at initial brine pH values 6, 5, 4 and 3 using the values of $K_a = 7.0 \times 10^{-5}$ and $K_{ow} = 3.0 \times 10^{-2}$.

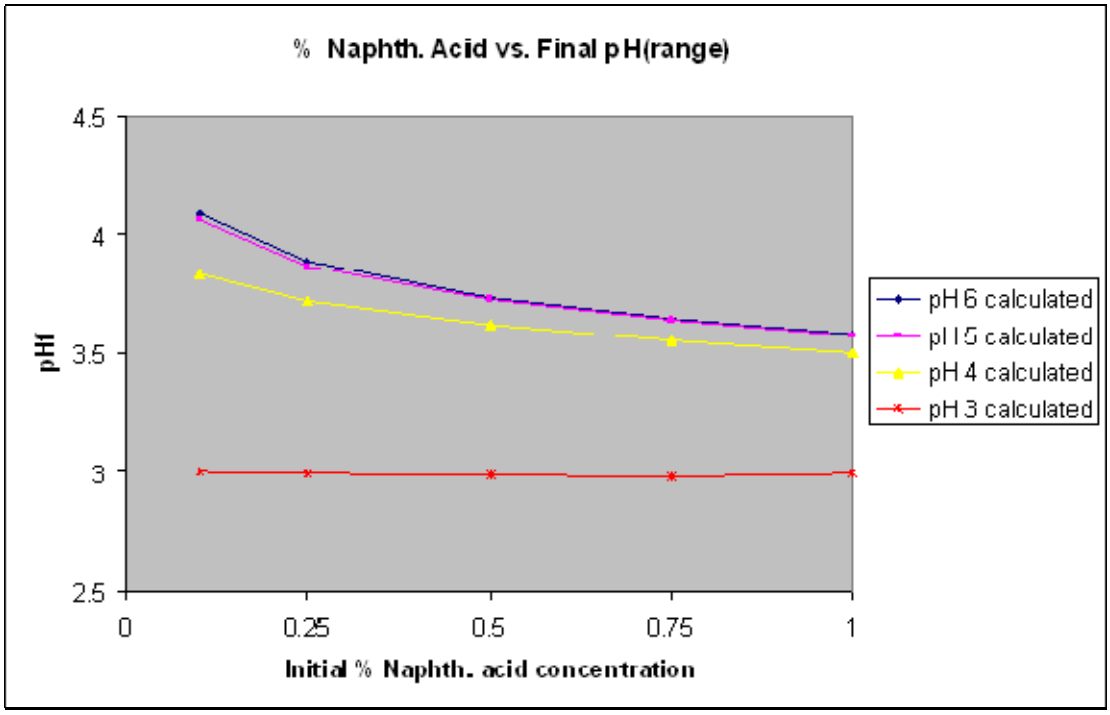

Figure 6.6: Plot of pH_f vs. initial % naphthenic acid for various values of initial pH (pH_i) for values of $K_a = 7.0 \times 10^{-5}$ and $K_{ow} = 3.0 \times 10^{-2}$.

Modelling Results—Approach 2

Another modelling approach was investigated that involved trying to match each individual experiment in Table 6.2 using an optimized solver. This solver was designed to find the best fit values of K_a and K_{ow} "for each individual pH change experiment." However, when this procedure was conducted, it was found that exact fits to the data were only possible by assuming that different sets of K_a and K_{ow} values applied for each of the initial brine pH values of 6, 5, 4, and 3. Table 6.3 shows the experimental data and data generated from the code, together with corresponding pairs for K_a and K_{ow} for each initial brine pH. A plot of the calculated final brine pH (pH_f) vs. initial % naphthenic acid $[HA]_{oi}$, using the data from Table 6.3, is also presented in Figure 6.7**.** A direct comparison with the experiment is made for this approach in Figure 6.8, in which it was observed that there was now a good quantitative and qualitative correlation between the experimental and the calculated data at higher pH values of 6 and 5, and a moderate qualitative match at lower pH values. The corresponding plots of best fit K_a and K_{ow} values vs. initial naphthenic acid concentration ($[HA]_{oi}$) for the individual experiments are shown in Figure 6.9**.** Clearly, there is no definite trend in these parameters with naphthenic acid concentration. This is not physically satisfactory and points to the fact that one of the assumptions of our simple model is not correct. This weak assumption ***may*** be due to the fact that a single naphthenic acid is assumed in the model, whereas the pH change experiments involved an extract from a calcium naphthenate field deposit, known (from Electrospray Mass Spectrometry and Atmospheric Pressure Chemical Ionisation Mass Spectrometry results) to have many naphthenic acid [HA] components (Mohammed and Sorbie, 2009).

Calculated					
Calc pH 6	5.448326	5.049786	4.749296	4.100036	3.45002
Calc pH 5	4.94995	4.449995	4.149965	3.950015	3.25013
Calc pH 4	3.854	3.467254	3.338684	3.259624	3.20317
Calc pH 3	2.986463	2.968053	2.941693	2.918893	2.89915
Experimental					
Exp pH 6	5.456	5.056	4.756	4.16	3.45
Exp pH 5	4.955	4.455	4.155	3.955	3.25
Exp pH 4	3.854	3.44	2.954	2.754	2.45
Exp pH 3	2.953	2.653	2.453	2.153	1.95
K_a					
pH/Conc.	0.0033M	0.0083M	0.0166M	0.025M	0.0333M
pH 6	0.000277	0.000852	0.00001	0.0000595	0.000772
pH 5	0.000416	0.0000199	0.000426	0.000505	0.00097
pH 4	0.000881	0.001	0.001	0.001	0.001
pH 3	0.001	0.001	0.001	0.001	0.001
K_{ow}					
pH/Conc.	0.0033M	0.0083M	0.0166M	0.025M	0.0333M
pH 6	0.00001	0.00001	0.001808	0.004206	0.004905
pH 5	0.00001	0.005505	0.000609	0.000909	0.0097
pH 4	0.002008	0.01	0.01	0.01	0.01
pH 3	0.01	0.01	0.01	0.01	0.01

Table 6.3: Calculated pH_f values from the code and the corresponding K_a and K_{ow} for each pH_i value.

It is important to note that K_a value of the naphthenic acid should have been one constant value within the range (pKa = 4 to 5) in carrying out the calculations, but rather in the actual sense the experiment was conducted using a multi-acid system whereas the model is based on the pseudo-component approach. It is this light several values of K_a were used for each different acid concentration in order to make model prediction. This approach yields better qualitative results based on the model prediction and experimental results.

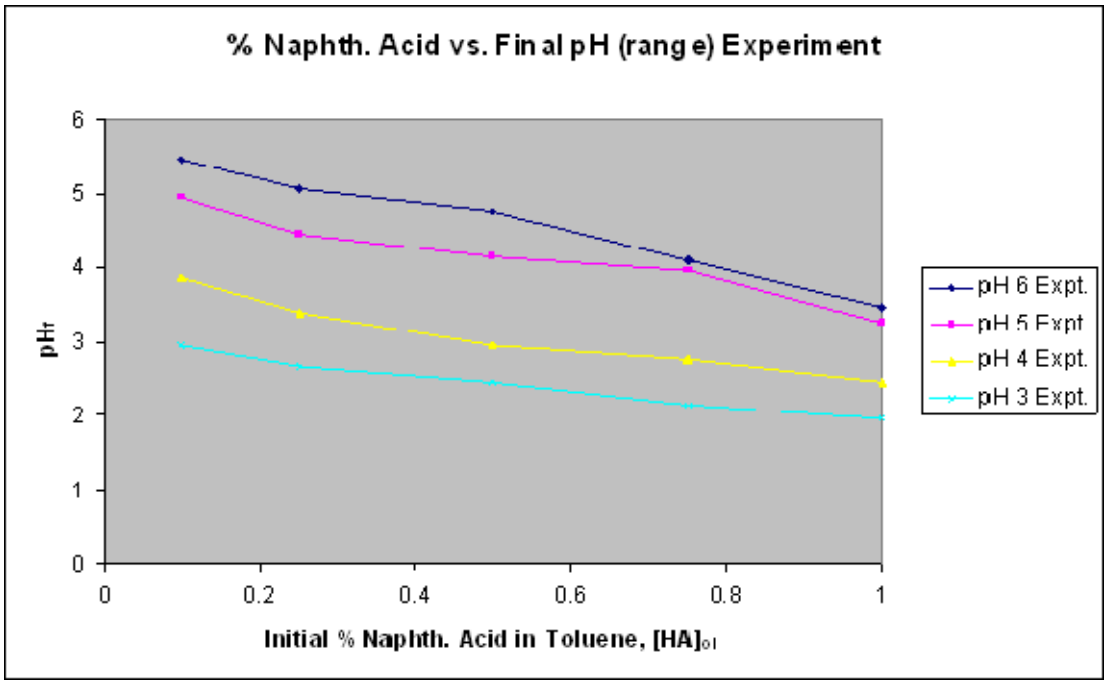

Figure 6.7: Plot of calculated pH_f vs. initial % naphthenic acid concentration for the cases where different K_a and K_{ow} values were found by optimizing fitting for each of the individual experiments.

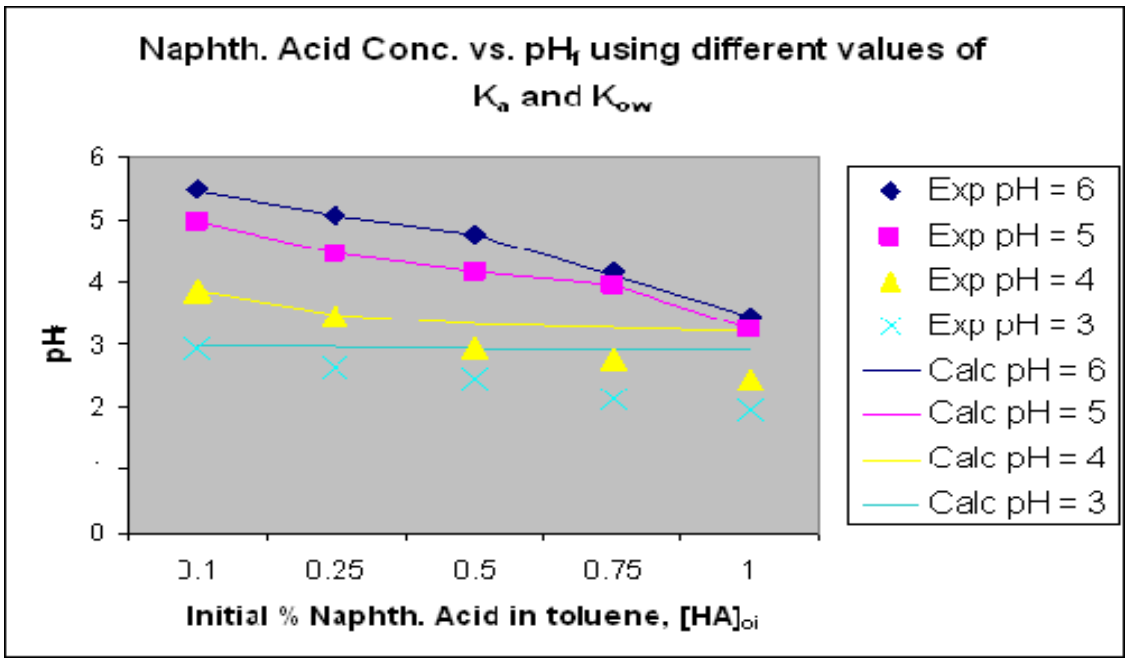

Figure 6.8: Comparison of the experimental pH change data with the calculated pH_f vs. initial % naphthenic acid concentration for the case where different K_a and K_{ow} values were found by optimized fitting for each of the individual experiments.

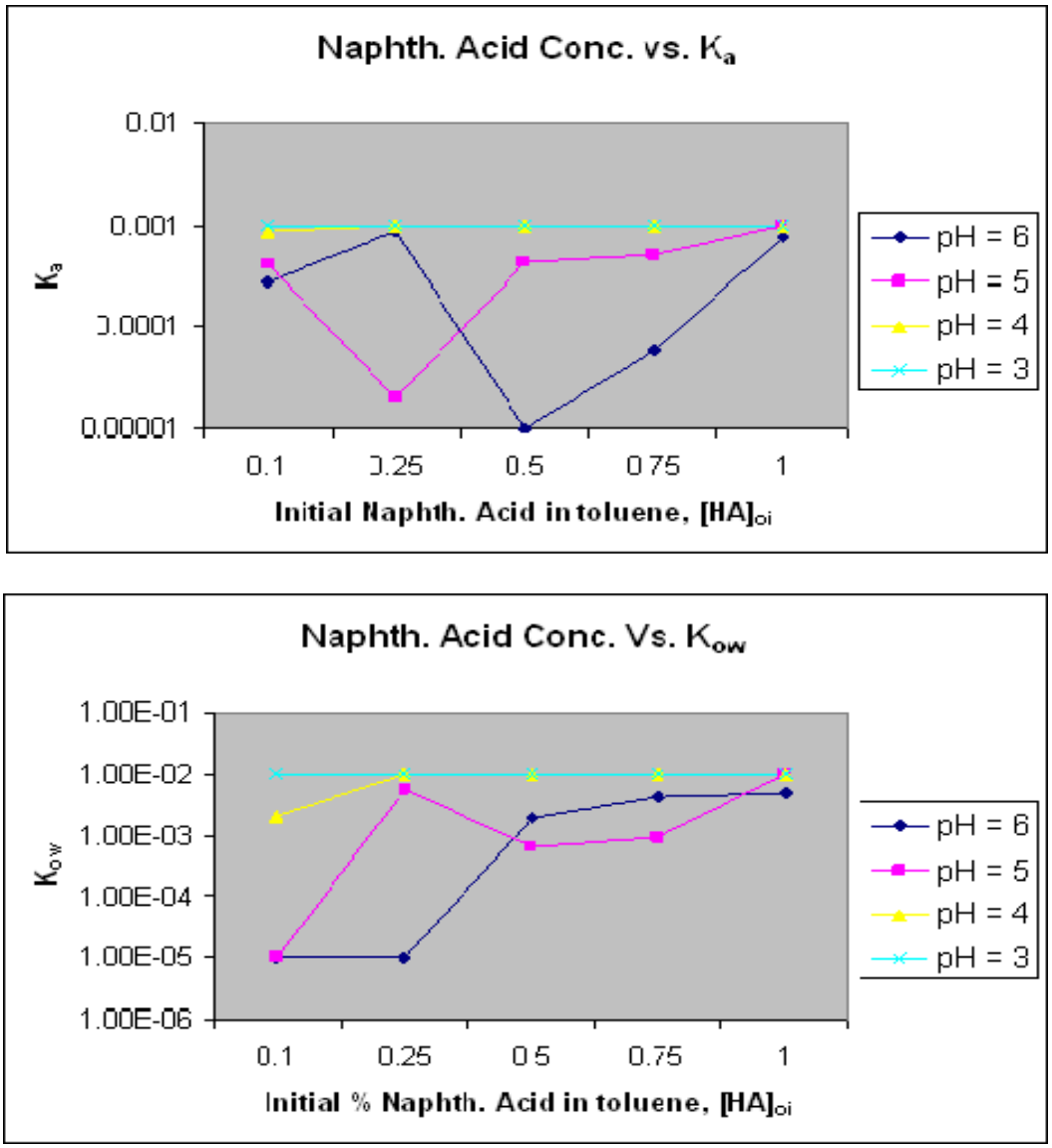

Figure 6.9: Plots of K_a vs. $[HA]_{oi}$ and K_{ow} vs. $[HA]_{oi}$ for the cases where K_a and K_{ow} are directly fitted for each pH change experiment; data in Table 6.3.

6.4 THERMODYNAMIC NAPHTHENATE PRECIPITATION MODELLING EXPERIMENT

In this section, the extension of the naphthenate thermodynamic model is now discussed to describe the chemistry of a simple partitioning naphthenate system, which may form a calcium naphthenate "precipitate", according to a solubility product type description. A single naphthenic acid, denoted [HA], is again used to represent the behaviour of the (much

more complex) range of naphthenic acids that is present in the oil; in this sense, [HA] is a "pseudo-component". This model acid can, as previously described (i) then partition between the oil and water phases, described by a partition constant, K_{ow}; (ii) it can dissociate as a weak acid in the aqueous phase, according to the dissociation constant, K_a; and (iii) it may precipitate/phase separate as a metal naphthenate, such as Na-A or Ca-A_2, described by a solubility product, such as K_{NaA} or K_{CaA_2}. All of the parameters that appear in this model are either well known or independently measureable physical data such as K_{ow}, K_a, K_{CaA_2} and K_w (the ionic product of water). A restricted version of this model was presented above to describe "pH change" experiments where an oil (toluene) containing naphthenic acids was brought into contact with a medium pH (pH ~ 9) aqueous phase, where naphthenic acid partitioning took place but no precipitate (or emulsion) formed. However, the pH changed from its initial value to a lower value. A full derivation of the naphthenate precipitation model is presented in Appendix A. Note that this derivation has been presented where outline previously but only a small number of numerical examples were given due to the difficulty in solving the equations numerically. The new derivation results in a reduced equation which has been solved in a recently written VBA code in Excel, using a much more robust Newton-Raphson numerical solution method. This code is then applied in a wide sensitivity study which makes some predictions about the way a precipitating Ca-Naphthenate (CaN) system behaves. The model was then applied to design three new experiments which were performed in the laboratory in order to test the model predictions. Before going into the details of the full naphthenate precipitation modelling, an experiment was carried out to determine the minimum brine pH which results in calcium naphthenate precipitation.

Naphthenate Precipitation Formation Experimental Results

The naphthenate precipitation experiment was carried out using naphthenic acid [HA] extract dissolved in toluene with [HA] = 7500 ppm and 3000 ppm, which were put into contact with a synthetic brine (composition: Na^+ = 25000 ppm and Ca^{++} = 20000 ppm) at various initial pH 6, 6.5, 7, 7.5, 8, 8.5 and 9. The results showed a very slight precipitation at brine pH 7.5, 8 and full precipitation formation of the naphthenates at pH 8.8 and 9 for

the naphthenic concentration [HA] in the oil phase equivalent to 7500ppm. However, formation of naphthenate precipitates at the lower concentration of naphthenic acid, of 3000pm in the oil phase, was observed slightly at brine pH 8. At brine pH 8.5, the naphthenate precipitation was at the interface and it was only at brine pH 9 that bulk naphthenate precipitation was observed. A descriptive chart of these results was compiled and is presented in Table 6.4 below. The final brine pH measured revealed a general decrease in the brine pH as the initial concentration of naphthenic acid in the oil phase increased. Furthermore, pH decreases for brine with initial pH of 9 were much higher than those for brine with initial pH of 6. The plot of the final brine pH versus the initial % naphthenic acid concentration in toluene is shown in Figure 6.10.

HA/brine pH	6	6.5	7	7.5	8	8.5	9
7500ppm	**No Precipitate**	**No Precipitate**	**No Precipitate**	**Very Slight Precipitate**	**Very Slight Precipitate**	**Precipitate**	**Precipitate (bulk)**
3000ppm	**No Precipitate**	**No Precipitate**	**No Precipitate**	**No Precipitate**	**Very Slight Precipitate**	**Precipitate (interface)**	**Precipitate**

Table 6.4: Calcium naphthenate precipitation chart at initial brine pH 6 to 9

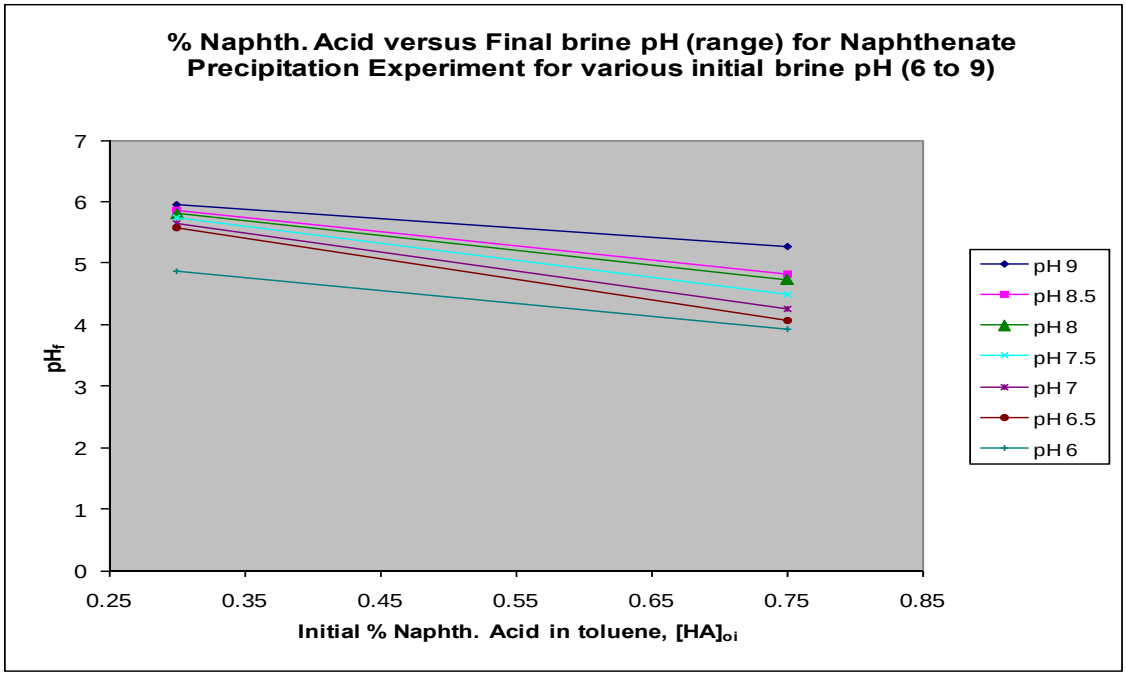

Figure 6.10: Plot of brine final pH_f versus initial % naphthenic acid concentration in toluene for various initial brine pH_i.

Sensitivity study using the naphthenate precipitation model

A wide ranging series of naphthenate precipitation calculations were performed which demonstrated the sensitivity of the model to the main input parameters. Recall that the main input parameters and initial values are shown in the algorithm for the numerical solution of the naphthenate model equation (Appendix A ---Table A1):

1. The **constant parameters** in the model – i.e. K_{ow}, K_a, K_{CaA_2} and K_w

2. The **initial values** of quantities – $\boldsymbol{x_{1i} = [HA]_{oi}}$, $\boldsymbol{x_{3i} = [H^+]_{wi}}$, and $\boldsymbol{x_{6i} = [Ca^{2+}]_{wi}}$

(Note $\boldsymbol{x_{5i} = [OH^-]_{wi}}$ is simply given as $\boldsymbol{x_{5i} = [OH^-]_{wi} = K_w / [H^+]_{wi}}$)

Although there appear to be several parameters in this model, they are actually quite constrained as discussed below for the constant parameters:

(i) ***Ionic product of water:*** $K_w = [H^+].[OH^-] = 1 \text{x} 10^{-14}$ – this could be varied in the calculations but it is simply maintained at this constant value in all of the calculations presented here;

(ii) ***Oil/water partition coefficient of HA:*** K_{ow} - the partition coefficient should reflect the fact that the naphthenic acid, [HA], is preferentially much more soluble in the oil than in the water, and it is most probably in the range K_{ow} ~ 0.001 - ~0.02, with a most probable value of ~0.01 - however, much wider range i.e. 1E-06 to 1 was considered in the sensitivity (although all values of $K_{ow} > 0.1$ are too high);

(iii) ***Dissociation constant of HA:*** K_a - most naphthenic acids are very weak acids with acid dissociation constants in the range $K_a \sim 1\text{x}10^{-5}$ - $1\text{x}10^{-4}$ (i.e. $pK_a \sim 5 - 4$). However, in this sensitivity calculation, the range was widened to 4 different values: $K_a \sim 1\text{x}10^{-6}$, $1\text{x}10^{-5}$, $1\text{x}10^{-4}$ and $1\text{x}10^{-3}$, although it should be noted that the latter value is probably too acidic.

(iv) ***Solubility model for CaA_2:*** K_{CaA_2} - the solubility product value for the $\boldsymbol{CaA_2}$ precipitate is the least well known of the constant parameters in the naphthenate system, as formulated here. It is given here by Eq. (4), $\boldsymbol{K_{CaA_2} = \left[Ca^{2+}\right]_f . \left[A^-\right]_f^2}$, but it is difficult to envisage what "realistic" values should be, since it involves the quantity $\left[A^-\right]_f^2$ which is very difficult to estimate *a priori* – indeed, it simply has to be calculated from the set of equations (where it is $\boldsymbol{x_4 = \left[A^-\right]_f}$). Again, it is stressed that, in principle, ***any*** mathematical model to describe metal naphthenate "precipitation" or "phase separation" can be inserted in the overall model. In fact, it was found out that typical equilibrium values of $\left[A^-\right]_f$ turn out to be , $\left[A^-\right]_f \sim 6\text{x}10^{-6}$ M - therefore, values of K_{CaA_2} which lead to a $\boldsymbol{CaA_2}$ precipitate are in the range used here, $K_{CaA_2} \sim 1\text{x}10^{-13}$, $1\text{x}10^{-12}$ and $1\text{x}10^{-11}$ - whereas values of $K_{CaA_2} \sim 1\text{x}10^{-10}$ do not lead to naphthenate precipitation.

In summary, the studies of the parameter sensitivity ranges are as follows:

	Actual Range Used in Sensitivity Calculations		
Parameter	**Low Values**	**Realistic range**	**High Values**
$K_w = [H^+].[OH^-]$	-	Fixed at $1x10^{-14}$	-
$K_{ow} = [HA]_{wf} / [HA]_{of}$	$1x10^{-6}$	~ 0.001 - ~0.02	0.1 - 1.00
$K_a = [H^+]_{wf}.[A^-]_{wf} / [HA]_{wf}$	$1x10^{-6}$	~ $1x10^{-5}$ - $1x10^{-4}$	$1x10^{-3}$
$\boldsymbol{K_{CaA_2} = \left[Ca^{2+}\right]_f . \left[A^-\right]_f^2}$	??	~$1x10^{-13}$ - $1x10^{-11}$	$1x10^{-10}$ no ppt. forms

A wide range of sensitivity calculations is presented in Figures 6.11 – 6.13. These figures show the sensitivity of the naphthenate precipitation model, showing (i) the final pH_f (pH_i = 9), (ii) the mass of CaA_2 precipitate and (iii) the %A in the precipitate as a function of K_{ow} (from 1E-06 to 1) for (a) $\boldsymbol{K_a}$ = = 1E-06; (b) $\boldsymbol{K_a}$ = 1E-05; (c) $\boldsymbol{K_a}$ = 1E-04; (d) $\boldsymbol{K_a}$ = 1E-03. Each figure is at a fixed value of solubility product, $\boldsymbol{K_{CaA_2}}$ **= 1E-13** (Figure 6.11), $\boldsymbol{K_{CaA_2}}$ **= 1E-12** (Figure 6.12), $\boldsymbol{K_{CaA_2}}$ **= 1E-11** (Figure 6.13). In each of the sub-figures, the value of $\boldsymbol{pH_f}$ at $\boldsymbol{K_{ow}}$ = 0.01 is also indicated. In general, these figures give the entire picture of the sensitivity of the model and, with very close study, they are extremely informative.

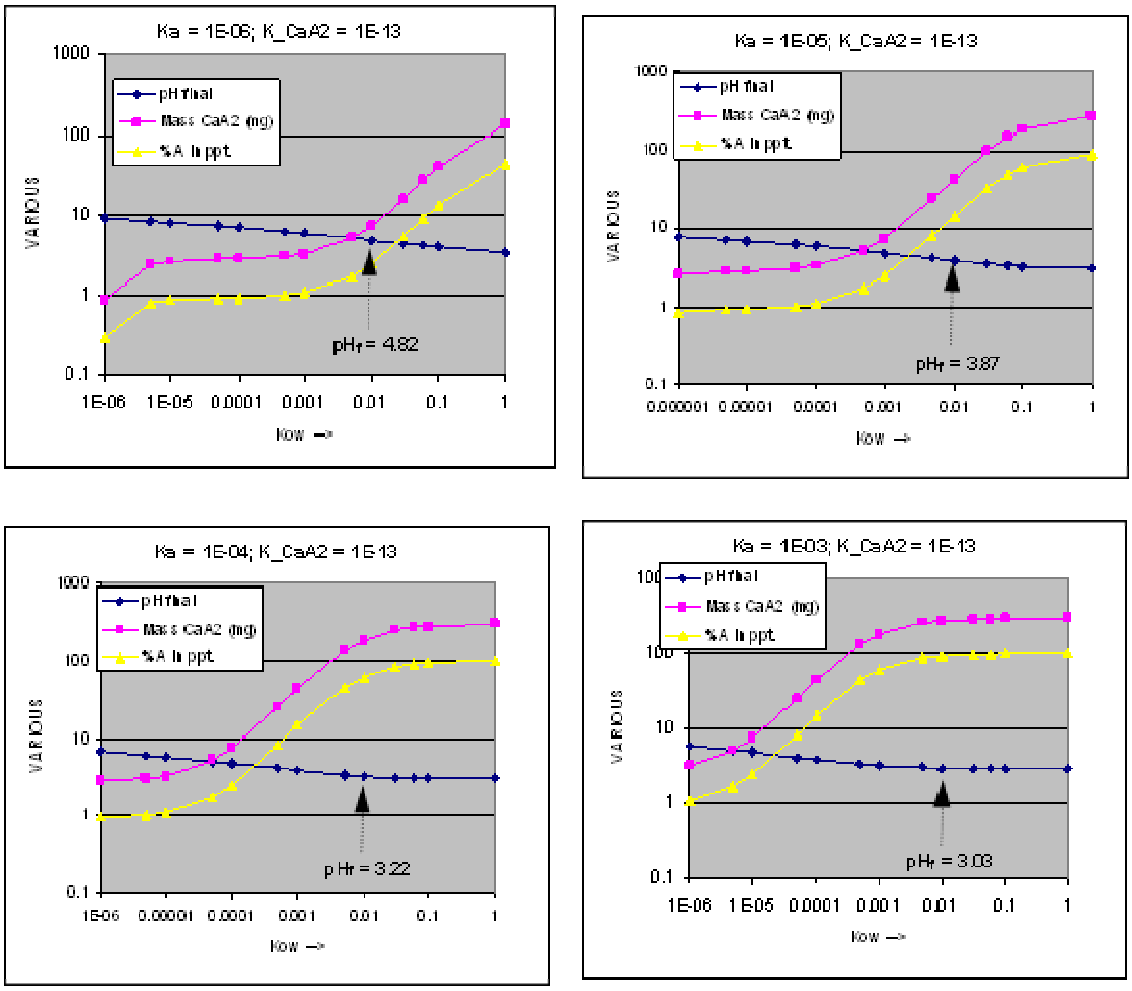

Figure 6.11: Sensitivity study of the naphthenate precipitation model, showing the final pH_f (pH_i = 9), the mass of CaA_2 precipitate and the %A in the precipitate as a function of K_{ow} (from 1E-06 to 1) for a fixed $\boldsymbol{K_{CaA_2}}$ **= 1E-13** and (a) $\boldsymbol{K_a}$ = = 1E-06; (b) $\boldsymbol{K_a}$ = = 1E-05; (c) $\boldsymbol{K_a}$ = = 1E-04; (d) $\boldsymbol{K_a}$ = = 1E-03. Value of $\boldsymbol{pH_f}$ at $\boldsymbol{K_{ow}}$ = 0.01 also indicated.

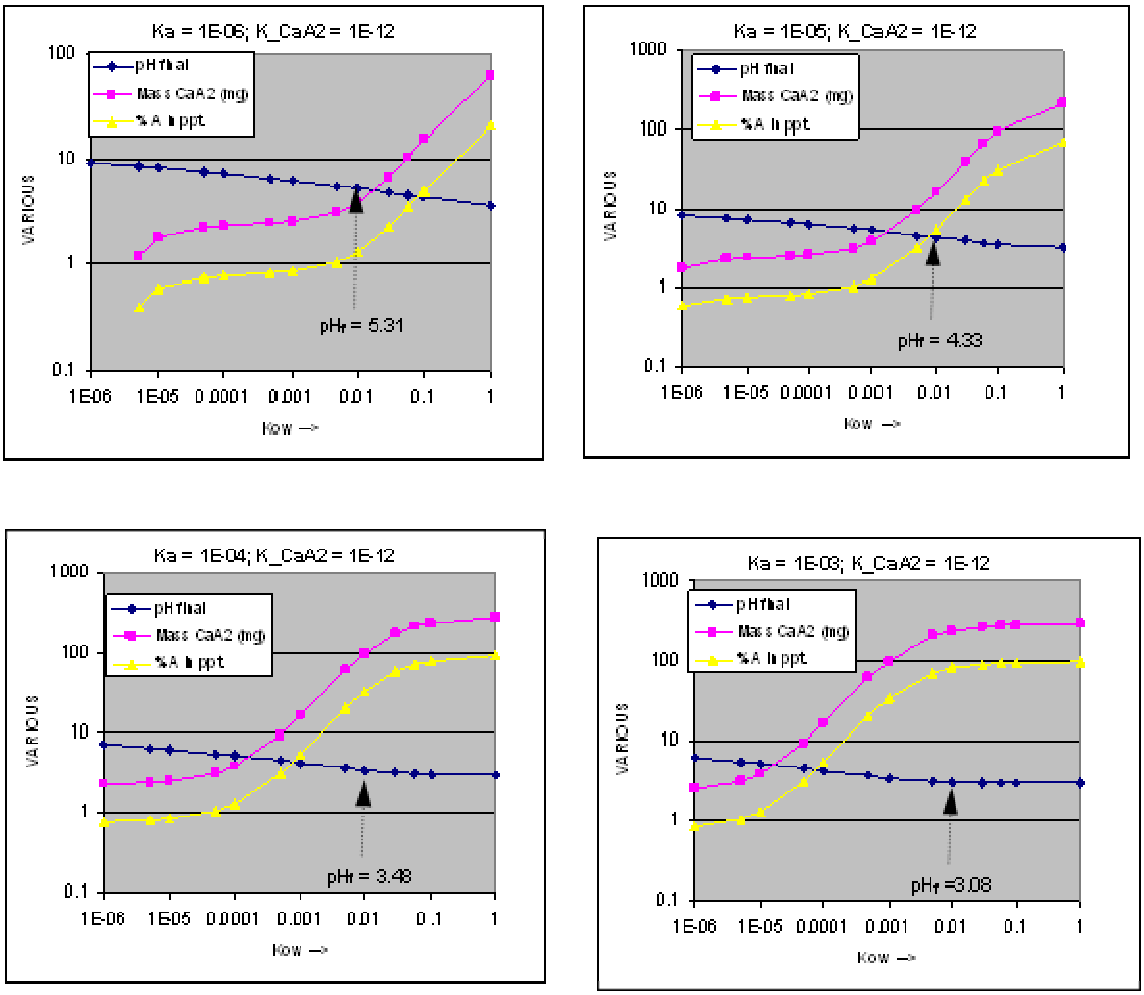

Figure 6.12: Sensitivity study of the naphthenate precipitation model, showing the final pH_f (pH_i = 9), the mass of CaA_2 precipitate and the %A in the precipitate as a function of K_{ow} (from 1E-06 to 1) for a fixed $\boldsymbol{K_{CaA_2}}$ **= 1E-12** and (a) $\boldsymbol{K_a}$ == 1E-06; (b) $\boldsymbol{K_a}$ == 1E-05; (c) $\boldsymbol{K_a}$ == 1E-04; (d) $\boldsymbol{K_a}$ == 1E-03. Value of $\boldsymbol{pH_f}$ at $\boldsymbol{K_{ow}}$ = 0.01 also indicated.

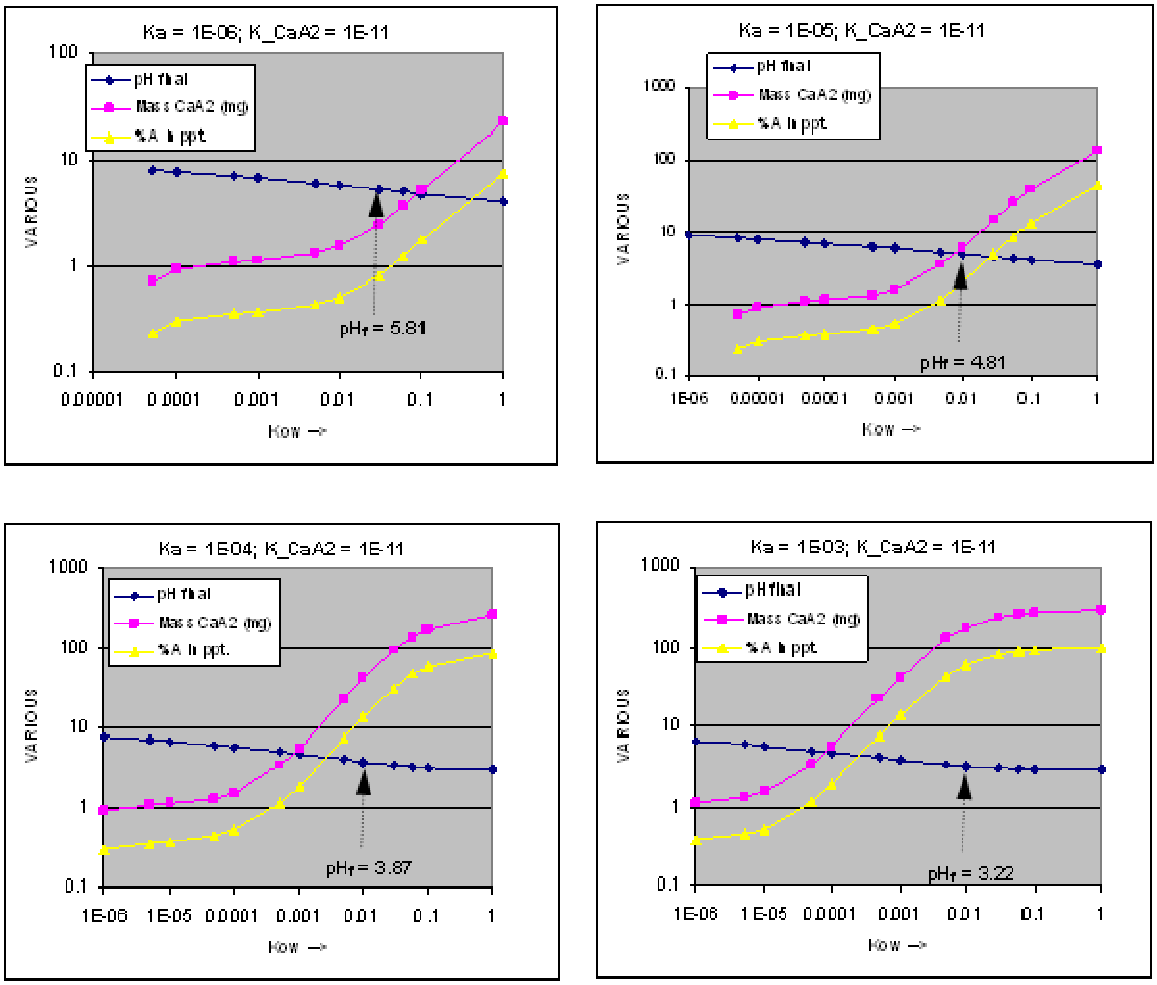

Figure 6.13: Sensitivity study of the naphthenate precipitation model, showing the final pH_f (pH_i = 9), the mass of CaA_2 precipitate and the %A in the precipitate as a function of K_{ow} (from 1E-06 to 1) for a fixed $\boldsymbol{K_{CaA_2}}$ **= 1E-11** and (a) $\boldsymbol{K_a}$ = = 1E-06; (b) $\boldsymbol{K_a}$ = = 1E-05; (c) $\boldsymbol{K_a}$ = = 1E-04; (d) $\boldsymbol{K_a}$ = = 1E-03. Value of $\boldsymbol{pH_f}$ at $\boldsymbol{K_{ow}}$ = 0.01 also indicated.

To summarise, the following conclusions can be deduced based on the information and naphthenate model sensitivity results in Figures 6.11 to 6.13 above:

1. Under ***all*** conditions at any fixed values of $\boldsymbol{K_{CaA_2}}$ and $\boldsymbol{K_a}$ (Figures 6.11 –6.13), then as K_{ow} increases (the [HA] becomes more soluble in the aqueous phase), the $\boldsymbol{pH_f}$ is lower, more $\boldsymbol{CaA_2}$ precipitate forms and a correspondingly larger %A appears in this precipitate.

2. As the solubility of the $\boldsymbol{CaA_2}$ reduces – i.e. as $\boldsymbol{K_{CaA_2}}$ decreases – then the amount of precipitate increases more rapidly as K_{ow} increases. This is best illustrated by selecting some results from Figures 6.11 – 6.13, as shown in Figure 6.14. Figure 6.14 shows the final pH_f (pH_i = 9) and the mass of CaA_2 precipitate as a function of $\boldsymbol{K_{ow}}$ (from 1E-06 to 1) for two values of the naphthenate solubility product, $\boldsymbol{K_{CaA_2}}$ **= 1E-13** and **1E-12 ,** for a **fixed** $\boldsymbol{K_a}$ **=** 1E-04. The "lag" in the rise in the amount of precipitate is clear in this figure, whereas the final pH behaviour is quite similar.

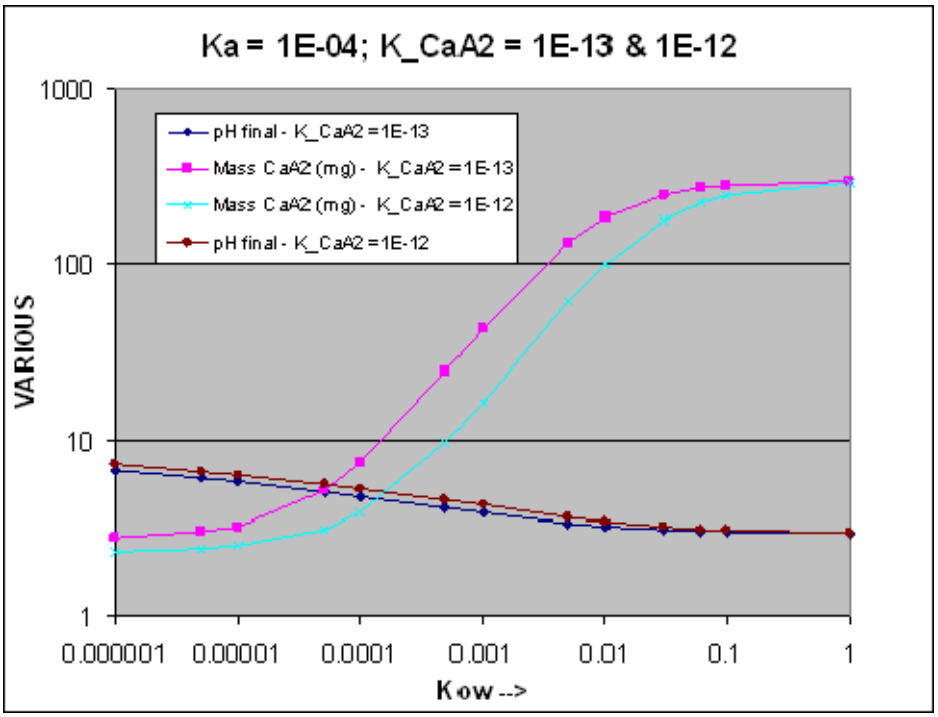

Figure 6.14: Sensitivity of the naphthenate precipitation model showing the final pH_f (pH_i = 9) and the mass of CaA_2 precipitate as a function of K_{ow} (from 1E-06 to 1) for two values of the naphthenate solubility product, $\boldsymbol{K_{CaA_2}}$ **= 1E-13** and **1E-12** for a fixed $\boldsymbol{K_a}$ **=** 1E-04.

3. Focusing on the probable quantitative behaviour of the naphthenate model, the final pH and the %A in the precipitate as a function of $\boldsymbol{K_a}$ for a fixed value of $\boldsymbol{K_{CaA_2}}$ **= 1E-12** and two "likely" values of $\boldsymbol{K_{ow}}$ = 0.001 and 0.01 are examined. Figures 6.15 and 6.16 show final pH and %A in precipitate results for these cases, respectively. Figure 6.16 is also

shown modified as Figure 6.17, where the "most likely" window of naphthenate parameters is shown on this figure; which was considered to be in the following range:

$$K_{CaA_2} = \text{1E-12}$$

$$\text{1E-05} \leq K_a \leq \text{1E-04}$$

$$\text{0.001} < K_{ow} \leq \text{0.02}$$

From Figure 6.17, it is clear that such parameters would lead to levels of **~2% to ~30% of naphthenic acid "A" being incorporated into the CaA_2 deposit**. This is quite clearly sufficient to lead to the types of observation made in the laboratory and most probably this is of the levels required to cause calcium naphthenate problems in the field. It also gives further support to the type of successive extraction experiment proposed in the next section, since, even at the highest values of K_a = 1E-04 and K_{ow} = 0.01, there is still a significant amount of [HA] remaining in the oil phase (~70%) after CaA_2 precipitates and the system is at equilibrium.

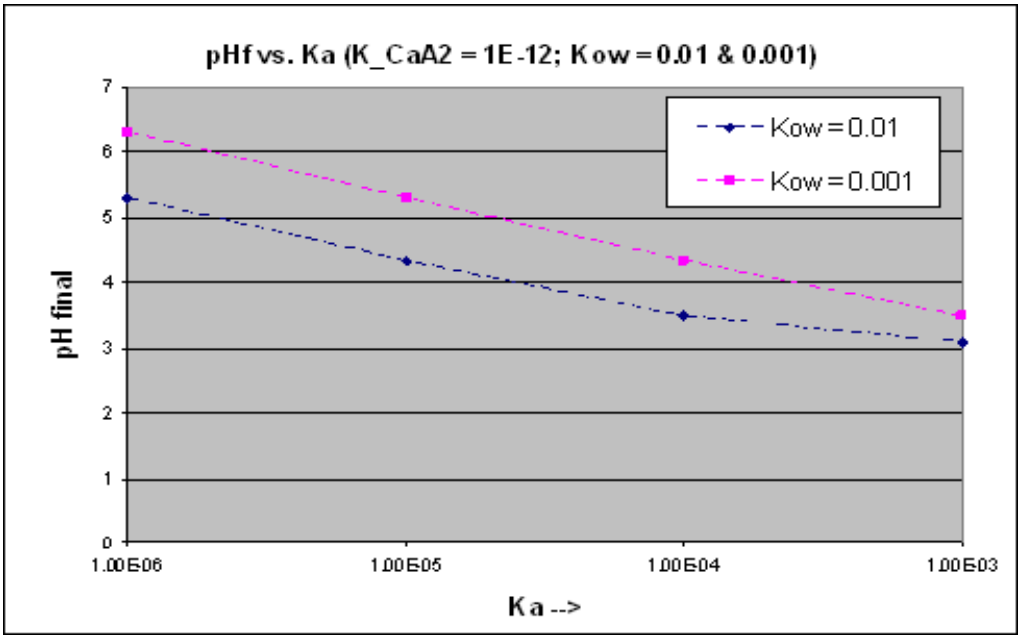

Figure 6.15: Sensitivity of the naphthenate precipitation model showing the final pH_f (pH_i = 9) vs. K_a (from 1E-06 to 1E-03) at two values of K_{ow} = 0.001 & 0.01 for fixed naphthenate solubility product, K_{CaA_2} **= 1E-12.**

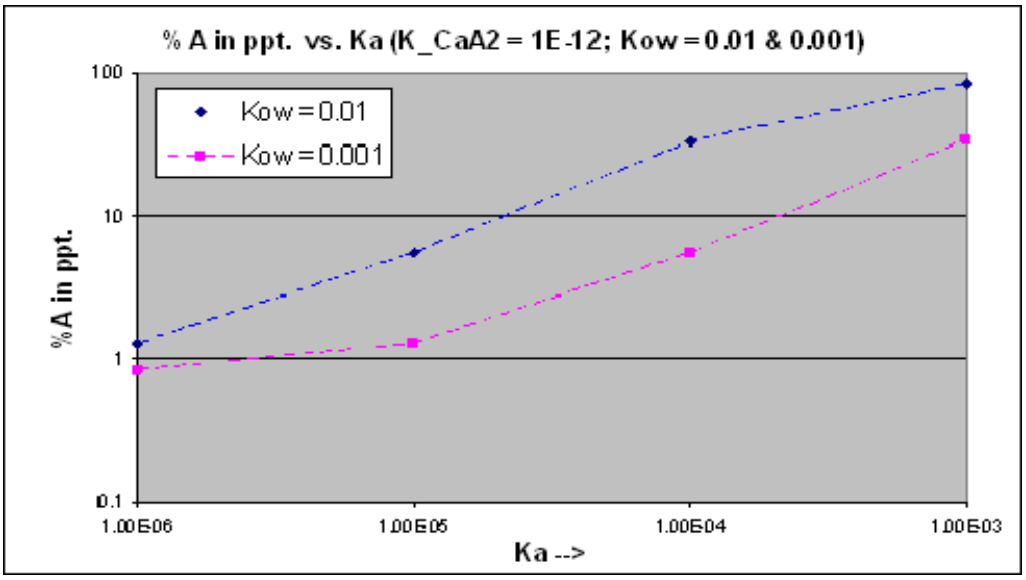

Figure 6.16: Sensitivity of the naphthenate precipitation model showing the %A in the CaA_2 precipitate vs. K_a (from 1E-06 to 1E-03) at two values of K_{ow} = 0.001 & 0.01 for fixed naphthenate solubility product, K_{CaA_2} = **1E-12.**

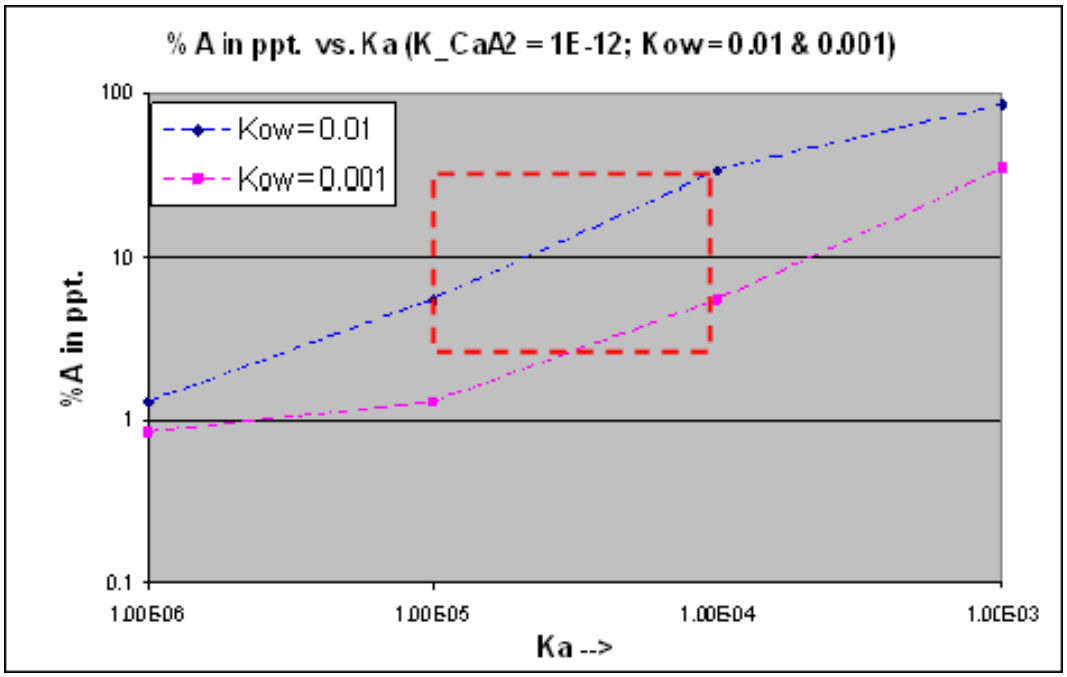

Figure 6.17: Sensitivity of the naphthenate precipitation model showing the %A in the CaA_2 precipitate vs. K_a (from 1E-06 to 1E-03) at 2 values of K_{ow} = 0.001 & 0.01 for fixed naphthenate solubility product, K_{CaA_2} = 1E-12. This is the modified Figure 6.16 showing the "most likely" window of properties.

4. From the sensitivity calculations in a Figures 6.11- 6.13, then a series of **phase diagrams for naphthenate precipitation** can be constructed, as shown in Figures 6.18 (a) – (d), and explained further in Figures 6.19 and 6.20. Figure 6.18 shows phase diagrams of the naphthenate precipitation regions in the K_{ow} - K_a plane at various CaA_2 solubilities: (a) K_{CaA_2} = 1E-13, (b) K_{CaA_2} = 1E-12 and (c) K_{CaA_2} = 1E-11. Each of these three figures (Figures 6.18(a) – 6.18(c)) shows the K_{ow} - K_a combinations required to obtain CaN precipitate, incorporating 5%, 10% and 50% of the original "A" (or [HA]) in the system. Figure 6.18(d) shows the K_{ow} - K_a combinations required to obtain a 5% A incorporation in CaA_2 for various levels of solubility (K_{CaA_2} = 1E-13, 1E-12 and 1E-11). These results are further elucidated in Figure 6.19 which shows phase diagrams of the naphthenate precipitation regions in the K_{ow} - K_a plane for CaA_2 solubility, K_{CaA_2} = 1E-13. The hatched region shows the K_{ow} - K_a combinations where very little CaN precipitate is formed; i.e. where < 5% of the original "A" (or [HA]) in the system is incorporated into the precipitate. Note also that, at a given K_a (for a fixed K_{CaA_2}) then more precipitate (i.e. %A incorporation) occurs as K_{ow} increases. Similarly, Figure 6.20 shows the "phase diagrams" of the naphthenate precipitation regions in the K_{ow} - K_a plane for CaA_2 solubilities, showing the 5%A boundary for incorporation in the precipitate at various K_{CaA_2} = 1E-13, 1E-12 and 1E-11. The hatched region shows the K_{ow} - K_a combinations where very little CaN precipitate is formed; i.e. where < 5% of the original "A" (or [HA]) in the system is incorporated into the precipitate. Note also that, at a given K_a a larger K_{ow} is required to give a 5 %A incorporation in the precipitate, as the solubility constant increases (from K_{CaA_2} = 1E-13 to K_{CaA_2} = **1E-11**).

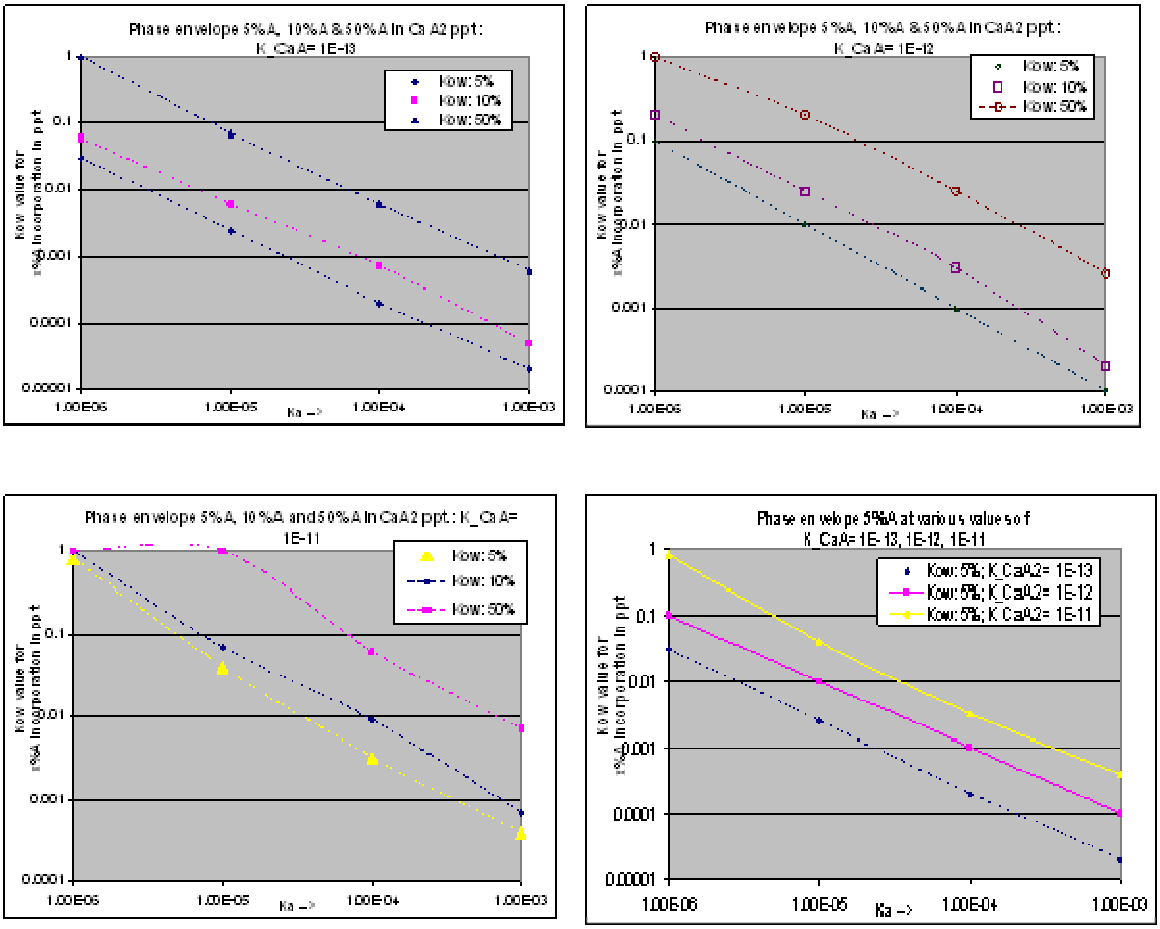

Figure 6.18: "Phase diagrams" of the naphthenate precipitation regions in the K_{ow} - K_a plane at various CaA_2 solubilities, (a) K_{CaA_2} = 1E-13, (b) K_{CaA_2} = 1E-12 and (c) K_{CaA_2} = 1E-11. Each of these 3 figures shows the K_{ow} - K_a combinations required to obtain CaN precipitate incorporating 5%, 10% and 50% of the original "A" (or HA) in the system. Figure 12(d) shows the K_{ow} - K_a combinations required to obtain a 5% A incorporation in CaA_2 for various levels of solubility (K_{CaA_2} = 1E-13, 1E-12 and 1E-11).

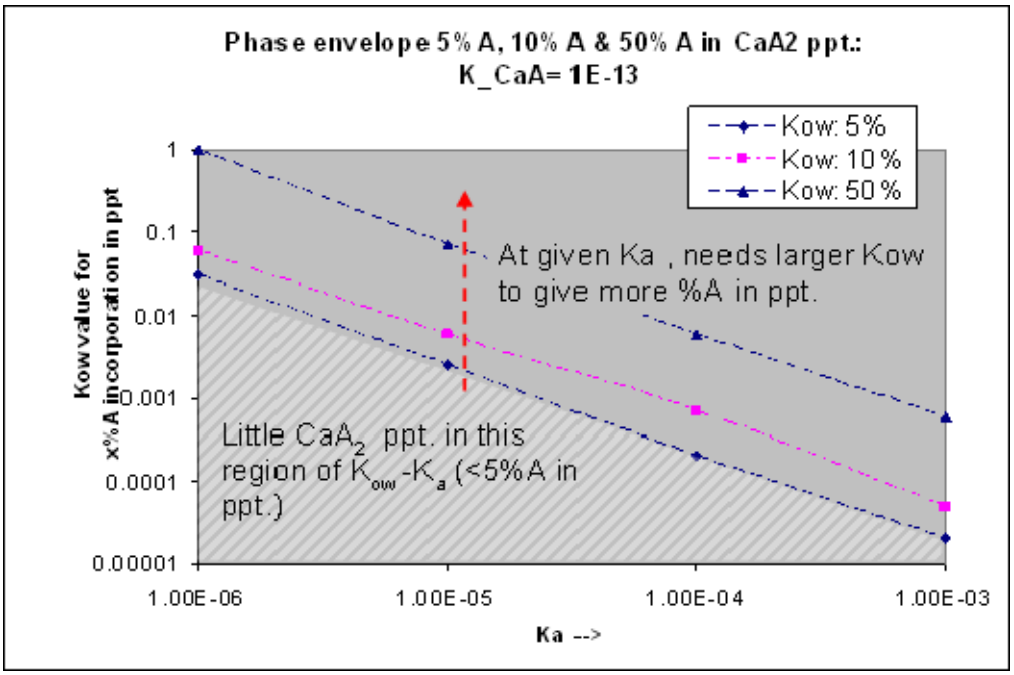

Figure 6.19: "Phase diagrams" of the naphthenate precipitation regions in the K_{ow} - K_a plane for CaA_2 solubilities, K_{CaA_2} = 1E-13. The hatched region shows the K_{ow} - K_a combinations where very little CaN precipitate is formed; i.e. where < 5% of the original "A" (or HA) in the system is incorporated into the precipitate. Note also that, at a given K_a (for a fixed K_{CaA_2}) then more precipitate (i.e. %A incorporation) occurs as K_{ow} increases.

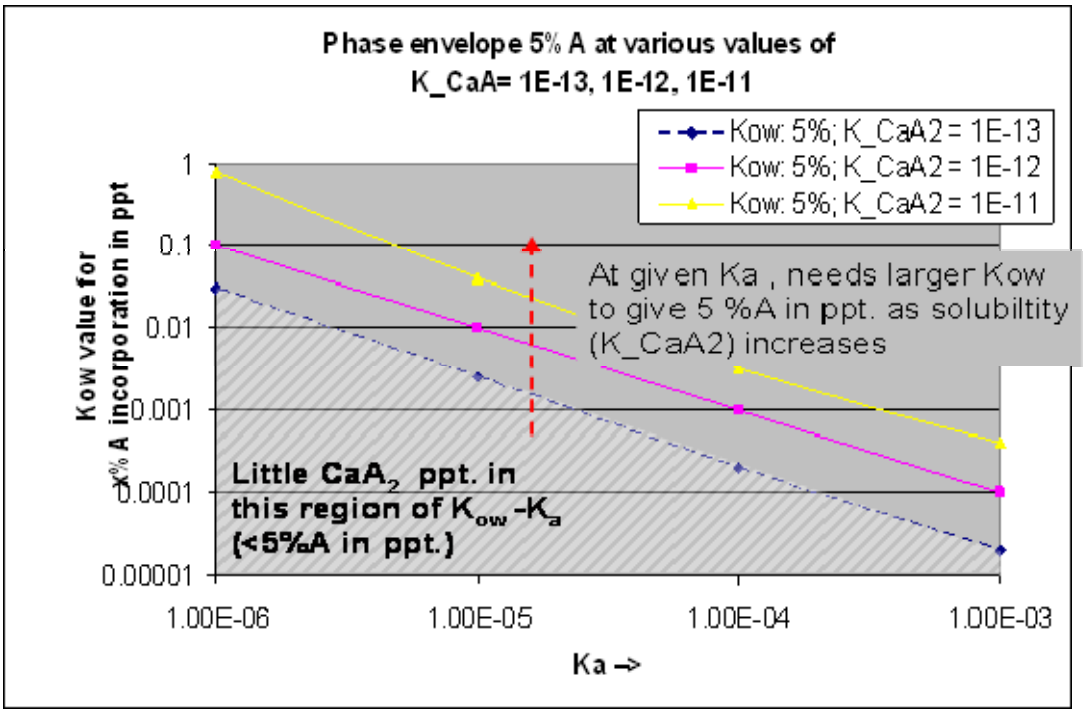

Figure 6.20: "Phase diagrams" of the naphthenate precipitation regions in the K_{ow} - K_a plane for CaA_2 solubilities, showing the 5%A boundary for incorporation in the precipitate at various K_{CaA_2} = 1E-13, 1E-12 and 1E-11. The hatched region shows the K_{ow} - K_a combinations where very little CaN precipitate is formed; i.e. where < 5% of the original "A" (or HA) in the system is incorporated into the precipitate. Note also that, at a given K_a a larger K_{ow} is required to give a 5 %A incorporation.

Predictions from Modelling for Experimental Verification

Example Modelling Results on Calcium Naphthenate (CaN) Deposition

The CaN naphthenate thermodynamic model derived in Appendix A essentially mimics the base case oil/brine precipitation experiment in Figure 6.21 and the species involved are shown schematically in Figure A1. The model is already described and all terms are explained in this appendix and the main parameters are K_{ow}, K_a, K_{CaA_2} and K_w. Table A2 summarises the model as 7 equations (4 equilibria, 2 mass balances and 1 charge balance) in 7 unknowns as follows: $[HA]_{of}, [HA]_{wf}, [H^+]_{wf}, [A^-]_{wf}, [OH^-]_{wf}, [Ca^{2+}]_{wf}$ *and* m_{CaA_2} These equations were solved numerically for various sets of parameters and initial conditions.

As an example, the "base case" CaN precipitation experiment was modelled and an acceptable match (*not* a prediction) was obtained using the parameters, K_{ow} = 0.01, K_a = $1x10^{-5}$, K_{CaA_2} = $1x10^{-11}$ and K_w = $1x10^{-14}$, along with the conditions, $V_w = V_o$ = 1 (litre), assuming M.Wt. of A= 300 (i.e. M.Wt. HA = 301) and the initial brine pH = 9. The initial naphthenic acid concentration in the oil was, $[HA]_{oi}$ = 0.001 M (300 ppm) and initial [Ca^{2+}] = 0.25M (10000 ppm). For this system, it was calculated that ~6.06 mg of CaN (CaA_2) would be formed and the final pH of the brine phase was predicted to be pH 4.81, and these results are in reasonable accord with experiment. However, it is also noted that, at equilibrium, only ~5% of the available original [HA] in the oil phase appeared in the precipitate i.e. ~95% of the [HA] was left in the oil phase. At equilibrium, the pH drops to 4.81 and the transfer of [HA] to the interface driven by its dissociation in the aqueous phase simply stops. This observation that ~ 95% of the original [HA] remains in the oil phase after 1 extraction process with pH 9 brine is the basis of for the "successive extraction" experimental predictions below.

Of the parameters in the model, K_{ow}, K_a and K_w are quite tightly constrained and have acceptable values in the example above, based on the known properties of naphthenic acids. However, the solubility product of the CaN (i.e. K_{CaA_2}) is the least familiar parameter here and this is estimated by approximate matching to experiment. However, it is emphasised here that in such complex natural systems, exact quantitative predictions of CaN precipitation (or final pH) are not granted, but it was hoped that semi-quantitative *trends* would be predicted (as in the experiments below).

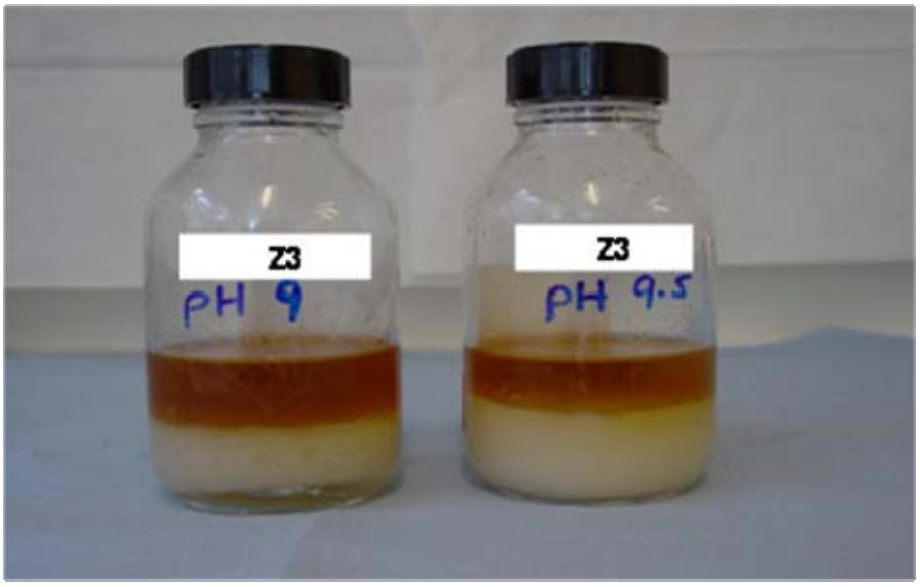

Figure 6.21: Naphthenate precipitation experiment using a (fully digested) field naphthenate extract (Z3 in (Mohammed and Sorbie, 2009)) at two brine pH adjusted values, pH = 9 and pH = 9.5

Successive Extraction Modelling Results

The basis for these experiments arises from the finding that, using reasonable parameters for (K_{ow}, K_a, K_{CaA_2} and K_w) in the base case model, then ~95% of the available [HA] remains in the oil phase, Thus, if successive extraction experiments of the type described in Section 3.4.6 are performed, then more CaN precipitation should occur as fresh pH 9 brine is mixed with the supernatant oil from the successive CaN precipitation experiments. Again in the calculations: $V_w = V_o = 1$ (litre), M.Wt. of A= 300 (i.e. M.Wt. HA = 301), K_{ow} = 0.01, $K_a = 1\text{x}10^{-5}$, $K_{CaA_2} = 1\text{x}10^{-11}$ and $K_w = 1\text{x}10^{-14}$. Initial conditions in the aqueous phase pH = 9 ($[H^+] = 1\text{x}10^{-9}$ mol/l); $[Ca^{2+}]$ = 0.25M– i.e. $[Ca^{2+}]$ = 10000 mg/l (ppm); in the oil phase, $[HA]_{oi} = 0.001$M (i.e. 0.3g/l or 300ppm [mg/l] based on M.Wt. A = 300; thus, the total initial mass of A in the system, V_w = 1 l, is 300mg.

This experimental "successive extraction" sequence is shown schematically in Figure 6.22 below. In fact, according to the model (with the parameters above), this type of sequential [HA] extraction experiment can be performed *many* times, causing further CaN formation

at each stage, using the same oil but fresh pH 9 brine each time. This is shown for the example above with $x_{1i} = [HA]_{oi}$ = 0.001M (300ppm – M.Wt. A = 300). The model was used to perform six successive identical oil/fresh pH 9 brine extraction experiments and results are shown in Table 6.5 and also in Figures 6.23 and 6.24. Figure 6.23 shows the depleting concentration [HA] in the oil at successive stages of extraction along with the %A remaining in the oil after CaN precipitation (an almost constant ~96.4%). Figure 6.24 shows that the final pH does rise slowly as the [HA] is depleted but it would appear to take ~8 - 9 extractions, for the final pH value to increase by ~0.1 pH unit. It was also noted from Table 6.5 that the predicted amount of CaN precipitate is approximately constant but decreases very slightly (this very small decrease in successive extractions could not be measured in the experiments). Results from such an experiment are reported below which test these model predictions.

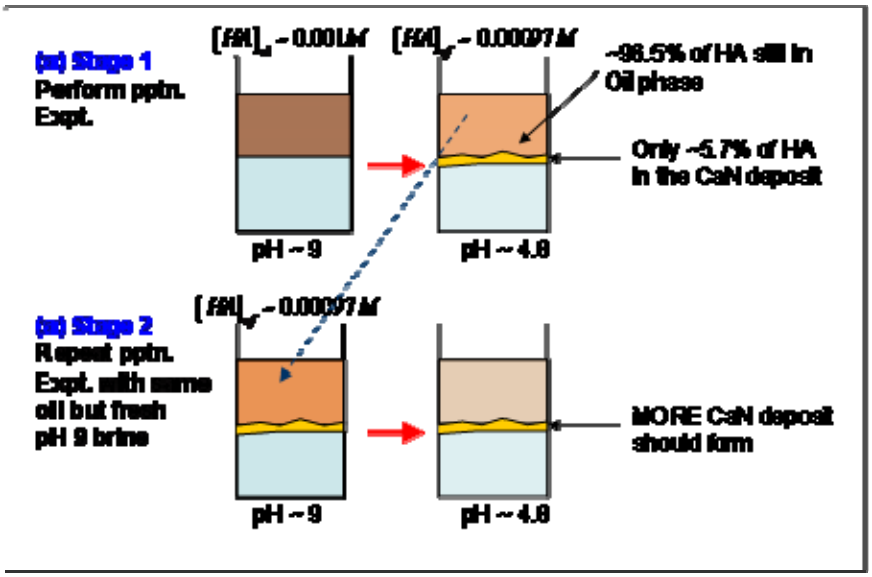

Figure 6.22: "Successive extraction" naphthenate precipitation experiments starting with (a) a field naphthenate extract in oil (toluene) and brine at pH = 9, followed by (b) treatment of the same (slightly HA depleted) oil with a fresh pH 9 brine. According to the naphthenate prediction model with likely values of K_{ow}, K_a, K_{CaA_2} and K_w, more CaN precipitate should form as shown schematically over several extraction stages.

Extraction step	x1i = $[HA]_{oi}$ (M)	x1i = $[HA]_{oi}$ (ppm)	Final x1 $[HA]_{of}$ (M)	Final x1 $[HA]_{of}$ (ppm)	Mass A in ppt. (mg)	%A in ppt. (%)	%A still in oil phase (%)	Total A still in system (mg)	Final pH
0				300			100		4.81
1	0.001	300	0.000965	289.5	5.67	1.89	96.51	300	4.81665
2	0.000965	289.5	0.000931	279.3	5.52	1.9	96.47	289.5	4.832
3	0.000931	279.3	0.000898	269.4	5.36	1.9	96.4	279.3	4.8478
4	0.000898	269.4	0.000866	259.8	5.21	1.93	96.4	264.4	4.8637
5	0.000866	259.8	0.000834	250.2	5.06	1.95	96.4	259.8	4.8796
6	0.000834	250.2	0.000803	240.9	4.91	1.96	96.3	250.2	4.8962

Table 6.5: Results of successive extraction experiments starting with the same oil (becoming gradually depleted in [HA]) and fresh brine at pH 9 [Ca] =0.25M (10,000 ppm).

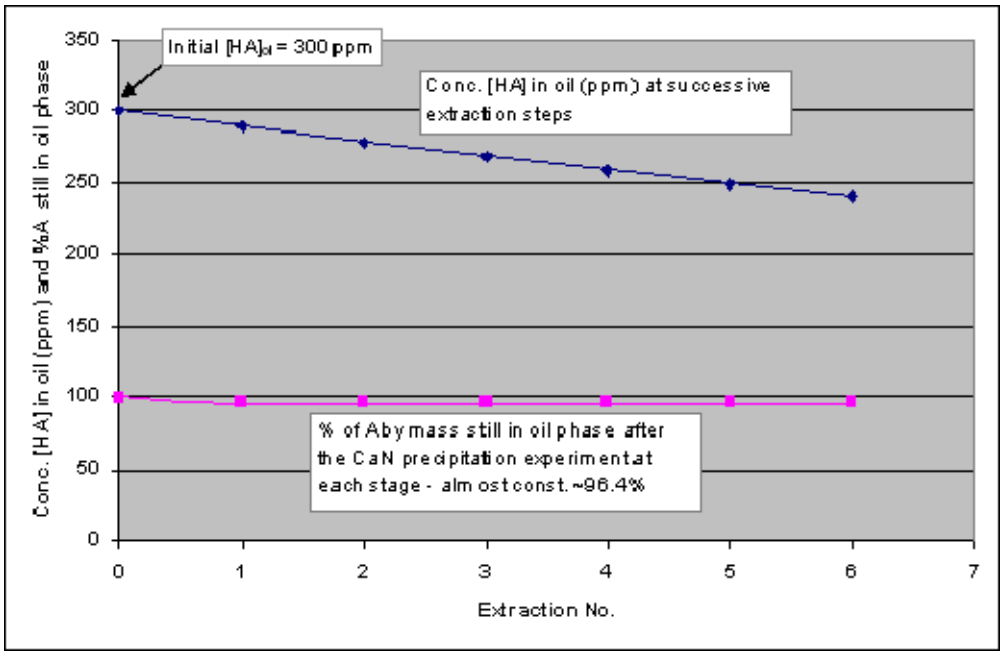

Figure 6.23: Results for [HA] in oil phase and % A left in the oil - from six successive identical oil/fresh pH 9 brine extraction experiments for the base case parameters used above, with the initial HA concentration in the oil phase being, $x_{1i} = [HA]_{oi}$ = 0.001M (300ppm, assuming M.Wt. of A = 300).

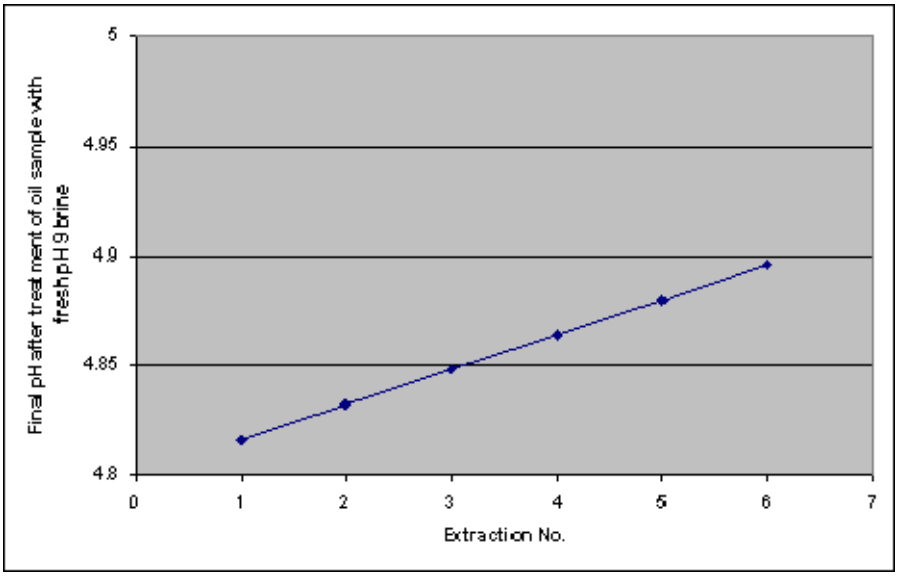

Figure 6.24: Final pH results - from six successive identical oil/fresh pH 9 brine extraction experiments for the base case parameters used above, with the initial HA concentration in the oil phase being, $x_{1i} = [HA]_{oi}$ = 0.001M (300ppm, assuming M.Wt. of A = 300).

Varying Water/Oil Volume (V_w/V_o) Ratio Modelling Results

In the equations for the naphthenate model (Appendix A - Table A2), the water/oil volume (V_w/V_o) ratio is incorporated in the equations. The effect of this volume ratio (or watercut, %W) is not immediately obvious from inspection of the equations. As described above, the varying (V_w/V_o) ratio experiments can be performed in two ways: i) Constant V_w and varying (V_w/V_o) ratio; ii) Constant total volume ($V_w + V_o$= constant) and varying (V_w/V_o) ratio. In fact, similar predictions were made for both types of experiment and so the predicted behaviour of the system is shown in a series of calculations for the constant volume (ii above) experiment in Table 6.6 below.

Predictions were carried out where the total volume of fluids, V_T, was kept constant, $V_T = (V_w + V_o)$, and then the proportion of each phase was varied such that % water cut varies from low to high. The model parameters considered in this calculation are as follows: V_T = 1 (litre) with V_w and V_o varying; M.Wt. A= 1000 (i.e. M.Wt. HA = 1001, this is close to the ARN value), K_{ow} = 0.01, $K_a = 1x10^{-5}$, $K_{CaA_2} = 1x10^{-13}$ and $K_w = 1x10^{-14}$. Initial conditions in aqueous phase are pH = 9 ($[H^+] = 1x10^{-9}$ mol/l); $[Ca^{2+}]$ = 0.50M – i.e. $[Ca^{2+}]$ = 20000 mg/l (ppm); in oil phase, $\left[HA\right]_{oi} = 0.001$M (i.e. 1.0 g/l of "A"); thus, the total initial mass of A, V_w = 1 l, is 1000mg; but this changes as V_w varies – see "mass available" in Table 6.6 below). The predictions for this case are shown in Table 6.6 below.

The predictions in Table 6.6 are plotted in Figure 6.25 and these results show that, quite unexpectedly, there is a *maximum* in the mass of CaN deposited with %watercut (around, %W ~70% watercut). This occurs despite the fact that less "A" is available (linearly) as watercut increases (Table 6.5). The prediction also shows that the %A in the CaN deposit rises sharply at high watercut (see Figure 6.25). It was also noted that the pH change is quite significant (Table 6.6) and gives a higher pH value at higher % watercuts.

K_{ow} = 0.01						
V_o (litre)	V_w (litre)	W'CUT (%W)	Mass_CaA_2 (mg)%a	%A	pH_final	Mass available (mg)
0.90	0.10	10.00	23.18	2.52	3.66	900.00
0.80	0.20	20.00	44.90	5.51	3.67	800.00
0.67	0.33	33.33	70.98	10.44	3.70	666.67
0.50	0.50	50.00	98.38	18.89	3.75	500.00
0.33	0.67	66.67	108.05	31.78	3.83	333.33
0.25	0.75	75.00	104.86	41.12	3.89	250.00
0.20	0.80	80.00	98.34	48.21	3.96	200.00
0.17	0.83	83.33	91.40	53.77	4.09	166.67
0.10	0.90	90.00	68.98	67.60	4.18	100.00
0.05	0.95	95.00	44.52	81.42	4.48	50.00

Table 6.6: Results predicted by the naphthenate model for the effect of varying the water/oil volumes, V_w and V_o such that $V_T = (V_w + V_o)$ is constant (1 litre) in a naphthenate precipitation experiment (type ii varying (V_w/V_o) ratio experiment in text)

This calculated maximum in mass of precipitated CaN (CaA_2) is quite a surprising prediction and is tested below experimentally for both types of varying (V_w/V_o) ratio experiment described above. It was noted that the same qualitative prediction, i.e. a maximum in CaN deposition at an intermediate %W value, was also predicted for the constant V_o, varying (V_w/V_o) experiments (Figure 6.25) but these results are not shown here.

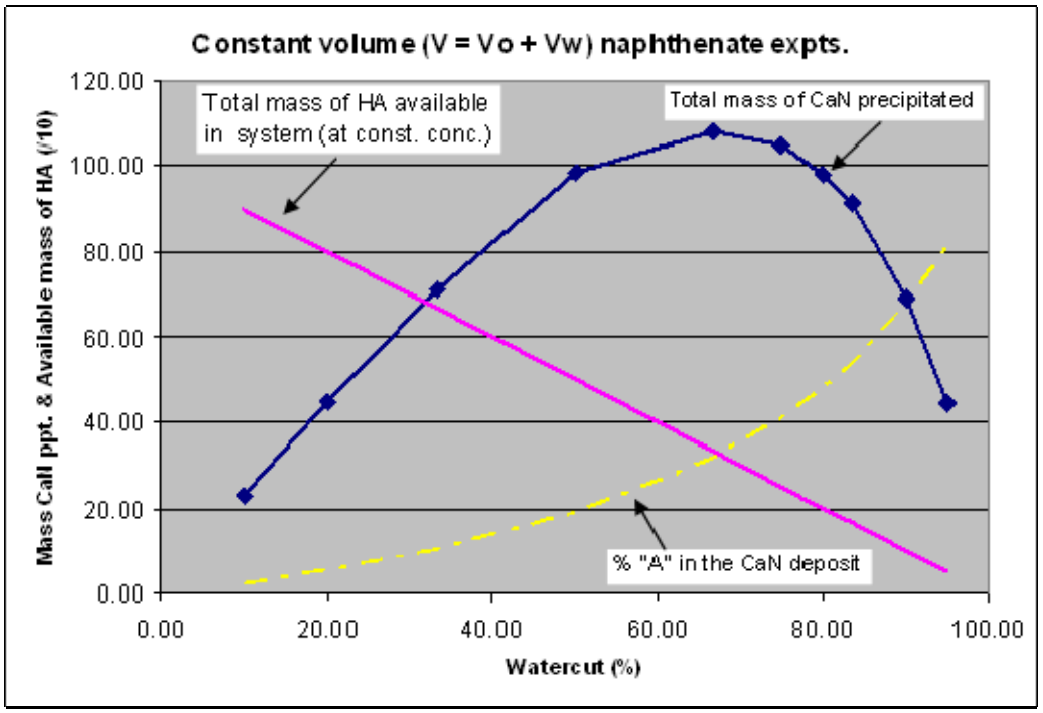

Figure 6.25: Results from the naphthenate precipitation model vs. % watercut; the mass of CaN deposited, the amount of "A" available and the %A in the CaN deposit are all shown vs. %watercut.

Experimental Results

The various types of experiments proposed in the modelling section above are now tested and the results are presented. Experiments were carried out using either three concentrations of naphthenic acid extract in toluene (1000 ppm, 3000 ppm and 7500 ppm), or 3000 ppm naphthenic acid in toluene and pH adjusted synthetic brine with composition (Na^+ = 25000 ppm and Ca^{++} = 20000 ppm). The initial brine pH in all the experiments conducted was pH 9. Preparations of the different concentrations of naphthenic acid extract in toluene and the synthetic brine have been reported in Mohammed *et al.,* 2009.

Successive Extraction Experimental Results

The "successive extraction" experiment, shown schematically in Figure 6.22 above, was carried out. The results from these laboratory experiments are presented in Table 6.7 below. The corresponding experimental plots of naphthenate precipitate formed (mg) vs. $[HA]_{oi}$ and final brine pH vs. $[HA]_{oi}$ are presented in Figures 6.26 and 6.27, respectively.

It is evident from the results in Table 6.7 and Figures 6.26 and 6.27 that the mass of naphthenate precipitated (mg) after each successive naphthenic acid extraction and precipitation with a fresh pH adjusted brine is quite similar in all the cases, for each naphthenic acid concentration (1000 ppm, 3000 ppm and 7500 ppm) and is in the range of 5mg to 7mg in each of the cases. However, it should be noted that not all of the precipitate formed was recovered, as some adhered to the walls of the bottle during filtration, although the approximate loss due to that should not be more than 10% at most.

Extraction step	**$[HA]_{oi}$ (ppm)**	**$[HA]_{oi}$ (M)**	**Mass precipitated (mg)**	**Final brine pH**
0	**1000**	**0.003**		
1		0.003	5	3.73
2			4	3.95
3			6	5.73
0	**3000**	**0.01**		
1		0.01	5	3.71
2			5	3.70
3			6	3.69
0	**7500**	**0.025**		
1		0.025	6	3.70
2			6	3.69
3			7	3.61

Table 6.7: Results of successive extraction experiments starting with the oil phase at various naphthenic acid concentrations (getting gradually depleted in HA) and fresh synthetic brine at pH 9 $[Ca^{++}]$ =0.5M (20000 ppm).

The final brine pH, measured after the filtration in each step of the successive extraction experiment, was observed to be slightly decreasing when using a particular naphthenic acid concentration e.g. a repeated extraction and precipitation using a naphthenic acid extract in toluene (7500 ppm = 0.025M) gives a final brine pH of 3.70, 3.69 and 3.61 after the first, second and third extractions respectively, and this trend was observed in all the other

experiments carried out using different naphthenic acid concentrations. It was observed that the experimental observations in Table 6.7 and Figures 6.26 and 6.27 are in approximate accord with the model predictions presented above.

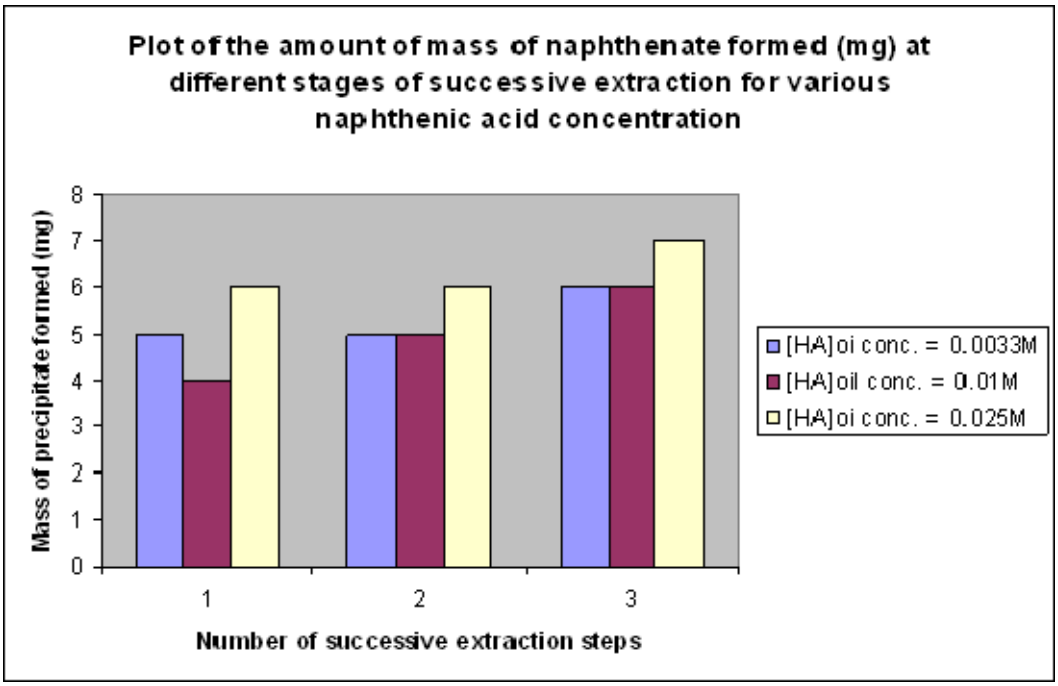

Figure 6.26: Plot of naphthenate precipitate formed (mg) at each successive extraction step for various naphthenic acid concentrations $[HA]_{oi}$.

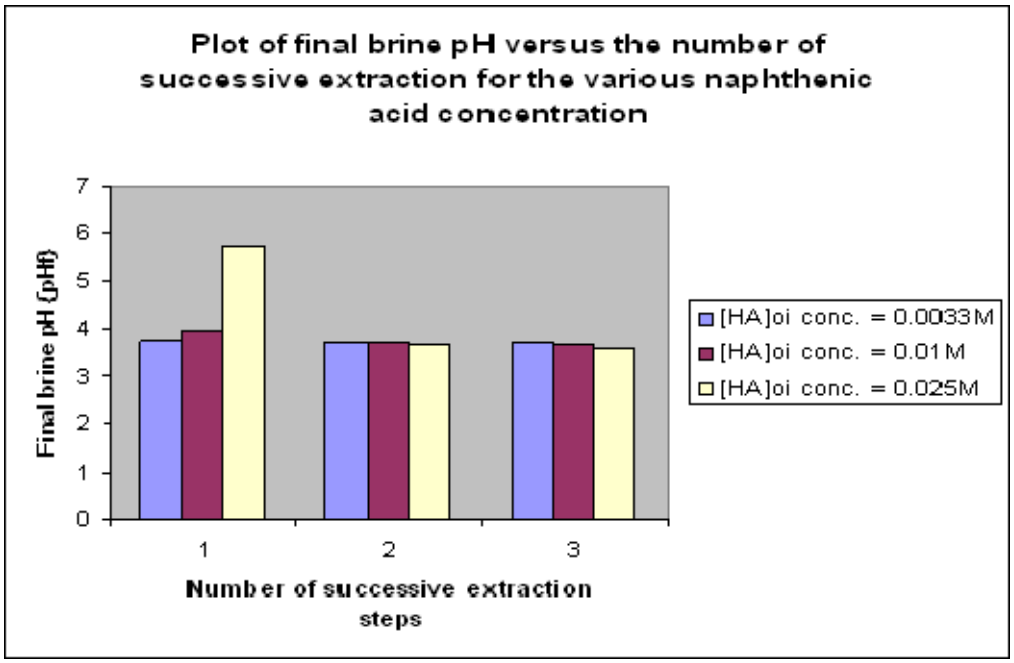

Figure 6.27: Plot of final brine pH at each successive extraction step versus for various naphthenic acid concentration $[HA]_{oi}$.

Although the model predicted a very slight decrease in successive masses of precipitation, within experimental error this would be observed as being approximately the same mass. Apart from one result in Table 6.7 (pH 5.73), the pH within each [HA] is approximately constant for successive extractions, in reasonable agreement with the model. Therefore, for this type of experiment, the model and experiment are in good qualitative agreement.

Varying Water/Oil Volume (V_w/V_o) Ratio Experimental Results

Fixed V_o, Variable (V_w/V_o) ***Ratio Experiments—Type (i):*** The laboratory results of the type (i) fixed V_o, variable (V_w/V_o) ratio experiments (Figure 6.28) are presented in Table 6.8 below, showing the mass of calcium naphthenate formed (mg) and the final brine pH. The actual static bottle test experiments are presented in Figure 6.28 showing the variable volume of water to oil ratio.

Mixing ratio V_w/V_o	Approx. % Water cut (%W)	$[HA]_{oi}$ (ppm)	$[HA]_{oi}$ (M)	Mass precipitated (mg)	Final brine pH (Average)
0.25/1	20	3000	0.01	40	3.10
0.50/1	33	3000	0.01	50	3.38
0.75/1	43	3000	0.01	60	3.49
1/1	50	3000	0.01	70	3.85
2/1	67	3000	0.01	90	4.23
5/1	83	3000	0.01	70	4.92
10/1	91	3000	0.01	40	5.25

Table 6.8: Results of fixed V_o, variable (V_w/V_o) ratio experiments with the oil phase at 3000ppm naphthenic acid concentration and synthetic brine at pH 9 $[Ca^{++}]$ =0.5M (20000 ppm).

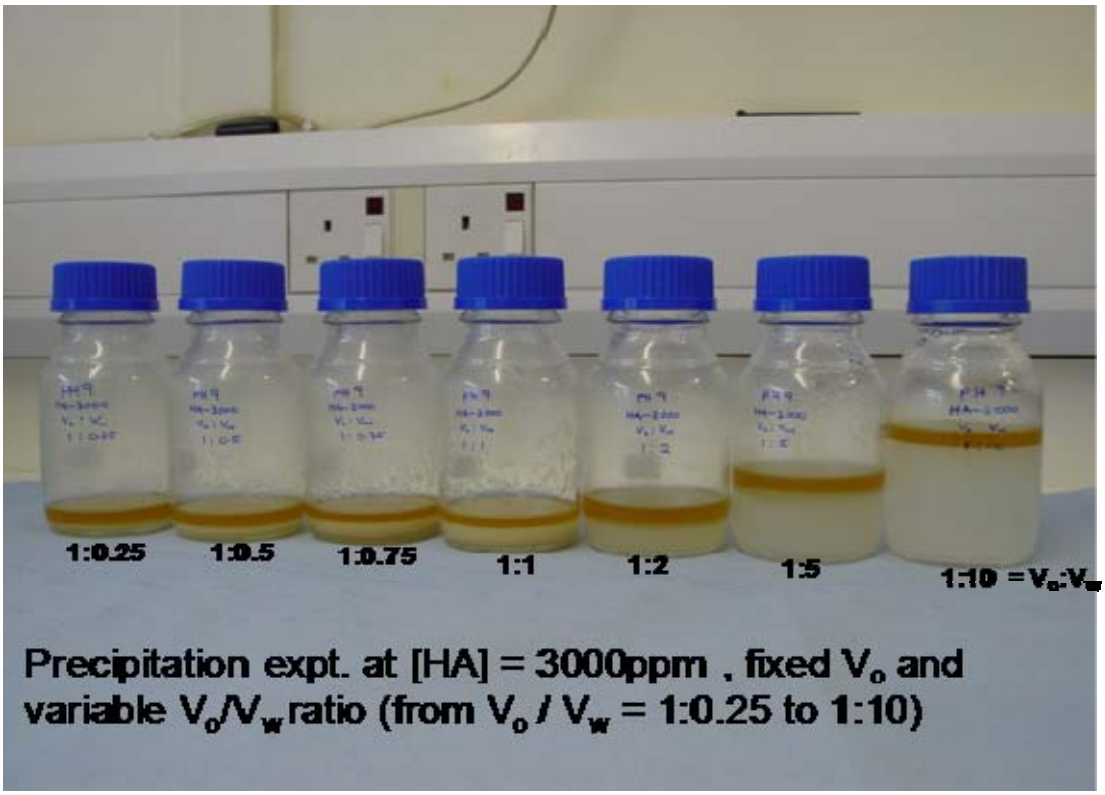

Figure 6.28: Static bottle test using fixed V_o and variable water/ oil volume (V_w / V_o) ratios at 3000 ppm naphthenic acid concentration $[HA]_{oi}$.

The laboratory results from the variable water/oil volume ratios in Table 6.8 indicate that the water to oil ratio is very important in the formation of naphthenate precipitate for each of the different naphthenic acid concentrations i.e. in this case 3000 ppm naphthenic acid concentration in toluene. Figure 6.29 shows the plot of the calcium naphthenate mass precipitated (mg) and final brine pH $[pH]_f$ vs. % watercut (%W). The plot in Figure 6.29 clearly shows that, as the ratio of water/oil volume gradually increases, then there is a clear maximum in the mass of CaN that is deposited around %W ~ 67%. A further increase in %W then leads to a *decrease* in the amount of calcium naphthenate formation.

The final brine pH increases as the water-oil volume (V_w/V_o) ratio or % watercut increases, which was considered to be due to the naphthenic acid in oil phase partitioning and dissociating to the water phase (brine). The laboratory experiment showed that, at a lower naphthenic acid concentration (say 1000 ppm =. 0.003M) and higher water/oil volume ratio, there was no formation of calcium naphthenate precipitate. However, this could be due to the fact that the unit volume of 1 in this experiment is represented to be 5ml. However, at a very high throughput, we may see some naphthenate formation, as the model also predicts, although the degree of naphthenate precipitation may not be severe (Turner and Smith, 2005). The results found from the laboratory experiment showed excellent agreement with the modelling results described above in Figure 6.25, although the actual type of experiment is slightly different.

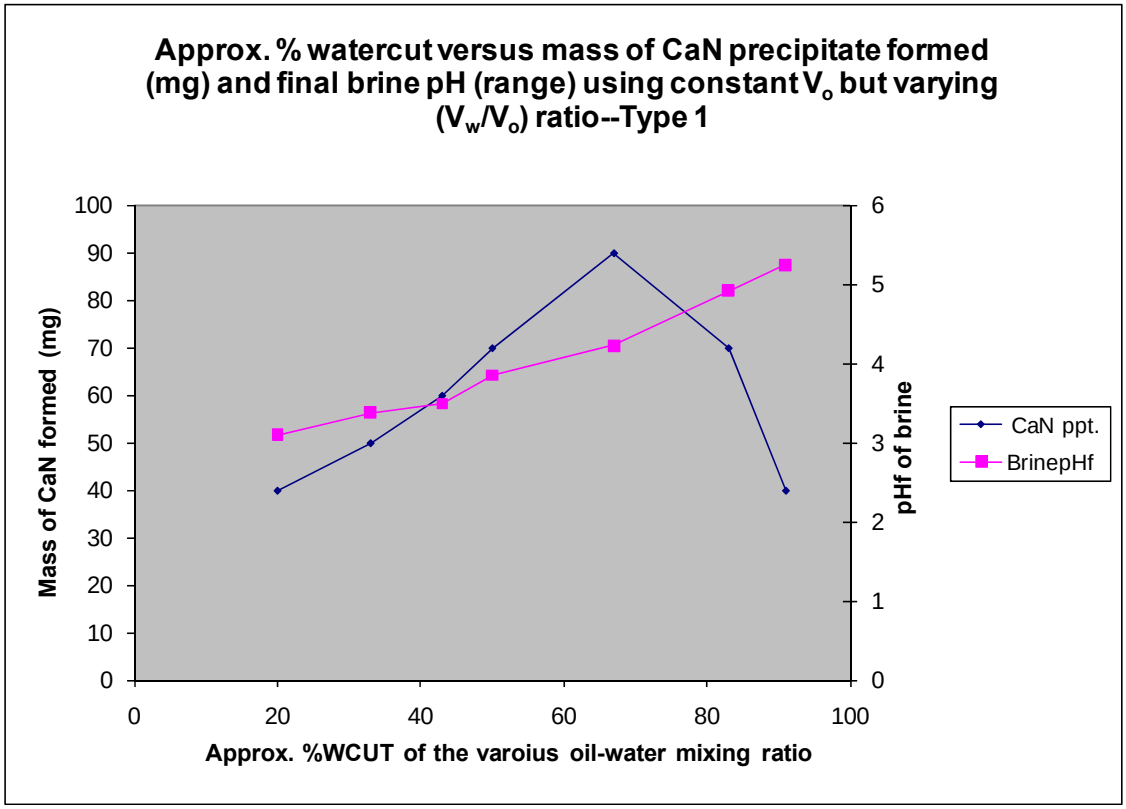

Figure 6.29: Plot of mass of CaN precipitate formed (mg) and final brine pH versus the approximate % water cut (V_w/V_o—variable and V_o constant).

Constant Total Volume ($V_T = V_w+V_o$), Variable (V_w/V_o) ***Ratio Experiments—Type (ii):*** In this case, a constant total volume, $V_T = V_w+V_o$, of both oil (naphthenic acid extract in toluene) and pH adjusted synthetic brine (pH 9) was used, and in this particular experiment $V_w + V_o = 40$ml. The mass of calcium naphthenate precipitation and final pH were then measured at different % watercuts, %W = 10%, 20%, 33%, 43%, 50%, 67%, 83% and 91%. The actual bottle tests for this type of experiment are shown in Figure 6.30. The results for the precipitation and final brine pH measurement are presented in Table 6.9 below. These results are plotted in Figure 6.31 which shows the mass of calcium naphthenate formed (mg) and final brine pH versus % watercut (%W), respectively. Again, the same qualitative observation on the precipitated mass of CaN is seen in this type (ii) varying (V_w/V_o) ratio experiment. In this case, the maximum mass of CaN precipitation is observed at %W ~ 60%. Above this value, a decrease in the amount of calcium

naphthenate precipitate was observed. The final brine pH increases monotonically and quite significantly as the % watercut increases.

This phenomenon of observed decrease in the amount of calcium naphthenate precipitate as % watercut increases beyond the optimum values had been previously reported during production (Sorbie, 2009).

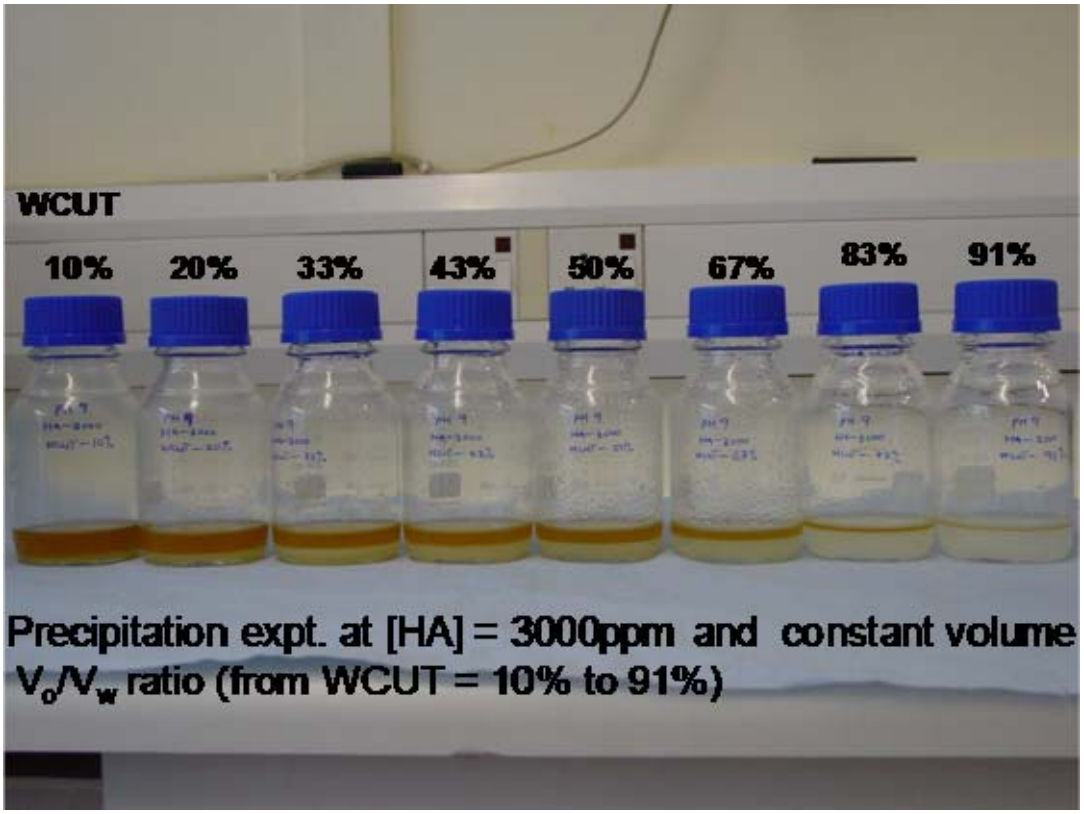

Figure 6.30: Static bottle test using constant total water/ oil volume (V_w / V_o) and varying V_w/V_o ratios at 3000 ppm naphthenic acid concentration $[HA]_{oi}$.

$V_w = V_o = 1$ And 1 unit = 40ml	% Water cut	$[HA]_{oi}$ (ppm)	$[HA]_{oi}$ (M)	Mass precipitated (mg)	Final brine pH (Average)
40	10	3000	0.01	40	2.91
40	20	3000	0.01	40	3.17
40	33	3000	0.01	50	3.43
40	43	3000	0.01	60	3.63
40	50	3000	0.01	70	3.78
40	67	3000	0.01	80	4.32
40	83	3000	0.01	70	4.53
40	91	3000	0.01	50	4.64

Table 6.9: Results of constant total ($V_w + V_o$) volume and varying V_w/V_o ratios experiments with the oil phase at 3000 ppm naphthenic acid concentration and synthetic brine at pH 9 [Ca] =0.5M (20000 ppm).

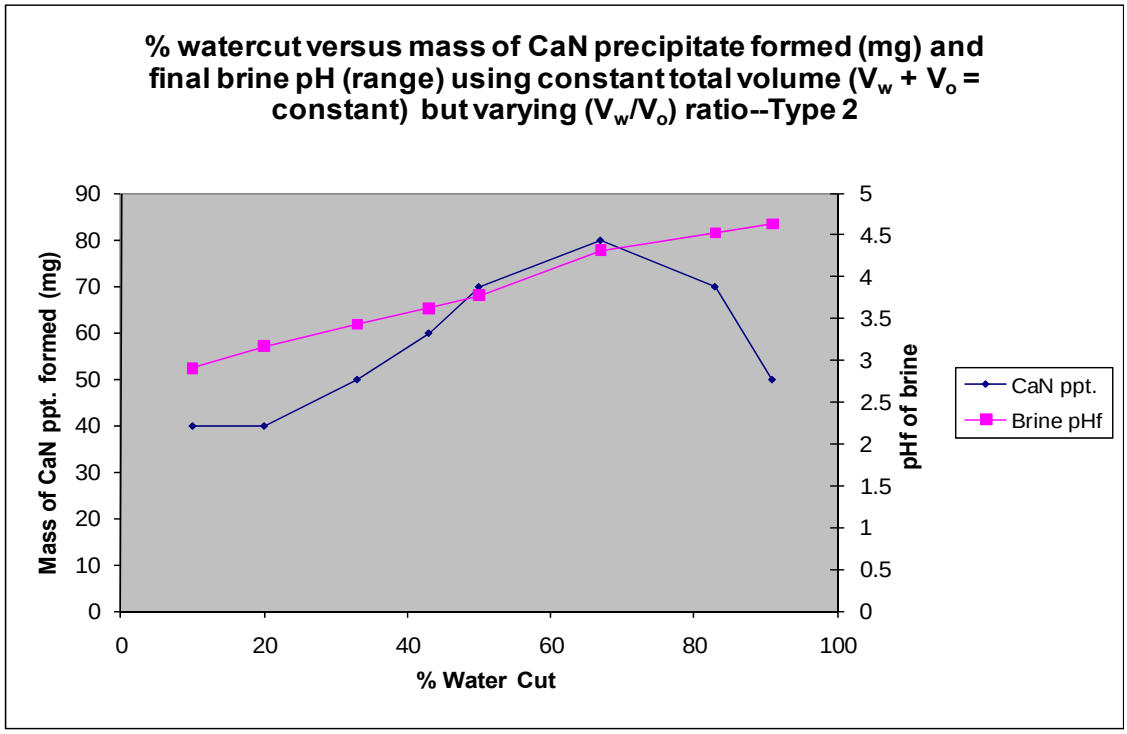

Figure 6.31: Plot of mass of CaN precipitate formed (mg) and final brine pH versus the % watercut (V_w/V_o—variable and V_T constant).

6.5 ADDITIONAL SENSITIVITY STUDIES

In this section, a range of additional sensitivity parameters were examined experimentally to study their effects on the formation of naphthenate in the oil-brine systems. These parameters are:

(i) the effect of increasing naphthenic acid [HA] concentration in the oil phase at a fixed brine composition (Na^+ = 25000 ppm and Ca^{++} = 20000 ppm) which is pH adjusted to pH 9;

(ii) the effect of non-shearing of the oil-water mix, i.e. conducting the precipitation experiment without shaking the mixed oil and water phases;

(iii) the effect of shearing and subsequently allowing the mixture (oil & water phases) to stand for some time (two weeks);

(iv) the effect of temperature on the formation of naphthenate;

(v) the effect of addition of bicarbonate (HCO_3^-) to the water phase (synthetic brine) prior to mixing with the oil phase; and, finally

(vi) the effect of the variation of calcium ions in the synthetic brine but with fixed concentration of sodium ions.

The composition of the water phase (synthetic brine) remains the same as in the previous experiments i.e. (Na^+ = 25000 ppm and Ca^{++} = 20000 ppm). The brine pH was adjusted to pH 9 whilst the concentration values of naphthenic acid in the oil phase were 1000 ppm, 3000 ppm and 7500 ppm. The results from these experiments are explained in detail below.

Naphthenate formation as a function of [HA] concentration

This experiment was specifically designed to see the effect of varying the concentration of naphthenic acid in the oil phase on the corresponding mass of naphthenate formation in the system where water phase (synthetic brine) is kept at pH 9. Table 6.10 below shows the amount of naphthenate precipitate formed at various naphthenic acid [HA] concentrations and the final brine ph measured.

$[HA]_{oi}$ (ppm)	$[HA]_{oi}$ (M)	Mass precipitated (mg)		Final brine pH	
		1	2 (duplicate)	1	2 (duplicate)
1000	**0.003**	4	4	3.75	3.74
3000	**0.01**	6	6	3.72	3.72
7500	**0.025**	7	8	3.70	3.71

Table 6.10: The mass of naphthenate precipitate formed at various naphthenic acid concentrations and the final brine pH measured.

The results showed a progressive increase of naphthenate mass precipitated as the concentration of naphthenic acid in the oil phase $[HA]_{oi}$ increased. This is attributed to the dissociation and partitioning of naphthenic acid in the oil phase, to react with the available cation (Ca^{++}) present in the water phase (synthetic brine) and after the system is equilibrated then the formation of naphthenate virtually ceased . The relation between the naphthenic acid concentration and the formation of naphthenate at water phase pH 9 is approximately linear. The final system brine pH measured showed a decrease as the concentrations of naphthenic in the oil phase increased, as seen in Table 6.10. The final brine pH value decreased from pH 9 at the beginning of the experiment prior to the addition of the oil phase to pH 3.75 at 1000 ppm naphthenic acid concentration and subsequently to pH 3.70 at 7500 ppm naphthenic acid concentration. This trend of the final pH decreasing from a higher value at a lower naphthenic acid concentration in the oil phase to a lower value at a higher naphthenic acid concentration was also predicted by the model in previous calculations (Mohammed *et al.,* 2009). The results from this experiment i.e. plots of naphthenate mass precipitate (mg) versus various concentrations of naphthenic acid oil phase $[HA]_{oi}$ and final system brine pH versus concentration of naphthenic acid in oil phase$[HA]_{oi}$ are presented in Figure 6.32 below.

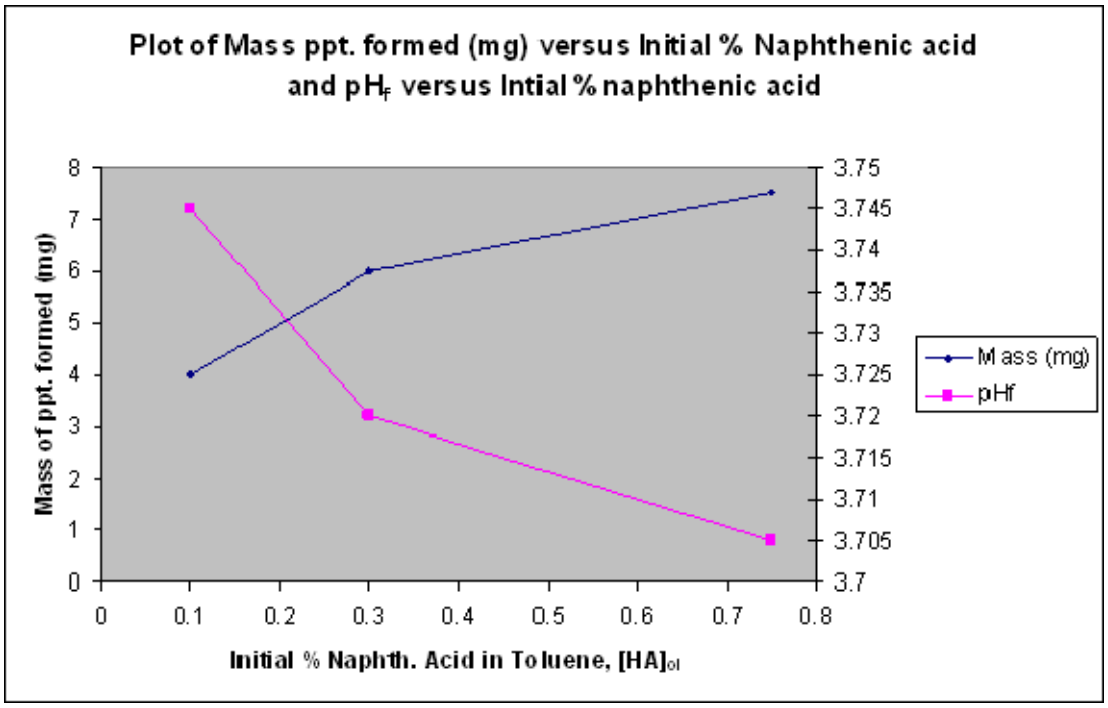

Figure 6.32: Plot of mass of calcium naphthenate ppt. formed (mg) versus initial % $[HA]_{oi}$ and pH_f versus initial % $[HA]_{oi}$.

Naphthenate Precipitation experiment without any shear (no turbulence)

The effect of non-shearing of the oil-water mix was examined, to study how it affects the formation of naphthenate in the precipitation experiment. These experiments again used a pH 9 adjusted water phase (synthetic brine) with an oil phase at various naphthenic acid concentrations. The experiment was conducted by mixing the two phases (oil and water) slowly with minimal disturbance or shaking. The resulting mixture was allowed to stand for about 10 minutes before any possible precipitation at the interface was observed and then the bottle containing the mixed phases (oil and brine) was allowed to stand undisturbed for two weeks with daily visual observation over that period. At the end of two weeks, the amount of naphthenate precipitate (if any) was quantified and the final brine pH was also measured. The results from this experiment are reported in Table 6.11 below.

$[HA]_{oi}$ (ppm)	$[HA]_{oi}$ (M)	Mass precipitated (mg)		Final brine pH measured	
		1	2 (duplicate)	1	2 (duplicate)
1000	**0.003**	N/A	N/A	5.83	5.85
3000	**0.01**	N/A	N/A	5.63	5.66
7500	**0.025**	N/A	N/A	5.49	5.48

Table 6.11: The mass of naphthenate precipitate formed (if any) and the corresponding final brine pH measured.

There was no formation of naphthenate precipitate after the two week period, as a clear interface between the oil and water phase was observed in all naphthenic acid concentrations in the oil phase. However, the final brine pH measured showed a decrease from 5.85 to 5.48 as the concentration of naphthenic acid [HA] in the oil phase increased. This is attributed to dissociation and partitioning of [HA] between the oil and water phases. A similar trend was observed in the pH change experiment which was reported in the earlier part of this chapter, although that type of experiment used a pH adjusted water phase at pH 6 and below, since precipitation did not occur at such pH values. It is very important to note that shear or shaking (turbulence) is one of the conditions for the formation of the naphthenate deposit. If there is ***no*** shear during the mixing between the oil and water phases, then no naphthenate precipitation will occur, as seen from the experimental results in the table above. The final brine pH also decreases from pH 9 at the beginning of the experiment to pH 5.48 by the end of the two weeks. However, the decrease in the brine pH value is totally dependent on the concentration of naphthenic acid in the oil phase. The results show that naphthenic acid in the oil phase at the beginning of the experiment $[HA]_{oi}$ must have dissociated and partitioned between the oil/water phases but the partitioned naphthenic acid did not react with the calcium cation (Ca^{++}) in the water phase at the interface to precipitate, due to the fact that there was no shear (turbulence); hence, the acid dissociation only leads to the change in the final brine pH. The visual observation on a daily basis is shown in Figure 6.33 and a plot of the final brine pH versus the naphthenic acid concentration $[HA]_{oi}$ is also presented in Figure 6.34 and we note the decrease in the final brine pH as the initial naphthenic acid concentration increases $[HA]_{oi}$.

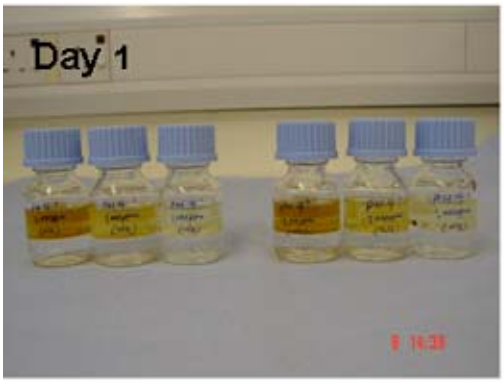
Day 1


Day 3


Day 2

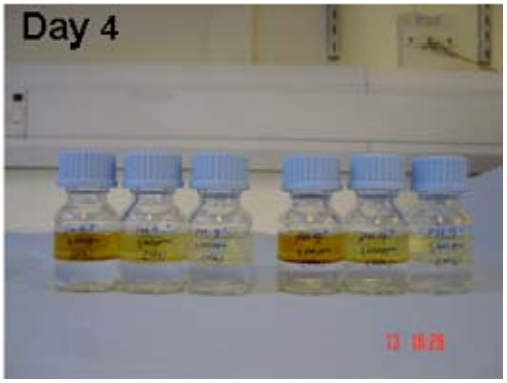
Day 4

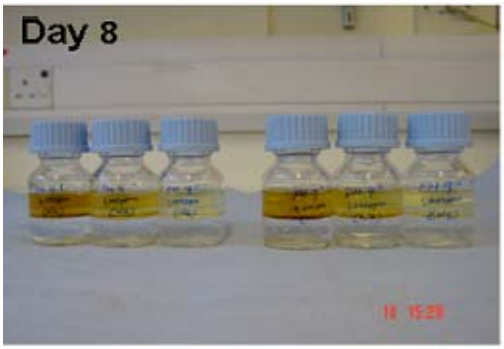
Day 8

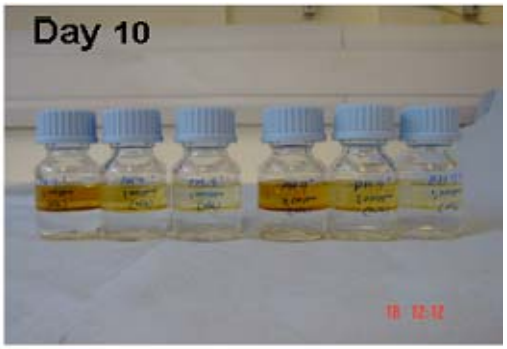
Day 10


Day 9

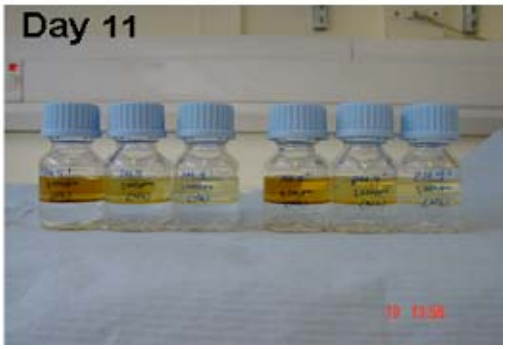
Day 11

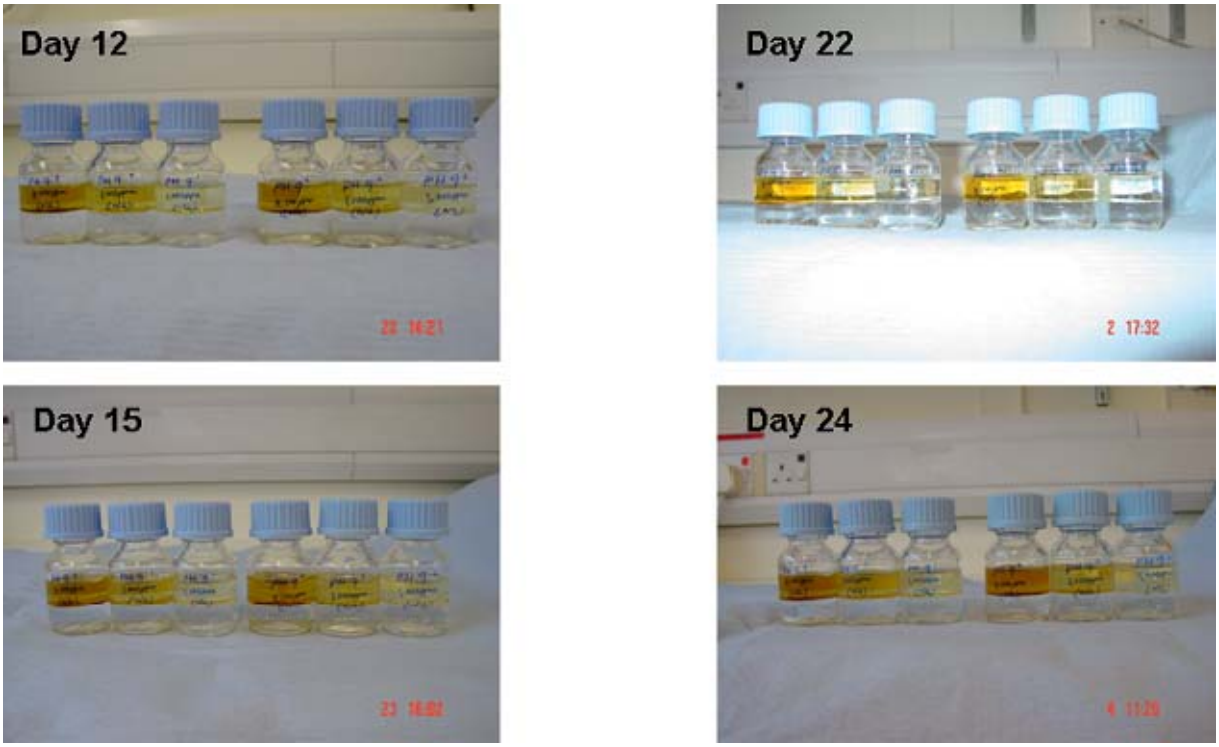

Figure 6.33: Visual observations for up to 24 days of the non-shear (no turbulence) naphthenate precipitation static bottle test experiment.

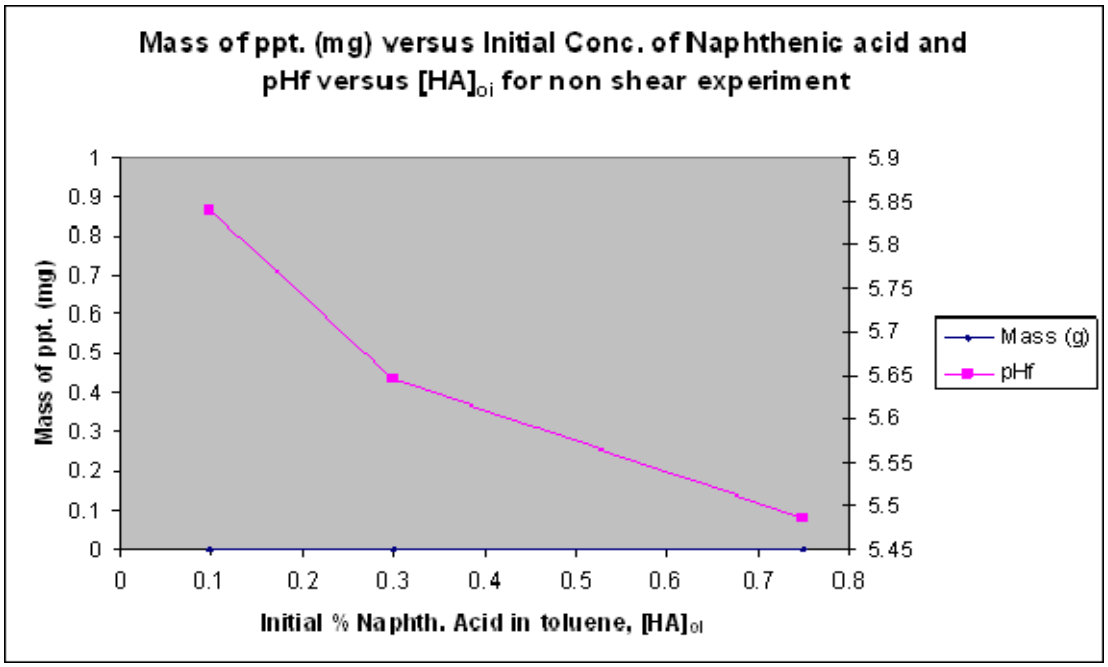

Figure 6.34: Plot of Final brine pH versus naphthenic acid concentration $[HA]_{oi}$ for non-shear naphthenate precipitation experiment

Naphthenate Precipitation with Shear then Standing

The effect of shear (turbulence) and then allowing the mixed phases to stand without further shear for a period of two weeks was studied in this experiment. The composition of the water phase (synthetic brine) remains the same as in the previous experiment, as does the naphthenic acid concentration $[HA]_{oi}$ in the oil phase. In this experiment, the water and oil phases were mixed together and mildly shaken for 30 seconds for each of the various naphthenic acid concentrations $[HA]_{oi}$ prior to leaving the mixed phases to stand undisturbed for 2 weeks; daily visual observations were conducted. At the end of the two week period, the amount of the naphthenate mass precipitated (mg) was measured and the final brine pH was determined. Table 6.12 shows the detailed results for the recovered naphthenate precipitate (mg) and the final brine pH after the two week period.

$[HA]_{oi}$ (ppm)	$[HA]_{oi}$ (M)	Mass precipitated (mg)		Final brine pH measured	
		1	2 (duplicate)	1	2 (duplicate)
1000	**0.003**	12	14	4.31	4.33
3000	**0.01**	18	16	3.86	3.87
7500	**0.025**	7	6	3.51	3.54

Table 6.12: The mass of naphthenate precipitated and the corresponding final brine pH measured after the 2 week period.

It was observed that at the beginning of the experiment, after mixing the 2 phases (oil/water) and then shaking for 30 seconds, there was formation of naphthenate precipitate. This deposit seemed to be distributed through the bulk of the solution, but daily visual observation when the whole mixture was allowed to stand, showed that the naphthenate precipitates started to settle at the oil/water interface. The photographic images of the daily observations are shown in Figure 6.35 which clearly shows that on the 1st day of the experiment, all the naphthenate precipitates were distributed through the bulk of the solution but, over time, the naphthenate precipitate started to congregate at the oil/water interface, leading to a clear water phase at the bottom of the bottle. It was also observed

that, at a very high concentration of naphthenic acid $[HA]_{oi}$, the amount of naphthenate precipitate formed gradually decreased progressively with the number of days the experiment was allowed to stand without shear, as can be seen from the image on day 15. However, this phenomenon is associated with the naphthenate precipitate formed from the oil phase with higher initial naphthenic acid concentration, i.e. $[HA]_{oi}$ = 7500 ppm. The oil phase with the moderate initial naphthenic acid [HA] concentration (say 3000 ppm) gave the optimum amount of naphthenate precipitation and even after the 24 days of standing, a substantial amount of precipitate was observed compared to the former i.e. $[HA]_{oi}$ = 7500 ppm. A plot of the amount of naphthenate precipitate formed after 24 days versus the initial concentration of naphthenic acid in the oil phase $[HA]_{oi}$ and final brine pH versus $[HA]_{oi}$ is shown in Figure 6.36.

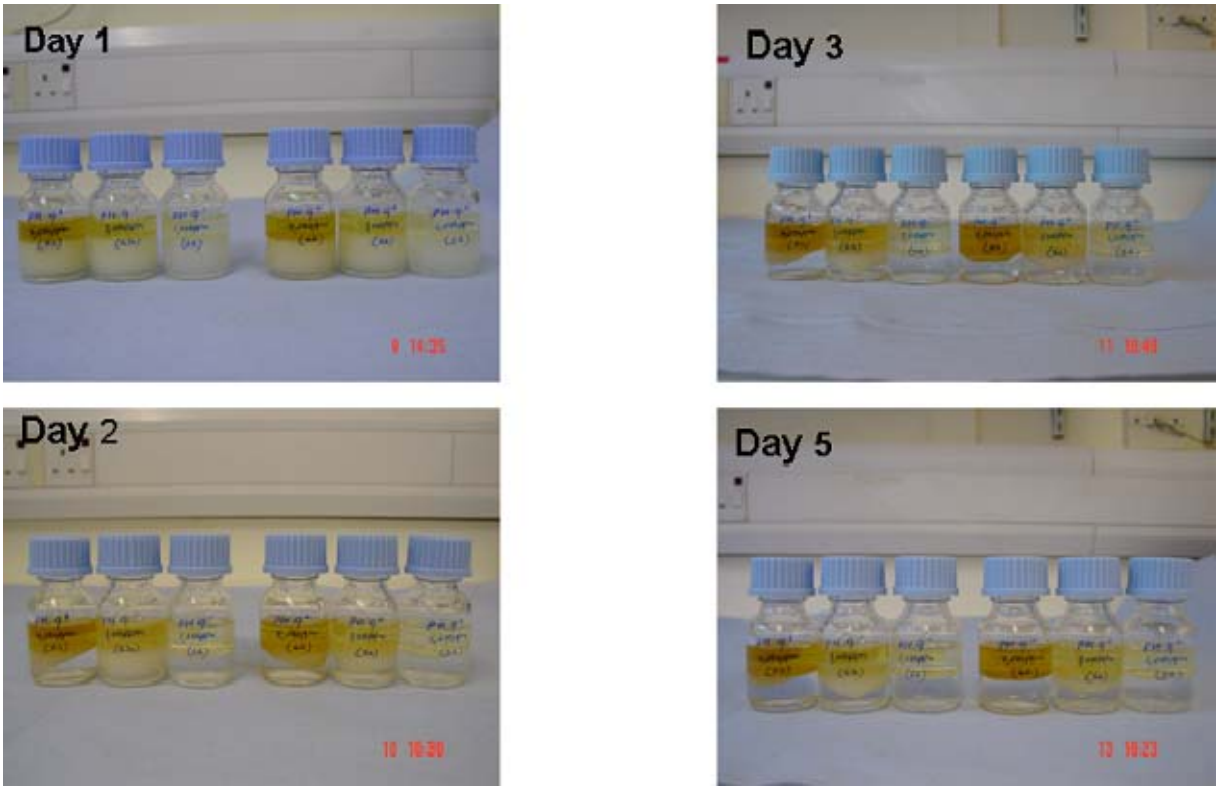

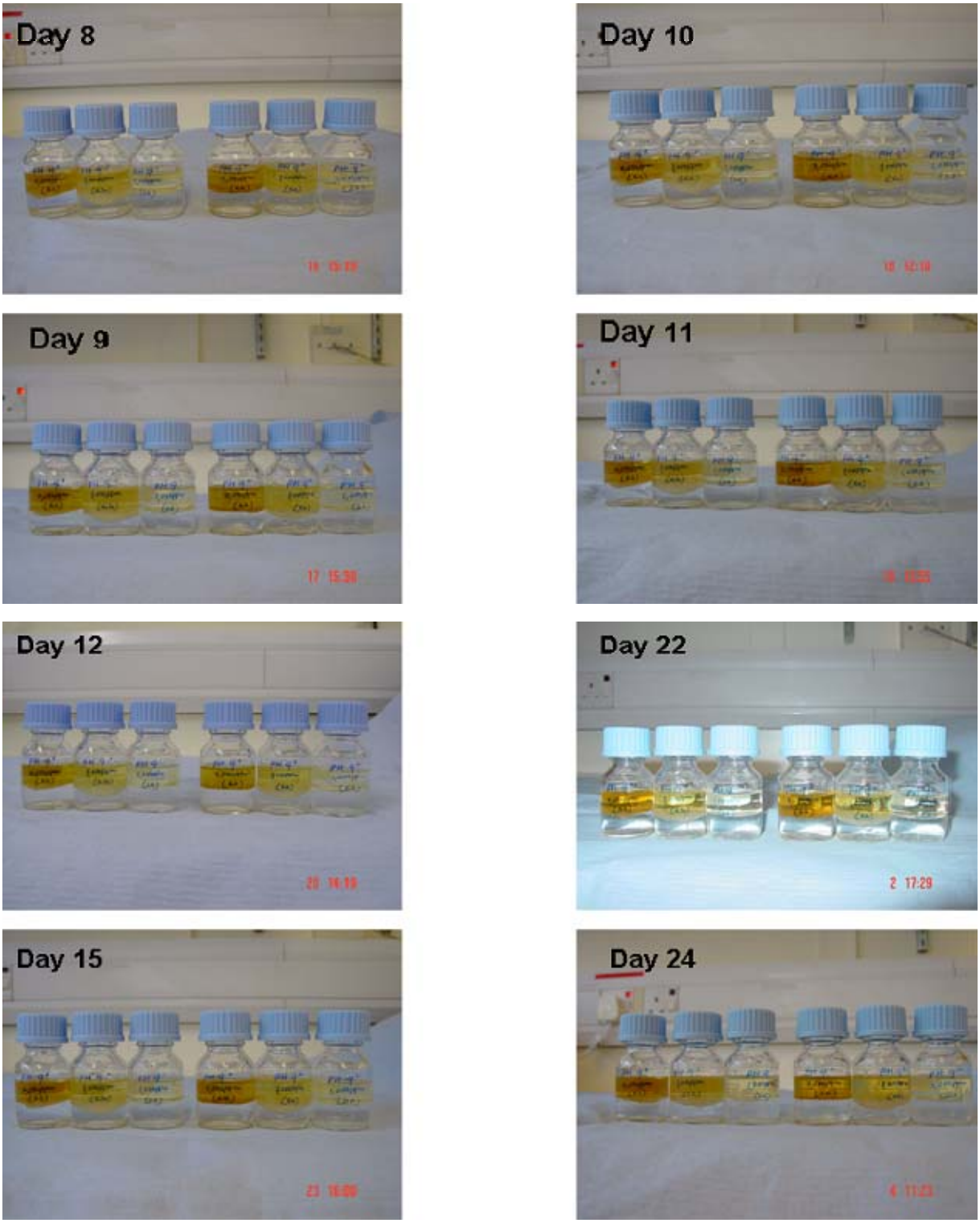

Figure 6.35: Visual observation of naphthenate precipitation static bottle test experiment with shear (turbulence) for 30 seconds then allowed to remain standing undisturbed for the remaining part of the experiment.

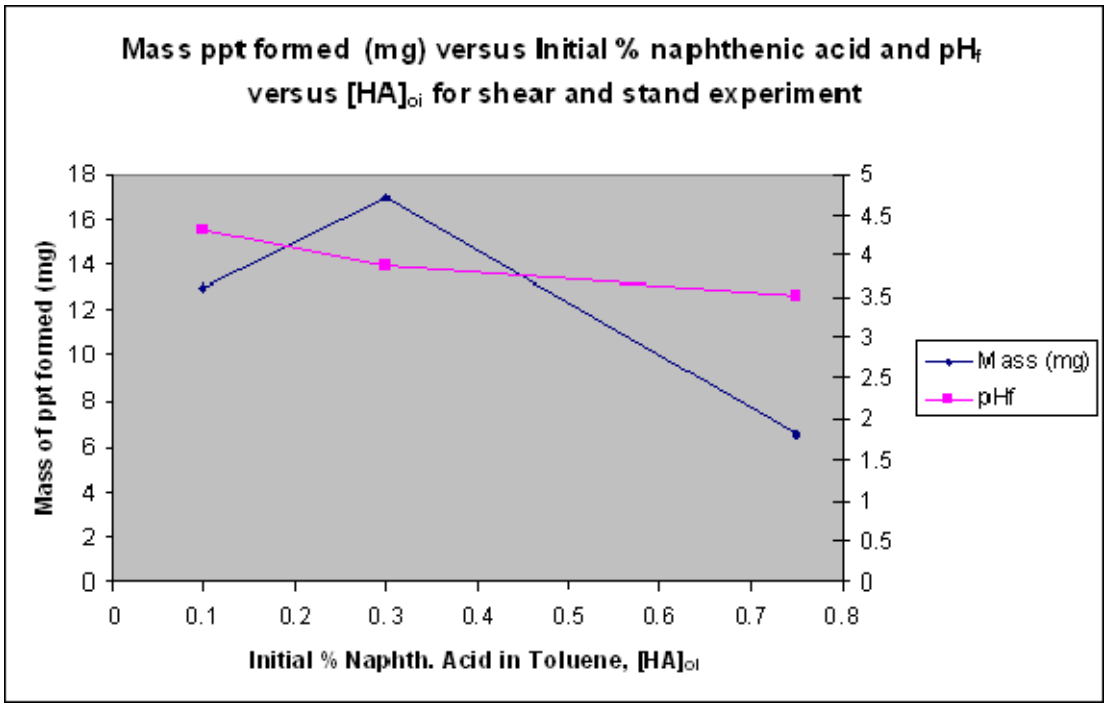

Figure 6.36: Naphthenate precipitate formed (mg) versus naphthenic acid concentrations $[HA]_{oi}$ and corresponding final brine pH measured for shear and subsequent standing naphthenate precipitation experiment.

Naphthenate Precipitation Experiment at a Higher Temperature (60^{o}C)

The effect of temperature on the quantity of naphthenate formation was studied here using the same composition of the water phase (Na^{+} = 25000 ppm and Ca^{++} = 20000 ppm) at pH 9 and an oil phase at various naphthenic acid [HA] concentrations i.e. (1000 ppm, 3000 ppm and 7500 ppm). In the oil industry, naphthenate formation is mostly observed in the separators, i.e. at certain temperature and pressure conditions, depending on the existing conditions during production operations. This particular experiment was designed to specifically heat both the oil and water (synthetic brine) phases to around 60^{o}C and mix them at that temperature to see the effect on the rate and quantity (mass) of naphthenate precipitate that can be formed. The total mass of naphthenate precipitate formed from this experiment and the final brine pH were measured and these results are presented in Table 6.13 below.

$[HA]_{oi}$ (ppm)	$[HA]_{oi}$ (M)	Mass precipitated (mg)		Final brine pH measured	
		1	2 (duplicate)	1	2 (duplicate)
1000	**0.003**	5	5	4.13	4.15
3000	**0.01**	7	8	3.84	3.85
7500	**0.025**	10	10	3.43	3.45

Table 6.13: The mass of naphthenate precipitated and the corresponding final brine pH measured for the naphthenate precipitation experiment carried out at a higher temperature.

Visual observation of the static bottle test experiment at 60^{o}C showed rapid naphthenate precipitation throughout the set of experiments carried out, with much a more substantial amount of naphthenate mass in bottles containing 3000 ppm and 7500 ppm naphthenic acid concentration in toluene, as shown in Figure 6.37. The amount of naphthenate precipitate generated is up to 10 mg for higher naphthenic acid concentrations, as can be seen from Table 6.13, whilst the oil phase with the lower naphthenic acid in it yields an amount of naphthenate precipitate similar to the test carried out at room temperature. The most important point to note here is that at such higher temperature the rate of naphthenate precipitation is higher than at room temperature, although this does not mean it would yield a higher mass of naphthenate precipitate. However, a higher throughput of both water and oil during production operations, coupled with the higher temperature in the separator, would lead to higher amounts of naphthenate formation. Similar work carried out by other researchers has shown that heating from 50^{o}C to 80^{o}C enhances naphthenate generation in both "end member" (sodium and calcium naphthenate) cases (Gallup and Star, 2004; Turner and Smith, 2005). The actual mechanism of how the temperature affects naphthenate formation is not well understood but it is probably simply related to its effect on the kinetics. Another point which should be noted is that, in all the experiments conducted, there was some recovery loss of the naphthenate formed which could be estimated to be around ~10% during filtration. A plot of the amount of naphthenate formed (mg) versus naphthenic acid concentration in the oil phase and final brine pH versus naphthenic acid concentration in oil phase is presented in Figure 6.38.

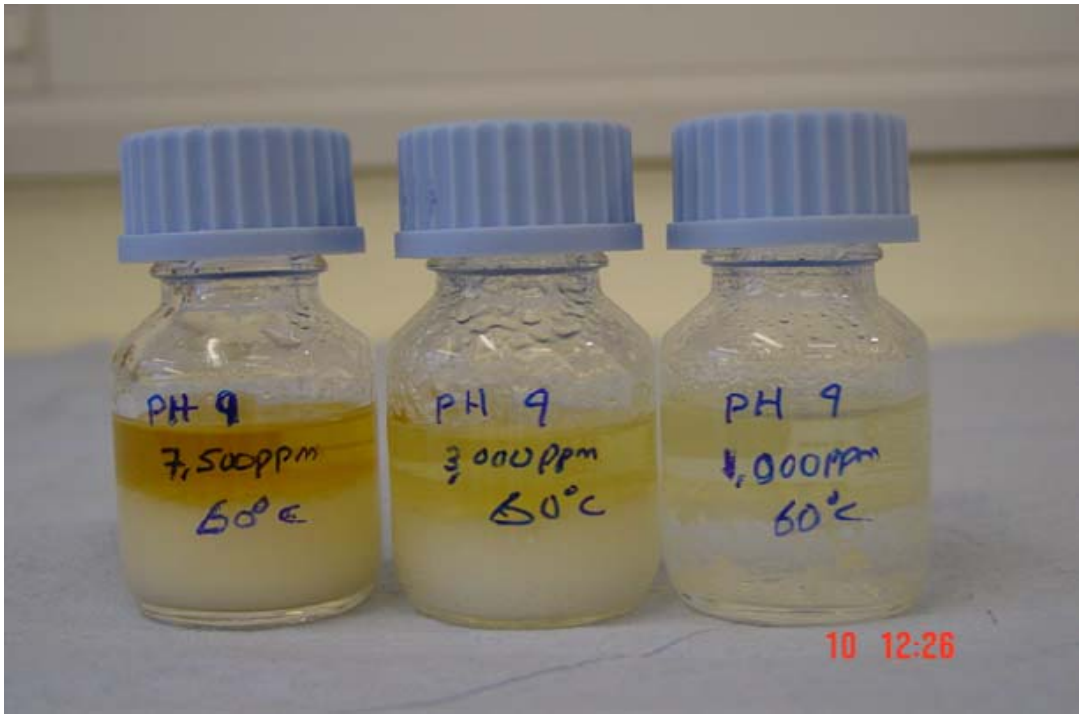

Figure 6.37: Visual observation of naphthenate precipitation static bottle test experiment at higher temperature (60°C) and various naphthenic acid [HA] concentrations.

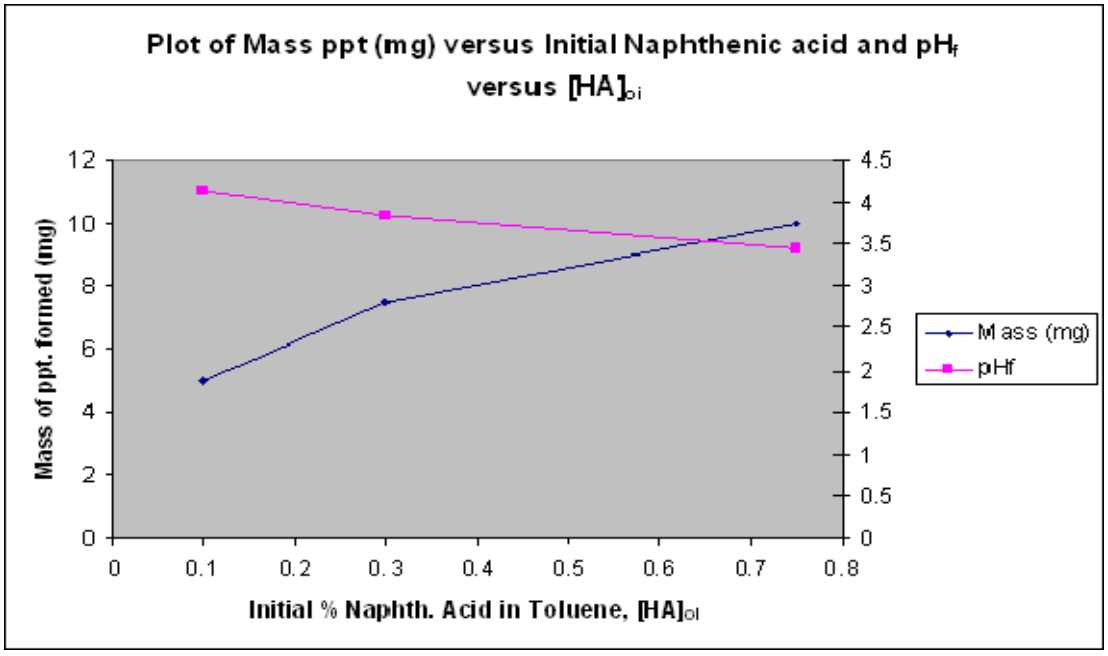

Figure 6.38: Plot of naphthenate precipitate formed (mg) versus naphthenic acid concentrations $[HA]_{oi}$ and final brine pH measured versus naphthenic acid concentration $[HA]_{oi}$ for experiment at higher temperature (60°C).

Effect of Bicarbonate (HCO_3^-) on Naphthenate Precipitation

This naphthenate deposition experiment was carried out to study the effect of bicarbonate (HCO_3^-) on the precipitation of naphthenate. The experiment was conducted using a pH 9 adjusted synthetic brine composition (Na^+ = 25000 ppm & Ca^{++} = 20000 ppm and various concentrations of HCO_3^- = 300 ppm, 600 ppm, 900 ppm) and an oil phase with various concentrations of naphthenic acid (1000 ppm, 3000 ppm and 7500 ppm). The concentration of bicarbonate was 300 ppm, 600 ppm and 900 ppm in each set of the experiments, to see the effect this would have on the formation of the naphthenate deposit. In each case the synthetic brine was pH adjusted to 9 prior to the addition of HCO_3^- before mixing the water and oil phases. The amount of naphthenate precipitate formed (mg) and the final brine pH values are presented in Tables 6.14 and 6.15 respectively.

$HA]_{oi}$ (ppm)	$[HA]_{oi}$ (M)	Mass of precipitate (mg)		
		With 300ppm HCO^3_-	With 600ppm HCO^3_-	With 900ppm HCO^3_-
0 (control)	**0**	N/A	N/A	N/A
1000	**0.003**	7	7	10
3000	**0.01**	12	12	15
7500	**0.025**	20	21	20

Table 6.14: The mass of naphthenate precipitate formed at various bicarbonate concentrations.

$HA]_{oi}$ (ppm)	$[HA]_{oi}$ (M)	Final brine pH measured		
		With 300ppm HCO_3^-	With 600ppm HCO_3^-	With 900ppm HCO_3^-
0 (control)	**0**	6.25	6.08	6.07
1000	**0.003**	6.46	6.40	6.34
3000	**0.01**	6.46	6.36	6.28
7500	**0.025**	6.46	6.34	6.21

Table 6.15: Final brine pH measured for naphthenate precipitation experiment carried out using various concentrations of bicarbonate.

Results from this experiment show an increase in the amount of naphthenate precipitation during the static bottle tests, as compared to those carried without the addition of bicarbonate to the synthetic brine. The final brine pH in all the cases appears to be similar irrespective of the amount of naphthenic acid in oil phase at the beginning of this study and this result is quite different from the one we have in the previous section above. A plot of the amount of naphthenate precipitate (mg) versus naphthenic acid concentration in toluene $[HA]_{oi}$ for each concentration of bicarbonate addition and final brine pH versus naphthenic acid concentration in toluene $[HA]_{oi}$ is presented in Figure 6.39. From this figure, we can clearly see in each case that as the naphthenic acid concentration $[HA]_{oi}$ in the oil phase increases and the concentration of the bicarbonate in the water phase increases, then a higher amount of naphthenate precipitation occurs. This may be due to the formation of both calcium carbonate and calcium naphthenate (mixed scales) whilst the final brine pH measured remains the same or slightly decreased with the increase of naphthenic acid concentration and bicarbonate, which can be seen from the graph in Figure 36. This phenomenon of mixed scale formation between carbonate and naphthenates has been reported previously (Rousseau *et al.,* 2001).

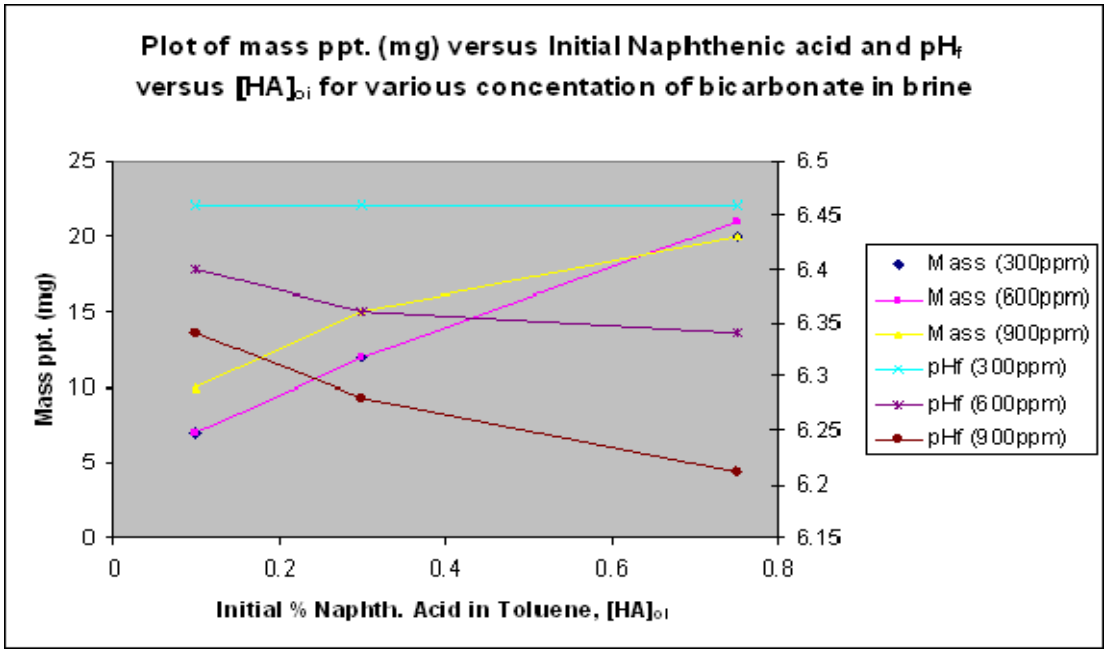

Figure 6.39: Plot of naphthenate precipitate formed (mg) versus naphthenic acid concentrations $[HA]_{oi}$ and final brine pH measured versus naphthenic acid concentration $[HA]_{oi}$ for experiment with addition of various concentration of bicarbonate.

Effect of Variable Concentrations of Ca^{++} ion in the Brine on Naphthenate Precipitation

The effect of varying the concentration of calcium ions in the brine (at fixed sodium ion concentration) was examined, to determine how it affects the formation of naphthenate in the oil-brine precipitation experiment. The experiment was carried out with fixed sodium ion concentration, i.e. 25000 ppm, and variable calcium ion concentrations i.e. 500, 1000, 2000, 5000, 10000 and 20000 ppm. The brine used was adjusted to pH 9 prior to mixing with oil phase which contains 7500 ppm naphthenic acid concentration. Table 6.16 below shows the amount of naphthenate precipitate (mg) and the final brine pH measure for each set of brine composition with variable Ca^{++} composition.

Na^{+} Concentration in the brine (ppm)	Ca^{++} Concentration in the brine (ppm)	Mass of CaN precipitated formed (mg)	Final brine pH measured (Average of two values)
25000	500	20	3.985
25000	1000	20	3.93
25000	2000	30	3.9
25000	5000	40	3.875
25000	10000	50	3.815
25000	20000	70	3.72

Table 6.16: The mass of naphthenate precipitate formed (mg) and the final brine pH measured from the experiment with variable Ca^{++} concentrations and fixed Na^{+} concentration.

The results show that as the calcium ion concentration (Ca^{++}) increased in the brine composition, then an increase in the amount of naphthenate precipitation was observed, as shown in Table 6.16 above. This is as expected, based on the naphthenate model, since when the Ca^{++} increases in the brine then there is some tendency of more calcium ions to be available for reaction with the naphthenic acid from the oil phase, which ultimately leads to the formation of more calcium naphthenate deposit. The static bottle test experiment carried out is presented in Figure 6.40. A plot of the mass of CaN naphthenate precipitate

versus Ca^{++} concentration in brine and final brine pH versus Ca^{++} concentration in brine is presented in Figure 6.41 below.

Figure 6.40: Static bottle test experiment using variable Ca^{++} concentration and fixed Na^{+} concentration in the brine at 7500 ppm naphthenic acid concentration in the oil phase.

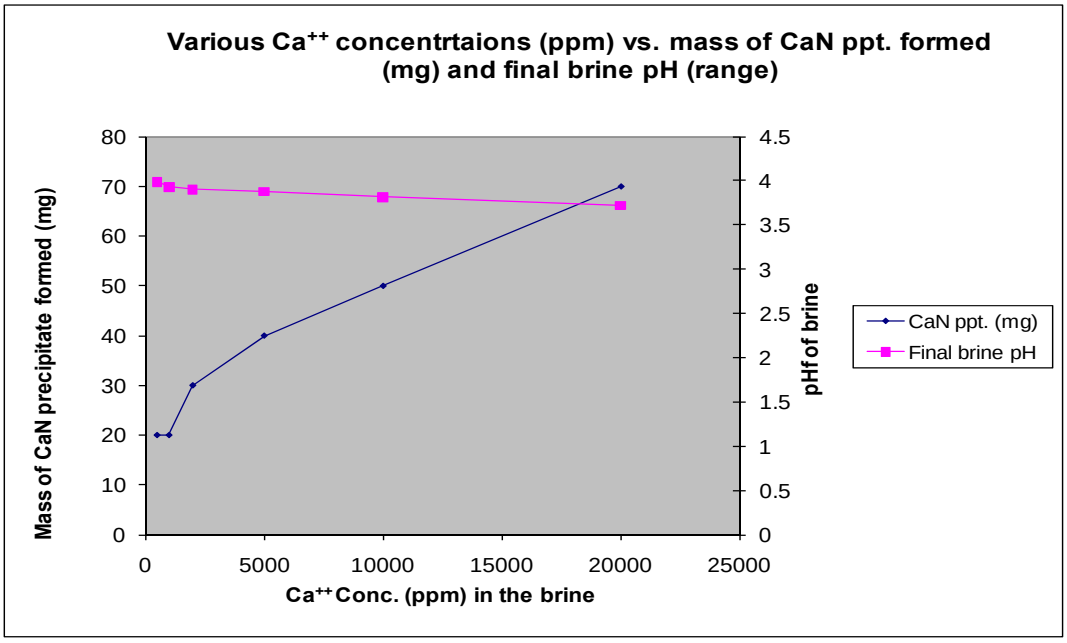

Figure 6.41: Plot of the mass of CaN precipitate formed (mg) versus Ca^{++} concentration in the brine and final brine pH versus Ca^{++} concentration in the brine.

6.6 SUMMARY AND CONCLUSIONS

In this chapter, the following have been described: (i) a simple pH change thermodynamic model was proposed where both prediction and experimental results were presented; (ii) a full model of naphthenate precipitation was described and a wide sensitivity study was performed using this model. In addition, a number of predictions were made and tested experimentally; and (iii) a range of other sensitivities were also studied experimentally in this chapter e.g. the effects of shear, temperature etc.

Thermodynamic pH Change Experiments

In this study, a simple thermodynamic model for naphthenic acid partitioning between oil and water was proposed and a full derivation is presented in Appendix A. The modelling was carried out by considering only a single "pseudo naphthenic acid" species denoted as [HA], which has been applied to experiments in which the naphthenate deposit does not actually appear—the so-called "pH change experiments." For this particular case, the change in brine pH from $pH_i \rightarrow pH_f$ is governed only by the parameters of K_a (naphthenic acid dissociation constant) and K_{ow} (oil-water partition coefficient) and the initial conditions (pH_i and $[HA]_{oi}$).

The pH change experimental results showed a progressive change in brine pH value (i.e., from high to low) when mixing the oil phase (extracted naphthenic acid dissolved in toluene) with the brine phase. Applying the thermodynamic naphthenate model to the pH change experiments reveals that, at a higher brine pH (pH 5 to 6), the model data agrees qualitatively with the experimental data, using a single fixed value of K_a and K_{ow}. However, using different sets of values of K_a and K_{ow} for each of the initial brine pH value (say 6, 5, 4, and 3) shows very good match between the model and experimental data, although having to adjust both of these quantities to match each experiment was not physically justified.

Thermodynamic Naphthenate Precipitation Experiments

A thermodynamic model describing calcium naphthenate (CaN) precipitation has been presented; a full derivation of this model is given in Appendix A which describes an

extension of an earlier simpler model (Mohammed *et al.,* 2009). This CaN prediction model was applied in a sensitivity study which made a number of specific predictions about the way a precipitating Ca-Naphthenate (CaN) system behaves. The model was then applied to design three new experiments which were performed in the laboratory in order to test the model predictions, as follows:

(a) The results of a series of "successive extraction" experiments: the model prediction here was that, at equilibrium in a two phase CaN deposit experiment, ~95% of the original naphthenic acid (HA) remained in the oil phase. Thus, successive extractions from the original oil sample with fresh pH 9 brine samples should give approximately equal masses of CaN deposit and a very slightly rising (but almost constant) low final pH value.

(b) Type (i) fixed V_o, variable (V_w/V_o) ratio set of experiments: In these experiments, a fixed volume of oil (V_o) containing naphthenic acid [HA] was taken and extracted by varying amounts of pH 9 brine. As the water fraction (%W) increased, a maximum was predicted in the mass of CaN deposited at around %W ~ 60 - 70% along with a continuously significantly rising final pH.

(c) Type (ii) fixed total volume, $V_T = (V_w+V_o)$, variable (V_w/V_o) ratio set of experiments: In these experiments, the total volume of oil and water was held constant and the proportion of each phase, the (V_w/V_o) ratio, was varied. The predictions for this type of varying %W experiment were qualitatively the same as the type (i) experiments (but quantitatively they were a little different).

The actual laboratory results for the above predicted experiments qualitatively agree very well with what the model predicts in all the three sets of experiments. In particular, the model quite unexpectedly predicts that there is **a maximum in the mass of CaN precipitated with %watercut (around ~60 - 70% watercut, %W)**. This occurs despite the fact that less "A" (naphthenate) is available (linearly) as % watercut increases in the type (ii) experiment; in the type (i) experiments, the same mass of naphthenic acid (but varying amounts of Ca^{2+}) is available for precipitation at all %W values. This is precisely

what is observed in both types of varying (V_w/V_o) ratio experiments. Thus, excellent semi-quantitative agreement is seen between the model predictions and the experimental findings.

Sensitivity studies Experiments

Additional sensitivity parameters were studied experimentally in this chapter to determine their effect on the formation of naphthenate, i.e., the effects of shear (or no shear), temperature, bicarbonate ions (HCO_3^-) and calcium ions (Ca^{++}) concentration in the water phase (brine). The results from this study revealed:

(a) Effect of non-shearing: Precipitation experiments with no shear (without shaking) after two weeks showed no visible formation of naphthenate precipitate, hence we can conclude that for the naphthenate to form there has to be some shear or turbulence.

(b) Shear and stand without shear: From this experiment, we were able to see that at the initial stage of the experiment, shear has an important role in the formation of naphthenate. However, as the experiment is allowed to stand for a long time, visual observation revealed that the amount of precipitate formed at the higher concentration of naphthenic acid in toluene decreased whilst in some cases the amount of naphthenate formed remains almost the same even after a two weeks period. Thus, it may be that there is an optimum concentration of naphthenic acid in the oil phase that would give the highest amount of naphthenate precipitate.

(c) Temperature effect: Results show that the reaction rate is favoured at a higher temperature, even although the amount of naphthenate precipitation does not significantly differ from the experiment conducted at room temperature. However, in a production system where the throughput is extremely high, coupled with the higher temperature, the effect of temperature would certainly have a strong role in the formation of naphthenates.

(d) Effect of the addition of bicarbonate (HCO_3^-): Addition of bicarbonate (HCO_3^-) to the pH adjusted water phase (synthetic brine) prior to mixing with the oil phase has generally

favoured the formation of naphthenate precipitate, as shown in Figure 36. However, increasing the concentration of bicarbonate does not make any substantial difference to the amount of naphthenate precipitation. The precipitate formed in this type of experiment may likely be due to the formation of mixed precipitates i.e. calcium carbonate and calcium naphthenates. Rousseau *et al.,* (2001) has reported formation of mixed deposits of calcium naphthenate and calcium carbonate in the production fields.

CHAPTER 7: NAPHTHENATES INHIBITION EFFICIENCY

7.1 INTRODUCTION

The objectives of the work in this chapter are: (a) to develop a methodology for assessing calcium naphthenate (CaN) inhibitors, and (b) to test this on a series of commercially available inhibitors for CaN. Eight naphthenate inhibitor samples were analysed in this study using; (i) calcium naphthenate extract from a field sample; (ii) sodium carboxylate emulsion extract from a field sample and (iii) emulsion forming crude oil spiked with naphthenic acid extract. The calcium naphthenate and sodium carboxylate emulsion extracts used in this study were extracted from the field samples supplied by FAST sponsor companies. Details for the naphthenic extraction have been fully described in Chapter 3, Sections 3.2.1 and 3.2.2, whilst the emulsion forming crude was supplied as an uncontaminated crude oil sample by one of the oil producing companies sponsoring FAST. The method development for the static inhibition efficiency experiment carried out in this thesis was presented in Chapter 3, Section 3.5.1.

The actual chemical composition of these inhibitors is not known, as the suppliers were not willing to release the information to the open literature. The proposed theory on the chemistry of these inhibitors and how they inhibit naphthenate formation is thought to be that the inhibitors exhibit surface active properties which cause them to congregate at the oil-water interface. The crowding of these inhibitors at the interface creates a layer (barrier) which inhibits the interactions between the carboxylic group of the naphthenic acids in the oil phase and cations in the water phase to form salts (which could either be a deposit of a substance or a carboxylate/emulsion type). In this way, these inhibitors prevent naphthenate formation.

A brief description of the naphthenate inhibitors studied is presented in Table 7.1 below. The short overview includes the code identification of the inhibitor, appearance description and % activity as supplied by the supplier.

The activity of these inhibitors was given as follows: (i) 40% active concentration for CNI 1, CNI 2, CNI 3 and CNI 4; (ii) 20% active concentration for CNI 5 and CNI 6; (iii) 50% active concentration for CNI 7; and (iv) 40% concentration for CNI 8. All efficiency inhibition calculations were based on % active concentration. The effect of these inhibitors on the final brine pH was also measured, along with that of the control (without the inhibitors).

Naphthenate inhibitor	**Colour description (closest)**	**% Activity**
CNI 1	Colourless	40
CNI 2	Light yellow	40
CNI 3	Light yellow	40
CNI 4	Colourless	40
CNI 5	Colourless	20
CNI 6	Colourless	20
CNI 7	Reddish brown	50
CNI 8	Light yellow	40

Table 7.1: Description of the 8 naphthenate inhibitor samples used in this study

7.2 RESULTS AND DISCUSSION

The results for the static inhibition efficiency experiment method development for the different naphthenate inhibitors are presented below. The main reason for this method development was to screen the available naphthenate inhibitors to determine which ones are suitable for inhibiting calcium naphthenate deposition and also what "minimum inhibitor concentration" (MIC) of these inhibitors could be deployed. The MIC in this context would be that broadly established by visual inspection rather than being a precise formula as is the case for mineral scale deposition.

Inhibition efficiency on calcium naphthenate extract

The eight naphthenate inhibitors viz: CNI 1, CNI 2, CNI 3, CNI 4, CNI 5, CNI 6, CNI 7 and CNI 8 were tested to establish the minimum inhibitor concentration (MIC) required to mitigate the formation of calcium naphthenate (CaN) precipitation in the laboratory, using the static bottle test. The oil phase used contained naphthenic acid extract at 1000 ppm, 3000 ppm and 7500** ppm acid concentration and synthetic brine, which is adjusted to pH 9. The initial screening of these inhibitors presented in the MIC chart showed that; (i) CNI 1, CNI 4, CNI 5, CNI 6 inhibitors can inhibit calcium naphthenate formation; (ii) CNI 7 and CNI 8 inhibitors mildly inhibit calcium naphthenate at a certain inhibition concentration range; and (iii) CNI 2 and CNI 3 were found to have a compatibility issue, as it was observed that even at 0 ppm concentration of naphthenic acid in the oil phase, there was formation of precipitate, which should not have formed. Because of this compatibility issue, experimental testing was restricted only to those inhibitors that show some potential for naphthenate inhibition, based on the laboratory studies.

****Note:** *Throughout this thesis, whenever 1 ppm of naphthenic acid in the oil phase is referred, this is actually (ρ_o/ρ_w) mg/L of the substance. In the aqueous phase, 1 ppm of any quantity is the normal 1 mg/L.*

CNI 1 Inhibitor

The minimum inhibitor concentration (MIC) chart is presented in Table 7.2. The corresponding static bottle test experiments together with the graphical plot of the final brine pH versus initial naphthenic acid concentration are presented in Figure 7.1. Static bottle tests using this inhibitor at various concentrations i.e. 150 ppm, 100 ppm, 50 ppm, 20 ppm and 0 ppm (control) revealed that at a very high concentration of naphthenic acid (say 7500 ppm) in the oil phase, the MIC is around 100 ppm, whilst at naphthenic acid concentration in the oil phase of 3000 ppm and 1000 ppm, the MIC was 50 ppm and 20 ppm, respectively. The final brine pH measured showed a progressive decrease but the trend can be explained as due to the dissociation of the naphthenic acid in the oil phase and subsequent partitioning between the oil and water phases, which results in the change of the brine pH. It is important to note in this case, for example, at 1000 ppm concentration of

naphthenic in the oil phase and 20 ppm of the inhibitor, the final brine pH measured was 5.98, whilst at the same naphthenic acid concentration in the oil phase and no inhibitor (0 ppm), the final brine pH was at 4.04. This observation was interesting, in the sense that addition of 20 ppm of CNI 1 inhibitor into the oil phase has substantially reduced the naphthenic acid partitioning from the oil phase to the water phase. This phenomenon can be explained by the inhibitor crowding at the oil-water interface which thus creates a thin layer to protect naphthenic acid from the oil phase from entering the water phase. When this naphthenic acid protection is achieved, then, ultimately, naphthenate formation will either be drastically reduced or completely stopped. This trend was observed in all of the various naphthenic acid concentrations in toluene (model oil phase) i.e. 3000 ppm and 7500 ppm.

Inhibitor\ HA	**7500 ppm**	**3000 ppm**	**1000 ppm**	**0 ppm**
250 ppm	N/A	N/A	N/A	N/A
200 ppm	N/A	N/A	N/A	N/A
150 ppm	**No Precipitate**	**No Precipitate**	**No Precipitate**	**No Precipitate**
100 ppm	**No Precipitate**	**No Precipitate**	**No Precipitate**	**No Precipitate**
50 ppm	**Very slight Precipitate**	**No Precipitate**	**No Precipitate**	**No Precipitate**
20 ppm	**Slight Precipitate**	**Slight Precipitate**	**No Precipitate**	**No Precipitate**
0 (control)	**Precipitate**	**Precipitate**	**Slight Precipitate**	**No Precipitate**

Table 7.2: Minimum inhibitor concentration chart (MIC) for CNI 1 inhibitor using CaN extract**.**

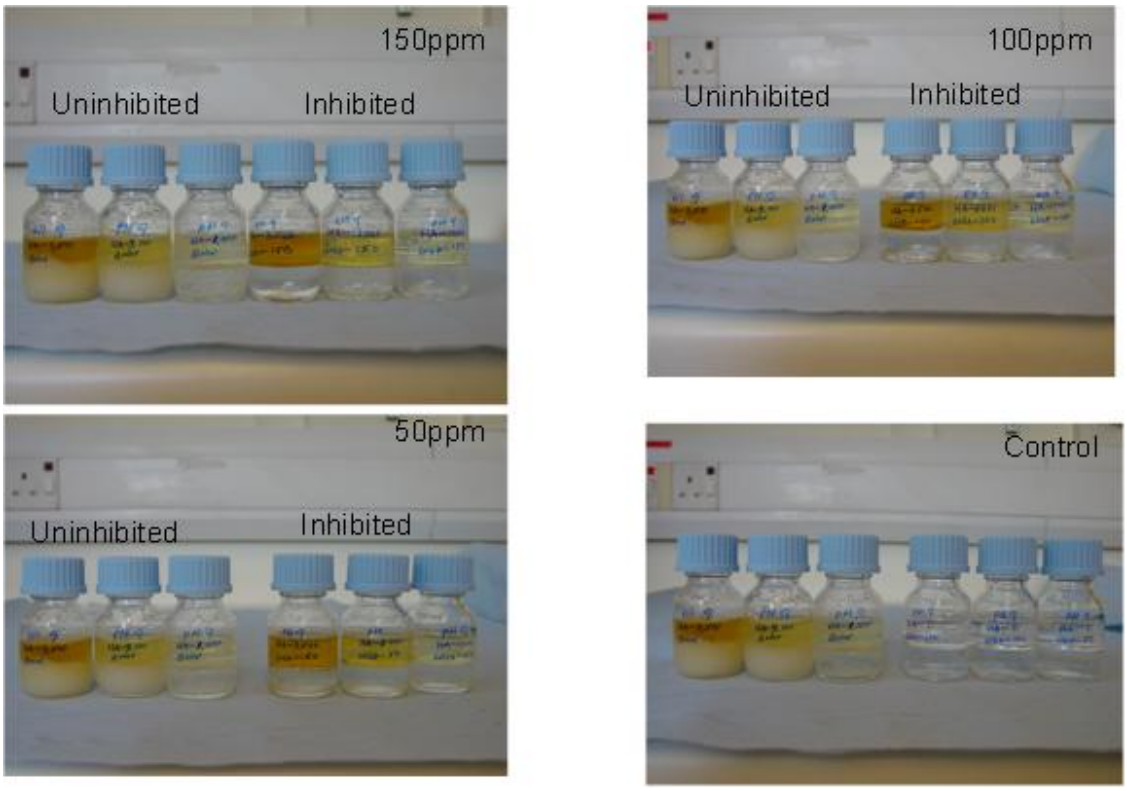

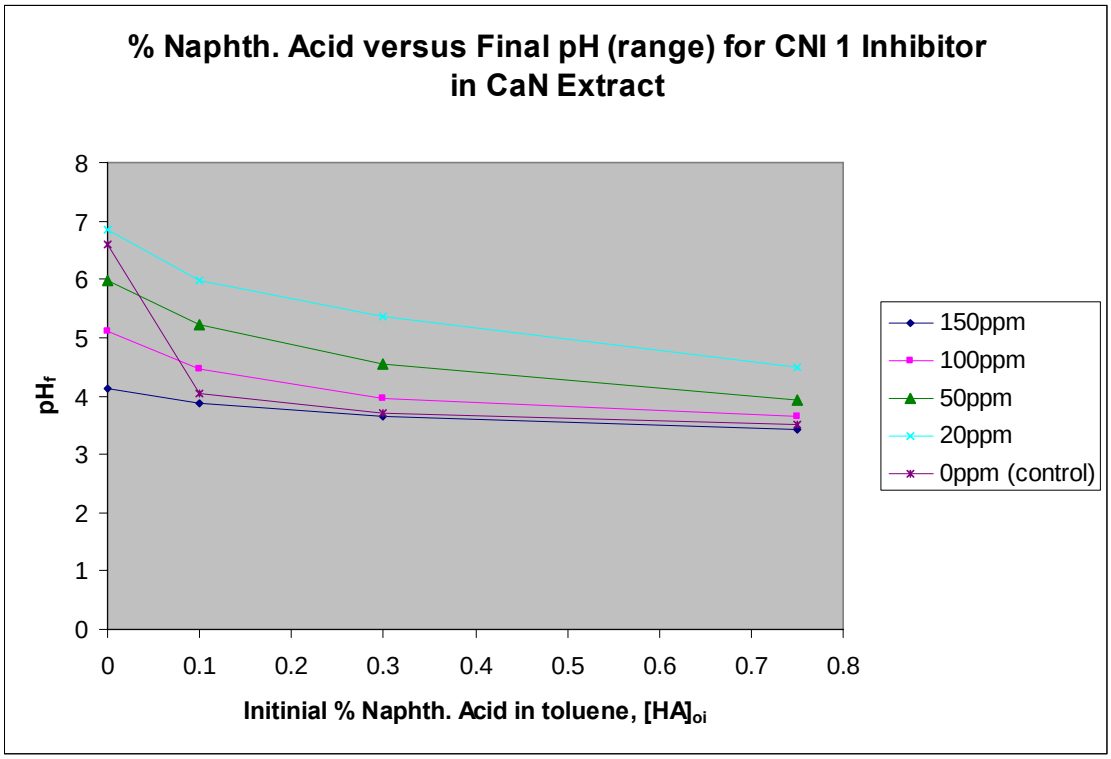

Figure 7.1: Static bottle test experiment (above) and the graphical plot of the final brine pH versus initial % naphthenic acid concentration, $[HA]_{oi}$ using CNI 1 inhibitor.

CNI 2 and CNI 3Inhibitors

The MIC charts for CNI 2 and CNI 3 inhibitors are presented in Tables 7.3 and 7.4, respectively, whilst an example of the static bottle inhibition efficiency test for the CNI 2 inhibitor is presented in Figure 7.2. Initial screening results from these inhibitors shows that both of them are incompatible. Therefore, further experimental study on these was discontinued. The results from the static inhibition efficiency study resulted in a formation of precipitate even at zero concentration of naphthenic (0ppm, $[HA]_{oi}$) in toluene and this can only be related to the fact that the inhibitors are incompatible with the synthetic pH adjusted brine. It is worth noting that the initial brine pH was 9 and was considered as a reference pH where naphthenate formation is observed, based on the previous naphthenate precipitation experiments.

Inhibitor\ HA	**7500 ppm**	**3000 ppm**	**1000 ppm**	**0 ppm**
250 ppm	N/A	N/A	N/A	N/A
200 ppm	N/A	N/A	N/A	N/A
150 ppm	**Precipitate**	**Precipitate**	**Precipitate**	**Precipitate**
100 ppm	**Precipitate**	**Precipitate**	**Precipitate**	**Precipitate**
50 ppm	**Precipitate**	**Precipitate**	**Precipitate**	**Precipitate**
20 ppm	**Slight Precipitate**	**Slight Precipitate**	**Slight Precipitate**	**Slight Precipitate**
0 (control)	**Precipitate**	**Precipitate**	**Slight Precipitate**	**No Precipitate**

Table 7.3: Minimum inhibitor concentration chart (MIC) for CNI 2 inhibitor, using CaN extract.

Inhibitor\ HA	**7500 ppm**	**3000 ppm**	**1000 ppm**	**0 ppm**
250 ppm	N/A	N/A	N/A	N/A
200 ppm	N/A	N/A	N/A	N/A
150 ppm	**Precipitate**	**Precipitate**	**Precipitate**	**Precipitate**
100 ppm	**Precipitate**	**Precipitate**	**Precipitate**	**Precipitate**
50 ppm	**Slight Precipitate**	**Slight Precipitate**	**Slight Precipitate**	**Slight Precipitate**
20 ppm	**Very slight Precipitate**	**Very slight Precipitate**	**Very slight Precipitate**	**Very slight Precipitate**
0 (control)	**Precipitate**	**Precipitate**	**Slight Precipitate**	**No Precipitate**

Table 7.4: Minimum inhibitor concentration chart (MIC) for CNI 3 inhibitor, using CaN extract.

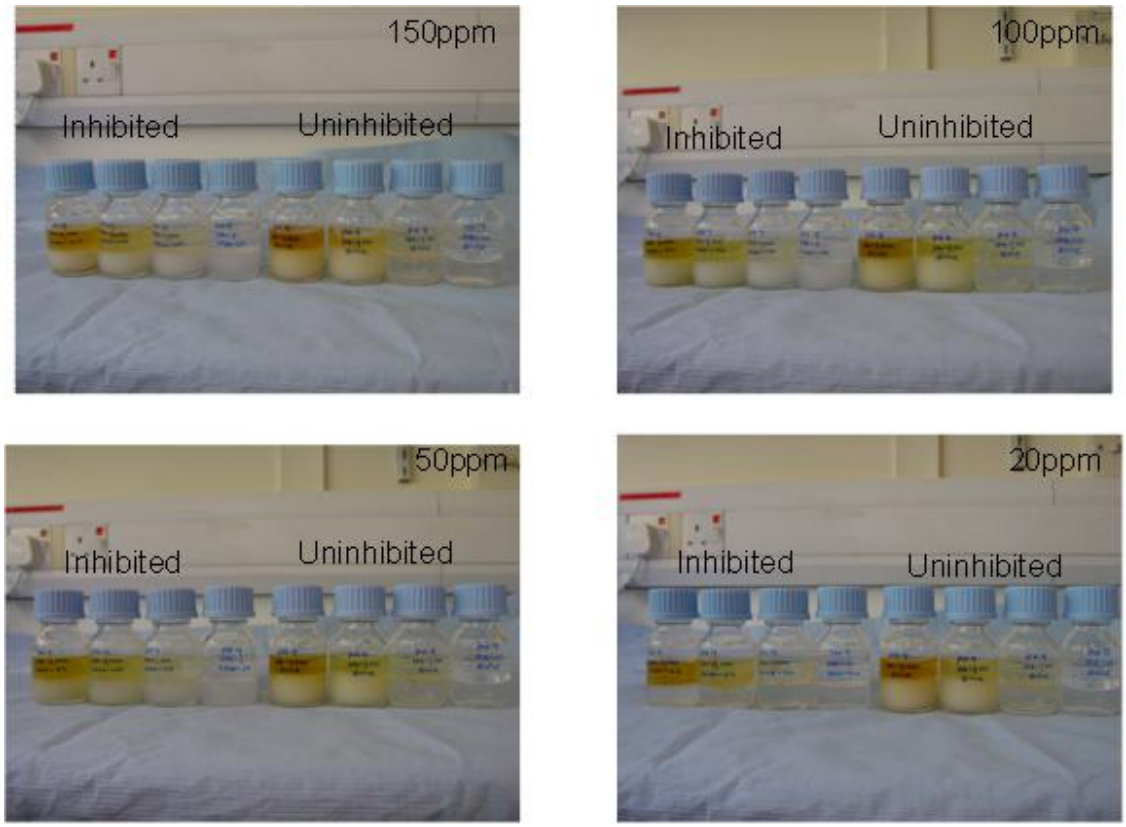

Figure 7.2: Static bottle test inhibition efficiency experiment for CNI 2 inhibitor, using various concentrations of naphthenic acid in toluene ($[HA]_{oi}$ = 1000 ppm, 3000 ppm and 7500 ppm) and pH 9 adjusted synthetic brine.

CNI 4 Inhibitor

The results are presented in Table 7.5 and Figure 7.3. Static bottle test efficiency studies using this inhibitor were carried out at various concentrations, i.e. 250 ppm, 200 ppm, 150 ppm, 100 ppm, 50 ppm, 20 ppm and 0 ppm (control), and initial naphthenic acid concentrations of 1000 ppm, 3000 ppm and 7500 ppm. These studies showed that the inhibitor CNI 4 can prevent the formation of calcium naphthenate. The MIC determined from the experiment was 200 ppm for naphthenic acid concentration of 7500 ppm, 100 ppm for 3000 ppm naphthenic acid concentration and 20 ppm for 1000 ppm naphthenic acid concentration, as can be seen in the MIC chart in Table 7.5 below. The plots of the final brine pH versus the initial % naphthenic acid concentration at various CNI 4 inhibitor concentrations showed a decrease in the final brine pH. A significant pH change was observed where zero (0 ppm) naphthenic acid was present, in relation to those compared with the presence of an inhibitor. Similar trends of final brine pH decrease were also observed from the study where CNI 1 inhibitor was used to mitigate formation of calcium naphthenate. The static inhibition efficiency bottle test experiment and plot of the final brine pH versus the initial % naphthenic acid concentration is presented in Figure 7.3.

Inhibitor\ HA	**7500 ppm**	**3000 ppm**	**1000 ppm**	**0 ppm**
250 ppm	**No Precipitate**	NA	NA	NA
200 ppm	**No Precipitate**	NA	NA	NA
150 ppm	**Dense Substance at interface**	**No Precipitate**	**No Precipitate**	**No Precipitate**
100 ppm	**Very slight Precipitate**	**No Precipitate**	**No Precipitate**	**No Precipitate**
50 ppm	**Very slight Precipitate**	**Cloudy at interface**	**No Precipitate**	**No Precipitate**
20 ppm	**Slight Precipitate**	**Cloudy at interface**	**No Precipitate**	**No Precipitate**
0 (control)	**Precipitate**	**Precipitate**	**Slight Precipitate**	**No Precipitate**

Table 7.5: Minimum inhibitor concentration chart (MIC) for CNI 4 inhibitor, using CaN extract.

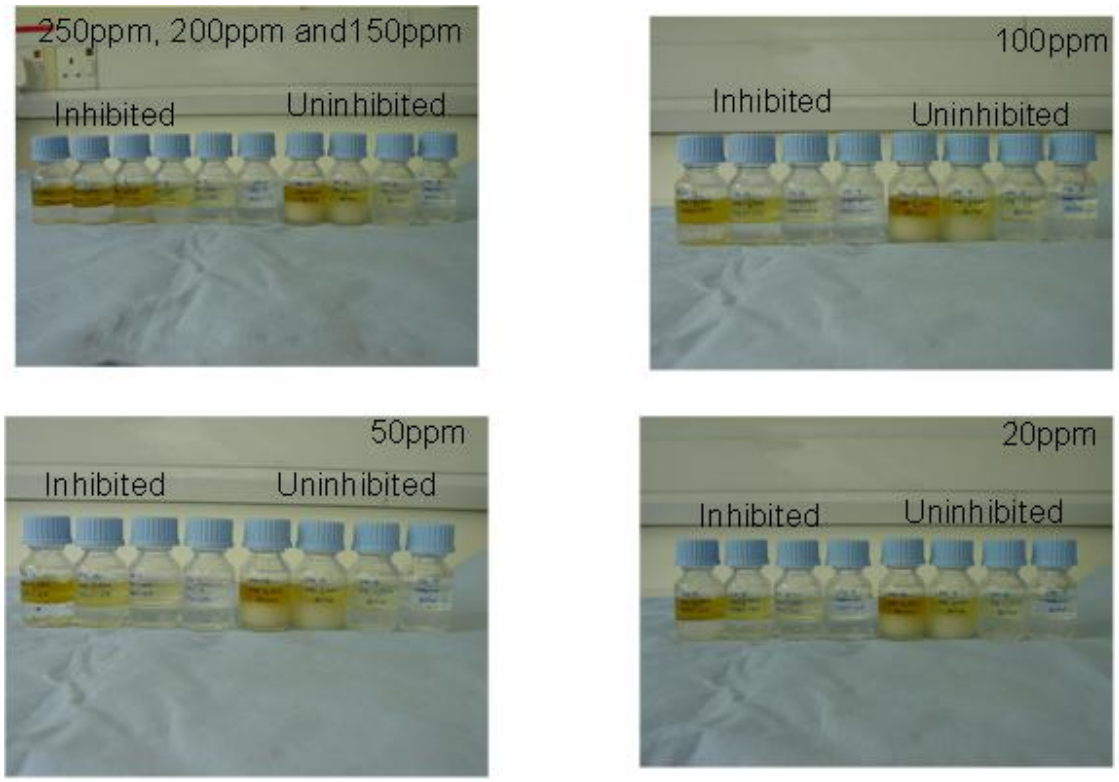

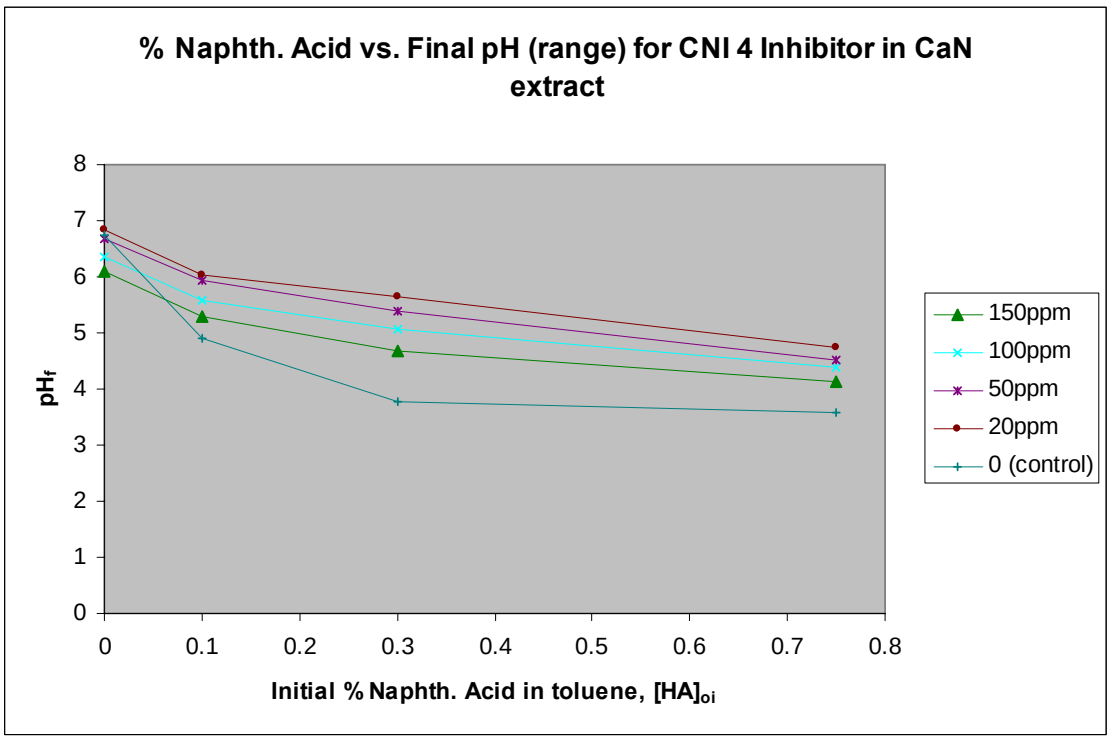

Figure 7.3: Static bottle test experiment (above) and the graphical plot of the final brine pH versus initial % naphthenic acid concentration, $[HA]_{oi}$ using CNI 4 inhibitor.

CNI 5 and CNI 6 Inhibitors

The MIC charts for CNI 5 and CNI 6 are presented below in Tables 7.6 and 7.7, respectively. Static bottle test efficiency studies using this inhibitor at various concentrations i.e. 250 ppm, 200 ppm, 150 ppm, 100 ppm, 50 ppm, 20 ppm and 0 ppm (control) and initial naphthenic acid concentrations at 1000 ppm, 3000 ppm and 7500 ppm showed that this inhibitor can prevent the formation of calcium naphthenate. For CNI 5 inhibitor, a concentration of 250 ppm was found to be effective in preventing deposition for oil with higher concentration of naphthenic acid present and 20 ppm was effective for oil with lower concentrations of naphthenic acid (say 1000ppm). The MIC determined for CNI 6 from the experiment was 200 ppm for naphthenic acid concentration of 7500 ppm, 150 ppm for oil with 3000 ppm and 1000 ppm naphthenic concentrations, as can be seen from the MIC chart in Tables 7.6 and 7.7 below. The plots of the final brine pH versus the initial % naphthenic acid concentration at various CNI 5 and CNI 6 inhibitor concentrations showed a decrease in the final brine pH. A significant pH change was observed where zero (0 ppm) naphthenic was present in the mix, whilst the addition of an inhibitor at a medium concentration (say 50 ppm to 100 ppm) was observed to stop precipitation; subsequent pH change of the brine is not significant compared to the control, where there is a drastic brine pH change. Static inhibition efficiency bottle test experiments and plots of the final brine pH versus the initial % naphthenic acid concentration are presented in Figures 7.4 and 7.5 respectively.

Inhibitor\ HA	7500ppm	1000ppm	0ppm
250ppm	No Precipitate	No Precipitate	No Precipitate
200ppm	Very slight Precipitate	No Precipitate	No Precipitate
150ppm	Very slight Precipitate	No Precipitate	No Precipitate
100ppm	Very slight Precipitate	No Precipitate	No Precipitate
50ppm	Slight Precipitate	No Precipitate	No Precipitate
20ppm	Precipitate	No Precipitate	No Precipitate
0 (control)	Precipitate	Very slight Precipitate	No Precipitate

Table 7.6: Minimum inhibitor concentration chart (MIC) for CNI 5 inhibitor, using CaN extract.

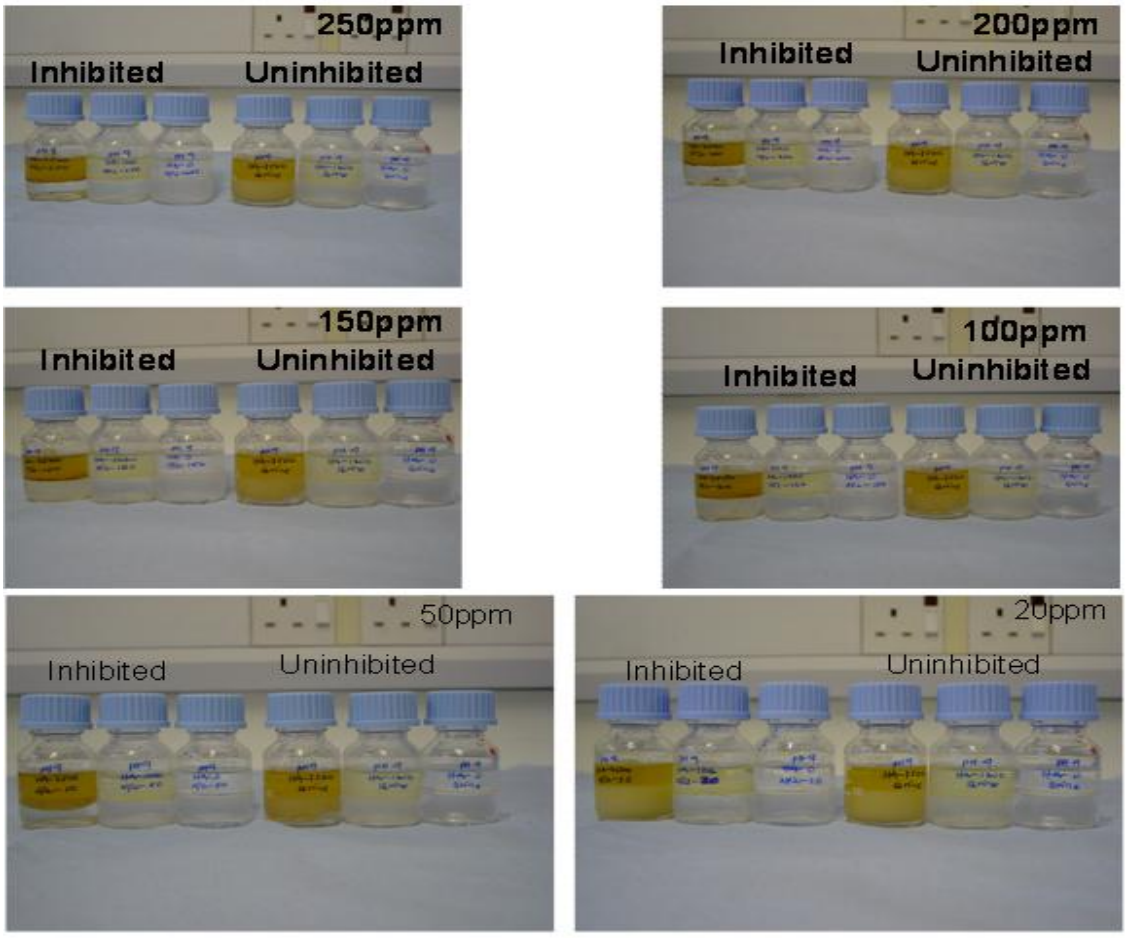

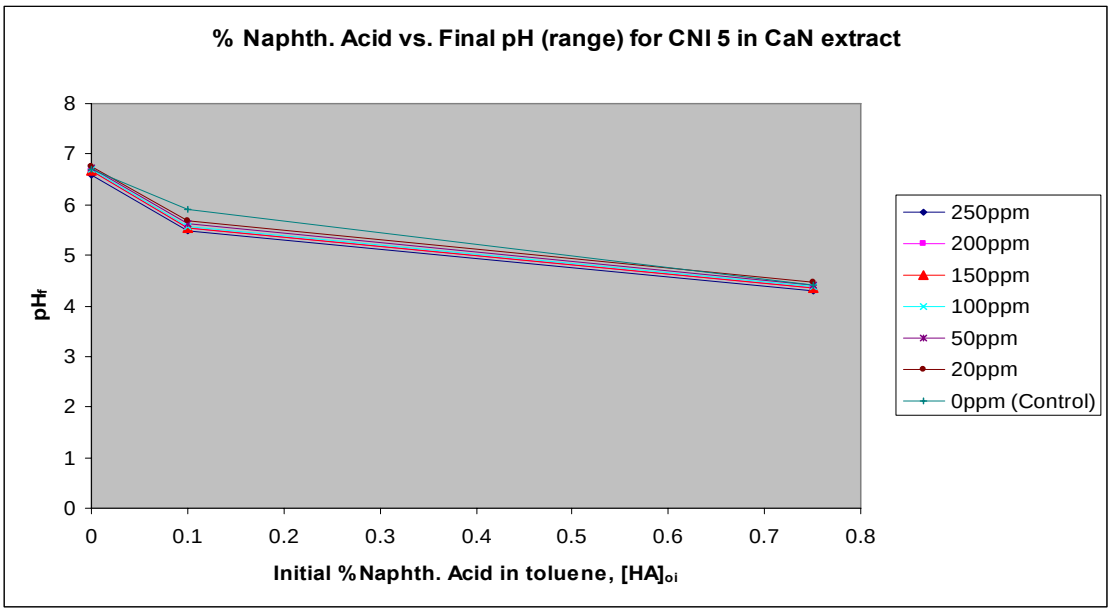

Figure 7.4: Static bottle test experiment (above) and the graphical plot of the final brine pH versus initial % naphthenic acid concentration, $[HA]_{oi}$ using CNI 5 inhibitor.

Inhibitor\ HA	7500 ppm	3000 ppm	1000 ppm	0 ppm
250 ppm	No Precipitate	No Precipitate	No Precipitate	No Precipitate
200 ppm	No Precipitate	No Precipitate	No Precipitate	No Precipitate
150 ppm	Very slight Precipitate	No Precipitate	No Precipitate	No Precipitate
100 ppm	Precipitate	Slight Precipitate	Very slight Precipitate	No Precipitate
50 ppm	Precipitate	Slight Precipitate	Very slight Precipitate	No Precipitate
20 ppm	Precipitate	Slight Precipitate	Very slight Precipitate	No Precipitate
0 (control)	Precipitate	Precipitate	Slight Precipitate	No Precipitate

Table 7.7: Minimum inhibitor concentration chart (MIC) for CNI 6 inhibitor, using CaN extract.

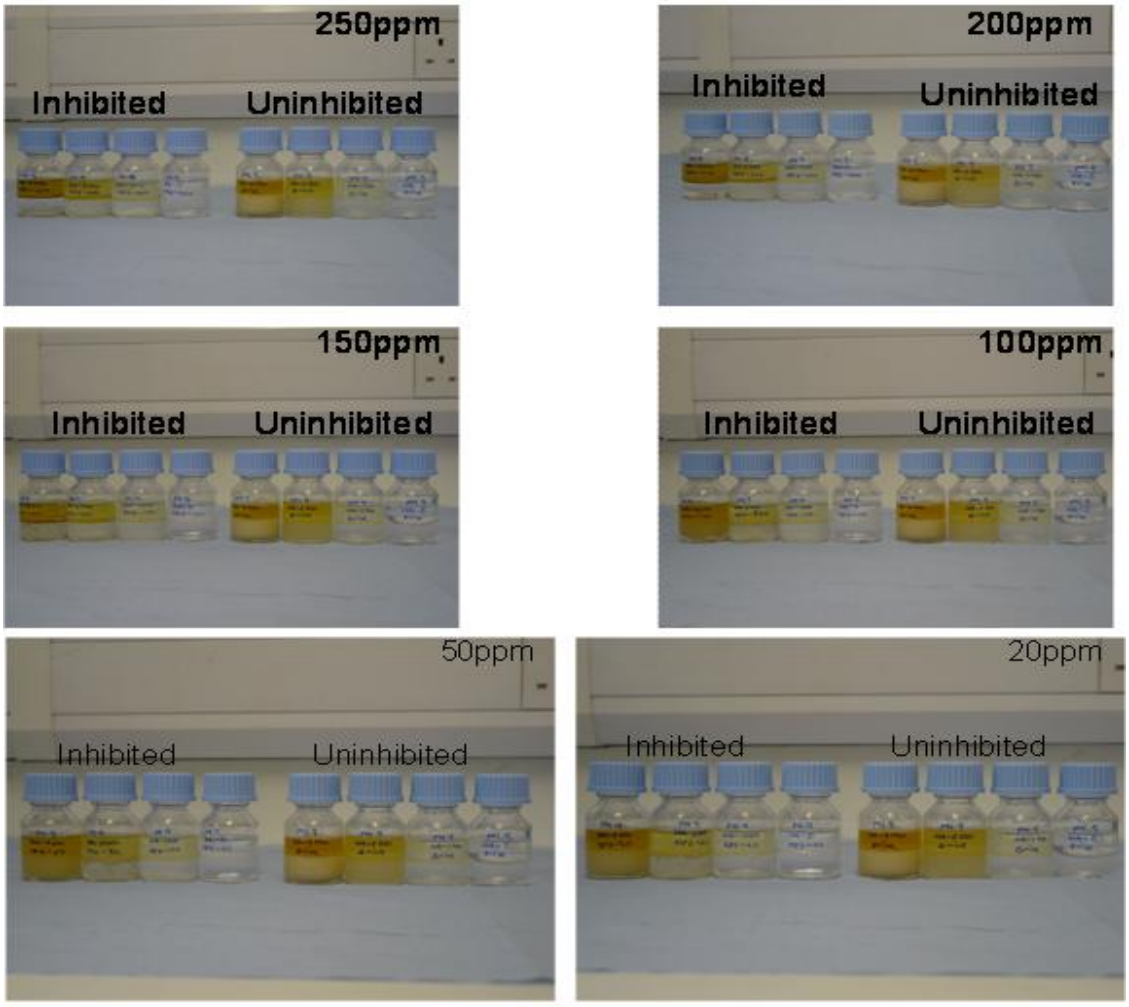

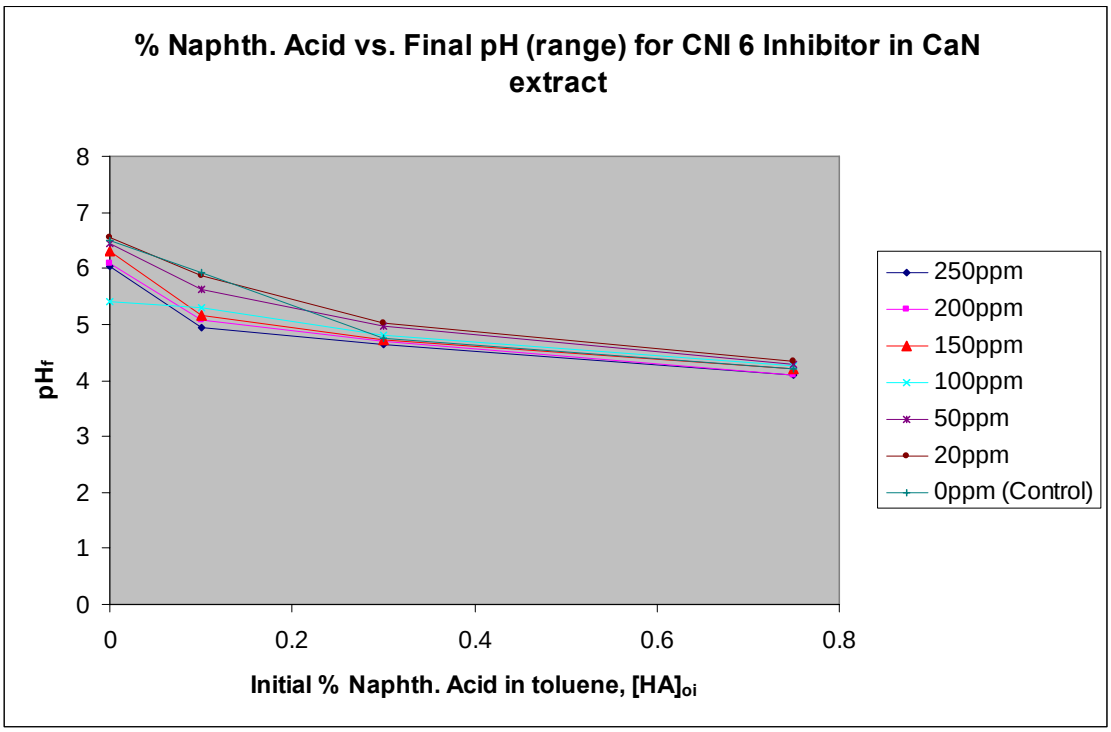

Figure 7.5: Static bottle test experiment (above) and the graphical plot of the final brine pH versus initial % naphthenic acid concentration, $[HA]_{oi}$ using CNI 6 inhibitor.

CNI 7 and CNI 8 Inhibitors

The minimum inhibition concentration charts for CNI 7 and CNI 8 are presented in Tables 7.8 and 7.9, respectively. It was found that the static bottle test efficiency studies using CNI 7 inhibitor did not give very good results. At both lower and higher concentration, the inhibitor (CNI 7) does not prevent calcium naphthenate formation, as can be seen from the chart in Table 7.8. At both 7500 ppm and 3000 ppm concentration of naphthenic acid in toluene (model oil phase) and higher concentrations of the inhibitors, these formulations precipitated. Furthermore, at lower concentration of the inhibitor (say between 10 ppm to 5 ppm), formation of a slight precipitate was observed in these experiments. However, inhibition efficiency experiments using CNI 8 showed a slight MIC window within which the inhibitor can prevent calcium naphthenate formation. The MIC window observed from these studies lies in the region of 50 ppm for oil with naphthenic acid concentration of 7500 ppm whereas an MIC of 20 ppm was observed from oil samples with 1000 ppm naphthenic acid concentration. The plot of the final brine pH versus the initial % naphthenic acid

concentration at various CNI 8 inhibitor concentrations and the photographs of the static bottle tests experiment are presented in Figure 7.6. The plot shows a decrease in the final brine pH generally, with considerable decrease at a higher inhibitor concentration.

Inhibitor\ HA	**7500 ppm**	**1000 ppm**	**0 ppm**
250 ppm	**Precipitate**	**Precipitate**	**Precipitate**
200 ppm	**Precipitate**	**Precipitate**	**Precipitate**
150 ppm	**Precipitate**	**Precipitate**	**Precipitate**
100 ppm	**Precipitate**	**Precipitate**	**Precipitate**
50 ppm	**Precipitate**	**Precipitate**	**Slight Precipitate**
20 ppm	**Precipitate**	**Precipitate**	**Slight Precipitate**
10 ppm	**Very slight Precipitate**	**Very slight Precipitate**	**No Precipitate**
5 ppm	**Slight Precipitate**	**Very slight Precipitate**	**No Precipitate**
0 (control)	**Precipitate**	**Very slight Precipitate**	**No Precipitate**

Table 7.8: Minimum inhibitor concentration chart (MIC) for CNI 7 inhibitor, using CaN extract.

Inhibitor\ HA	**7500ppm**	**1000ppm**	**0ppm**
100ppm	**Slight Precipitate**	**Very slight Precipitate**	**Very slight Precipitate**
50ppm	**No Precipitate**	**Very slight Precipitate**	**No Precipitate**
20ppm	**Very slight Precipitate**	**No Precipitate**	**No Precipitate**
10ppm	**Slight Precipitate**	**Very slight Precipitate**	**No Precipitate**
5ppm	**Precipitate**	**Very slight Precipitate**	**No Precipitate**
0 (control)	**Precipitate**	**Very slight Precipitate**	**No Precipitate**

Table 7.9: Minimum inhibitor concentration chart (MIC) for CNI 8 inhibitor, using CaN extract.

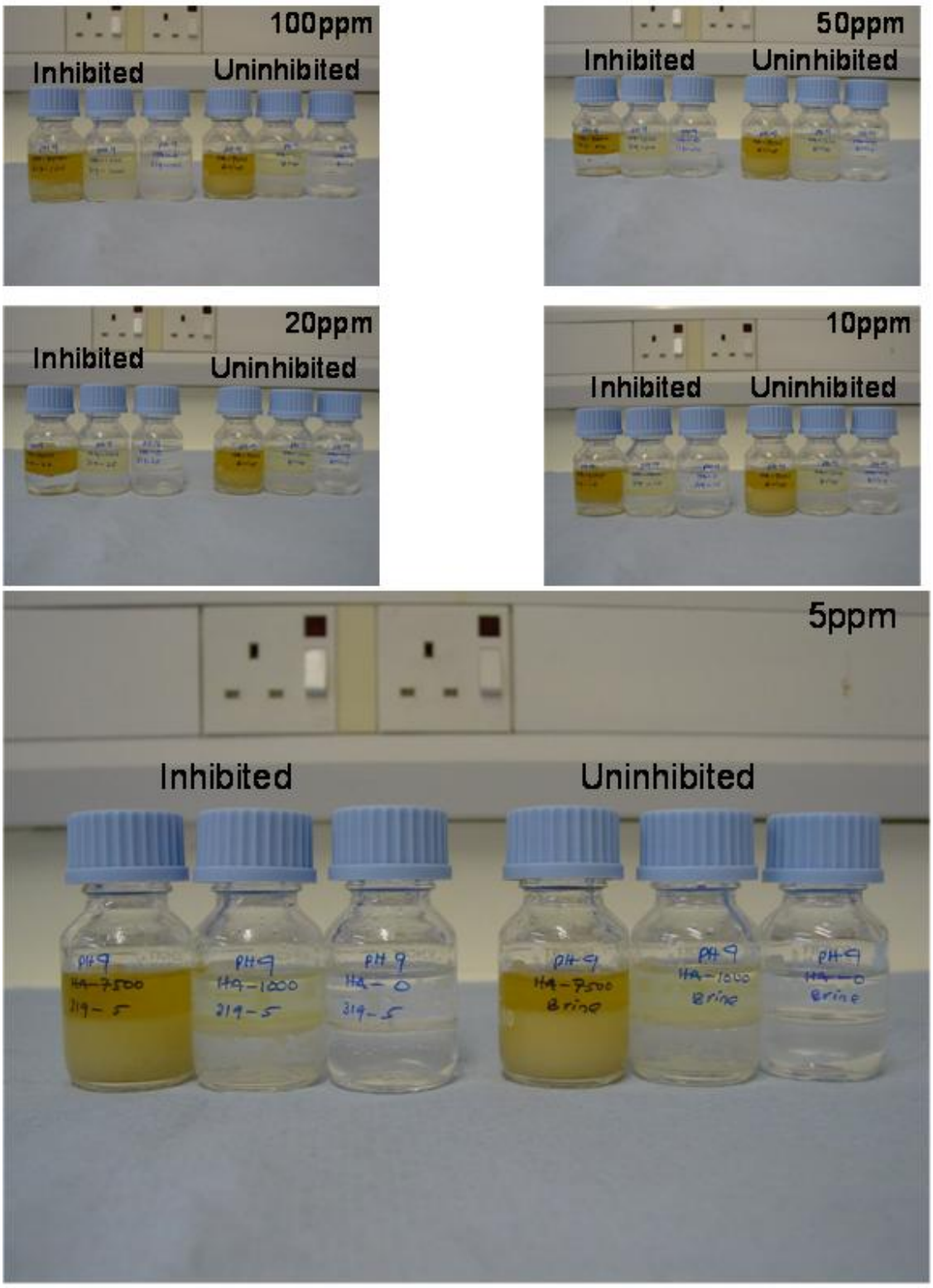
100ppm
Inhibited
Uninhibited
50ppm
Inhibited
Uninhibited
20ppm
Inhibited
Uninhibited
10ppm
Inhibited
Uninhibited
5ppm
Inhibited
Uninhibited

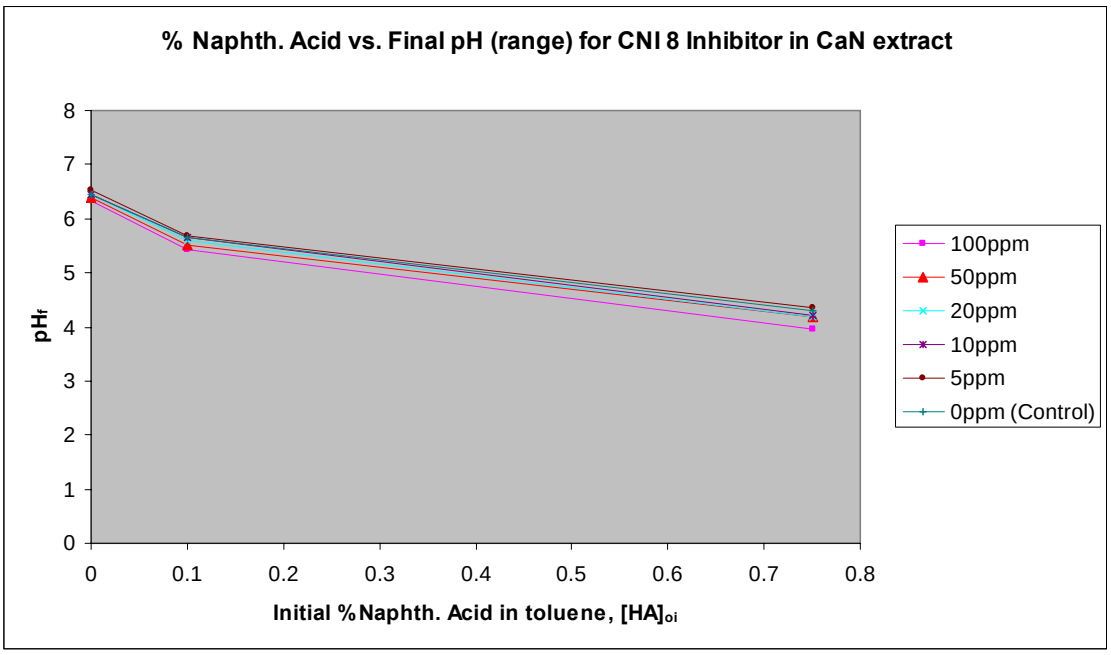

Figure 7.6: Static bottle test experiment (above) and the graphical plot of the final brine pH versus initial % naphthenic acid concentration, $[HA]_{oi}$ using CNI 8 inhibitor.

Inhibition Efficiency for Sodium Carboxylate/Emulsion Extracts

These naphthenate inhibitors were used for the study of sodium carboxylate/emulsion inhibition, although they were not meant for this purpose; their manufacturers claimed that these were specifically developed for calcium naphthenate inhibition. However, it was decided to test these same inhibitors on sodium carboxylate/emulsion and also emulsion forming crude oil, to see whether the inhibitors can be useful in addressing the soft emulsion type problem. The eight inhibitors used for this study were as follows: CNI 1, CNI 2, CNI 3, CNI 4, CNI 5, CNI 6, CNI 7 and CNI 8. These inhibitors were tested to establish the minimum inhibitor concentration (MIC) required to prevent the formation of sodium carboxylate/emulsion in an oil-water system in the laboratory, using the static bottle test. The oil phase used contained naphthenic acid extract dissolved in toluene at various concentrations of 1000 ppm, 3000 ppm, 7500 ppm and the water phase (synthetic brine) was pH adjusted to pH 9. The CNI 2 and CNI 3 inhibitors were not used in this study, due to the compatibility problem observed during the calcium naphthenate inhibition efficiency experiments.

Inhibitors CNI 1 and CNI 4

The static inhibition efficiency study using these inhibitors on sodium naphthenate extract at various concentrations of naphthenic acid extract and synthetic brine, which is pH adjusted to pH 9, revealed that the inhibitor can minimise or prevents formation of sodium carboxylate/emulsion, as observed. The MIC chart for the inhibitors CNI 1 and CNI 4 are presented in Tables 7.10 and 7.11, respectively.

For CNI 1, the minimum inhibition concentration for the oil-brine composition with higher concentration of naphthenic acid in the oil phase (say 7500 ppm) was around 200 ppm, whilst for moderate and lower naphthenic acid concentration of 3000 ppm and 1000 ppm it was 50ppm, in both cases. It is also important to note that there was emulsion formation in the control experiment, where no inhibitor was added. The static bottle inhibition efficiency experiment, together with the plot of the final brine pH versus the initial naphthenic acid concentration in the oil phase for the various inhibitor concentration is presented in Figure 7.7. It is clearly evident that the final brine pH decreases with the increasing naphthenic acid concentrations.

For the CNI 4 inhibitor, the static bottle inhibition efficiency experiment pictures, together with a plot of the final brine pH versus initial naphthenic acid concentration, $[HA]_{oi}$ is presented in Figure 7.8. Inhibition efficiency tests on sodium naphthenate extract using the CNI 4 inhibitor show a slightly different minimum inhibitor concentration value, with the MIC of 200 ppm for higher naphthenic acid concentration in the oil phase (7500 ppm) and MIC of 150 ppm and 50 ppm for naphthenic acid concentration of 3000 ppm and 1000 ppm in the oil phase, respectively. The final brine pH measured gave a similar trend to the CNI 1 inhibitor, showing a decrease in the final brine pH as the concentration of naphthenic acid in the sodium naphthenate extracts (oil phase) increased, as shown in Figure 7.8. It is worth noting that sodium naphthenate inhibition was clearly observed when the CNI 4 inhibitor was applied.

Inhibitor\ HA	7500 ppm	3000 ppm	1000 ppm	0 ppm
250 ppm	No Emulsion	No Emulsion	No Emulsion	No Emulsion
200 ppm	No Emulsion	No Emulsion	No Emulsion	No Emulsion
150 ppm	Very Slight (interface)	No Emulsion	No Emulsion	No Emulsion
100 ppm	Very Slight (interface)	No Emulsion	No Emulsion	No Emulsion
50 ppm	Slight Emulsion	No Emulsion	No Emulsion	No Emulsion
20 ppm	Emulsion	Slight Emulsion	Slight Emulsion	No Emulsion
0 (control)	Emulsion	Emulsion	Slight Emulsion	No Emulsion

Table 7.10: Minimum inhibitor concentration chart (MIC) for CNI 1 inhibitor using sodium carboxylate/emulsion extracts.

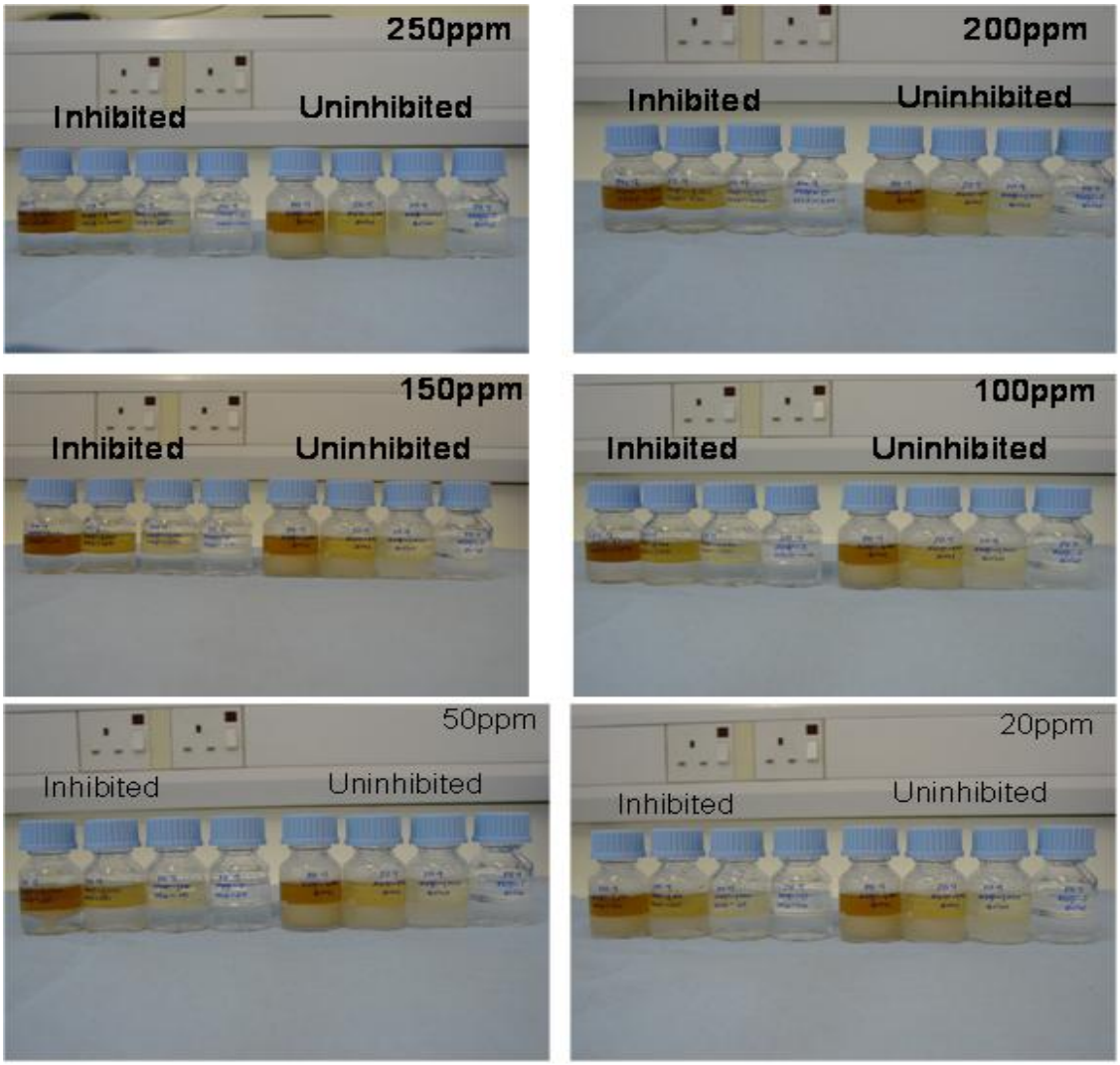

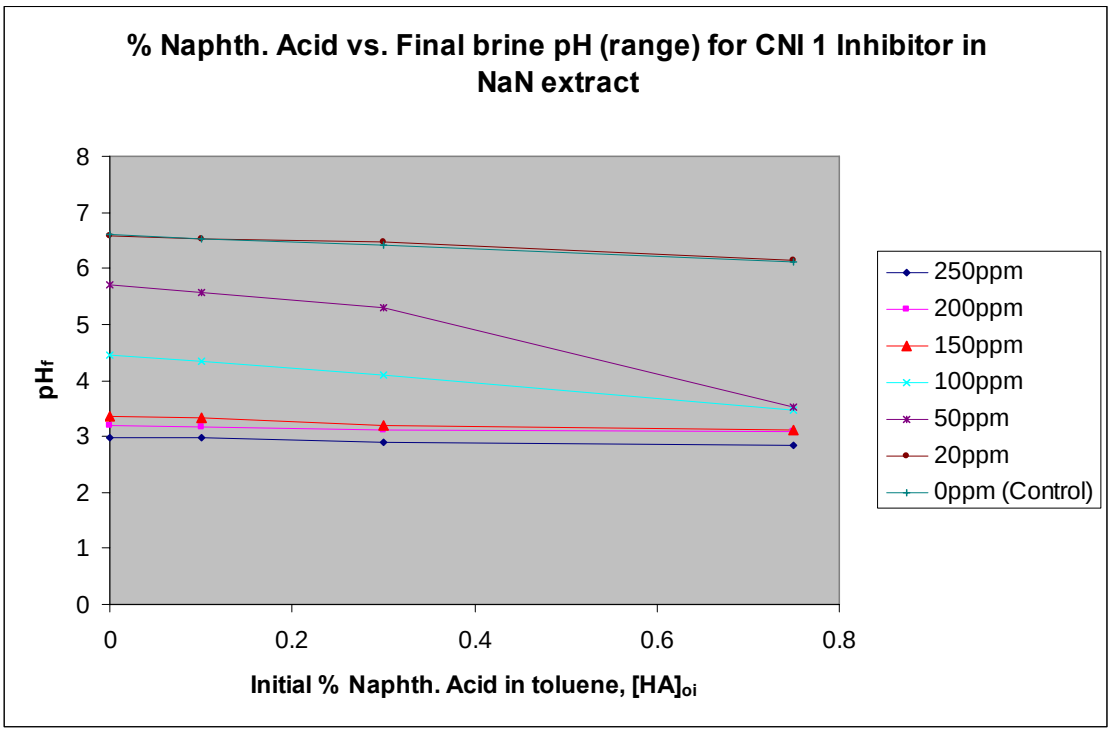

Figure 7.7: Static bottle test experiment (above) and the graphical plot of the final brine pH versus initial % naphthenic acid concentration, $[HA]_{oi}$ using CNI 1 inhibitor in NaN extract.

Inhibitor\ HA	7500 ppm	3000 ppm	1000 ppm	0 ppm
250 ppm	No Emulsion	No Emulsion	No Emulsion	No Emulsion
200 ppm	No Emulsion	No Emulsion	No Emulsion	No Emulsion
150 ppm	Very Slight (interface)	No Emulsion	No Emulsion	No Emulsion
100 ppm	Very Slight (interface)	Very Slight (interface)	No Emulsion	No Emulsion
50 ppm	Very Slight (interface)	Very Slight (interface)	No Emulsion	No Emulsion
20 ppm	Slight Emulsion	Very Slight (interface)	Very Slight (interface)	No Emulsion
0 (control)	Emulsion	Emulsion	Slight Emulsion	No Emulsion

Table 7.11: Minimum inhibitor concentration chart (MIC) for CNI 4 inhibitor using sodium carboxylate/emulsion extracts.

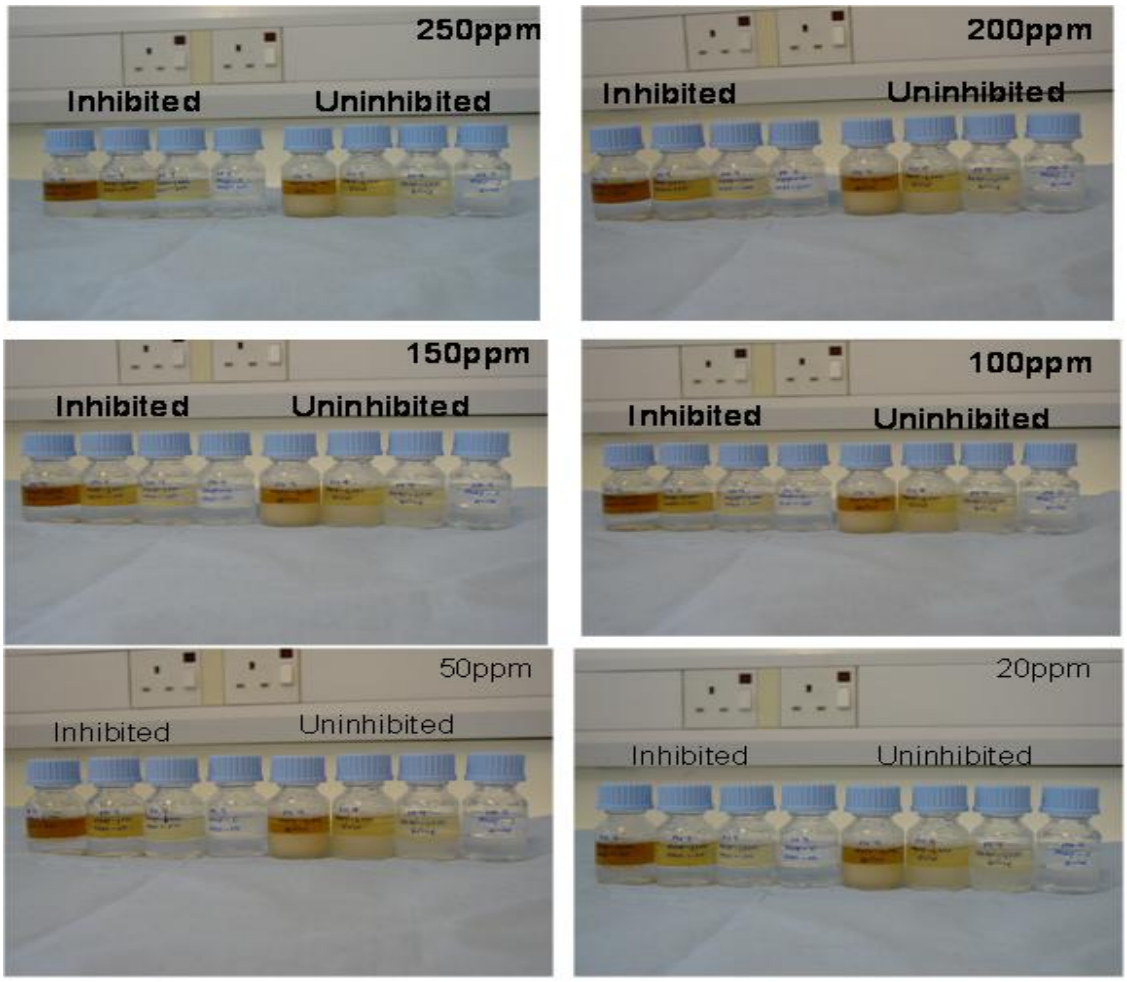

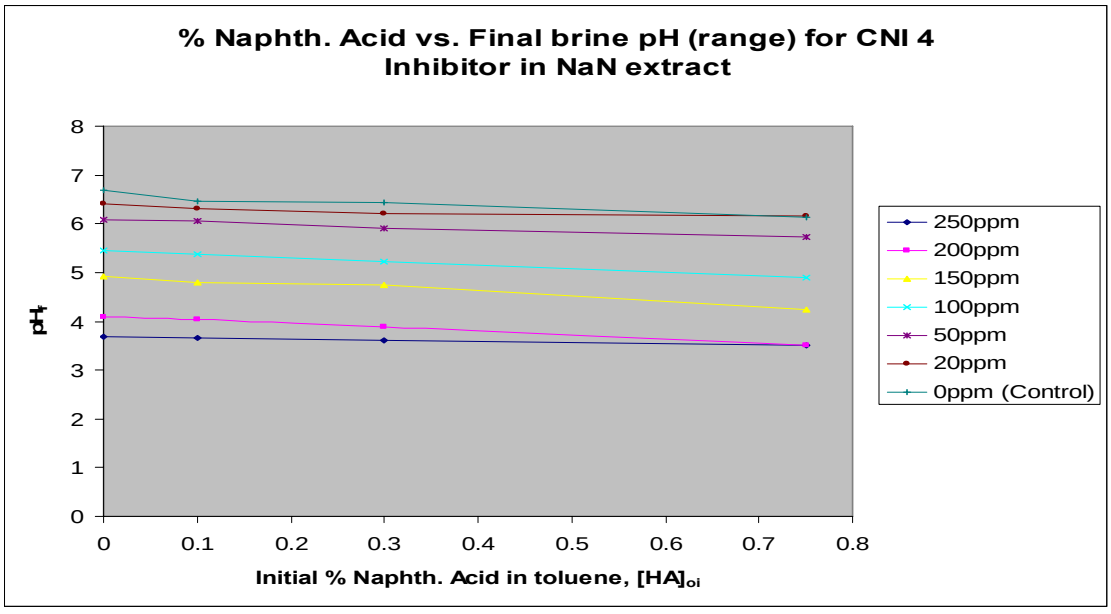

Figure 7.8: Static bottle test experiment (above) and the graphical plot of the final brine pH versus initial % naphthenic acid concentration, $[HA]_{oi}$ using CNI 4 inhibitor in NaN extract.

Inhibitors CNI 5 and CNI 6

The results from the static inhibition efficiency studies using CNI 5 inhibitor showed that, at higher naphthenic acid concentration in toluene (oil phase), i.e. 7500 ppm, the MIC was 200 ppm and for the naphthenic acid concentration of 1000 ppm in the oil phase, the MIC observed was 20 ppm. Note that two different naphthenic acid concentrations (7500 ppm and 1000 ppm) in toluene (model oil) were used when testing the CNI 5 inhibitor. The CNI 6 naphthenate inhibitor shows a slightly different result with the MIC of 150ppm at higher concentration of naphthenic acid in the oil phase (~7500 ppm), whilst medium and lower concentrations of naphthenic acid (3000 ppm and 1000 ppm) in the oil phase gave a MIC of 100 ppm. The summary charts for the MIC results of CNI 5 and CNI 6 are presented in Tables 7.12 and 7.13, respectively. Generally, the final brine pH measured after the experiment shows decreases with the increasing concentration of naphthenic acid in the oil phase, which is associated with the naphthenic acid going into the brine phase from the water phase. Application of the inhibitor at higher concentrations, coupled with the higher naphthenic acid concentration in the oil phase showed much more drift in the final brine pH, whilst application of the inhibitors at a medium concentration (sufficient to prevent sodium carboxylate/emulsion formation) gave less of a pH decrease, even when compared with the control experiment, where there is no addition of the inhibitor. The plot of the final brine pH versus initial naphthenic acid concentration, $[HA]_{oi}$ for the CNI 5 inhibitor is presented in Figure 7.9, and the static bottle inhibition efficiency experiment picture, together with plot of the final brine pH versus initial naphthenic acid concentration, $[HA]_{oi}$, for CNI 6 is presented in Figure 7.10.

Inhibitor\ HA	7500 ppm	1000 ppm	0 ppm
250 ppm	No Emulsion	No Emulsion	No Emulsion
200 ppm	No Emulsion	No Emulsion	No Emulsion
150 ppm	Very slight Emulsion	No Emulsion	No Emulsion
100 ppm	Very slight Emulsion	No Emulsion	No Emulsion
50 ppm	Slight Emulsion	No Emulsion	No Emulsion
20 ppm	Emulsion	No Emulsion	No Emulsion
0 (control)	Emulsion	Slight Emulsion	No Emulsion

Table 7.12: Minimum inhibitor concentration chart (MIC) for CNI 5 inhibitor using sodium carboxylate/emulsion extracts.

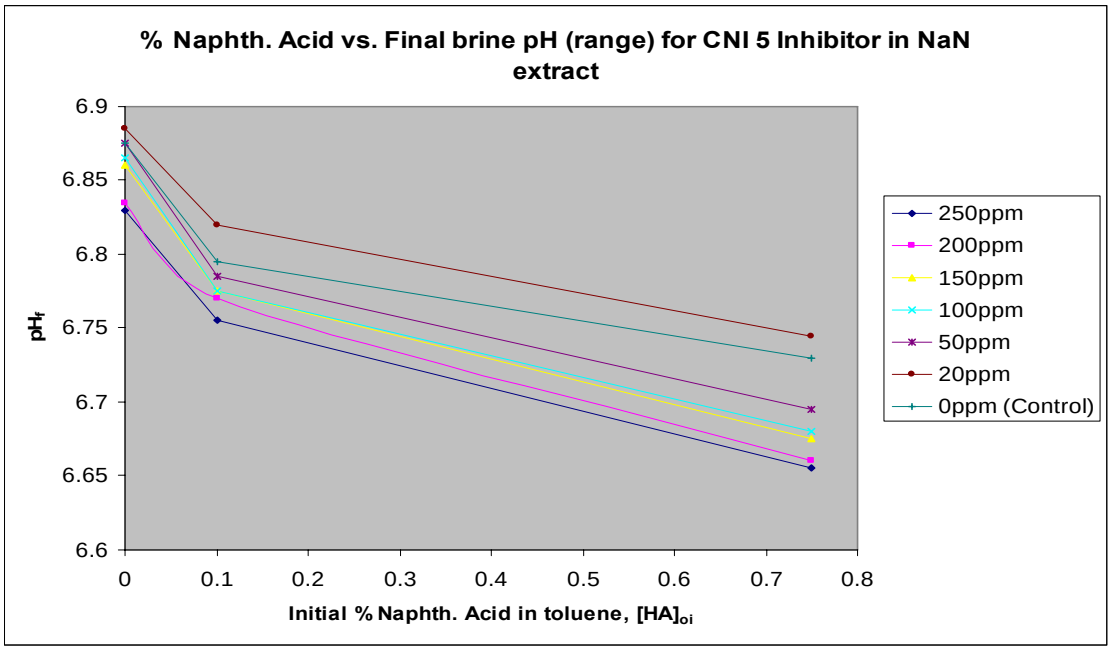

Figure 7.9: Plot of the final brine pH versus initial % naphthenic acid concentration, $[HA]_{oi}$ using CNI 5 inhibitor in NaN extract.

Inhibitor\ HA	7500 ppm	3000 ppm	1000 ppm	0 ppm
250 ppm	No Emulsion	No Emulsion	No Emulsion	No Emulsion
200 ppm	No Emulsion	No Emulsion	No Emulsion	No Emulsion
150 ppm	No Emulsion	No Emulsion	No Emulsion	No Emulsion
100 ppm	Very slight Emulsion	No Emulsion	No Emulsion	No Emulsion
50 ppm	Very slight Emulsion	Very slight Emulsion	Very slight Emulsion	No Emulsion
20 ppm	Emulsion	Slight Emulsion	Very slight Emulsion	No Emulsion
0 (control)	Emulsion	Emulsion	Slight Emulsion	No Emulsion

Table 7.13: Minimum inhibitor concentration chart (MIC) for CNI 6 inhibitor using sodium carboxylate/emulsion extracts.

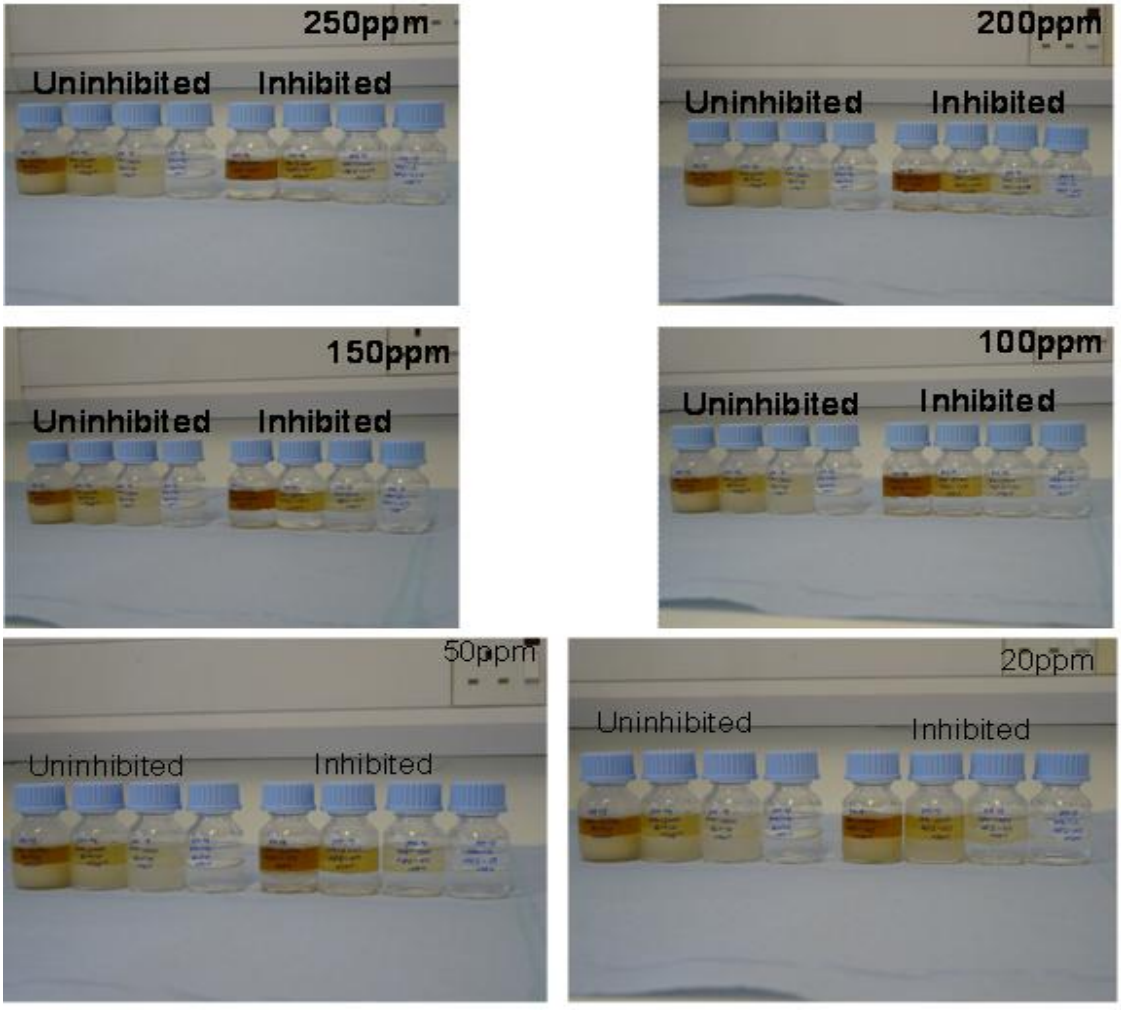

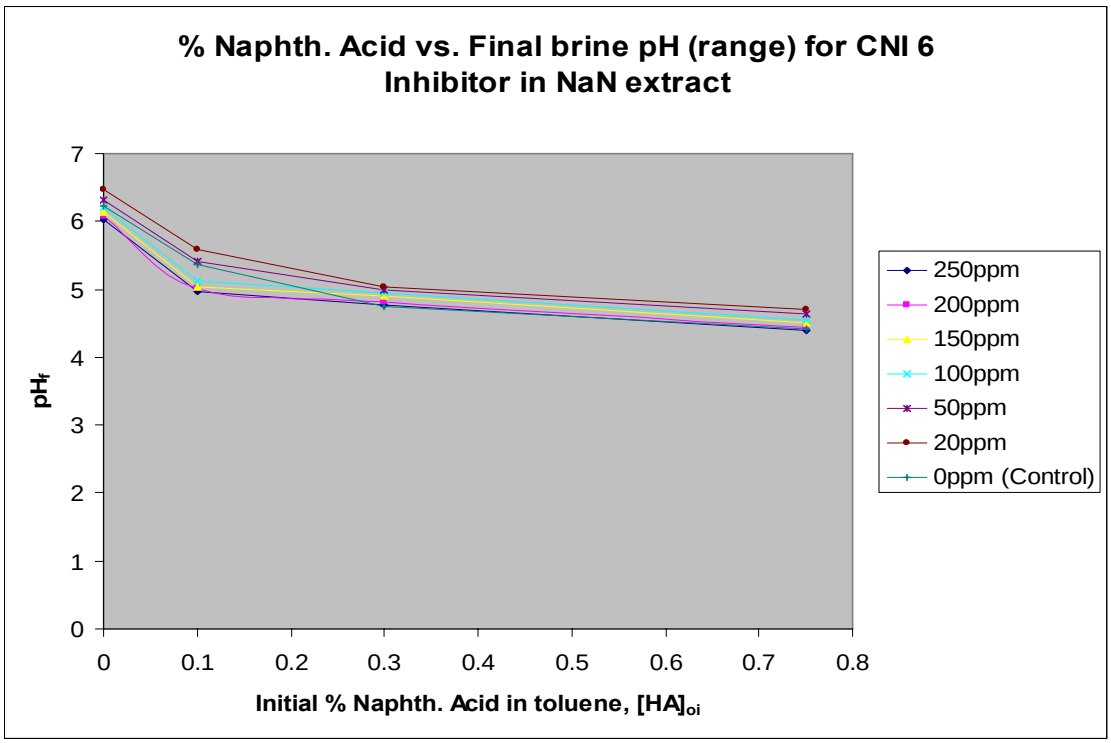

Figure 7.10: Static bottle test experiment (above) and the graphical plot of the final brine pH versus initial % naphthenic acid concentration, $[HA]_{oi}$ using CNI 6 inhibitor in NaN extract.

Inhibitors CNI 7 and CNI 8

The sodium carboxylate/emulsion inhibition efficiency studies using CNI 7 and CNI 8 showed a very narrow concentration range where a MIC value was observed. The observed MIC values in both cases do not give good inhibition, as can be seen from the Tables 7.14 and 7.15 for CNI 7 and CNI 8, respectively. Application of these inhibitors at higher or lower naphthenic acid concentration in the oil phase resulted in emulsion formation. The observed effect of the inhibitor/inhibition effect was worst in the case of CNI 7 inhibitor which formed an emulsion, even at 0 ppm naphthenic acid concentration. This type of incompatibility was also observed in the case of the CNI 2 and CNI 3 naphthenate inhibitors. Static bottle inhibition experiments using the CNI 7 inhibitor showed a slight inhibition at 10 ppm inhibitor for 7500 ppm naphthenic acid concentration in the oil phase, whilst, at a lower naphthenic acid concentration of 1000 ppm, a MIC of 5 ppm was observed. However, the CNI 8 inhibitor showed only a slight inhibition (MIC ranging

between 20 ppm – 10 ppm) at a lower naphthenic acid concentration in the oil phase, i.e. 1000 ppm. The final brine pH measured showed a general decrease as both the naphthenic acid concentration in the oil phase and the inhibitor concentration increased. A plot of the final brine pH versus the initial concentration of naphthenic acid in toluene (oil phase) together with the static bottle tests experiment photographs for CNI 8 inhibitor is shown in Figure 7.11 below.

Inhibitor\ HA	7500 ppm	1000 ppm	0 ppm
250 ppm	Emulsion	Emulsion	Emulsion
200 ppm	Emulsion	Emulsion	Emulsion
150 ppm	Emulsion	Emulsion	Emulsion
100 ppm	Emulsion	Emulsion	Emulsion
50 ppm	Emulsion	Emulsion	Emulsion
20 ppm	Slight Emulsion	Slight Emulsion	Slight Emulsion
10 ppm	No Emulsion	Very slight Emulsion	Very slight Emulsion
5 ppm	Very slight Emulsion	No Emulsion	No Emulsion
0 (control)	Emulsion	Slight Emulsion	No Emulsion

Table 7.14: Minimum inhibitor concentration chart (MIC) for CNI 7 inhibitor using sodium carboxylate/emulsion extracts.

Inhibitor\ HA	7500 ppm	1000 ppm	0 ppm
100 ppm	Emulsion	Slight Emulsion	Very slight Emulsion
50 ppm	Very slight Emulsion	Very slight Emulsion	No Emulsion
20 ppm	Very slight Emulsion	No Emulsion	No Emulsion
10 ppm	Slight Emulsion	No Emulsion	No Emulsion
5 ppm	Emulsion	Very slight Emulsion	No Emulsion
0 (control)	Emulsion	Slight Emulsion	No Emulsion

Table 7.15: Minimum inhibitor concentration chart (MIC) for CNI 8 inhibitor using sodium carboxylate/emulsion extracts.

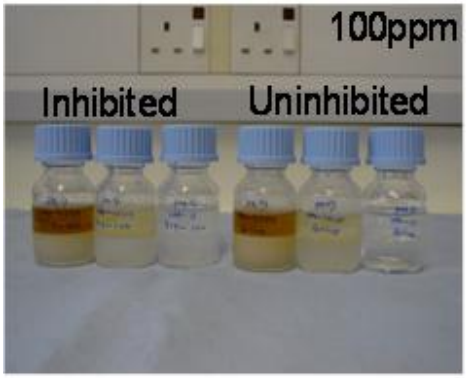
100ppm
Inhibited
Uninhibited

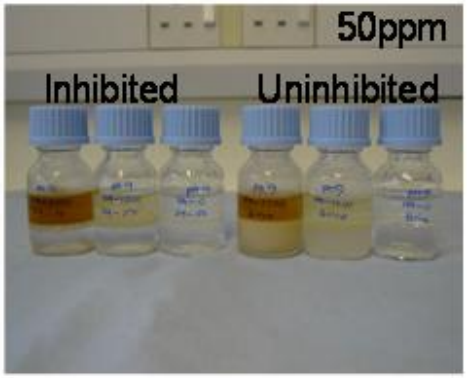
50ppm
Inhibited
Uninhibited

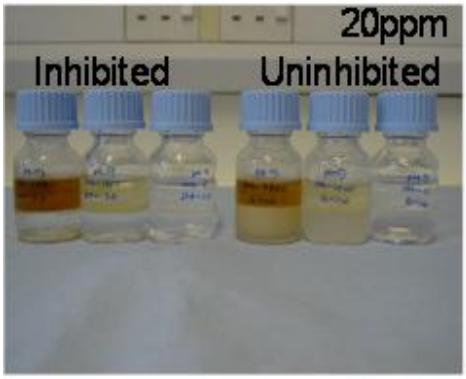
20ppm
Inhibited
Uninhibited

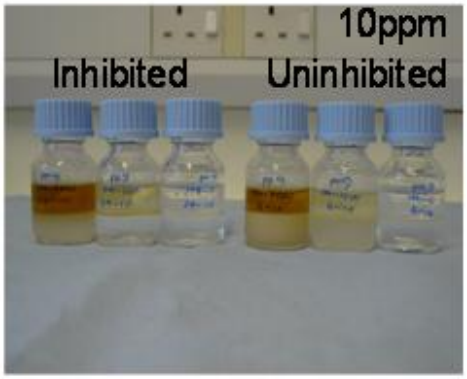
10ppm
Inhibited
Uninhibited

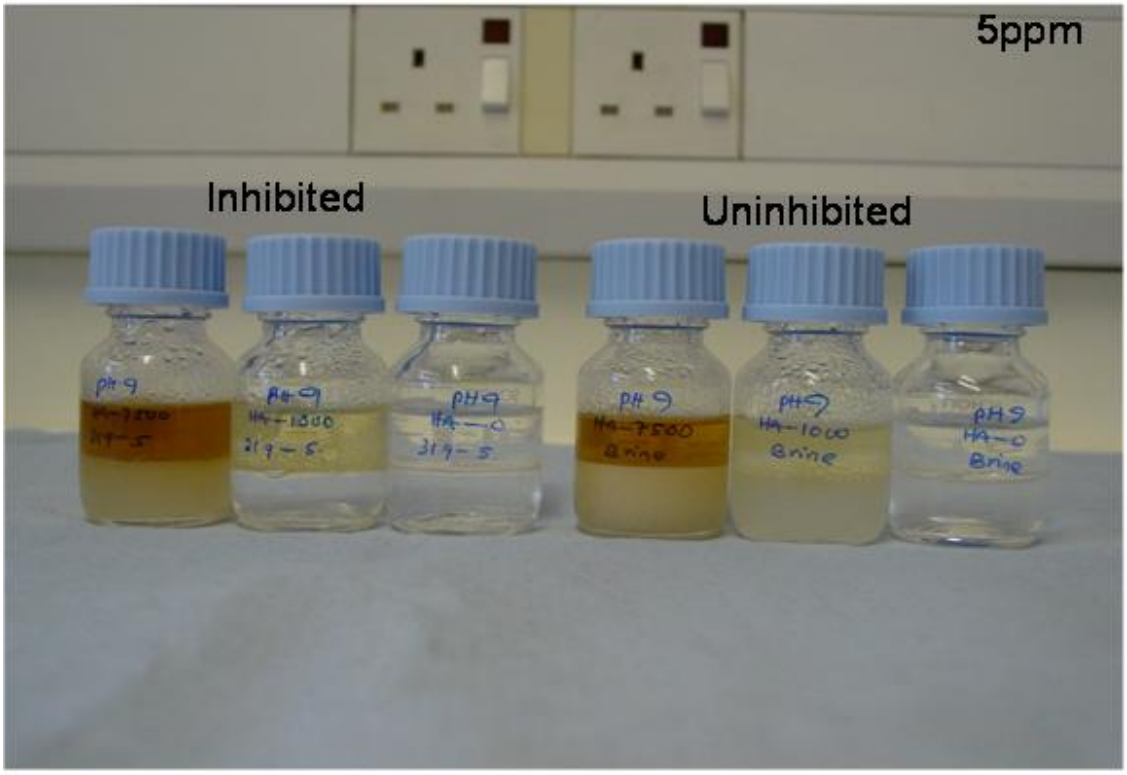
5ppm
Inhibited
Uninhibited

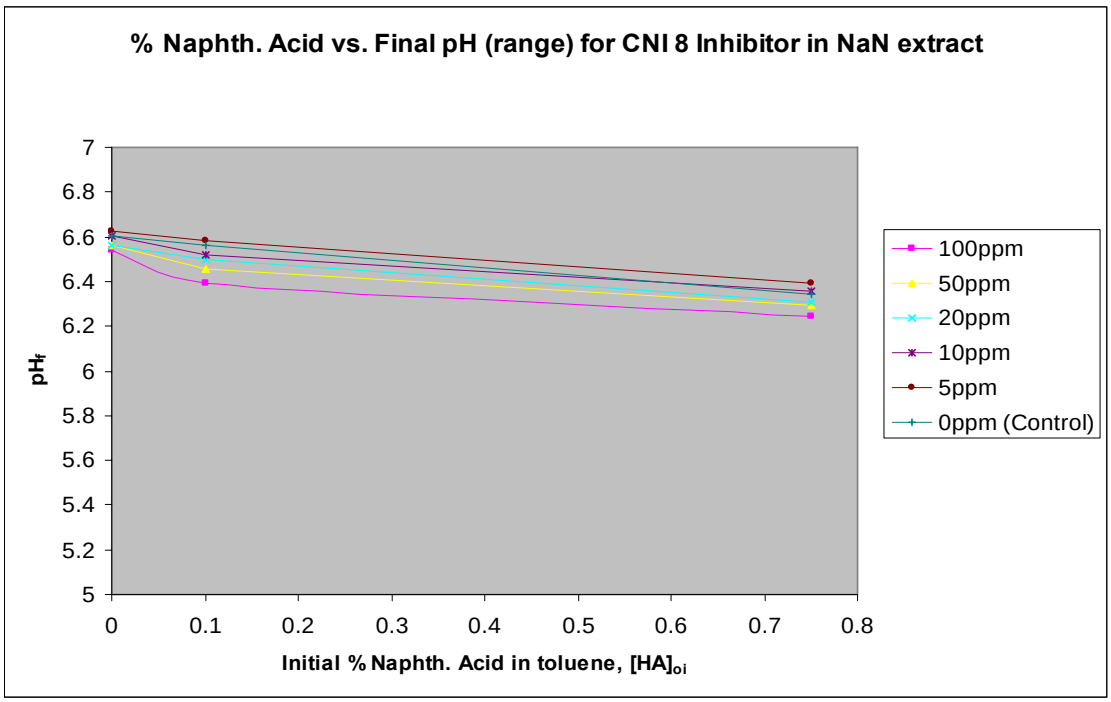

Figure 7.11: Static bottle test experiment (above) and the graphical plot of the final brine pH versus initial % naphthenic acid concentration, $[HA]_{oi}$ using CNI 8 inhibitor in NaN extract.

Inhibition Efficiency of Crude Oil Spiked with Naphthenic Acid Extract

A static inhibition efficiency study was performed using a crude oil sample spiked with naphthenic acid extract (extracted from a field calcium naphthenate deposit) to test the three chosen best performing inhibitors i.e. inhibitors CNI 1, CNI 4 and CNI 5**.** This type of experiment was carried out deliberately, to see if the naphthenate inhibitors can still perform in a real crude oil containing naphthenates, rather than the model oil (field naphthenate extract in toluene). The crude oil sample used in this study was an emulsion forming crude but has been reported by the supplier as being an "uncontaminated" sample (i.e. it had not been treated with a naphthenate inhibitor or any other chemical treatments). The crude oil sample was spiked with various concentrations (7500 ppm, 3000 ppm and 1000 ppm) of CaN forming naphthenic acid extract. In addition, one control set was carried out with the non-spiked crude oil to see whether it would form an emulsion upon contact with the synthetic pH adjusted brine (pH 9). The results from this study were quite

interesting, in the sense that the inhibitors tested were able to inhibit formation of both emulsion and calcium naphthenate formation, for this case.

Inhibitors CNI 1 and CNI 4

Minimum inhibitor concentrations (MIC) were established for CNI 1 and CNI 4 inhibitors tested and are presented in Tables 7.16 and 7.17, respectively. The minimum inhibitor concentrations (MIC) for both inhibitors are 250 ppm for the crude oil sample spiked with 7500 ppm concentration of naphthenic acid, 150 ppm for the crude oil sample spiked with 3000 ppm and 20 ppm for the crude oil sample spiked with 1000 ppm concentration of naphthenic acid. One interesting observation was the formation of emulsion in the case where the crude oil was *not* spiked with the naphthenic acid extract. Hence, these inhibitors can also be used for the prevention of either emulsions or solid deposits. The final brine pH measured indicated a decrease with the increasing concentration of naphthenic acid extract in the crude oil and it is important to note that at lower concentration of naphthenic acid in crude oil (say 1000 ppm), the change in the final brine pH when inhibitor is added was lower as compared with that without addition. This may be due to the fact that the inhibitor acts at the interface to prevent partitioning of the dissociated naphthenic acid to the water phase from the oil phase, hence minimising or preventing naphthenate formation in the system. The final brine pH measured for the crude oil spiked with 1000 ppm naphthenic acid extract when using 20 ppm of inhibitor CNI 1 was pH ~ 5.80. This can be compared with the final brine pH at the same naphthenic acid extract concentration in crude oil with no inhibitor (0 ppm), which was pH ~ 4.3; this is a good indication of how the naphthenate inhibitor at this naphthenic acid concentration plays a strong role in minimising the substantial decrease in the final brine pH. A similar trend was noted when naphthenate inhibitor CNI 4 was used, which can be seen from the plots of the final brine pH versus initial % naphthenic acid concentration in crude oil, $[HA]_{oi}$. The static inhibition efficiency experiment photographs and the plot of the final brine pH versus initial % naphthenic acid concentration in the crude oil for inhibitors CNI1 and CNI 4 are presented in Figures 7.12 and 7.13, respectively.

Inhibitor\ HA	7500 ppm	3000 ppm	1000 ppm	0 ppm
250 ppm	No Precipitate	No Precipitate	No Precipitate	No Precipitate
200 ppm	Very slight Precipitate	No Precipitate	No Precipitate	No Precipitate
150 ppm	Very slight Precipitate	No Precipitate	No Precipitate	No Precipitate
100 ppm	Very slight Precipitate	Very slight Precipitate	No Precipitate	No Precipitate
50 ppm	Slight Precipitate	Very slight Precipitate	No Precipitate	No Precipitate
20 ppm	Slight Precipitate	Very slight Precipitate	No Precipitate	No Precipitate
0 (control)	Precipitate	Precipitate	Slight Precipitate	Emulsion

Table 7.16: Minimum inhibitor concentration chart (MIC) for CNI 1 inhibitor, using crude oil spiked with naphthenic acid extract from calcium naphthenate deposit.

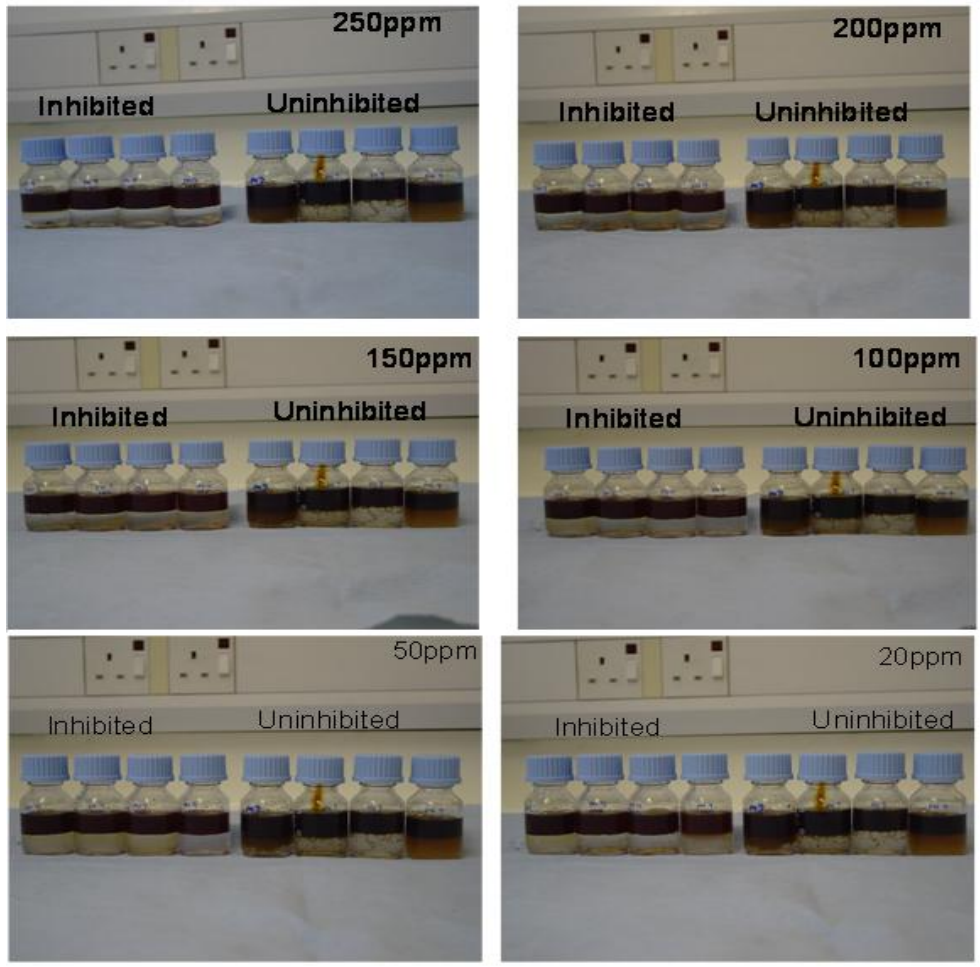

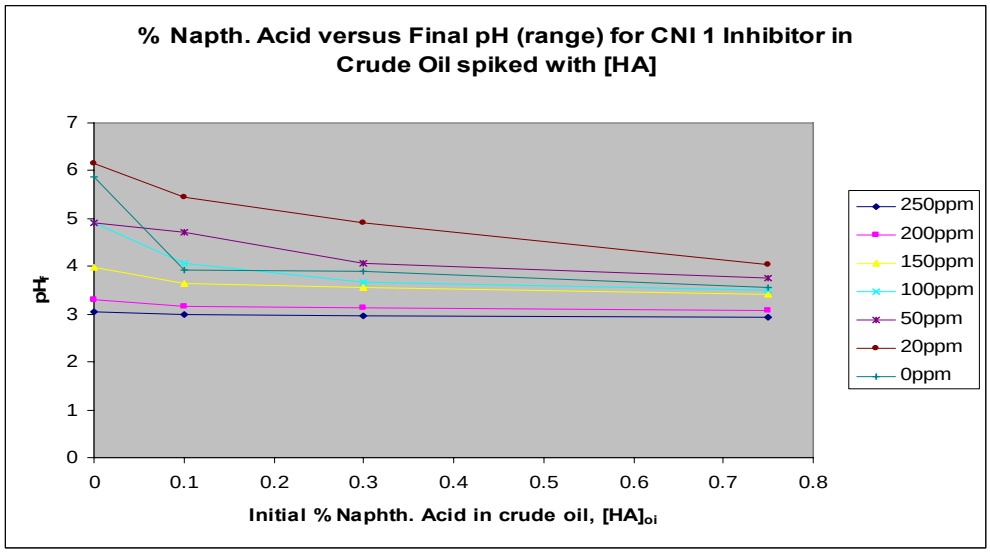

Figure 7.12: Static bottle test experiment (above) and the graphical plot of the final brine pH versus initial % naphthenic acid concentration, $[HA]_{oi}$ using CNI 1inhibitor for crude oil naphthenate inhibition.

Inhibitor\ HA	7500 ppm	3000 ppm	1000 ppm	0 ppm
250 ppm	No Precipitate	No Precipitate	No Precipitate	No Precipitate
200 ppm	Very slight Precipitate	No Precipitate	No Precipitate	No Precipitate
150 ppm	Very slight Precipitate	No Precipitate	No Precipitate	No Precipitate
100 ppm	Very slight Precipitate	Very slight Precipitate	No Precipitate	No Precipitate
50 ppm	Very slight Precipitate	Very slight Precipitate	No Precipitate	No Precipitate
20 ppm	Slight Emulsion	Very slight Precipitate	No Precipitate	No Precipitate
0 (control)	Precipitate	Precipitate	Slight Emulsion	Emulsion

Table 7.17: Minimum inhibitor concentration chart (MIC) for CNI 4 Inhibitor, using crude oil spiked with naphthenic acid extract from calcium naphthenate deposit.

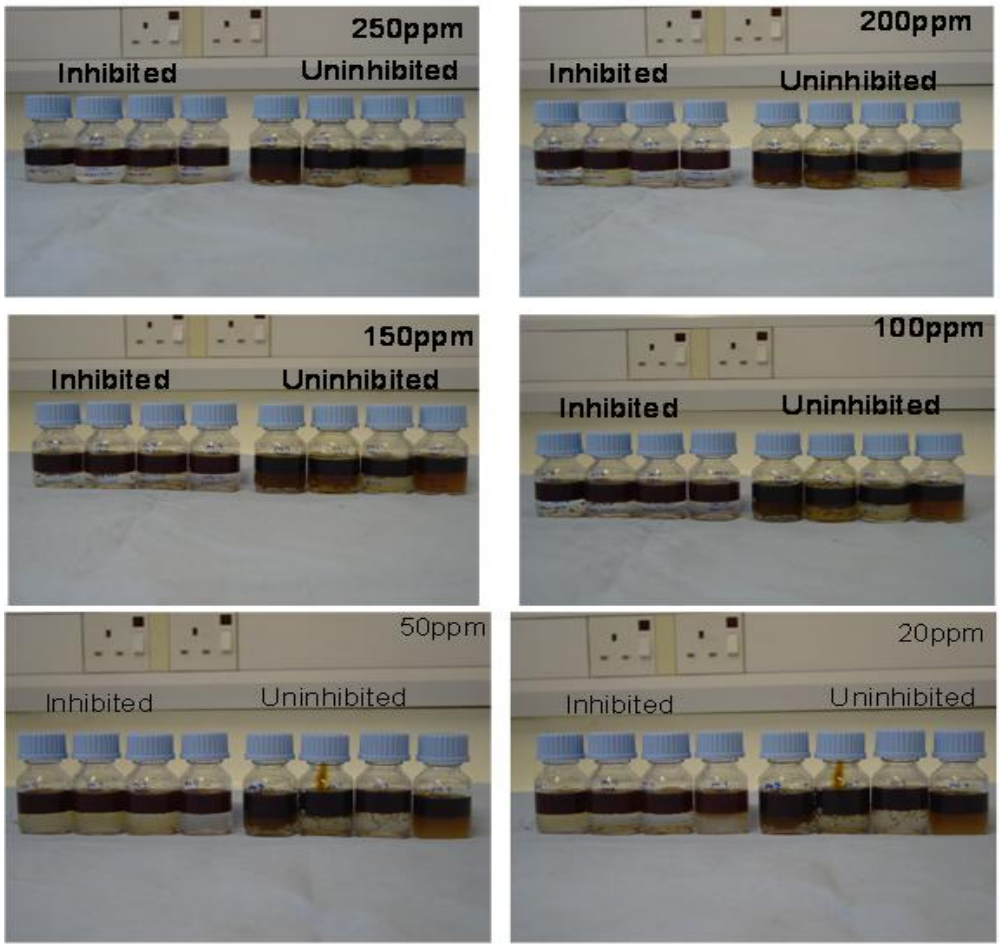

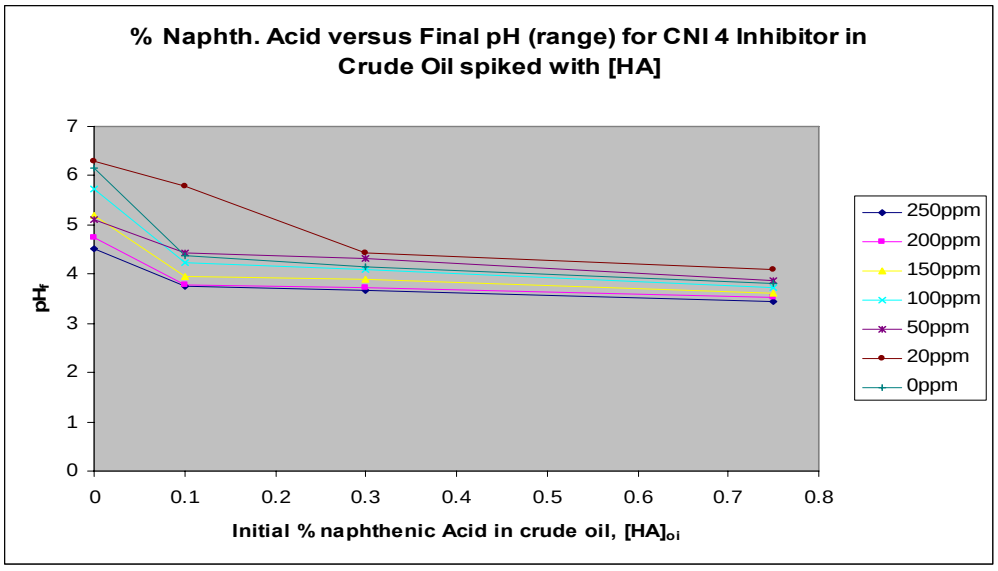

Figure 7.13: Static bottle test experiment (above) and the graphical plot of the final brine pH versus initial % naphthenic acid concentration, $[HA]_{oi}$ using CNI 4inhibitor for crude oil naphthenate inhibition.

Inhibitor CNI 5

The MIC chart for the CNI 5 inhibitor is presented in Table 7.18 below. This inhibitor (CNI 5) shows a very good inhibition effect at both higher and lower naphthenic acid concentrations in the crude oil sample. As mentioned earlier above, the emulsion forming crude was spiked with naphthenic acid extract from calcium naphthenate deposit and was subsequently used as the oil phase for the inhibition efficiency analysis. A minimum inhibitor concentration of 100 ppm was observed for crude oil sample spiked with 7500 ppm concentration of naphthenic acid, 50 ppm for crude oil sample spiked with 3000 ppm and 20 ppm for crude oil sample spiked with 1000 ppm concentration of naphthenic acid. Also, formation of an emulsion was observed even in the case when the crude oil was not spiked with the naphthenic acid extract. Measurement of the final brine pH showed a pH value decrease with the increase in the naphthenic acid concentration and higher inhibitor concentration. It is also interesting to note that the change in the final brine pH when an inhibitor was added was lower at inhibitor concentrations 20 ppm and 50 ppm for all three naphthenic acid concentrations, i.e. at 7500 ppm, 3000 ppm and 1000 ppm, as compared with the case were there was no addition of naphthenate inhibitor. Furthermore, even at 100 ppm inhibitor concentration, the final brine pH change was lower for medium and lower concentrations of naphthenic acid in the crude oil as compared to the one with no addition of naphthenic acid in the crude oil. This observation can be seen from the plot of the final brine pH versus initial % naphthenic acid concentration in crude oil, $[HA]_{oi}$ which is presented in Figure 7.14 below.

Inhibitor\ HA	7500 ppm	3000 ppm	1000 ppm	0 ppm
250 ppm	No Precipitate	No Precipitate	No Precipitate	No Precipitate
200 ppm	No Precipitate	No Precipitate	No Precipitate	No Precipitate
150 ppm	No Precipitate	No Precipitate	No Precipitate	No Precipitate
100 ppm	No Precipitate	No Precipitate	No Precipitate	No Precipitate
50 ppm	Slight Precipitate	No Precipitate	No Precipitate	No Precipitate
20 ppm	Slight Precipitate	Very slight Precipitate	No Precipitate	No Precipitate
0 (control)	Precipitate	Slight Precipitate	Very Slight Precipitate	Emulsion

Table 7.18: Minimum Inhibitor Concentration Chart (MIC) for CNI 5 Inhibitor using crude oil spiked with naphthenic acid extract from calcium naphthenate deposit.

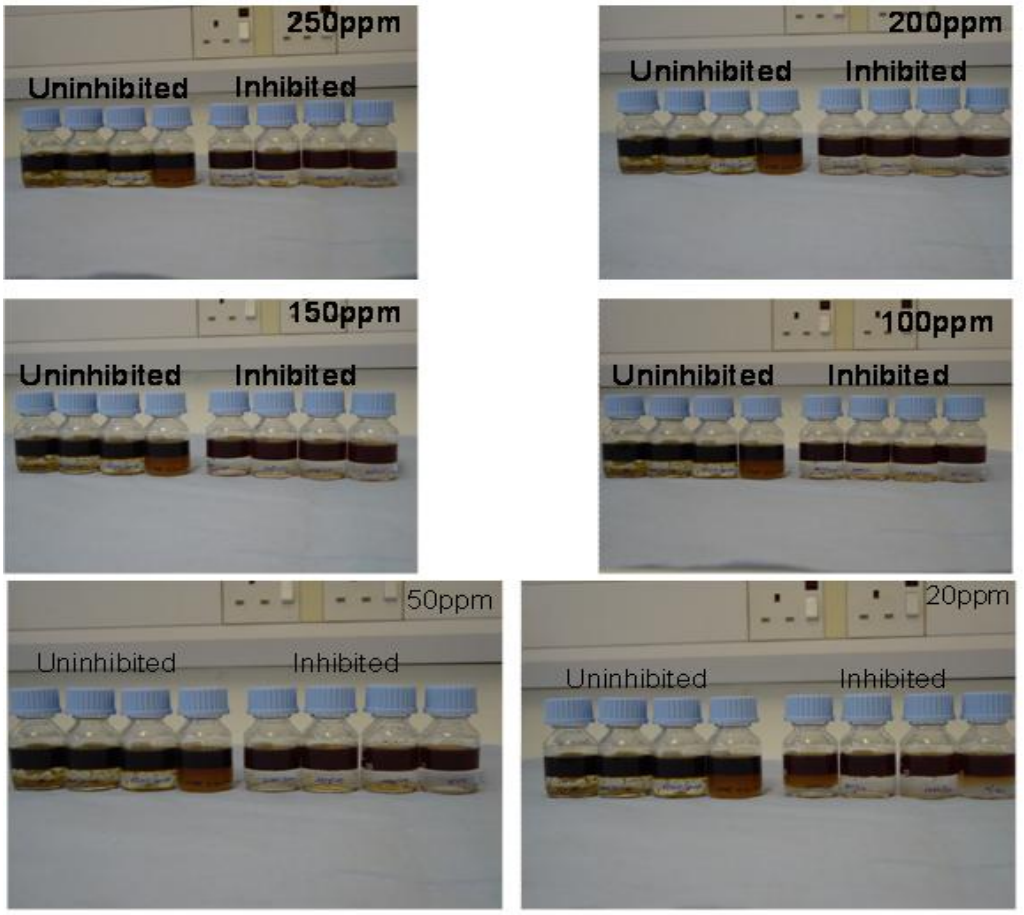

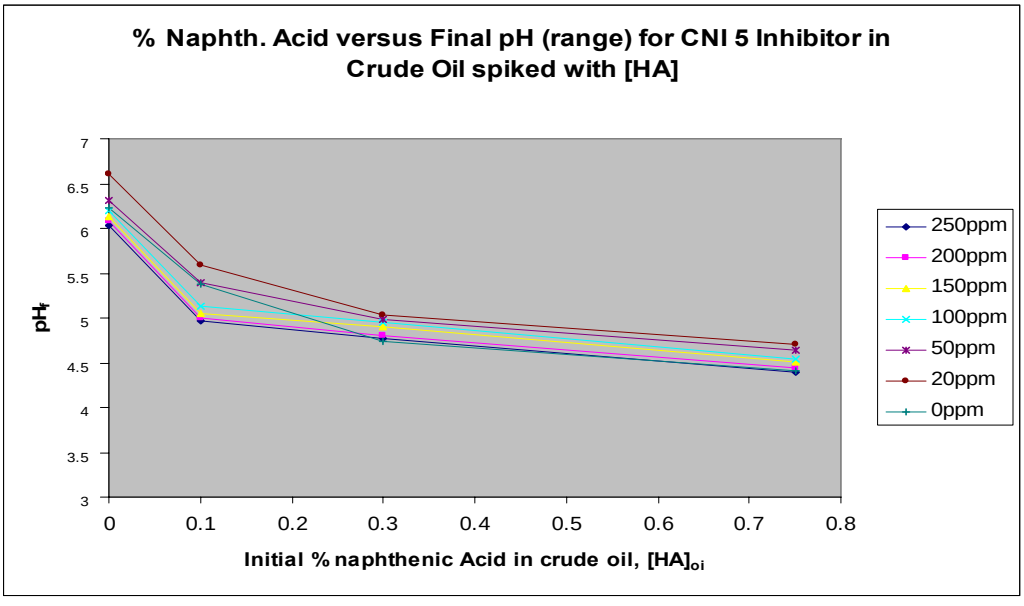

Figure 7.14: Static bottle test experiment (above) and the graphical plot of the final brine pH versus initial % naphthenic acid concentration, $[HA]_{oi}$ using CNI 5inhibitor for crude oil naphthenate inhibition.

Inhibition Efficiency on Emulsion Forming Crude Oil Samples

An emulsion forming crude oil sample which was mentioned in the earlier part of this chapter as being "uncontaminated" was used as supplied, to test the inhibition efficiency using three types of naphthenate inhibitors i.e. CNI 6, CNI 7 and CNI 8. These naphthenate inhibitors are meant to be for calcium naphthenate inhibition but were also tested on sodium carboxylate/emulsion and crude oil (emulsion forming).

Inhibitors CNI 6, CNI 7 and CNI 8

Static inhibition efficiency experiments carried out using these inhibitors showed that CNI 6 worked extremely well whilst CNI 7 does not and CNI 8 works mildly at a certain range of inhibitor concentration. The result from CNI 6 showed total elimination of emulsion formation at a MIC of 100 ppm. Furthermore, at 50 ppm inhibitor concentration there was an inhibition of about 80% efficiency, as can be seen from the photographs of static bottle test experiments presented in Figure 7.15 below. Interestingly, even addition of just 20 ppm inhibitor concentration (CNI 6 inhibitor), was observed to give a reasonable level of inhibition of about 50% efficiency, based on the observations from Figure 7.15. This can be clearly observed when compared with the control experiment where there was no addition of inhibitor in the emulsion forming crude oil sample. A chart for the inhibition efficiency is presented in Table 7.19. The final brine pH measured showed a decrease as the concentration of inhibitor increased in the oil phase (emulsion forming crude). The brine pH value decrease was slight compared with the control experiment, where there was no addition of inhibitor. Upon addition of 150 ppm inhibitor concentration in the oil phase, the brine pH changed from initial pH 9 to a final pH 6.64, whilst in the case of the control the brine pH changed from pH 9 to pH 6.50. Therefore, addition of naphthenate inhibitor has prevented the dissociation and partitioning of the naphthenic acid from the oil phase into the water phase. A plot of the final brine pH measured versus the concentration of inhibitor in the oil phase is plotted and presented in Figure 7.16 below.

Inhibitor	Crude oil
250 ppm	No Emulsion
200 ppm	No Emulsion
150 ppm	No Emulsion
100 ppm	No Emulsion
50 ppm	Very slight Emulsion
20 ppm	Slight Emulsion
0 (control)	Emulsion

Table 7.19: Minimum inhibitor concentration chart (MIC) for CNI 6 inhibitor tested on emulsion forming crude oil sample.

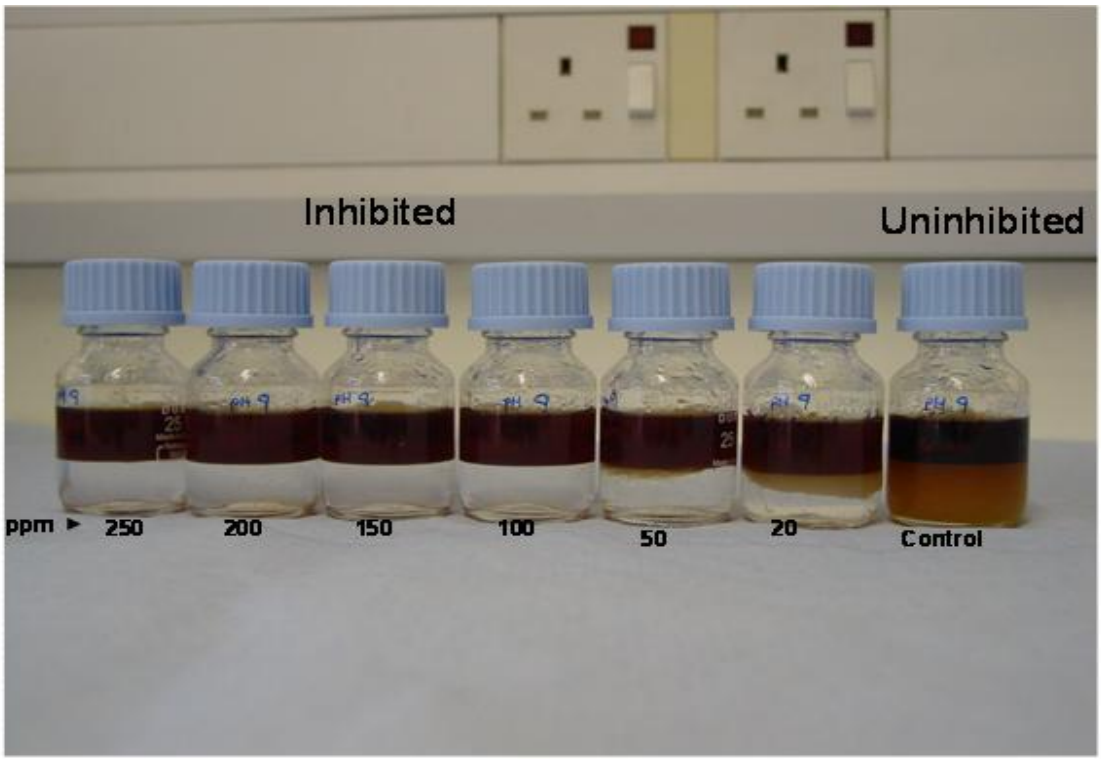

Figure 7.15: Static bottle test efficiency experiment using CNI 6 inhibitor on emulsion forming crude.

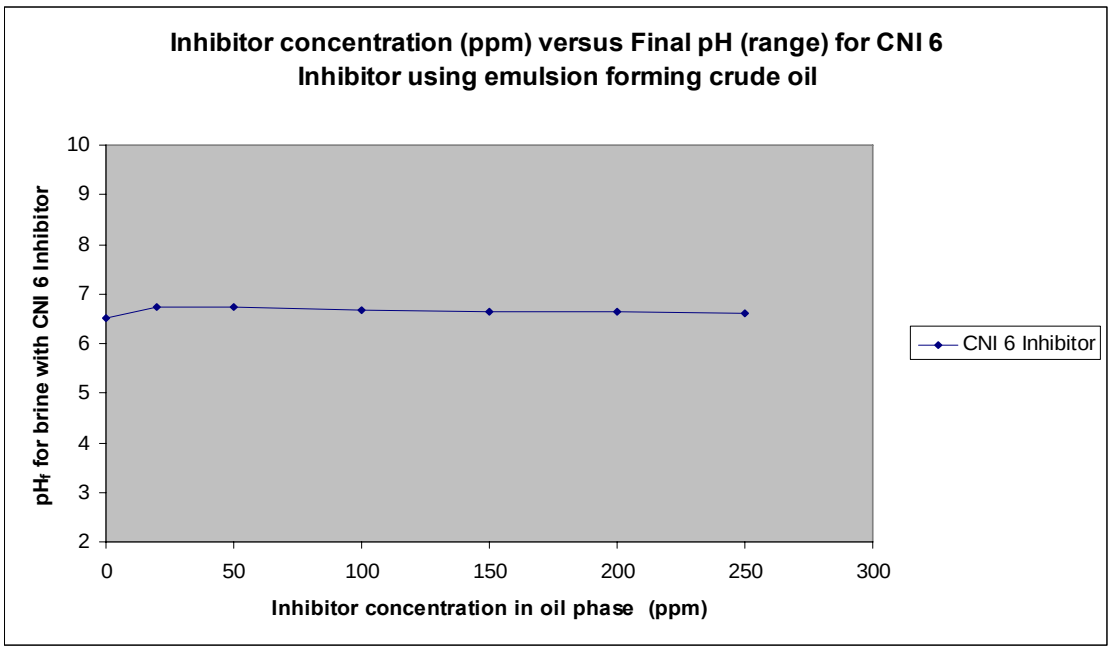

Figure 7.16: Graphical plot of the final brine pH versus concentration of naphthenate inhibitor in the oil phase (ppm).

However, inhibition efficiency studies using naphthenate inhibitors CNI 7 and CNI 8 showed that formation of emulsion could be minimised only at certain inhibitor concentrations and even then, it does not completely stop the formation of emulsion. It was observed from the static studies that CNI 7 inhibitor was able to achieve inhibition at about 10 ppm inhibitor concentration, with some slight inhibition at 5 ppm, whilst the CNI 8 naphthenate inhibitor shows some promise at inhibitor concentrations of ~20 ppm and 10 ppm, although the inhibition efficiency was not good enough to be used. The final brine pH was not measured, as most of these tests led to the formation of emulsions. Therefore, it was difficult to separate the final water phase for any pH measurement. The minimum inhibition concentration charts for CNI 7 and CNI 8 are presented in Tables 7.20 and 7.21, respectively, and photographs of the static bottle test efficiency experiment for CNI 8 is presented in Figure 7.17.

Inhibitor	Crude oil (Emulsion forming)
250 ppm	**Emulsion**
200 ppm	**Emulsion**
150 ppm	**Emulsion**
100 ppm	**Emulsion**
50 ppm	**Emulsion**
20 ppm	**Emulsion**
10 ppm	**No Emulsion**
5 ppm	**Very slight Emulsion**
0 (control)	**Emulsion**

Table 7.20: Minimum inhibitor concentration chart (MIC) for CNI 7 inhibitor tested on emulsion forming crude oil sample.

Inhibitor	Crude oil
250 ppm	**Emulsion**
200 ppm	**Emulsion**
150 ppm	**Emulsion**
100 ppm	**Emulsion**
50 ppm	**Slight Emulsion**
20 ppm	**Very slight Emulsion**
10 ppm	**Very slight Emulsion**
5 ppm	**Slight Emulsion**
0 (control)	**Emulsion**

Table 7.21: Minimum inhibitor concentration chart (MIC) for CNI 8 inhibitor tested on emulsion forming crude oil sample.

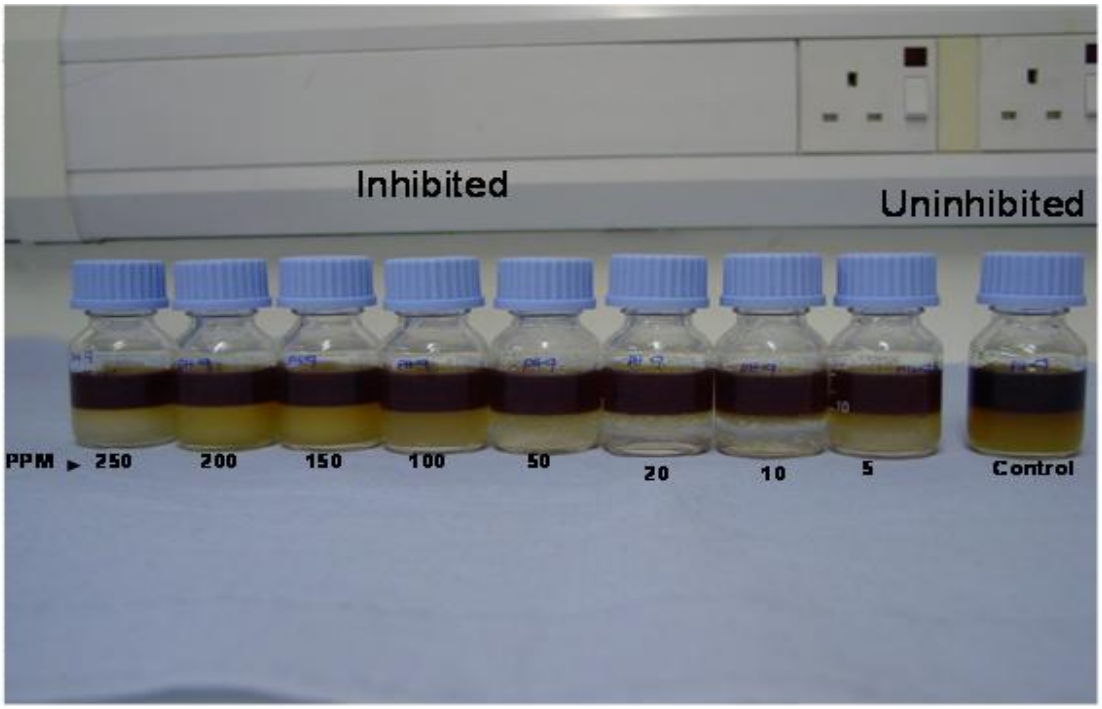

Figure 7.17: Static bottle test efficiency experiment using CNI 8 inhibitor on emulsion forming crude.

Inhibition Efficiency of Calcium Naphthenate Extract at Higher Temperature (60^{o}c)

A static inhibition efficiency study was carried out using naphthenic acid extract from a field calcium naphthenate deposit, which was dissolved in toluene to give the "pseudo" oil phase and a synthetic brine with composition: Na^{+}= 25000 ppm and Ca^{++} = 20000 ppm, which had been pH adjusted to pH 9. The concentration of naphthenic acid extract in toluene was 7500 ppm in both sets of experiments. Both the pH adjusted brine and the oil phase (naphthenic acid extract dissolve in toluene) were heated in a water bath to attain the required temperature prior to mixing of both phases to determine the minimum inhibitor concentration (MIC) in each case.

Inhibitors CNI 1 and CNI 4

The results from the static inhibition experiments were quite remarkable, with the MIC for CNI 1inhibitor being 20 ppm at 7500 ppm naphthenic acid extract concentration in the oil phase, as compared with an MIC of 100 ppm at the same concentration at room temperature. The MIC for CNI 4 inhibitor was 100 ppm at 60^{o}C compared with an MIC of

200 ppm at the same 7500 ppm concentration of naphthenic acid extract in the oil phase at room temperature. This result was very interesting in the sense that applying these inhibitors at higher temperature yields a better result compared to their application at room temperature. The reason for this better performance at higher temperature may be due to the fact that the reaction mechanism of these inhibitors is favoured at higher temperatures than the room temperature, due to possible kinetic effects. Therefore, significantly enhanced naphthenate inhibitor performance was observed when applying them at higher temperatures. The minimum inhibition efficiency (MIC) chart for CNI 1 and CNI 4 inhibitors are presented in Tables 7.22 and 7.23, respectively, whilst the static bottle inhibition efficiency photographs and the plots of the final brine pH vs. inhibitor concentration in the oil phase for CNI 1 and CNI 4 inhibitors are presented in Figure 7.18.

Inhibitor\ HA	**7500 ppm (CNI 1 Inhibitor)**
250 ppm	**No Precipitate**
200 ppm	**No Precipitate**
150 ppm	**No Precipitate**
100 ppm	**No Precipitate**
50 ppm	**No Precipitate**
20 ppm	**No Precipitate**
0 (control)	**Precipitate**

Table 7.22: Minimum inhibitor concentration chart (MIC) for CNI 1 inhibitor tested on naphthenic acid extract from calcium naphthenate at higher temperature (60^{o}C).

Inhibitor\ HA	7500 ppm (CNI 4 Inhibitor)
250 ppm	No Precipitate
200 ppm	No Precipitate
150 ppm	No Precipitate
100 ppm	No Precipitate
50 ppm	Very slight Precipitate
20ppm	Slight Emulsion
0 (control)	Precipitate

Table 7.23: Minimum inhibitor concentration chart (MIC) for CNI 4 inhibitor tested on naphthenic acid extract from calcium naphthenate at higher temperature (60^{o}C).

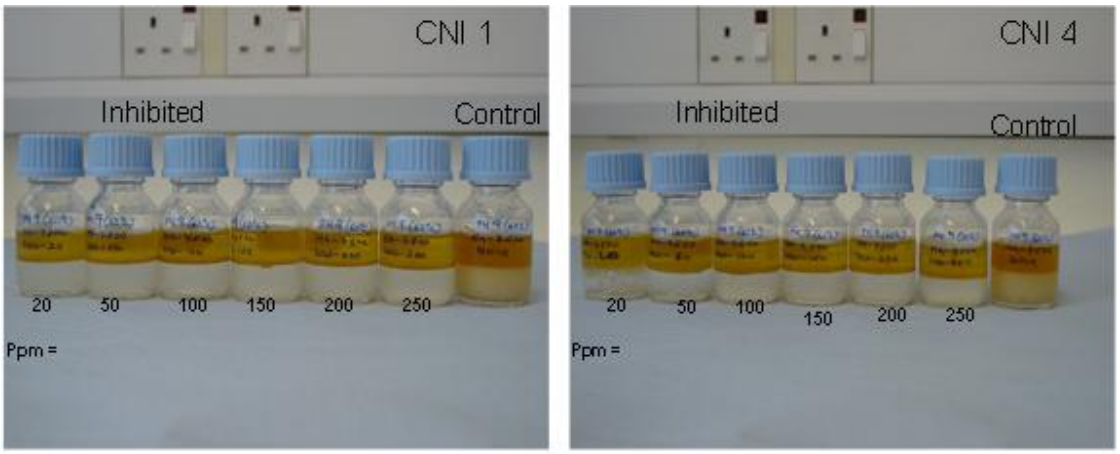

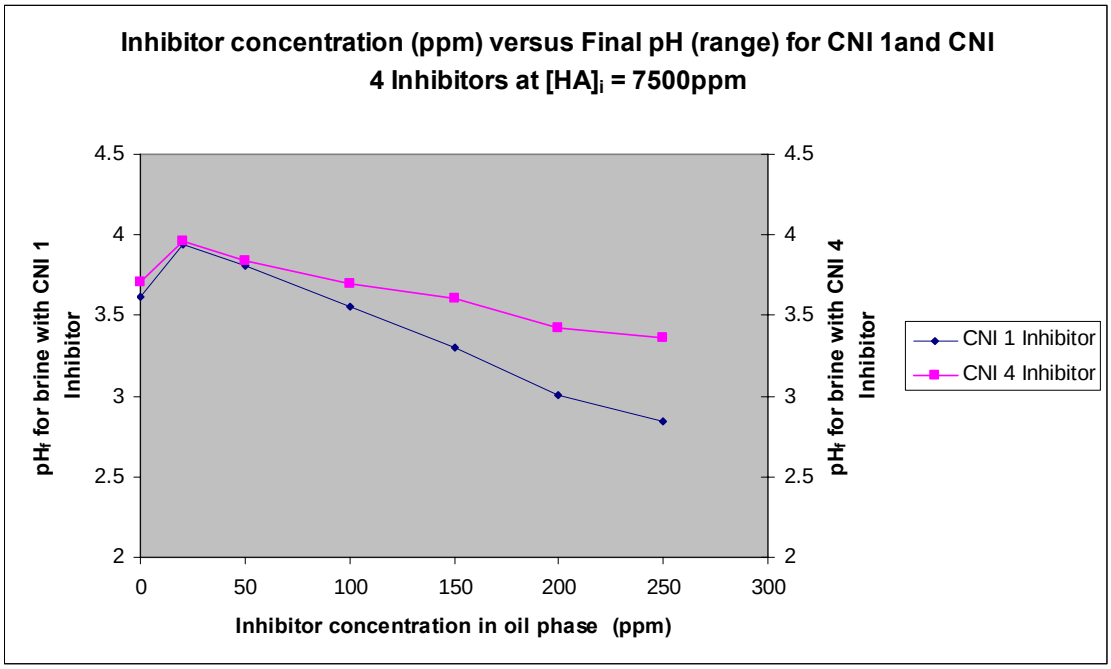

Figure 7.18: Static bottle test inhibition efficiency experiment (above) and the graphical plot of the final brine pH (for CNI 1 & CNI 4 inhibitor) versus inhibitor concentration in the oil phase (ppm).

7.3 SUMMARY AND CONCLUSIONS

Static inhibition efficiency studies of calcium naphthenate and sodium carboxylate/ emulsion prevention were carried out using eight different naphthenate inhibitors supplied by 3 different oil service companies who sponsor the FAST JIP. The key objective of this study was to develop a test methodology for these inhibitors in order to test these species for preventing or minimising the formation of either calcium naphthenate or sodium carboxylate in oil production facilities. Also, the effect of temperature was investigated on the best two performing inhibitors. The following conclusions were derived from the studies:

Calcium Naphthenate Inhibition

Static inhibition efficiency studies were carried out on the eight different types of naphthenate inhibitors, viz. CNI 1, CNI 4, CNI 5, CNI 6 and CNI 8. Several of these species can inhibit the formation of calcium naphthenate at various MIC levels, depending

on the chemistry of the inhibitor. However, CNI 7 inhibitor did not give any good results whilst naphthenate inhibitors CNI 2 and CNI 3 were found to have compatibility problems, even with the control experiment, which led to the formation of precipitates. Therefore, studies using these two inhibitors, CNI 2 and CNI 3, were discontinued. The results showed that effective inhibition of calcium naphthenate formation could be obtained with the following MIC values: (i) 100 ppm and 20 ppm MIC for higher and lower naphthenic acid extract concentration, in the case of CNI 1 inhibitor; (ii) 200 ppm and 20 ppm was observed at higher and lower concentrations of naphthenic acid extract in the oil phase for CNI 4 inhibitor; (iii) 250 ppm and 20 ppm for higher and lower concentration of naphthenic acid extract in the oil phase for CNI 5 inhibitor; and (v), interestingly, CNI 8 performed within a certain concentration range with 50 ppm for higher acid compositions in the oil phase and 20 ppm for lower acid compositions in the oil phase. It was observed that at higher inhibitor concentrations, then the formation of calcium naphthenate was observed.

Sodium Carboxylate/Emulsion

Sodium carboxylate/emulsion static inhibition efficiency experiments were also performed. Note that these inhibitors were specifically designed for calcium naphthenate prevention. The six inhibitors tested were CNI 1, CNI 4, CNI 5, CNI 6, CNI 7 and CNI 8. These inhibitors were found to be effective in the prevention of sodium carboxylate/emulsion formation at various MIC values, depending on the amount of naphthenic acid present in the "pseudo" oil phase. For example, CNI 1 and CNI 4 inhibitors prevented sodium carboxylate formation at MIC levels of 200ppm and 20ppm for higher and lower concentration of naphthenic acid extract in the oil phase. The corresponding MIC levels for CNI 5 were 200 ppm and 20 ppm for two concentrations in the oil phase (i.e. 7500 ppm and 1000 ppm). It was observed that CNI 7 and CNI 8 behave differently from the other inhibitors, in that they tend to have a narrow range of MIC values and any deviation outside this range leads to the formation of emulsion. CNI 7 inhibitor has an MIC of 10 ppm for higher acid concentration in the oil phase and 5 ppm for the lower concentration of acid in the oil phase. Application of either CNI 7 or CNI 8 inhibitor slightly above or below the MIC value resulted in the formation of an emulsion.

Crude Oil Spiked with Naphthenic Acid Extract from Calcium Naphthenate Deposit

Three inhibitors were used for this study: CNI 1, CNI 4 and CNI 5 and these were found to inhibit naphthenates from an emulsion forming crude oil spiked with naphthenic acid extract quite effectively, in our static bottle test experiments. MIC levels of 250 ppm and 20 ppm for CNI 1, 200 ppm and 20 ppm for CNI 4 and 100 ppm and 20 ppm for CNI 5 were observed for higher and lower concentrations of naphthenic acid extract in the crude oil.

Emulsion Forming Crude Oil Sample

The static inhibition efficiency study on the emulsion forming crude oil was carried out using the CNI 6, CNI 7 and CNI 8 inhibitors. Each of these three inhibitors has its own particular inhibition characteristics. Results from our study showed a MIC of 100 ppm for the CNI 6 inhibitor, whereas CNI 7 had an MIC window of ~10 ppm for effective inhibition. Inhibitor concentrations above or below 10 ppm resulted in the formation of an emulsion. However, the CNI 8 inhibitor could not give any reasonable MIC values for effective inhibition, based on the experiments conducted. It was noted that, at around 20 to 10 ppm inhibitor concentration, there was a little inhibition but this slight level of inhibition would not be adequate in field production facilities, where there would be very large throughputs of both oil and water.

Calcium Naphthenate Inhibition at Higher Temperature (60^{o}C)

Calcium naphthenate static inhibition efficiency experiments at a higher temperature (60 ^{o}C) were conducted on the best two performing naphthenate inhibitors, based on the earlier results. CNI 1 and CNI 4 inhibitors were used in this study at 60^{o}C and these chemicals showed improved performance over the initial room temperature results. The study was carried out with a naphthenic acid extract concentration in the oil phase (7500 ppm). The MIC levels found from this study were 20 ppm for the CNI 1inhibitor and 100 ppm for the CNI 4 inhibitor, as compared to an MIC of 100 ppm for the CNI 1 inhibitor and 200 ppm for CNI 4 inhibitor, at the same naphthenic acid concentration in the oil phase, at room temperature. Clearly, these naphthenate inhibitors show an improved performance at elevated temperatures, which may be due to the better kinetics at such temperatures.

CHAPTER 8: CONCLUSIONS AND RECOMMENDATIONS

8.1 CONCLUSIONS

The key objectives of the work undertaken in this PhD thesis were as follows:

(i) To extract and characterise the composition of naphthenate deposits from various calcium naphthenate field deposits and sodium carboxylate/emulsion samples, as well as from some corresponding crude oil samples that either form calcium naphthenate or sodium carboxylate/emulsion;

(ii) To study the geochemistry of some naphthenate forming crude oils from different parts of the world, to attempt to establish whether any of the geochemical marker species give any clues to whether the crude will be prone to naphthenate deposits/emulsions and, if so, what type of deposit/emulsion it might form;

(iii) To carry out thermodynamic naphthenate modelling predictions (using both simple pH change and precipitation experiments) and also study some sensitivity parameters such as % watercut, brine pH, bicarbonate and temperature;

(iv) To develop an experimental method to evaluate chemical naphthenate inhibitors and to apply this method to evaluate a range of commercially available inhibitors as supplied by some of the FAST oil service sponsor companies.

In Chapter 4, results of different types of naphthenic acid extraction methods and the subsequent characterization (using ESMS and APCI-MS techniques) of a range of field samples from the North Sea (UK and Norway sectors), South East Asia and West Africa were presented. From the analysis of the calcium naphthenate deposits, it was possible to distinguish quite clearly the various compositions of naphthenic acids in each of the samples, as well as the effect of using different types of spectroscopy in the naphthenic acid extract characterization. The analysis of naphthenic acid extracts in the deposit, using electrospray mass spectrometry (ESMS) and atmospheric pressure chemical ionisation mass spectrometry (APCI-MS), showed calcium naphthenate deposits fall into one of the following classifications: (i) consisting of a broad distribution of lower molecular weight naphthenic acids in the range of m/z 200 to m/z 650 and containing a narrow but significant

ion peak of higher molecular weight naphthenic acid (ARN) in the range of ~m/z 1230 ; or (ii) showing only a very pronounced significant ion peak of higher molecular weight naphthenic acids at around m/z 1230 and containing almost no lower molecular weight naphthenic acids. When present, the composition of the lower molecular weight naphthenic acids in all the extracts analysed consisted of acyclic, monocyclic, bicyclic and alkylbenzoic naphthenic acid species. It has been established that the APCI-MS analysis technique gives much better speciation of the higher molecular weight naphthenic acids, compared to ESMS. However, analysis of the sodium carboxylate extract revealed only the presence of lower molecular weight naphthenic acid (mainly acyclic type) with a distribution pattern with a preference of even-over-odd carbon numbers, whilst other remaining extract analysis of emulsions revealed the presence of lower molecular weight naphthenic acids (acyclic, bicyclic, monocyclic and alkylbenzoic) in the range of m/z 200 to m/z 650.

Also, analysis of extracts from crude oil samples using different extraction techniques (solid phase Acid-IER i.e. QAE-Sephadex and alcohol KOH) was carried out. The general conclusion based on this analysis is that only lower molecular naphthenic acids were detected from the crude oil itself; the higher molecular weight acids were too difficult to detect, which is most probably due to their very low concentration levels in the crude oil samples. This extensive naphthenic acid extraction and characterization work has finally addressed the issue of the true composition of naphthenate field deposits. It has been clearly established that there are various types of acid distribution in different naphthenate field samples, which are field specific. These specific distributions can probably be associated with the petroleum system where the oil was generated and possibly other secondary activities which may occur during oil migration and in the reservoir.

In Chapter 5, the study of the geochemistry of naphthenate forming crude oils i.e. both calcium naphthenate and sodium carboxylate/emulsion forming crudes were examined. The aim of the study was to separate the various crude oil samples into the different fractions (aliphatic, aromatic and polar) and then subsequently analyse these fractions using gas chromatography (GC) and gas chromatography mass spectrometry (GCMS) to detect a

range of molecular biomarkers. The objective here was to try to establish whether any relationship existed between the observed patterns of geochemical marker molecules and the likelihood of the oil producing naphthenate deposits and, if so, which type. The key conclusions derived from the results in Chapter 5 are as follows: (i) that most of the calcium naphthenate forming crudes tend to have high total acid number (TAN) as compared to the sodium carboxylate /emulsion forming crudes, although this is not always the case; (ii) all of the calcium naphthenate forming crudes were found to have a higher percentage of diasterane as compared to sodium carboxylate/emulsion forming crudes; and (iii) the calcium naphthenate forming crudes show some level of biodegradation, compared to the sodium carboxylate/emulsion forming crudes. This type of prediction study using certain geochemical parameters is at the preliminary stage and more needs to be done to establish how reliable and generally applicable this technique actually is.

In Chapter 6, an experimental and model prediction of naphthenate deposition is developed. Two types of experiment are described – one involving a simple pH change and another where full naphthenate precipitation occurs. This model was used to investigate the naphthenate precipitate mechanism and a wide range of sensitive parameters has been studied. In addition, other factors have been studied experimentally which may have some influence on the formation of naphthenate precipitates e.g. shear rate, bicarbonate, %watercut, brine pH, calcium ion concentration in the brine and temperature. The main conclusions in this chapter are as follows:: (i) in the pH change experiment; the prediction modelling results agree much better for the higher initial brine pH results (pH 5 and 6), whereas at lower brine pH the naphthenic acid dissociation and partitioning are much less obvious; (ii) in the precipitation results, for the "successive extraction" experiments, it was observed that at each stage almost equal amounts of naphthenate were observed, as predicted by the model, (iii) two types of variable watercut experiment were performed i.e. fixed V_o, variable (V_w/V_o) ratio and fixed total volume, $V_T = (V_w+V_o)$, variable (V_w/V_o) ratio. In both of these, the mass of naphthenate precipitate first increases with the increasing %watercut, up to around 70% watercut and then subsequently decreases. This was predicted by the model and was then observed experimentally; (iv) it was also observed that shear has a significant role to play in the formation of naphthenate and also

that the addition of bicarbonate resulted in an increased amount of naphthenate precipitate formation, which may be related to the formation of both calcium naphthenate and calcium carbonate together. Formation of calcium naphthenate at higher temperature is favoured, although the amount of naphthenate precipitate did not drastically increase; however, the *rate* at which the naphthenate is formed was observed to be faster than in the room temperature experiments.

In Chapter 7 results from the naphthenate static bottle test inhibition efficiency experiments were presented. The main objective of this work was to develop a test methodology in order to screen some commercially available naphthenate inhibitors, using extracts from calcium naphthenate deposits, sodium carboxylate/emulsion and emulsion forming crude oils. The key findings from these naphthenate static inhibition efficiency experiments are as follows: (i) 5 of the naphthenate inhibitors i.e. CNI 1, CNI 4, CNI 5, CNI 7 and CNI 8 were found to inhibit the formation of calcium naphthenate over a range of MICs values. The MIC also varies according to the concentration of naphthenic acid extract in the oil phase; as expected, MIC increases as $[HA]_i$ increases. For example, one of the best naphthenate inhibitors (CNI 1) showed inhibition at 100 ppm and 20 ppm for higher and lower naphthenic acid extract concentrations (7500 ppm and 3000 ppm) in the oil phase; (ii) the inhibitors tested on the sodium carboxylate/emulsion extract show good inhibition performance although they were not designed for inhibiting these types of emulsion (they were developed for CaN prevention). The naphthenate MIC values also varied according to the different chemical composition of each inhibitor. Two of the inhibitors i.e. CNI 7 and CNI 8 behave different to the others, in that they have a narrow range of concentrations where they perform effectively; (iii) studies carried out on an emulsion forming crude spiked with naphthenic acid extract and the untreated emulsion forming crude showed that good inhibition performance could be obtained for the inhibitors tested; and (iv) it was observed when these inhibitors were tested at higher temperatures, the efficiency of the inhibitors is improved. The MIC for CNI 1 inhibitor at 60^{o}C and 7500 ppm naphthenic acid extract concentration in the oil phase was 20 ppm as compared to 100 ppm at room temperature. This improved efficiency was associated with the faster kinetics between the inhibitor and the acids in the oil phase.

8.2 RECOMMENDATIONS FOR FUTURE WORK

This thesis has covered four major areas as follow:

(i) Characterization of naphthenates using spectrometry;

(ii) Geochemical studies of crude oil composition;

(iii) Thermodynamic modelling of naphthenates (pH change and precipitation); and

(iv) Static inhibition efficiency study of chemical naphthenate inhibitors.

Although, much has been discovered, there are still many aspects of naphthenate formation, deposition, prediction and characterisation which should be studied more closely in the future. Some of these areas for further study are listed below:

(i) Additional work on the geochemistry studies of naphthenate forming crudes could include analysing more representative samples from various producing fields which have tendency to produce calcium naphthenate deposit, sodium carboxylate/emulsion and even oils that do not give any naphthenate problems. This will help to establish whether our preliminary geochemical correlations are general and reliable for predictive purposes. This type of detailed study will certainly give better information and possibly employ these techniques in naphthenate prediction, prior to any observed naphthenate formation. If this can be achieved, then this will be of great benefit to the oil industry and large amounts of money may be saved. The study conducted in this thesis was very preliminary and, from the results, it shows some good promise as an alternative tool for naphthenate prediction in the field.

(ii) With respect to the thermodynamic modelling, the use of real crude oil rather than model oil may be the next step in the modelling work. In addition, the possibility of incorporating the effects of temperature and pressure in the naphthenate model code should be assessed. The use of real crude oil is much more complex, as these oils contain many components which are less well understood. However, incorporating these into the precipitation model in commercial software would be of great industrial and practical interest.

(iii) Another area for further work is on naphthenate inhibition efficiency studies, using a tube blocking rig. In this thesis, detailed work on the static bottle test experiment has been carried out using extracts from calcium naphthenate deposit, sodium carboxylate/emulsion and emulsion forming crude oil. An attempt was also made to use a conventional tube blocking rig with minor modification to carry out dynamic naphthenate efficiency work. However, this could not be achieved due to the current design of the equipment and therefore results from that study are not reported in this thesis. Future work regarding the improvement of the rig design and dynamic inhibition will be worthwhile and this will allow us to extend the test conditions to higher temperature and pressure using both model oils and real crude oils. Ultimately, this type of study will be very beneficial to the oil industry in addressing the costly and difficult problem of naphthenate deposition.

APPENDIX A DERIVATION OF THE NAPHTHENATE MODEL EQUATIONS (NAPHTHENATE PRECIPITATION)

In this appendix, a full derivation of partitioning/precipitating naphthenate model is described. Real crude oils often contain many hundreds of naphthenic acid components, as shown for example in the ESMS and APCI-MS spectra of the field calcium naphthenate deposit (Mohammed and Sorbie, 2009). In the model described below, the naphthenic acid in the model oil is represented by a *single* component, denoted [HA] which may appear to be quite a severe approximation. However, [HA] can be considered as a "pseudo-component" which represents the collective effect of the wide range of actual naphthenic acids. In some cases, however, it is thought that a single tetra-protic naphthenic acid (or small family, known as "ARN") dominates the calcium naphthenate deposit, as is the case for the field example reported in (Mohammed and Sorbie, 2009). Thus, a single [HA] component model may be a much more reasonable approximation for such cases.

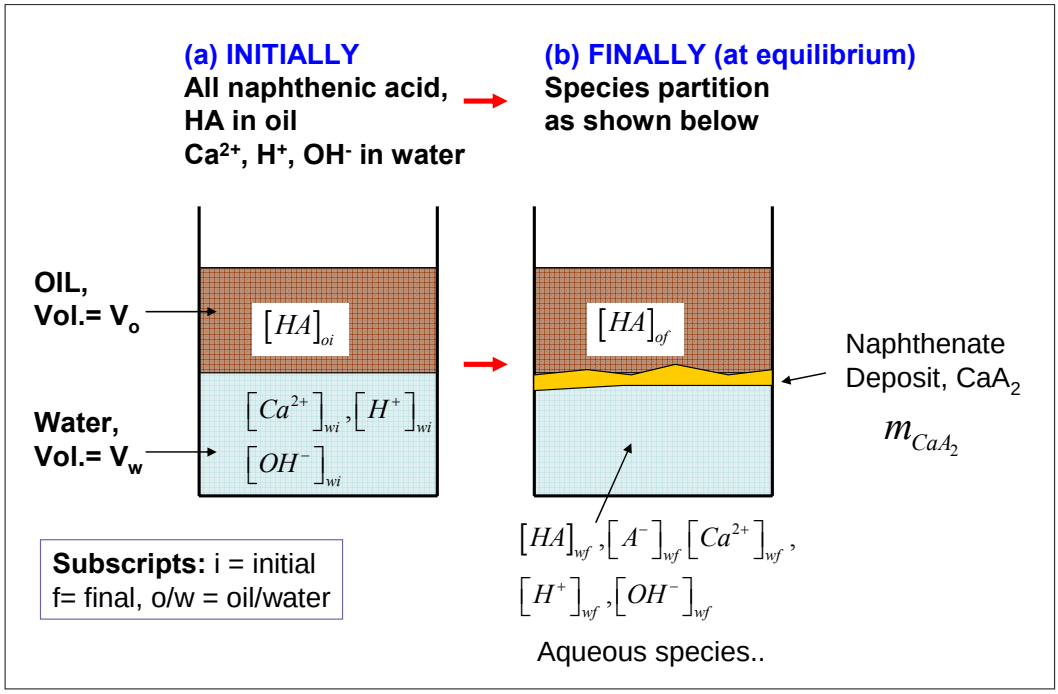

Figure A-1: The schematic of a model naphthenate system, [HA] (a) at initial conditions with all the naphthenic acid in the oil and (b) at equilibrium where the [HA] has partitioned between the oil and aqueous phases and may have precipitated as a calcium salt (CaA_2 in this case). V_o and V_w are the volumes of oil and water, respectively (assumed that $V_o = V_w$ here). In the development of the naphthenate precipitation model, refer to the schematic of CaN precipitation experiment in Figure A1 above. This mirrors the observed base case

CaN precipitation experiment shown in Figure 6.21 (Chapter 6). The model acid, [HA], may then behave as follows:
it may partition between the oil and water phases, described by a partition constant, K_{ow};

it can dissociate as a weak acid in the aqueous phase, according to the dissociation constant, K_a; and

it may precipitate/phase separate as a metal naphthenate, such a Na-A or Ca-A_2, described by a solubility product, such as K_{NaA} or K_{CaA_2}; experimentally, this deposit usually appears at the interface (Figures 6.21 and A1).

All of the parameters in this model are either well known or they are independently measurable physical data such as K_{ow}, K_a, K_{CaA_2} and K_w (the ionic product of water). A restricted version of this model was used previously to describe "pH change" experiments (Mohammed et al., 2009) where an oil (toluene) containing naphthenic acids was contacted with a medium pH (pH ~ 3 – 6) aqueous phase, where naphthenic acid partitioning took place but no precipitate (or emulsion) formed; however, the pH changed from its initial value to a lower value e.g. pH 6.5 → pH4 (Mohammed *et al.,* 2009). This pH change is described by the same model but without the "solubility product" expression for precipitation, i.e. it is governed only by the parameters, as K_{ow}, K_a and K_w. Indeed, such "pH change" experiments may be performed to establish the values of K_{ow} and K_a, which can then be used in the full precipitation model where, for a calcium naphthenate, the quantity K_{CaA_2} must be found. Therefore, the pH change model is considered as a subset of the full precipitation model.

In this thesis, the full derivation of the naphthenate precipitation model in the form that it is actually solved in the computer code (in VBA in Excel) is presented. This code is then applied in a wide sensitivity study which makes some predictions about the way a precipitating Ca-Naphthenate (CaN) system behaves. These results supply designs for the predictive experiments presented in the main text of this thesis. Several novel predictions arise from the applications here which, to my knowledge, have not been reported previously. These are then tested by the experiments described in this thesis.

Before presenting the details of the model for naphthenic acid partitioning between oil and water and its subsequent precipitation as calcium salt in the aqueous phase, the ***principle*** of the approach is outline to derive the set of constraint equations, viz:

1. Describe the partitioning of the naphthenic acid between the oil and water phases, by a water oil partition factor, K_{ow} (see below);

2. Write the equilibrium expressions for dissociation of the weak naphthenic acid, [HA] (described by K_a), the ionic product of water (K_w) and precipitation of the calcium naphthenate (CaA_2 in this case);

3. From the initial conditions of naphthenic acid in the oil only where $[HA] = [HA]_{oi}$ and calcium in the water only, $[Ca^{2+}] = [Ca^{2+}]_{wi}$ set up the mass balance equations (one for "A" and one for Ca);

4. Write the one charge balance equation for the aqueous phase.

As will be shown below, going through the procedure in steps 1 – 4 above leads to 7 equations in 7 unknowns, which can be solved numerically given certain initial conditions. These unknowns are as follows:

7 Unknowns => $[HA]_{of}, [HA]_{wf}, [H^+]_{wf}, [A^-]_{wf}, [OH^-]_{wf}, [Ca^{2+}]_{wf}$ *and* m_{CaA_2}

For simplicity of manipulation of the equations below, the unknown 7 equations are identified as follows:

Equilibrium conc. of HAin the oil phase,	$x_1 = [HA]_{of}$;
Equilibrium conc. HA in the aq. phase,	$x_2 = [HA]_{wf}$;
Equilibrium H^+ ion conc. in aq. phase,	$x_3 = [H^+]_{wf}$;
Equilibrium A^- ion conc. in aq. phase,	$x_4 = [A^-]_{wf}$;
Equilibrium OH^- ion conc. in aq. phase,	$x_5 = [OH^-]_{wf}$;
Equilibrium Ca^{2+} ion conc. in aq. phase,	$x_6 = [Ca^{2+}]_{wf}$; *and*
Equilibrium mass (no. moles) of CaA_2,	$x_7 = m_{CaA_2}$

Table A1: Notation in derivation of naphthenate model equations

These main species are shown in the schematic of Figure A1 where the initial conditions are shown in Figure A1a and the final (equilibrium) situation is shown in Figure A1b. The volumes of oil and water are V_o and V_w, respectively. Also note that the quantities $\boldsymbol{M_{HA}}$, $\boldsymbol{M_A}$, $\boldsymbol{M_{Ca}}$ and $\boldsymbol{M_{CaA_2}}$ are the molecular/atomic weights of the various species (where approximately $\boldsymbol{M_{HA} \approx M_A}$ and $\boldsymbol{M_{CaA_2} = M_{Ca} + 2M_A}$ etc.); below, "i" and "f" subscripts denote the initial and final (equilibrium) concentrations of the various species in the aqueous (subscript "aq") and oil (subscript "o") phases. Ions, such as H^+, Ca^{2+}, A^-, do not require any subscripts since they only appear in the aqueous phase.

The set of equations governing this system can be written as follows:

Equilibrium partitioning and solution equilibrium

(i) The partitioning of the naphthenic acid between the water and the oil is described by a partition coefficient, K_{ow}, given by:

$$\boldsymbol{K_{ow} = \frac{[HA]_{aq.f}}{[HA]_{o.f}}} \qquad (1)$$

note that the [HA] may become less soluble as the salinity of the aqueous phase increases i.e. K_{ow} will be lower at higher ionic strengths. Note that it is numerically convenient to define K_{ow} as the ratio of the lower phase solubility of the species (water) than in higher phase solubility (oil).

(ii) The dissociation of the weak naphthenic acid and water are given by the usual K_a expressions as follows:

$$K_a = \frac{\left[H^+\right]_f . \left[A^-\right]_f}{\left[HA\right]_{aq.f}} \qquad (2)$$

where it is known that, typical pK_a values ($-\log_{10}K_a$) for these species are in the range 4 to 5, and

$$K_w = \left[H^+\right]_f . \left[OH^-\right]_f \qquad (3)$$

where K_w is of order, 1.0×10^{-14}.

(iii) the solubility product of the precipitated calcium naphthenate - assumed formula, CaA_2 - is given by:

$$K_{CaA_2} = \left[Ca^{2+}\right]_f . \left[A^-\right]_f^2 \qquad (4)$$

but in principle any mathematical solubility expression may be included here.

Mass balance

(iv) The (known) initial mass of the "A" species in **Moles**, m_{Ai}, is as follows:

$$m_{Ai} = \left[HA\right]_{oi} . V_o \qquad (5)$$

while, at equilibrium, the "A" appears in several components and the final mass (in Moles) is given by the expression:

$$m_{Af} = \left[HA\right]_{of} . V_o + \left[HA\right]_{wf} . V_w + \left[A^-\right]_f . V_w + 2 . m_{CaA_2} \qquad (6)$$

where, by material balance, $m_{Ai} = m_{Af}$

(v) The initial mass of the Ca species in **Moles**, $m_{Ca,i}$, is as follows:

$$m_{Ca,i} = \left[Ca^{2+}\right]_{wi} . V_w \qquad (7)$$

while, at equilibrium, the Ca appears both in solution and also in the precipitated CaA_2 and the final mass in Moles is given

$$\boldsymbol{m_{Ca,f} = \left[Ca^{2+}\right]_f .V_w + m_{CaA_2}} \qquad (8)$$

where, again by material balance, $\boldsymbol{m_{Ca,i} = m_{Ca,f}}$ (in moles)

Charge balance

(iv) Finally, the equilibrium concentrations must be constrained by ensuring that there is charge balance. The initial (known) total charge in the system, C_i - considering only the active ions - is as follows:

$$\boldsymbol{C_i = \left(2\left[Ca^{2+}\right]_{wi} + \left[H^+\right]_i - \left[OH^-\right]_i\right).V_w} \qquad (9)$$

and this charge is set by the initial conditions by specifying $\boldsymbol{\left[Ca^{2+}\right]_{wi}}$ ***and*** $\boldsymbol{\left[H^+\right]_i}$. The final charge at equilibrium is given by:

$$\boldsymbol{C_f = \left(2\left[Ca^{2+}\right]_f + \left[H^+\right]_f - \left[OH^-\right]_f - \left[A^-\right]_f\right).V_w} \qquad (10)$$

where, by charge conservation, $\boldsymbol{C_f = C_i}$.

Thus, the 7 unknowns

$$\Rightarrow \quad [HA]_{of}, [HA]_{wf}, \left[H^+\right]_{wf}, \left[A^-\right]_{wf}, \left[OH^-\right]_{wf}, \left[Ca^{2+}\right]_{wf} \ \textit{and} \ m_{CaA_2}$$

can be found by solving the 7 equations => Equations (1), (2), (3), (4), (6), (8) and (10), and a summary of the model equations, using the notation in Table A1, above is given in Table A2 below:

The set of model equations in Table A2 are solved numerically for the parameters and quantities of interest and results are discussed in the main text of the thesis.

Naphthenate Model Equation	**In Notation of Table A1**
Eq. (1) $\boldsymbol{K_{ow}} = \dfrac{\left[\boldsymbol{HA}\right]_{aq.f}}{\left[\boldsymbol{HA}\right]_{o.f}}$	Eq. A1 $\dfrac{\boldsymbol{x}_2}{\boldsymbol{x}_1} = \boldsymbol{K_{ow}}$
Eq. (2) $\boldsymbol{K_a} = \dfrac{\left[\boldsymbol{H^+}\right]_f . \left[\boldsymbol{A^-}\right]_f}{\left[\boldsymbol{HA}\right]_{aq.f}}$	Eq. A2 $\dfrac{\boldsymbol{x}_3 . \boldsymbol{x}_4}{\boldsymbol{x}_2} = \boldsymbol{K_a}$
Eq. (3) $\boldsymbol{K_w} = \left[\boldsymbol{H^+}\right]_f . \left[\boldsymbol{OH^-}\right]_f$	Eq. A3 $\boldsymbol{x}_3 . \boldsymbol{x}_5 = \boldsymbol{K_w}$
Eq. (4) $\boldsymbol{K_{CaA_2}} = \left[\boldsymbol{Ca^{2+}}\right]_f . \left[\boldsymbol{A^-}\right]_f^2$	Eq. A4 $\boldsymbol{x}_6 . \boldsymbol{x}_5^2 = \boldsymbol{K_{CaA_2}}$
Eq. (6) – Mass balance "A" $\boldsymbol{m_{Af}} = \left[\boldsymbol{HA}\right]_{of} . \boldsymbol{V_o} + \left[\boldsymbol{HA}\right]_{wf} . \boldsymbol{V_w} + \left[\boldsymbol{A^-}\right]_f . \boldsymbol{V_w} + 2 . \boldsymbol{m_{CaA_2}}$	Eq. A5 $\boldsymbol{x}_{1i} = \boldsymbol{x}_1 + \left(\dfrac{\boldsymbol{V_w}}{\boldsymbol{V_o}}\right) . \boldsymbol{x}_2 + \left(\dfrac{\boldsymbol{V_w}}{\boldsymbol{V_o}}\right) . \boldsymbol{x}_4 + \left(\dfrac{2}{\boldsymbol{V_o}}\right) . \boldsymbol{x}_7$ where $\boldsymbol{x}_{1i} = \boldsymbol{[HA]_{oi}}$
Eq. (8) – Mass balance "Ca" $\boldsymbol{m_{Ca,i}} = \boldsymbol{m_{Ca,f}} = \left[\boldsymbol{Ca^{2+}}\right]_f . \boldsymbol{V_w} + \boldsymbol{m_{sol}}$	Eq. A6 $\boldsymbol{x}_{6i} = \boldsymbol{x}_6 + \left(\dfrac{1}{\boldsymbol{V_w}}\right) . \boldsymbol{x}_7$ where $\boldsymbol{x}_{6i} = \boldsymbol{[Ca^{2+}]_{wi}}$
Eq. (10) – Charge balance $\boldsymbol{C_i} = \boldsymbol{C_f} = \boldsymbol{V_w}(2\left[\boldsymbol{Ca^{2+}}\right]_f + \left[\boldsymbol{H^+}\right]_f - \left[\boldsymbol{OH^-}\right]_f - \left[\boldsymbol{A^-}\right]_f)$	Eq. A7 $2\boldsymbol{x}_6 + \boldsymbol{x}_3 - \boldsymbol{x}_5 - \boldsymbol{x}_4 = \boldsymbol{C_i}$ where $C_i = 2\boldsymbol{x}_{6i} + \boldsymbol{x}_{3i} - \boldsymbol{x}_{5i}$ that is => $C_i = 2\left[\boldsymbol{Ca^{2+}}\right]_{wi} + \left[\boldsymbol{H^+}\right]_{wi} - \left[\boldsymbol{OH^-}\right]_{wi}$

Table A2: Summary of the equation in the naphthenate model – using notation in Table A1.

.

REFERENCES:

Acevedo S., Escobar G., Ranaudo M. A., Khazen J., Borges B., Pereira J. C., Mendez B., 1999, *Isolation and characterization of low and high molecular weight acidic compounds from Cerro Negro extra heavy crude oil: Role of these acids in the interfacial properties of the crude oil emulsions*, Energy and Fuels, **13**, 333-335.

Ajienka J. A., Ogbe N. O., Ezeaniekwe B. C., 1993, *Measurement of dielectric constant of oilfield emulsions and its application to emulsion resolution*, Journal of Petroleum Science and Engineering, **9** (4), 331-339.

ASTM D 664, 2004, *Standard Test Method for Acid Number of Petroleum Products by Potentiometric Titration*; ASTM International: West Conshohocken, PA, 2004

Babaian-Kibala E., Petersen P. R., Humphries M. J., 1998, *Prepr.-Am. Chmen. Soc., Div. Pet. Chem*., **3**, 106-110.

Barakat A. O., Mostofa A., El-Gayar M. S., Rullkotter J., 1997, *Source-dependent biomarker properties of five crude oils from the Gulf of Suez, Egypt,* Organic Geochemistry, **26**, 441-450.

Barnard P. C., Bastow M. A., *Hydrocarbon generation, migration, alteration, entrapment and mixing in the Central and Northern North Sea*, 1991, Petroleum Migration, Geological Society, Special Publication, England W. A and Fleet A. J (editors), 167-190.

Barrow M. P., *Characterization of the naphthenic acid content in crude oil extracts using Fourier-Transform ion cyclotron resonance mass spectrometry*, 2003, Internal presentation for Total at the Department of Chemistry, University of Warwick, UK.

Baugh P. J., 1993, *Gas Chromatography: a practical approach*. Oxford University Press, Oxford, 426pp.

Baugh T. D., Wolf N. O., Mediaas H., Vindstad J. E., Grande K., 2004, *Characterization of a calcium naphthenate deposit – The Arn acid discovery*, American Chemical Society, Division of Petroleum Chemistry, **49** (3), 274-276.

Baugh T D., Grande K., Mediaas H., Vindstad J. E., Wolf N. O., 2005a, *The discovery of high molecular weight naphthenic acids (Arn acid) responsible for calcium naphthenates deposits*, SPE 93011, presented at the 7th International Symposium on Oilfield Chemistry, Aberdeen, UK, May 11-12.

Baugh T., Grande K. V., Mediaas H., Vindstad J. E., Wolf N. O., 2005b, *The discovery of high molecular weight naphthenic acids (Arn acid) responsible for calcium naphthenate deposits*, proceedings of the Chemistry in the Oil Industry IX, RSC/EOSCA, Manchester, UK, October 31-November 2.

Brandal, Ø., 2005, *Interfacial (O/W) Properties of naphthenic Acids and Metal Npahthenates, Naphthenic Acid Characterization and Metal naphthenates Inhibition*. PhD Thesis at NTNU.

Brient J. A., Wessner P. J., Doyle M. N., 1995, *Naphthenic acids In Encyclopedia of Chemical Technology* (Kirk-Othmer, Ed.), John Wiley & Sons, New York.

Brocart B., Hurtevent C., Volle J. L., 2005, *Analytical detection of Arn-type naphthenic acids in crudes*, presented at the 6th Petroleum Phase Behavior and Fouling Conference, Amsterdam, The Netherlands, June 25-29.

Chang, S. Hsu., Dechert, G. J., Robbins, W. K., Fukuda, E.K., 2000, *Naphthenic Acids in Crude Oils Characterized by Mass Spectrometry*, Energy & Fuels, **14** 217-223.

Curiale J., Lin R., Decker J., 2005, *Isotopic and molecular characteristic of Miocene-reservoired oils of the Kutei Basin, Indonesia*, Organic Geochemistry, **36** 405-424.

Didyk B. M., Simoneit B. R. T., Brassell S. C., Eglinton G., 1978, *Organic geochemical indicators of palaeoenvironmental conditions of sedimentation,* Nature, **272**, 216-222.

Dyer S. J., Graham G, M., Arnott C., 2003*, Naphthenate scale formation – examination of molecular controls in idealised systems*, SPE 80395, presented at the 5th International Symposium on Oilfield Scale, Aberdeen, UK, January 29-30.

Dyer S. J., Williams H. L., Graham G. M., Cummine C., Melvin, K B., Haider F., Gabb A. E., 2006, *Simulating calcium naphthenate formation and mitigation under laboratory conditions*, SPE 100632, presented at the 8th International Symposium on Oilfield Scale, Aberdeen, UK, May 31-June 1.

Dzidic I., Somerville A. C., Raia J. C., Hart H. V., 1988, *Determination of naphthenic acids in California crudes and refinery wastewaters by fluoride ion chemical ionization mass spectrometry*, Analytical Chemistry, **60**, 1318-1323.

Ekweozor C. M., Okogun J. I., Ekong D. E. U., Maxwell J. R., 1979, *Preliminary organic geochemical studies of samples from the Niger Delta (Nigeria). I. Analysis of crude oils for triterpanes*, *Chemical Geology*, **27**, 11-28.

Ese M. H., Kilpatrick P. K., 2004, *Stabilization of water-in-oil emulsion by naphthenic acids and their salts: model compounds, role of pH, and soap/acid ratio*, Journal of Dispersion Science and Technology, **25** (3), 253-261.

Fan T. P., 1991, *Characterization of naphthenic acids in petroleum by Fast Atom Bombardment mass spectrometry*, Energy and Fuels, **5**, 371-375.

Fan T., Buckley J.S., 2002, *Rapid and Accurate SARA Analysis of Medium Gravity Crude Oils*, Energy and Fuels, **16**, 1571-1575.

Gallup D. G., Smith P. C., Chipponeri J., Abuyazid A., Mulyono D., 2002, *Formation and mitigation of metallic soap sludge, Attaka, Indonesia field*, SPE 73960, presented at the International Conference on Health Safety and Environment in Oil and Gas Exploration and Production, Kuala Lumpur, Malaysia, March 20-22.

Gallup D. G., Star J., 2004, *Soap sludges: aggravating factors and mitigation measures*, SPE 87471, presented at the 6th International Symposium on Oilfield Scale, Aberdeen, UK, May 26-27.

Gallup D. G., Smith P. C., Star J. F., Hamilton S. H., 2005, *West Seno deepwater development case history, production chemistry*, SPE 92969, presented at the International Symposium on Oilfield Chemistry, Houston, Texas, USA, February 2-4.

Gallup D. L., Curiale J. A., Smith P. C., 2007, *Characterization of sodium emulsion soaps formed from production fields of Kutei Basin, Indonesia*, Energy and Fuels, **21**, 1741-1759.

Gallup D L., Denny V., Khandekar C Y., *Inhibition of Sodium Emulsions, West Seno, Indonesia,* 2010, SPE 130506, presented at the 10th International Oilfield Scale Symposium, Aberdeen, UK, May 26-27.

Goldszal A., Hurtevent C., Rousseau G., 2002, *Scale and naphthenate inhibition in deep-offshore fields*, SPE 74661, presented at the 4th International Oilfield Scale Symposium, Aberdeen, UK, January 30-31.

Hao C., Headley J. H., Peru K. M., Frank R., Yang P., Solomon K. R., 2005, *Characterization and pattern recognition of oil-sand naphthenic acids using comprehensive two dimensional gas chromatography/time of flights mass spectrometry*, Journal of Chromatography A, **1067**, 277-284.

Havre T. E., 2002. *Formation of Calcium Naphthenate in Water/Oil System, Naphthenic Acid Chemistry and Emulsion stability,* PhD thesis, Department of Chemical Engineering, Norwegian University of Science and Technology, Trondheim, Norway.

Headley J. V., Peru K. M., Mac Martin D. W., Winkler M., 2002, *Determination of dissolved naphthenic acids in natural water by using negative-ion electrospray mass spectrometry*, Journal of the AOAC International, **85** (1), 182-187.

Holowenko F. M., MacKinnon M. D., Fedorak P. M., 2002, *Characterization of naphthenic acids in oil sands wastewaters by gas chromatography-mass spectroscopy*, Water Research, **36**, 2843-2855.

Hsu C. S., Dechert G. J., Robbins W. K., Fukuda E. K., 2000, *Naphthenic acids in crude oils characterized by mass spectrometry*, Energy and Fuels, **14**, 217-233.

http://www.chm.bris.ac.uk/ms/theory/apci-ionisation.html

Hurtevent C., Ubbels S., 2006, *Preventing naphthenate stabilized emulsions and naphthenate deposits in fields producing acidic oils*, SPE 100430, presented at the 8th International Symposium on Oilfield Scale, Aberdeen, UK, May 31-June 01.

Idem R. O., Ibrahim H. H., 2002, *Kinetics of CO_2-induced asphaltene precipitation from various Saskatchewan crude oils during CO_2 miscible flooding*, Journal of Petroleum Science and Engineering, **35**, 233-246.

Jones D. M., Watson J. S., Meredith W., Chen M., Bennett B., 2001, *Determination of naphthenic acids in crude oils using nonaqueous ion exchange solid phase extraction*, Analytical Chemistry, **73**, 703-707.

Kim S., Stanford L., Rodgers R. P., Marshall A. G., Walters C. C., Qian K., Wenger L. M., Mankiewicz P., 2005, *Microbial alteration of the acidic and neutral polar NSO compounds*

revealed by Fourier transform ion cyclotron resonance mass spectrometry, Organic Geochemistry, *36*, 1117-1134.

Klein G, C., Rodgers R, P., Larter S. R., Bennett B., Marshall A. G., 2006, *A comprehensive comparison of the polar NSO compounds in a suite of biodegraded oils by ESI FTICR MS*, presented at the 17th International Mass Spectrometry Conference, Prague, Czech Republic, August 27- September 1.

Koike L., Reboucas L. M. C., Reis A. M, Marsaioli A. J., Richnow H. H., Michaelis W., 1992, *Naphthenic acids from crude oil of Campos Basin*, Organic Geochemistry, **18** (6), 851-860.

Kuzmanovic B., Kuipers N. J. M., De Haan A. B., Kwant G., 2005, *Reactive extraction of carboxylic acids from a polar hydrocarbons using aqueous sodium hydrogen carbonate with back-recovery using carbon dioxide under pressure*, Separation and Purification Technology, **47** (1-2), 58-72.

Langmuir I., Schaefer V. J., 1937, *The effect of dissolved salts on insoluble monolayers*, Journal of the American Chemical Society, **59**, 2400-2414.

Laredo G. C., Lopez C. R., Alvarez R. E., Cano J. L., 2004, *Naphthenic acids, total acid number and sulfur content profile characterization in Isthmus and Maya crude oils*, Fuel, **83** (11), 1689-1695.

Lutnaes B. J., Brandal O., Sjoblom J., Krane J., 2006, *Archaeal C80 isoprenoid tetracids responsible for naphthenate deposition in crude oil processing*, Organic and Biomolecular Chemistry, **4**, 616-620.

Moldowan J. M., Dahl J., Huizinga B. J., Fago F. G., Hickey L. J., Peakman T. M., Taylor D. W., 1994, *The molecular fossil record of Oleanane and its relation to angiosperm*, Science, **256**, 768-771.

Mackenzie A. S., Patience R. L., Maxwell J. R., Vandenbroucke M., Durand B., 1980, *Molecular parameters of maturstion in the Toarcian shales, Paris Basin, France-I. Changes in the configuration of acyclic isoprenoids alkanes, steranes, and triterpanes,* Geochimica et Cosmochica Acta, **44**, 1709-1721.

Marshall A. G., Hendrickson C. L., Jackson G. S., 1998, *Fourier transform ion cyclotron resonance mass spectrometry: a primer*, Mass Spectrometry Reviews, **17**, 1-35.

Mediaas H., Grande K., Hustad B-M., Rasch A., Rueslatten H, G., Vindstad J. E., 2003, *The Acid-IER method – a method for selective isolation of carboxylic acids from crude oils and other organic solvents*, SPE 80404, presented at the 5th International Symposium on Oilfield Scale, Aberdeen, UK, January 29-30.

Mediaas H., Grande K., Hustad B-M., Hovik K. R, Kummernes H., Nergard B., Vindstad J. E., 2005, *A unique laboratory test rig reduces the need for offshore tests to combat calcium naphthenate deposition in oilfield process equipment*, presented at Tekna Oilfield Chemistry Symposium, Geilo, Norway, March 13-16.

Meredith W., Kelland S-J., Jones D. M., 2000, *Influence of biodegradation on crude oil acidity and carboxylic acid composition*, Organic Geochemistry, **31**, 1059-1073.

Mohammed M. A., Sorbie K. S., Shepherd, A. G., 2009, *Thermodynamic Modeling of Naphthenate Formation and Related pH Change Experiments*, SPE Production & Operation Journal, August edition, 466-472.

Mohammed M. A., Sorbie K. S., 2009, *Naphthenic acid extraction and characterization from naphthenate field deposits and crude oils using ESMS and APCI-MS*, Colloids and Surface a: Physiochem. Eng. Aspect, **349**, 1-18.

Mullins O. C., Sheu E. Y., Hammani A., Marshall A. G., 2007, *Asphaltenes, heavy oils, and petroleomics*, Springer.

Nascimento L. R., Rebouças L. M. C., Koike L., Reis F, A. M., Soldan A. L., Cerqueira J. R., Marsaioli A. J., 1999, *Acidic biomarkers from Albacora oils, Campos basin, Brazil*, Organic Geochemistry, **30**, 1175-1191.

Pearson K., 2004, *Separator profiling: Kuito FPSO case study*, SPE 8847, presented at the 11th International Petroleum Exhibition and Conference, Abu Dhabi, UAE, October 10-13.

Peters, K. E., Moldowan, J. M., 1993. *The Biomarker Guide*: *Interpreting molecular fossil in petroleum and ancient sediments*. Prentice Hall, 363pp.

Petex, 1990, Treating *Oilfield Emulsions*, University of Texas at Austin, Petroleum Extension Service.

Philips, 1996, *Environmental scanning electron microscopy. An introduction to ESEM*, 2nd edition, Philips Electron Optics.

Qian K., Robbins W. K., Hughey C. A., Cooper H. J., Rodgers R. P., Marshall A. G., 2001, *Resolution and identification of elemental composition for more than 3000 crude acids in heavy petroleum by high-field Fourier-Transform ion cyclotron resonance mass spectrometry*, Energy and Fuels, **15**, 1505-1511.

Robbins W. K., 1998, *Challenges in the characterization of naphthenic acids in petroleum*, presented before the Division of Petroleum Chemistry Inc. 215th National Meeting, American Chemical Society, Dallas, Texas, USA, March 29-April 3.

Rogers V. V., Liber K., MacKinnon M. D., 2002, *Isolation and characterization of naphthenic acids from Athabasca oil sands tailings pond water*, Chemosphere, **48**, 519-527.

Ronald M. A., 1981, *Microbial Degradation of Petroleum Hydrocarbon: an Environmental Perspective,* Microbiological Reviews, **45** (1), 180-209.

Roques D. E., Overton E. B., Henry C. B., 1994. *Using gas chromatography/mass spectrometry fingerprint analyses to document process and progress of oil degradation*. Journal of Environment. Qual. **23** 581-855.

Rowland S. J., Hird S. J., Robson J. H., Venkatesan M. I., 1990, *Hydrogenation behaviour of two highly branched C_{25} dienes from Antartic marine sediments,* Organic Geochemistry, **15**, 215-18.

Rousseau G., Zhou H., Hurtevent C., 2001, *Calcium Carbonate and Naphthenate Mixed Scale in Deep-Offshore Fields,* SPE 68307 presented at the International Symposium on Oilfield Scale, Aberdeen, 30–31 January.

Rudzinski W. E., Oehlers L., Zhang Y., Najera B., 2002, *Tandem mass spectrometric characterization of commercial naphthenic acids and Maya crude oil*, Energy and Fuels, **16**, 1178-1185.

Saab J., Mokbel A. C., Razzouk A. C., Ainous N., Zydowicz N., Jose J., 2005, *Quantitative extraction procedure of naphthenic acids contained in crude oils-Characterization with different spectroscopic methods*, Energy and Fuels, **19**, 525-531.

Sarac S., Civan F., 2007, *Experimental Investigation and Modeling of Naphthenate Soap Precipitation Kinetics in Petroleum Reservoirs*, SPE 106074 presented at the International Symposium on oilfield Chemistry, Houston, Texas, USA, 28 February – 02 March.

Sartori G., Savage C. W., Ballinger B. H., Dalrymple D. C., 2001, *Process for extraction of naphthenic acids from crudes*, US Patent 6281328 B1.

Seifert W.K., Teeter R. M., Howells W.G., Cantow M.J.R., 1969, *Analysis of crude oil carboxylic acids after conversion to their corresponding hydrocarbons*, Journal of Analytical Chemistry, **41**, 1638-1647.

Seifert W. K., Moldowan J. M., 1978, *Application of steranes, terpanes, and monoaromatics to the maturation, migration and source of crude oils*, Geochimica et Cosmochimica Acta, **42**, 77-92.

Seifert W. K., Moldowan J. M., 1986, *Use of biological markers in petroleum exploration. In: Johns, R. B. (ed) Biological Markers in the Sedimentary Record,* Methods in Geochemistry and Geophysics, Elsevier, New York, pp.61-290.

Shepherd A. G., Thomson G., Westacott R., Neville A., Sorbie K. S., 2005, *A Mechanistic Study of Naphthenate Scale Formation*, SPE 93407, presented at the SPE International Symposium on Oilfield Chemistry, Houston, Texas, USA.

Shepherd A. G., 2008, *A Mechanistic Analysis of Naphthenate and Carboxylate Soap-forming Systems in Oilfield Exploration and Production*, PhD thesis at the Institute of Petroleum Engineering, Heriot-Watt University Edinburgh, UK.

Skippins J., Johnson D., Davies R., 2002, *Corrosion-mitigation program*, Oil and Gas Journal, **98** (37)**,** 64-68.

Smith P. C.*,* 2004, *Soap (naphthenates) scales management from deepwater flow assurance aspects to oil terminal sludge processing*, presented at IQPC Flow Assurance. A Holistic Approach Meeting, Kuala Lumpur, Malaysia, December 1-2.

Somasundaran P., Ananthapadmanabhan K. P., Ivanov I. B., 1984, *Dimerization of oleate in aqueous solutions*, Journal of Colloid and Interface Science, **99** (1), 128-135.

Sorbie K.S., Shepherd A.G., Turner M., Smith P.C., Westacott R.E., 2005. *Naphthenate Formation in Oil Production: General Theories and Field Observations. Proc.,* Chemistry in the Oil Industry IX, Manchester, UK, 31 October–2 November.

Speight, J.G., 1999, *The chemistry and technology of petroleum*. New York, Marcel Dekker.

Stenius P., Zillacus C. H., 1971, *Association equilibria and micelle formation of fatty acid sodium salts. I. A survey of potentiometric measurements on salts with 2-6 carbon atoms at high ionic strength*, Acta Chimica Scandinavica, **25**, 2232-2250.

St John W. P., Rughani J., Green S. A., McGinnis G. D., 1998, *Analysis and characterisation of naphthenic acids by gas chromatography-electron impact mass spectrometry of tert-butyldimethylsilyl derivatives*, Journal of Chromatography A, **807**, 241-251.

Thomas D.B., Knut V.G., Mediaas H., Vindstad J.E., Nicholas O.W., 2005, *The discovery of higher molecular weight naphthenic acids (ARN acid) responsible for calcium naphthenate deposits*, SPE/IADC 93011, in: Presented at 7th International Symposium on Oilfield Scale, Aberdeen, UK.
Tissot B. P., Welte D.H., 1978, Petroleum Formation and Occurrence, Springer-Verlag, New York, USA.

Tomczyk N. A., Winans R. E., Shinn J. H., Robinson R. C., 1998, *Results of treatment on acid content in a California heavy crude*, presented before the Division of Petroleum Chemistry Inc. 215th National Meeting, American Chemical Society, Dallas, Texas, USA, March 29-April 3.

Tomczyk N. A., Winans R. E., Shinn J. H., Robinson R. C., 2001, *On the nature and origin of acidic species in petroleum 1. Detailed acid type distribution in a California crude oil*, Energy and Fuels, **15**, 1498-1504.

Turner M., Smith C. P., 2005, *Controls on soap scale formation, including naphthenate soaps - drivers and mitigation*, SPE 94339, presented at the 7th International Symposium on Oilfield Scale, Aberdeen, UK, May 11-12.

Vindstad J. E., Bye A. S., Grande K. V., Hustad B. M., Hustvedt E., Nergard B., 2003, *Fighting naphthenate deposition at the Heidrun field*, 2003, SPE 80375, presented at the 5th International Symposium on Oilfield Scale, Aberdeen, UK, January 29-30.

Volkman, J. K., Maxwell. J. R., 1986, *Acyclic isoprenoids as markers. In: Johns, R. B. (ed) Biological markers in the Sedimentary Record,* Elsevier, New York, pp1-42.

Watson J.S., Jones D.M., Swannell R.P.J., van Duin A.C.T., 2002, *Formation of carboxylic acids during aerobic biodegradation of crude oil and evidence of microbial oxidation of hopanes,* Organic Geochem. **33**, 1153-1169.

Weiss H. H., Wilhelms A., Mills N., Scotchmer J., Hall P. B., Lind K., Brekket T., 2000, *NIGOGA – The Norwegian industry guide to organic geochemistry analysis*, published by the Norwegian Petroleum Directorate.